Catalytic co-pyrolysis of biomass and waste polymers using zeolite catalysts for upgrading bio- oils

Andrew Colin Dyer

Submitted in accordance with the requirements for the degree of Doctor of Philosophy as part of the integrated PhD with MSc in Bioenergy

July 2019

Centre for Doctoral Training

School of Chemical and Process Engineering

University of Leeds

Declaration of Authorship

The candidate confirms that the work submitted is his own and that appropriate credit has been given where reference has been made to the work of others.

Publications and outputs

Dyer, A., Williams, P. and Nahil, M.A., Catalytic co-pyrolysis of biomass and polymer waste as a pathway towards improved bio-oil production. In: 9th International symposium on feedstock recycling of polymeric materials, Ostrava, Czech Republic, p32. Editor Stanislav Honus

Dyer, A., Williams, P. and Nahil, M.A., Upgrading of oils from catalytic co-pyrolysis of waste plastics and biomass using ex-situ metal/zeolite catalysts. In: 12th Eccria Conference (The European conference on fuel and energy research and its applications), Cardiff, UK, p82. Editor Tony Ward

Acknowledgements

Abstract

This research has used catalytic pyrolysis and catalytic co-pyrolysis of biomass and plastics with upgrading of oils to make them more suitable for fuel use or as chemical feedstocks.

Pyrolysis of biomass at 500°C produced char, gas and liquid products, with the liquid containing both oil and water. All of the compounds which were identified in the bio-oil contained oxygen which is the primary cause of poor fuel properties in pyrolysis bio-oils through increased acidity and instability and reduced energy density.

Catalytic pyrolysis using ZSM-5 reduced the yield of liquid products by formation of deoxygenation gases (carbon monoxide and carbon dioxide) and light hydrocarbon gases (C_2-C_4) through zeolitic cracking. The proportion of oil within the liquid yield was also reduced with further deoxygenation reactions forming water. The Zeolite catalyst acts as a solid acids through two main sites, Strong Brönsted acid sites donate protons (H^+) whilst weaker Lewis acid sites accept electrons often in the form of a hydride (H^-) ion. Deoxygenation reactions include decarbonylation, decarboxylation and hydrodeoxygenation.

Metal-impregnated ZSM-5 catalysts were produced and used during pyrolysis as a pathway towards further upgrading of oils. These metal catalysts improved or maintained the oil yield observed for unmodified ZSM-5 and had varying effects on the oxygenated compounds in the oils. Gallium impregnated ZSM-5 (5 wt.%) produced the lowest proportion of oxygenated compounds. The gallium impregnated zeolites appear to function as bifunctional catalysts with the gallium atoms enhancing the acidity of the Brönsted acid sites. This allowed for decarbonylation of furan derived from cellulose into allene compounds which could then be further converted into aromatic compounds.

Catalytic co-pyrolysis using plastics was identified as another method for upgrading bio-oils through hydrogen donation. Plastics produce high oil yields when pyrolysed and these oils have low oxygen content. Co-pyrolysis oils of biomass and plastics, therefore, had a lower abundance of oxygenated compounds and greater oil yields than biomass alone. There were also synergistic effects observed which altered the oil yields beyond what was expected. These synergy effects involved free radical interactions between biomass and the plastics leading to hydrogen donation from the plastics to the biomass as well as natural catalytic effects involving char produced during biomass thermal decomposition. This was particularly notable in co-pyrolysis of

biomass and polystyrene where deoxygenation was enhanced during fixed-bed experiments.

Catalytic co-pyrolysis of biomass and polystyrene at different mixing ratios was examined in more detail using metal-loaded ZSM-5 catalysts. The metal impregnated ZSM-5 catalyst were able to reduce the oxygenated compound abundance in the pyrolysis oils compared to unmodified ZSM-5 in many cases. At a 1:1 mixture ratio cobalt-ZSM-5 produced the highest oil yields and joint lowest oxygenated compound abundance. At 4:1 gallium-ZSM-5 produced the highest liquid yield and lowest oxygenated compound abundance. This deoxygenation involved a mixture of decarbonylation, decarboxylation and hydrodeoxygenation reactions. The formation of carbon oxides during decarbonylation and decarboxylation reactions removed oxygen from the oil whilst reducing the oil yield directly as a result of carbon removal. Hydrodeoxygenation to remove oxygen in the form of water could also cause indirect loss of oil yield through carbon loss by enhanced coke formation. This is a particular problem where hydrogen content is depleted such that high yields of alkene and aromatic compounds are not viable. For efficient deoxygenation of bio-oil, the balance of these deoxygenation reactions should lead to maximum oxygen removal with minimal loss of carbon as carbon oxides or coke. Catalytic co-pyrolysis experiments using different metal-impregnated ZSM-5 catalysts gave varied results both for yield and composition of pyrolysis products with variation in the sample composition strongly influencing the effectiveness of a particular catalyst.

Table of Contents

List of Tables

List of Figures

Abbreviations

BEIS	Department for Business Energy and Industrial Strategy
BECCS	Bioenergy with carbon capture and storage
BTX	Benzene, Toluene and Xylene
CHNS	Carbon, hydrogen, Nitrogen and Sulphur Analysis
DEFRA	Department for Environment, Food and Rural Affairs
DP	Degree of polymerisation
EDX	Energy dispersive X-ray
EFW	Energy from waste
FCC	Fluid catalytic cracking
FID	Flame ionization detector
GC	Gas chromatography
GRP	Glass reinforced plastic
GWP	Global warming potential
HDO	Hydrodeoxygenation
HDPE	High-density polyethylene
IC	Internal combustion
LDPE	Low-density polyethylene
MS	Mass spectrometry
MSE	Secondary electron multiplier detector
Mtoe	Million Tonnes of oil equivalent
NIST	National institute of standards and technology
PAH	Polyaromatic hydrocarbons
PET	Polyethylene terephthalate

PP	Polypropylene
PS	Polystyrene
RDF	Refuse-derived fuel
RF	Response factor
RSD	Relative standard deviation
SE	Secondary electron
SEM	Scanning electron microscope
TCD	Thermal conductivity detector
TPD	Temperature programmed desorption
TPO	Temperature programmed oxidation
XRD	X-ray diffraction
XRF	X-ray Fluorescence spectrometry
ZSM-5	Zeolite Socony Mobile-5

Chapter 1: Introduction

1.1 Concerns regarding fossil derived fuels

Figures produced by the International Energy Agency for 2017 [1] put Global supply of energy at approximately 13,972 Mtoe (Million Tonnes of Oil Equivalent) of which 81.3% was sourced from fossil fuels. According to the study, these fossil fuels led to the release of an estimated 32,840 Mt of CO_2. These figures are understandably enormous but do not begin to explain the toll that is accounted on the Earth by the extraction and use of such large quantities of fossil fuels. It is worth listing several of the more serious consequences caused by fossil fuels: oil spillage or leakage during transportation and extraction; greenhouse gas emissions caused by leakage and combustion exhaust gases, leading to climate change; acid precipitation caused by combustion exhaust gases; air quality problems caused by emissions of nitrogen oxides, incompletely combusted hydrocarbons and particulates during fuel combustion which can through interaction with nitrous oxides lead to, photochemical smog; environmental damage caused by drilling and digging into ocean beds and landscapes to draw out the fuels, damaging not only the landscapes themselves but also the ecosystems which inhabit them [2, 3].

On top of this damage caused by using fossil fuels as a source of energy there are also consequences from the use of fossil fuels to produce chemicals and raw materials such as plastics. These materials eventually come to the end of their useful lives and are disposed of, leading to more environmental damage such as landfill sites, air pollution from combustion, water pollution and climate change due to greenhouse gases released during decomposition or unstable materials. The more stable materials are also problematic due to their long persistence in the environments to which they become part [4].

1.2 Current energy usage

These issues accumulate to provide an environmental imperative to reduce the use of fossil fuels from the current level. Unfortunately, the issues with fossil fuels are counter balanced by their usefulness for many purposes. They are excellent energy carriers and useful chemical building blocks, which coupled with their abundance, versatility and relatively low extraction and processing costs, makes them attractive.
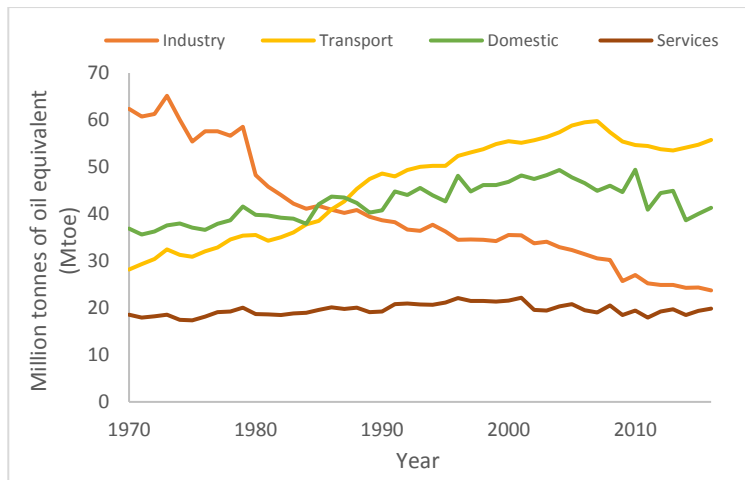
Figure 1.1: Energy use by various sectors in the UK – adapted from data published in BEIS, "Energy consumption in the UK - 2017" [5].

It is therefore no surprise, that in the UK, they account for a high proportion of energy supply, and figures from the department for business, energy and industrial strategy (BEIS) show that transport makes up a large, and growing, part of that energy demand. In 2016 transport accounted for approximately 40% of energy used in the UK with domestic at 29%, industry at 17% and the service sector at 14% [5] – (Figure 1.1).
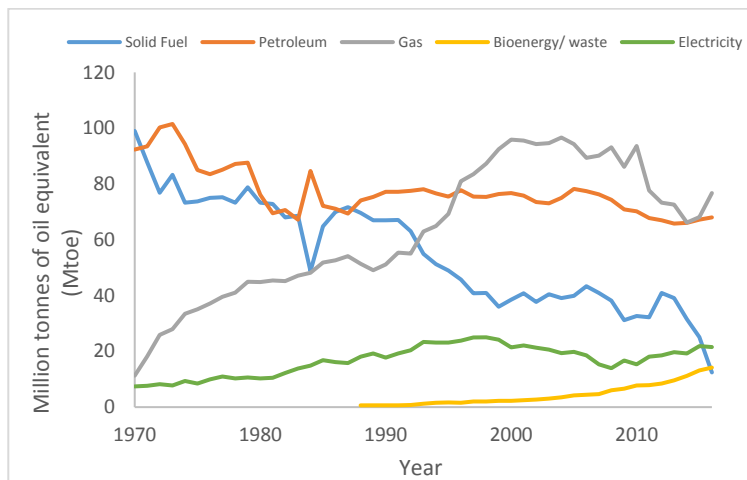
Figure 1.2: Energy use in the UK by type of fuel– adapted from data published in BEIS, "Energy consumption in the UK - 2017" [5].

Figure 1.2 shows the energy use by type of fuel and the two largest sections using this division are fossil derived fuels, petroleum and gas. This trend appears to be continuing although there has been significant progress made on

reducing the reliance on solid fossil fuels such as coal. This appears to have been offset largely by use of gaseous fuels which have increased at a similar rate to solid fuels decreases. Petroleum however, has remained largely constant which is almost certainly due to the dependence of the transport sector on liquid fuels (Figure 1.3). Further statistics from the "Energy consumption in the UK - 2017" report indicate that of the transport sector road transport (74%) accounted for the main energy use followed by air transport (23%) [5]. In 2017, Department for Transport figures regarding licensed vehicles in the UK give the number of road vehicles at approximately 38 million which saw a small increase of 1.7% from the previous year. Of this number, 31.3 million of these were cars and during the period July through to September in 2017 54.1% of new registrations were petrol fuelled, 40.5% diesel fuelled and 5.4% electric vehicles (both plug in (2.3%) and non-plug in hybrids (3.1%)) [6].
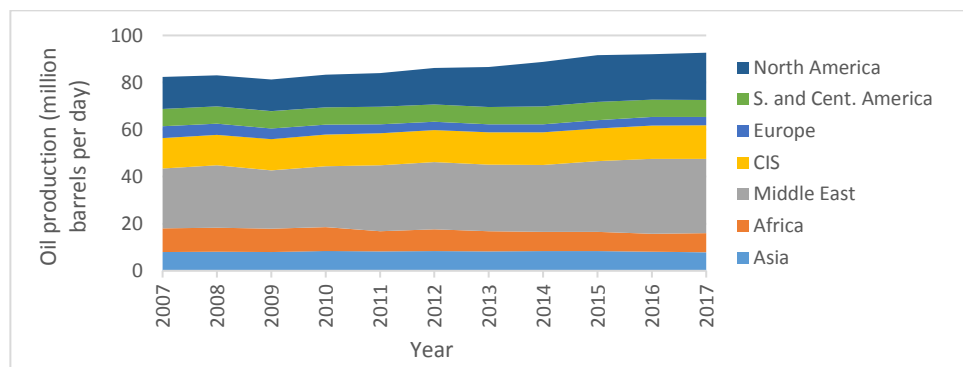
Figure 1.3: Global oil production during the previous decade, adapted from "BP Statistical review of world energy June 2018" [7].
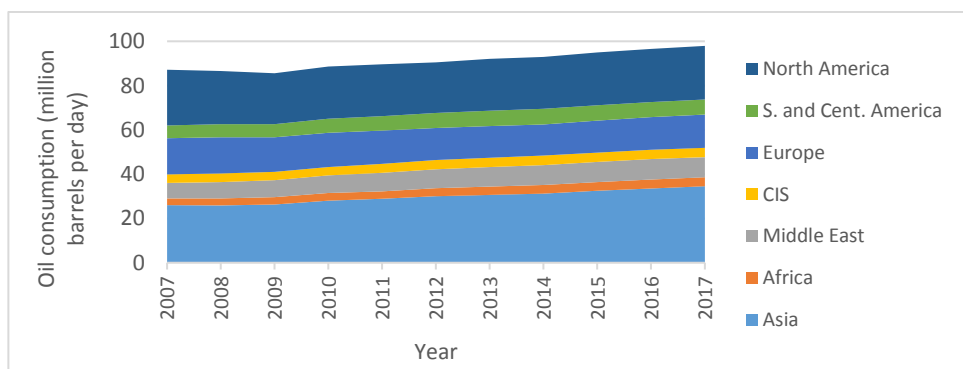
Figure 1.4: Global oil consumption during the previous decade [7].

This is probably most strikingly seen by examining global consumption and production figures for the fossil-based material, crude oil. Statistics compiled by

BP in their report "BP Statistical review of world energy June 2018" show that both demand and supply have increased consistently during the last decade [7] (see Figure 1.4).

1.3 Replacing fossil fuels

1.3.1 The three main fossil fuels

As can be observed from these figures and graphs, the use of fossil fuels is dominant both in the UK and globally with long term trends suggesting they will remain a significant part of the global energy mix. In the UK, transport is one of the biggest consumers of energy and this energy is sourced almost exclusively from petroleum. There are many advantages of using fossil fuels and if their use is to be reduced or replaced there is a need to understand why they are so attractive.

Solid fuels such as coal have seen extensive use for providing heat and for power generation [8, 9]. Coal extraction, transportation and combustion are all environmentally damaging with public perception of solid fuel combustion as unclean leading to reduced use for power generation in the UK. Coal still holds considerable importance to the steel manufacturing industry. The reduction in use of coal for power generation and for heating in the UK has mostly been replaced by renewable technologies such as solar, wind and nuclear energy as well as use of cleaner burning natural gas. Gaseous fuels were originally used for lighting but in modern times find use for cooking, domestic heating and power generation [10]. Liquid fuels which are usually derived from petroleum which can be extracted from underground reservoirs trapped in geological formations and can then be separated by fractional distillation to give many different hydrocarbon products [11].

1.3.2 Bio-sourced fuels

Efforts are being made to replace fossil fuels with both liquid and gaseous fuels. In the UK and across Europe bioethanol and biodiesel are routinely used as part of the transport fuel mix although concerns about land use change, through use of first generation / food biomass derived fuels, have indicated to policy makers that these are only a starting point on a road to fossil fuel replacement [12]. Second generation biofuels which are derived from non-food crops and third generation biofuels which used organisms, such as microalgae, to produce fuels directly are another potential source of non-fossil derived fuel although these are young technologies and have only had limited development. Gaseous

fuels such as biomethane and hydrogen are also an important possibility. These have the advantage of being able to be used with current internal combustion (IC) engine technology with only minor alteration of operational parameter. However, the low energy density of gaseous fuels makes them challenging to store. Hydrogen combusts extremely cleanly producing just water as a by-product, however, it is currently expensive and energy intensive to produce thereby limiting its potential.

1st (Corn, sugar beat, sugar cane)	• Bioethanol • Biodiesel • Unmodified oils
2nd (short rotation coppice, straw/ arable husks, organic waste)	• Cellulosic ethanol • Biomethane / biogas • Pyrolysis oil • Solid fuels
3rd (Algae, microalgae)	• Biodiesel • Petroleum • Methane • Vegetable oil
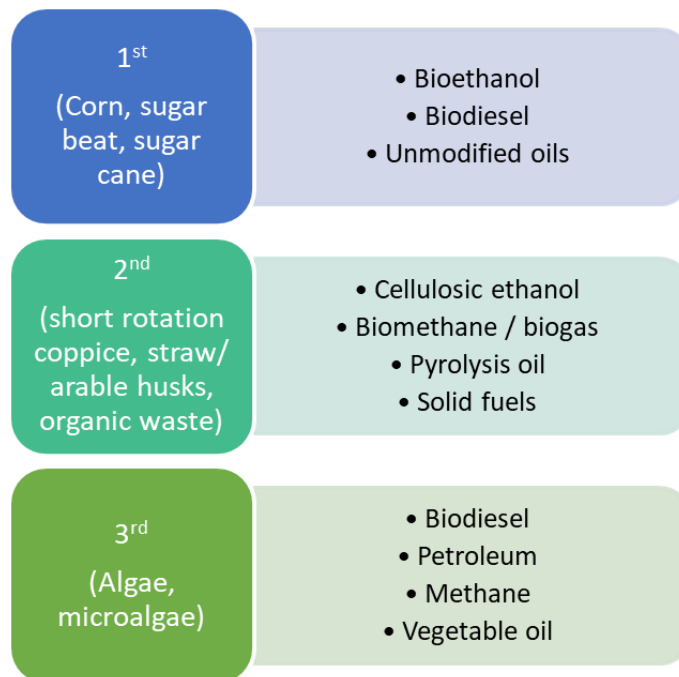
Figure 1.5: Examples of 1st, 2nd and 3rd generation biofuels [13, 14].

1.4 Disposal of waste materials

1.4.1 Plastic waste

Petroleum is used to produce fuel, but it is also used as a feedstock for a range of chemicals and materials which impact all areas of modern life, areas such as food, clothing, construction materials as well as medicine. This introduces a secondary issue which is the production of high quantities of waste; material which is no longer suitable for its primary purpose and has limited value. This waste includes synthetic plastics, much of which is derived from fossil hydrocarbons, for example in 2015 global production of resins and fibres was 380Mt of material. Equivalent to a compound annual growth since the 1950s of approximately 9%. Half of the plastic ever produced was made in the last 13 years [15]. This is a problem which continues to expand and if it is not treated

as a priority it has the potential to cause environmental damage in many ways as serious as those observed from fossil fuel use.

1.4.2 Biomass waste

Biomass waste is also produced on a large scale, however because it is a natural material, unless it is chemically treated it readily undergoes biodegradation, if not protected from the natural environment. This is advantageous in that it does not linger in an environment and in degrading gives nourishment and habitats for a wide range of organisms which are vital to life on planet earth [10]. However, if it degrades naturally it produces methane gas which has a high global warming potential (GWP). Biomass waste is produced at scale but also in great variety. Biomass can be extremely complex in nature with one plant such as a tree producing many different biomass products, leaves, bark, trunk wood, roots which are each composed of many cellular structures and materials. The nature of each of these materials can vary based on many conditions including weather, soil, nutrients, age, maturity and season of the year, to name a few. This makes utilisation of biomass extremely complicated [16, 17].

Lignocellulosic biomass derived from the main trunk of a tree, with bark and leaves removed, is a feedstock used in several industries including construction, furniture making and paper making and each of these produces waste biomass material both at the production stage and at the end-of-life of products. Unfortunately, many waste materials from these sources are contaminated with chemicals used to treat the materials to improve their longevity or functionality [10]. Another major source of biomass waste is as a direct result of plant cultivation, these include forestry, arboriculture, sawmill residues as well as agricultural residues [18].

1.4.3 Fate of UK waste

The process by which waste material is handled will be an important factor in determining environmental damage, therefore it is important to examine the current destination of UK waste. Data collected by the charity Recoup, which focuses on the use and recycling of plastic packaging within the UK domestic market in 2017 gives a helpful overview. 1.02 Million Tonnes of plastic packaging was collected with the purpose of recycling from a total 2.26 Mt of packaging on the market. This equates to a recycling rate of just under 45%. From this recycled fraction 63% was exported and 37% was recycled domestically. The other 1.24 Mt was either sent to landfill or disposed of through energy recovery processes [19]

From this data it could be inferred that 16.7% of total packaging was recycled domestically and 28.4% exported with the intention of recycling but the outcome of the recycling process is more challenging to establish. The residual waste, which is the fraction collected by waste authorities without the purpose of being recycled or reused, was also examined by the Recoup report. It found that 36% was reported to be utilised for energy from waste purposes (EFW), 28% to landfill, 23% converted to RDF (refuse derived fuel) and 13% recycled. The report also looked at the financial details and indicates that in 2015 the average mixed bottle price was £70 per tonne of material. If this value remains unchanged then the value of bottles which were not recycled could be worth more than £17 million and cost £25 million for disposal [19]. This indicates that there is a large amount of material which is collected and sorted and has the potential to be utilised and is not currently being used in the UK market. There would be a financial incentive to making use of this material which as a commodity has a comparatively low cost and at the same time has a cost associated with disposal.

Another source of UK waste data, are UK government values published by the department for environment, food and rural affairs (DEFRA) [20]. These compare many different aspects of waste management on a quantitive basis, highlighting patterns of change and explain the causes of these variations. The key section that will be examined below are statistics on packaging waste. The EC Directive 94/62/EC sets targets for recycling of packaging and packaging waste which were to be met by participating countries by 2008 from which point these targets remained in place or could be superseded by more tight restrictions implemented by each country. The figures for plastics waste in 2016 are the same as those given in the recoup report (2017) and the recycling / recovery rate of 44.9% exceeds the EU target of 22.5%. The wood collection figure is 1.31 Mt with only 0.41 Mt recycled a rate of 30.9% compared to the EU target of 15.0% thereby, current waste targets are being exceeded [20].

1.5 Conversion of biomass and waste materials into useful products via Pyrolysis

1.5.1 Biomass as a resource

Defra statistics indicate that biomass is more likely to be used for energy recovery rather than recycled [20]. Chemically impregnated and low-grade wood can be carefully combusted during an EFW process to reduce the risk of contaminated material causing environmental damage. However, this waste makes up only a limited proportion of the variable and complex biomass

resource available. Table 1.1 shows several different biomass sources outlined by the Forest Research [21].

Table 1.1: Biomass resources categorised according to their sources [21].

Virgin wood	Energy Crops	Agricultural residues	Food waste	Industrial waste
Logs	Short rotation tree plantations	Plant husks	Food Production waste	Treated & untreated wood
Bark	Grasses	Straw	Household waste	Wood composites and laminates
Sawdust	Non-woody energy crops	Animal litter	Cooking oils	Paper industry waste pulps
Woodchips	Agricultural energy crops (sugar beet)			Textiles
Brash	Water crops (seaweed and algae)			Sewerage sludge

Due to the complexities arising from determining the potential biomass resource, studies have been undertaken to calculate the amount and type of biomass resource which can be realistically made available for replacement of fossil fuel. A study at the Tyndale Centre for Climate Change Research (Manchester UK) examined the potential for UK sourced biomass resources to replace fossil-based resources with emphasis on forwards planning to meet 4 scenarios [18].

The 4 scenarios focused on:

- Prioritisation of food security.
- Economic development and competition as a priority.
- Conservation of biodiversity and land as a priority.
- Producing energy through biomass as a priority.

The study found that without undermining food security the UK could meet up to 44% of its energy demand by 2050 through biomass resources produced within the UK land area. The resource with the most reliability and robustness was the use of residues from agriculture, forestry and associated industry which could potentially provide up to 6.5% of primary energy by 2050. On top of this, waste materials could potentially provide up to 15.4% and crops grown with the direct purpose of providing energy or as a source of biomass as much as 22%. The study found that this resource is not automatically available and would

need to be achieved through strategic decision making, planning and implementation which are not currently in line with UK bioenergy strategies [18].

There is also an abundant biomass resource that could be utilised from outside the UK whilst still adhering to sustainability targets. Drax power station in North Yorkshire, which has seen conversion from coal as the primary fuel through to a mixture of coal and biomass fuels, notably imports wood pellets mainly from North America (83% - 2017, 5.6 Mt) as well as some from Europe (including UK) and South America [22]. Data from Drax for 2017 presents the types of biomass which was used for power generation – (Figure 1.6).
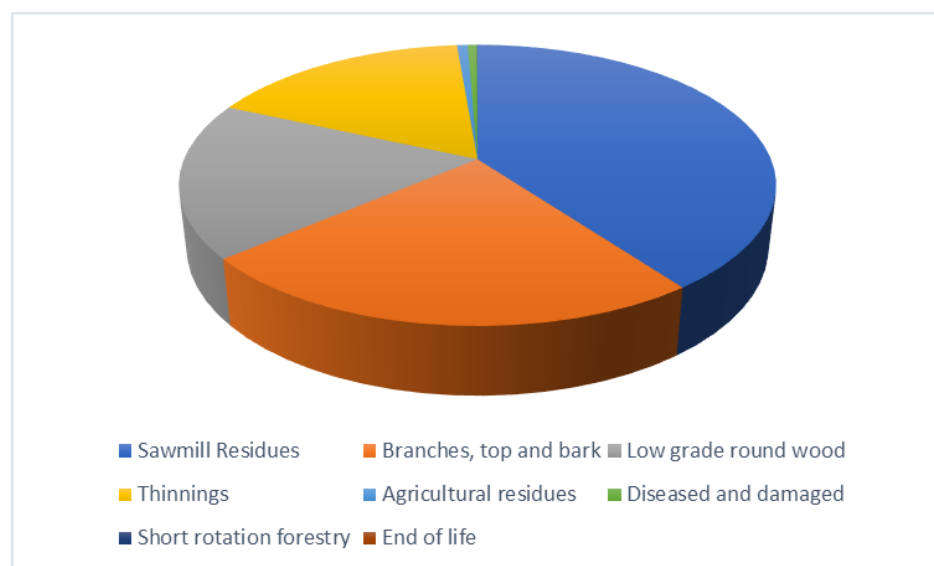
Figure 1.6: Biomass types used at Drax power station - 2017 [22].

1.5.2 Sustainable biomass utilisation

However, utilisation biomass resource is not straight forward and use of biomass is not sustainable unless the material is sourced in a responsible way and leads to reduction of emissions when compared to the alternative. The UK government published a bioenergy strategy in 2012 [23] which highlighted that bioenergy is the only resource able to readily supply all the UK energy requirements (heat, transport and electricity) and was important to meet carbon reduction targets. This was announced with the important proviso that it **must** be sustainably sourced or greater damage could be caused than carbon reduction alleviated.

The strategy indicated that use of bioenergy would initially be focused on heat and power generation but envisaged transport becoming the key utiliser of bioenergy by 2030 and continuing through to 2050 regardless of whether

carbon capture and storage technology was available. Although, bioenergy with carbon capture and storage (BECCS) could potentially lead to negative emissions where more carbon dioxide might be removed from the atmosphere than released to produce the energy and is therefore a vital technology for long term greenhouse gas reductions [23].

Utilisation of biomass has sometimes attracted criticism even between researchers with disagreements at times handled in the public eye. One such dispute was between Chatham House and IEA bioenergy who had differing views with regards to accounting of carbon sequestration in forests [24, 25]. Both parties however, agreed that biomass has the potential to replace for fossil fuels, but this must only be undertaken where sustainability is achieved.

The IEA report comments on its vision for the role of biomass as fuel source with the following quote - "Biomass is a renewable resource with large potential for expansion, and unlike other renewable resources, biomass can be stored and converted to different energy carriers. It can thus play a critical role in facilitating transition to low-carbon energy systems" [25]. This highlights the key value of biomass utilisation, but sustainability must also be achieved.

1.6 Current conversion technologies

1.6.1 Conversion possibilities

There are four main categories of processing for conversion of biomass materials into useful and valuable commodities, physical, biological, chemical and thermal. The first, physical could include milling and grinding of materials or pressing as is the case with olives to force natural oils away from the bulk of the biomass material to produce a pure liquid product separated from a solid residue. Biological systems are also widespread and are used for production of ethanol from sugar containing crops through fermentation. Anaerobic digestion is also used for the decomposition of food and plant waste which contains high moisture content. The gases produced such as methane are then able to be upgraded or combusted directly thereby removing a compound with a high global warming potential whilst potentially producing useful heat or energy [10].
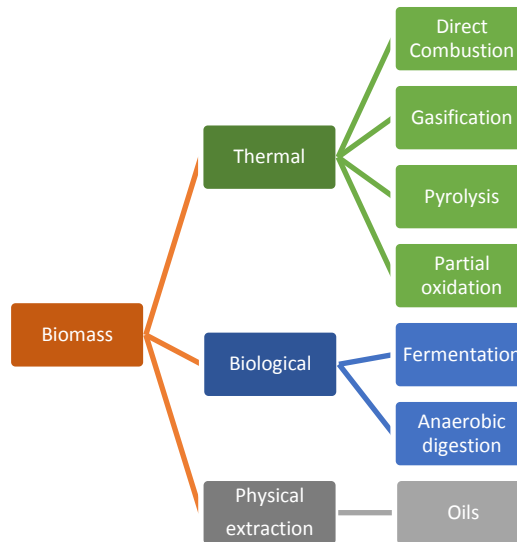
Figure 1.7: Potential conversion pathways for biomass material - adapted from handbook of alternative fuel technologies [26].

Chemical technologies are also widespread but are usually specifically designed for each feedstock and end use. There is ongoing development in fields such as chemical conversion of lignin into chemicals, however due to the highly specific nature of the chemical processes they will not be considered further in this study.

Thermal processing includes a wide range of technologies and processes which use thermal energy to break bonds within a material with the purpose of producing lower molecular weight compounds.

In direct combustion of a hydrocarbon material the aim is often full conversion of a material into ash, carbon dioxide and water, with the aim of producing useful energy or to dispose of bulky materials. This can produce very high temperatures and usually utilises managed air flow to control completeness of combustion and product formation.

Gasification seeks to reduce high molecular weight hydrocarbons down to useful low molecular weight, gaseous, compounds such as hydrogen, carbon monoxide or methane with the aim of producing chemical feedstocks or energy carrier gases which can be combusted at a later stage. This usually uses temperatures of around 700-1000°C, often with reduced oxygen to hinder combustion processes although gasification above this temperature range is also possible.

Processes such as partial oxidation and torrefaction are at the other end of the thermal scale and uses comparatively gentle conditions such as temperatures

below 300°C to decompose targeted compounds within a material such as hemicellulose with the aim of producing a solid fuel with favourable physical or mechanical characteristics. This is very similar to the process used to roast coffee beans to produce a substance similar in nature to the original material, but which is more easily mechanically ground and where extraction of compounds using boiling water is augmented.

Pyrolysis is a process which stands part way between partial oxidation and gasification (400-600°C) and is usually used to produce either a solid fuel such as char, a liquid such as bio-oil or a combination of the two. These thermal processes are more of a spectrum than a binary set of processes and use controlled temperature, atmosphere and pressure to determine yields of products [10, 26, 27].

1.6.2 Pyrolysis

When biomass is heated in the absence of oxygen there are 3 major components produced, char, gas and condensed liquid (bio-oil). If pyrolysis is used to produce liquid fuel then it is the bio-oil which is the most important product, however the gas and char are likely to be useful as well. Bio-char is similar in nature to charcoal and several different uses have been suggested including as a soil additive or decarbonisation of steelmaking. The gaseous yield are normally a mixture of permanent gases and hydrocarbons and might be possible to use as a fuel or a chemical feedstock, however when producing bio-oil they would most likely be combusted to produce heat for the pyrolysis process [27-29].
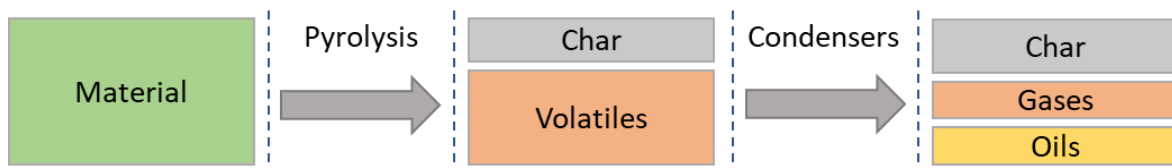
Figure 1.8: A schematic representation of the pyrolysis process.

1.6.3 Catalytic Pyrolysis

Bio-oil can be upgraded post pyrolysis through several processes, notably, Zeolite cracking (FCC), hydrotreating and hydrocracking. Each process is used routinely in crude oil refining and are effective although with varying efficiency and each have drawbacks. Catalytic pyrolysis is a similar thermal process to

standard pyrolysis however the vapours produced during devolatilisation are passed through a catalyst before condensation occurs. If post pyrolysis catalytic treatments are used the yield is condensed and then reheated to undergo the catalytic process and this can lead to many different side reactions occurring which will change the bio-oil. The advantage of catalytic processes directly to vapours is the reduction or elimination of these unwanted reactions. Hydrogen is used routinely to assist in reactions to remove oxygen from bio-oils however this increases the cost and the energy input of the total process thereby reducing efficiency. Some literature has suggested that polymers could be used as hydrogen donor materials alongside catalytic processes to aid removal of oxygen. The exact processes will be examined further during the literature review [27, 28, 30]
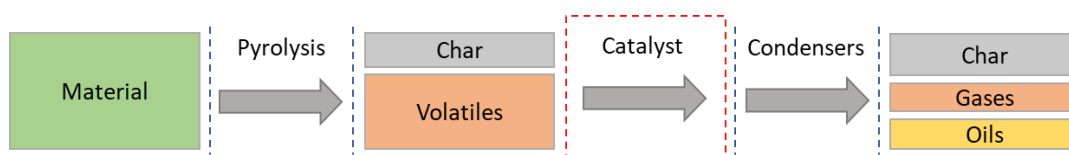
Figure 1.9: A schematic representation of a catalytic pyrolysis process.

1.7 Aims

This project aims to examine the catalytic pyrolysis of a standard wood pellet sample alongside plastic samples representative of waste plastics utilised globally in large quantities. The plastics studied are polyethylene terephthalate (virgin/reinforced), low density polyethylene (virgin), high density polyethylene (recycled), polypropylene (recycled) and polystyrene (recycled) which are available in a homogenous pelletised form. The wood sample and plastic samples will be pyrolysed in a two-stage fixed bed reactor both individually and in various combinations to investigate co-pyrolysis of biomass and plastics. Ex-situ catalysis using ZSM-5 and metal impregnated (Co, Cu, Fe, Ga, Ni, Mg and Zn) ZSM-5 catalysts, produced through wet impregnation of commercially available ZSM-5, will also be examined to investigate the effect of these modified and unmodified zeolites on the yield and composition of pyrolysis products. The effect of combining co-pyrolysis and catalytic pyrolysis using the metal-impregnated zeolites will also be investigated. The products from these pyrolysis experiments will be analysed to determine if oils suitable for fuel production or production of chemical feedstocks may be possible using this

process catalytic pyrolysis / co-pyrolysis process. The composition of the pyrolysis products and the yield of products will both be important for assessing then suitability of each pyrolysis output for fuel or chemical feedstock production.

The analysis of the products will investigate the effect of co-pyrolysis on the yields of liquid, solid and gaseous products with analysis of the liquid yield undertaken to identify changes to the amount of water formed during pyrolysis such as through hydrodeoxygenation reactions which may reduce the oxygen content of the oil. Semi-quantitive GC-MS analysis of the oils will also be used to compare the types of compounds identified in the oils produced through the various co-pyrolysis mixtures and through catalytic co-pyrolysis. This will be used in conjunction to quantitive gas chromatography of gaseous products and Karl-Fischer titration of the liquid yield to identify the cause of observed variations between the compounds identified in the oils.

The project will also examine the catalysts after pyrolysis has been completed to identify whether coke deposition is enhanced or minimised through co-pyrolysis or through deposition of the metals onto ZSM-5.

1.8 Objectives

1. To determine the yield and character of the pyrolysis products obtained by pyrolysis of a sample of biomass. This biomass sample is a commercially produced wood pellet from virgin wood with a homogenous composition and consistent moisture content. The pyrolysis will use a two-stage fixed-bed reactor which remains unchanged throughout further pyrolysis experiments such that comparison can be drawn between pyrolysis of different samples. Solid yield is to be determined through comparison of sample weight before and after pyrolysis. Liquid yield is to be determined by comparison of the condenser weight before and after pyrolysis. Gas yield is to be determined through calculations using quantitative gas chromatography analysis of permanent and hydrocarbon gases. Oil yield is to be determined through Karl-Fischer titration of the liquid samples to determine the water content of the liquid which is subtracted from the liquid yield to determine the oil yield. The composition of the oils is to be determined through semi-quantitative gas chromatography with mass spectrometry such that variations between the compounds which are identified in the oil samples might be

observed. These values may not be treated as absolute values but where variations are present between two oil samples these should be observed. Analysis of oil composition will focus on the proportion of the compounds identified in the oil which contain oxygen and those which contain aromatic or polyaromatic features. Quantitive gas chromatography and Karl-Fischer titration are to be used in conjunction with the GC-MS analysis to identify the cause of changes in the oil composition such as through deoxygenation products, water, carbon dioxide and carbon monoxide.

2. To determine the effect that a commercial ZSM-5 catalyst has on the yield and characteristics of products from pyrolysis of the biomass sample. This will be through comparison of results obtained through non-catalytic and ex-situ catalytic pyrolysis using the same fixed bed reactor and product collection equipment used for pyrolysis of the biomass sample.

3. To produce metal impregnated ZSM-5 catalysts at a 5 wt.% loading (metal is present as 5% of the weight of the catalyst produced) by wet impregnation of the commercially available ZSM-5 using metal nitrate hydrates followed by calcination and reduction using hydrogen. The metals used for impregnation are copper, cobalt, iron, gallium, nickel, magnesium and zinc.

4. To use the metal impregnated ZSM-5 (Co, Cu, Fe, Ga, Ni, Mg and Zn) for ex-situ catalytic pyrolysis of the biomass sample to identify the effect they have on the yields and compositions of the pyrolysis products under the same conditions as the previous experiments.

5. To observe the pyrolysis of plastics using the ex-situ unmodified ZSM-5 catalyst for comparison against the pyrolysis products for the biomass sample. The plastics are polyethylene terephthalate (virgin-reinforced), low density polyethylene (virgin), high density polyethylene (recycled), polypropylene (recycled) and polystyrene (recycled). Analysis is to be completed as with the biomass sample to allow for comparison.

6. To observe the effect of co-pyrolysis of the biomass sample with plastic samples at a 1:1 mixing ratio (by weight) in the presence of the unmodified ZSM-5 catalyst. The yields of pyrolysis products and the composition are to be analysed such that comparison can be undertaken to the results obtained for pyrolysis of the individual samples of biomass and plastics during objectives 2 and 5.

7. To observe ex-situ catalytic co-pyrolysis of biomass and plastics (HDPE, PET, PS) using unmodified ZSM-5 at different mixing ratios (1:1, 4:1 and

9:1 by weight) with biomass in each case being the greater proportion of the sample. This will be undertaken for polyethylene terephthalate, high density polyethylene and polystyrene.

8. To analyse non-catalytic thermal decomposition of the biomass and plastic samples using TGA-MS to identify the profile of decomposition. This is to be compared against the thermal decomposition of the combined biomass and the plastic samples to identify interactions or synergy effects which may be observed between the biomass and plastic samples during the devolatilisation process.

9. To undertake ex-situ catalytic co-pyrolysis of the biomass sample and polystyrene using the metal impregnated ZSM-5 catalysts at different mixing ratios (1:1 and 4:1) and compare the effect of changing the mixing ratio and catalyst on the pyrolysis yields and composition of these products.

10. To observe the effect of changes to mixing ratio (1:1, 4:1, 19:1, 99:1 and 1:0) and catalyst temperature (450°C, 500°C, 550°C and 600°C) on the yield and composition of pyrolysis products during ex-situ catalytic co-pyrolysis of biomass and polystyrene using gallium impregnated ZSM-5 as the catalyst.

11. To identify the coke deposition on the catalyst which are used for pyrolysis of the biomass and plastic samples using temperature programmed oxidation. This can provide insight into the poor performance of a catalyst or identify whether a catalyst might be susceptible to enhanced deactivation during pyrolysis.

12. To identify the coke deposition on the catalyst which are used for co-pyrolysis of the biomass with the plastic samples using temperature programmed oxidation to provide insight into the potential that co-pyrolysis using a particular mixture of biomass and plastic might enhance or reduce coke formation.

13. To compare the simulated distillation profile of oils produced using pyrolysis and co-pyrolysis of biomass and plastics in order to compare against the standard profile for a fuel. This is to identify whether co-pyrolysis or the use of metal impregnated catalysts may lead to improvements for the purpose of fuel production and to identify the limitations of these improvements.

1.9 Thesis structure

Chapter 1 introduces and details the global and local (UK) environmental concerns to which catalytic pyrolysis may be able to provide a solution. This chapter gives the basic process of catalytic pyrolysis and examines the reasons that catalytic pyrolysis could provide a suitable solution to the issues identified.

Chapter 2 gives a state-of-the-art literature review identifying the current understanding concerning catalytic pyrolysis of biomass and plastics and examining the effect of co-pyrolysis of biomass with different plastics. This chapter also examines the production, action and effect of both unmodified and metal impregnated ZSM-5 catalysts to provide upgrading to pyrolysis vapours. This chapter also identifies the way in which changes to catalysts, pyrolysis conditions and pyrolysis feedstock might affect the products of pyrolysis both in a beneficial or a detrimental manner.

Chapter 3 provides the experimental methodology which was used for pyrolysis experiments and for analysis of the products of pyrolysis. This chapter also examines the processes which were used for data analysis, identifying the significance of results which were obtained using these analytical methodologies. The composition of the samples which were used for pyrolysis were also reported alongside the methodologies used to determine these results.

Chapter 4 investigates the non-catalytic (objective 1) and catalytic pyrolysis (objective 2) of the biomass sample to identify the way in which the use of a commercial ZSM-5 catalyst effects the product yield during pyrolysis using the two-stage fixed bed reactor and to identify the changes in oil compounds identified during oil analysis. Metal impregnated ZSM-5 produced (objective 3) through wet impregnation of the commercial ZSM-5 used in objective 2 are then used for ex-situ pyrolysis of the biomass sample in the two-stage fixed bed reactor (objective 4) with pyrolysis product yields and compositions compared against those for the unmodified catalyst to determine if oils which are more suitable for fuel production or chemical feedstock formation have been produced. The unmodified ZSM-5 and metal modified ZSM-5 catalysts were investigated through temperature programmed oxidation (TPO) (objective 11) to identify coke deposition during pyrolysis to determine if metal impregnation of ZSM-5 might cause enhanced or reduced coke formation.

Chapter 5 used thermogravimetric analysis with online mass spectrometry (TGA-MS) to examine the temperature profile for the thermal decomposition of the biomass and plastic samples and to identify changes in the devolatilisation

profile during co-pyrolysis of biomass with the plastics (objective 8). The mass spectrometry was used to observe the evolution of water, carbon dioxide, carbon monoxide and hydrogen gas during the thermal degradation process to identify any changes which might indicate that co-pyrolysis is producing an effect on the chemical reactions which are occurring during decomposition.

Chapter 6 investigates catalytic co-pyrolysis of the biomass and plastics in the two-stage pyrolysis reactor using unmodified ZSM-5. Initial investigations examine pyrolysis of the individual plastic samples in the presence of the unmodified ZSM-5 catalyst (objective 5) before examining co-pyrolysis of the biomass sample with the plastic samples in a 1:1 mixing ratio by weight (objective 6). Further investigations examined co-pyrolysis of the biomass with high-density polyethylene, polyethylene terephthalate and polystyrene at different mixing ratios (1:1, 4:1 and 9:1) to observe what effect this had on the yield and composition of pyrolysis products (objective 7). The catalysts which were used during pyrolysis were examined by TPO to identify whether co-pyrolysis of the biomass sample with these plastics resulted in enhanced coke deposition (objective 12).

Chapter 7 investigates the catalytic co-pyrolysis of biomass and polystyrene using metal-impregnated ZSM-5 catalysts at two different mixing ratios (1:1 and 4:1) to identify the effect that the different mixing ratio had on the effectiveness of each metal impregnated catalyst to produce oils suitable for fuel use or to produce chemical feedstocks (objective 9). Further analysis was conducted using one of the metal-impregnated catalysts (Ga-ZSM-5 (5 wt.%)) which performed effectively in the previous chapters. This further analysis examined the effect of varying the temperature of the catalyst bed and varying the mixing ratios used during co-pyrolysis further (objective 10). Simulated distillation was used to compare the distillation profile of oils produced during pyrolysis and co-pyrolysis using the metal modified and unmodified ZSM-5 catalysts to identify to what extent the changes introduced to the experiments were able to produce an oil suitable for fuel use and to compare this against the profile expected for a standard fuel (objective 13).

Chapter 8 concludes the results obtained during catalytic co-pyrolysis of biomass and plastics using ZSM-5 catalysts. This highlights the advantages and limitations regarding the catalytic upgrading of pyrolysis oils to produce fuels or chemical feedstocks. This chapter also identifies further work which would improve or expand on the results obtained, particularly focussing on the differences between this methodology, optimised for research, and a process which might be used commercially.

Chapter 2: Literature review

2.1 Introduction

This research examines the catalytic co-pyrolysis of biomass and polymers with the desired result of producing oils suitable for fuel use or for production of chemical feedstocks. In order to evaluate these oils it is valuable to understand the processes which are occurring during pyrolysis. This will include the thermal effects, the effects of interactions between samples and catalytic effects. It is also important to ascertain how the changes brought about through upgrading might change the oils, and to establish how these upgraded products might compare to gasoline derived through petroleum crude oil sources.

2.2 Pyrolysis of biomass

Pyrolysis is a process which can be used to convert biomass into gaseous, liquid and solid products which is a potential pathway towards replacement of petroleum derived transportation fuels, the basic process is concisely defined by the encyclopaedia Britannica [31].

"**Pyrolysis**, the chemical decomposition of organic (carbon-based) materials through the application of heat. Pyrolysis … occurs in the absence or near absence of oxygen, and it is thus distinct from combustion." – Encyclopaedia Britannica [31].

Lignocellulosic biomass may provide an abundant renewable resource for the [26] production of such bio-derived fuel with thermal degradation of biomass through pyrolysis leading to three major products, bio-oil (or tar), bio-char and non-condensable gases [29, 32]. Lignocellulosic biomass is composed of three major components, cellulose, hemi-cellulose and lignin with each component involved in different decomposition pathways leading to different compound mixtures. Adding to the complexity of biomass pyrolysis, each of the three components, cellulose, hemi-cellulose and lignin has varied and complex composition which can vary widely between biomass type and as the pyrolysis process progresses these compounds are able to interact with each other leading to an even greater range of pyrolysis products. As well as the major constituents of lignocellulosic biomass, the minor components, such as extractives and char, may have a significant impact on secondary reactions and therefore the final composition of pyrolysis products [33-35].

The literature review will initially examine the processes which affect a single particle of biomass and will then continue by focusing on the fates of individual

components during pyrolysis. This will include examining variations in method which would affect the output from pyrolysis. Once this is established the review will examine reaction pathways which may lead to upgrading of the pyrolysis products with a particular focus on catalytic pathways.

2.2.1 Devolatilisation of biomass

Pyrolysis of biomass is a similar process to combustion of lignocellulosic biomass with the major difference being the absence or near absence of oxygen. This means that whilst thermal decomposition of the material occurs there is a halt before the highly exothermic thermal oxidation stage which is often referred to as combustion or oxidation. Figure 2.1 describes the processes which compose the combustion of a particle of biomass. Combustion of biomass typically has three main processes [10, 36].

a) Drying

b) Devolatilisation

c) Oxidation / combustion
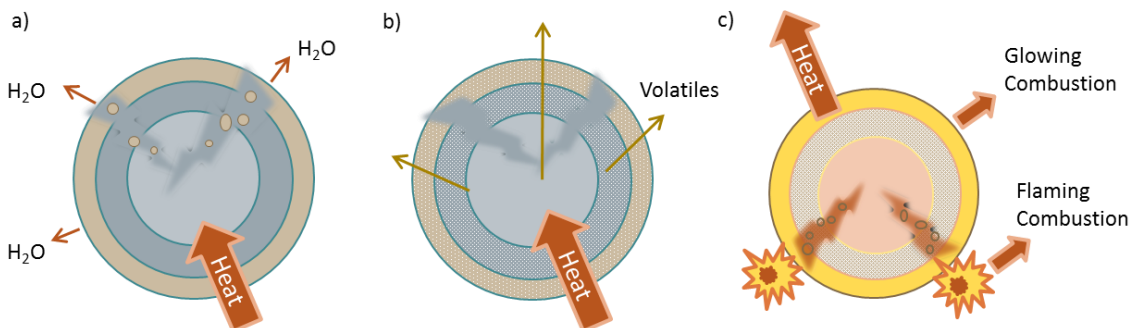
Figure 2.1: Stages during thermal degradation of biomass [10, 36].

The moisture content of biomass can vary widely between biomass sources and can be significantly affected by storage or pre-treatment. In an undried sawdust sample it might have a range of 25%-60% moisture which often drops to around 10% or below in a wood pellet. In the first stage of combustion (a), which takes place at temperatures of <100°C, the material dries as moisture is driven off the particle. As the biomass particle heats further (b) water or steam is forced out of the particle and in doing so drives channels in the fabric of the particle. If the particle continues to be heated above 250°C, the various components of the lignocellulosic biomass begin to break down and release volatiles which also force their way out of the particle either through the

channels previously formed or creating their own channels as they exit. The temperature at which this process occurs is dependent on the composition of the biomass [34]. As the volatiles leave the particle they can begin secondary reactions with species in the particle, or with other species in the gas phase such as other volatiles or low boiling point metals. In this way both homogeneous and heterogeneous cracking reactions are present even without the presence of a dedicated catalyst.
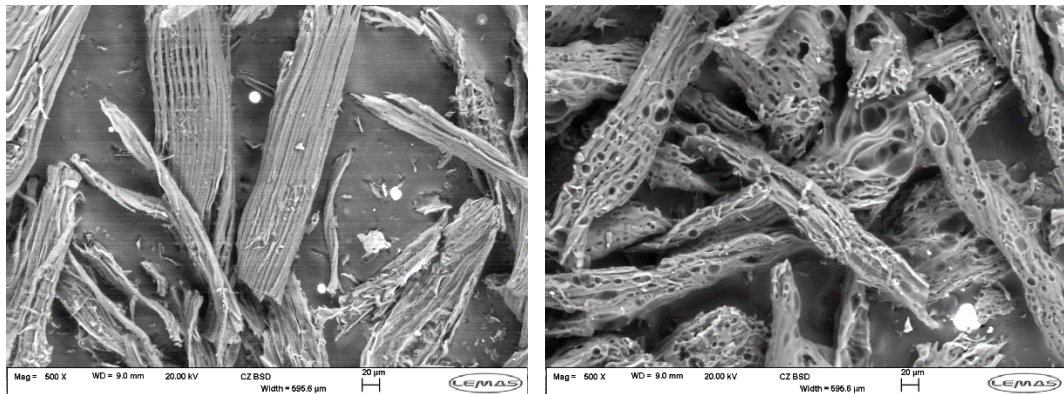
Figure 2.2: SEM images at 500x magnification of pine which has been devolatilised by heating from room temp to 1000°C in a nitrogen atmosphere. Left - low heating rate (10°Cmin^{-1}) Right - high heating rate (1000°Cmin^{-1}).

Figure 2.2 shows SEM images of a pine sample which has been devolatilised at a low heating rate and a high heating rate with these images clearly indicating the effect of the moisture and volatiles rapidly expelled from the sample.

Generally, above 600°C these devolatilisation reactions cease. In an oxidising atmosphere such as air, the particle may then undergo a third stage which is oxidation or combustion. There are two types of oxidation, initially as volatiles leave the particle they can become ignited which is referred to as flaming combustion the remaining material can also become ignited and oxidise from the exterior of the particle through to the centre which is called glowing combustion. It is possible for glowing combustion to happen without flaming combustion [36].

During pyrolysis, where there is an absence of an oxidising agent, the third stage is avoided. Instead the volatile vapours either react within the sample, condense or polymerise onto the exterior of particle or become entrained into the gas flow through the reactor where further decomposition may occur, or

they are carried through to the condenser system. In the condenser system low temperatures or electrostatic precipitators can be used to condense volatiles. Gases which are non-condensing continue through the condenser system and might be collected for utilisation or analysis or vented [10, 37, 38].

2.2.2 Pyrolysis conditions and yields

Carbonisation has been used for centuries to convert lignocellulosic biomass into charcoal, a solid with high carbon content. In principle it is a very similar process to pyrolysis which produces three products which are utilised char, oil and gas although the oil or the char is usually the priority product from pyrolysis [10, 26].

Table 2.1 outlines three pyrolysis technologies, slow or conventional pyrolysis, fast pyrolysis and flash pyrolysis. Slow pyrolysis much like carbonisation comprises relatively slow heating rates and long residence times and favours the production of solid products although moderate gas yields are also observed. Fast pyrolysis is designed to maximise the yield of liquid products and uses high heating rates and short residence times with the aim of reducing secondary reactions of volatile gases. Flash pyrolysis usually aims to produce gaseous hydrocarbon products, utilising extremely short residence times and rapid heating rates generally linked with raised temperatures to achieve this. These are not the only pyrolysis processes possible but they helpfully describe how variation in process conditions can be used to direct the pyrolysis products [27, 29, 30].

The conditions which can be achieved during pyrolysis are highly dependent on the equipment which is being used. There are a wide range of reactor designs which encompass gasification, pyrolysis and combustion and each has its own advantages or disadvantages for each purpose. The main reactors which are currently used for pyrolysis are bubbling fluidised bed (BFB), circulating fluidised bed (CFB), rotating cone, screw kiln, auger, ablative and fixed bed. Each design may also be modified both in scale and function to optimise the usefulness of the technology [26].

Table 2.1: The effect of changing conditions on the yield of pyrolysis products [26, 27, 29, 30].

Pyrolysis technology	Conditions			Product yields		
	Residence time	Heating rate	Temperature (°C)	Char (%)	Bio-oil (%)	Gases (%)
Slow / Conventional	5-30 min	<50 °C min^{-1}	400-600	<35	<30	<40
Fast pyrolysis	<5 s	~1000 °C s^{-1}	400-600	<25	<75	<20
Flash pyrolysis	<0.1 s	~1000 °C s^{-1}	650-900	<20	<20	<70

The differences in reactor design have implications on the conditions to which the pyrolysis material is exposed during pyrolysis. The major variation is the method of heat application (friction, conduction, convection and radiative) which often directly relates to the rate of heat transfer. The reactor type usually also affects the size distribution of material which can be used for pyrolysis as well as the residence time for the pyrolysis products such as char and vapour before these are removed from the effect of high temperature zones within the reactor. There are also implications with regards to separation of particular pyrolysis products. With biomass pyrolysis, for example, catalytically active species in the char material can enhance secondary reactions with the volatiles which may lead to an increased formation of coke rather than other more desirable products. The reactor design is also likely to have implications with regards to whether batch or continuous feed is possible with some designs more suitable for scale-up than others. In general, the greater the pyrolysis heating rate that is required, the more advanced the technology which is needed to rapidly deliver the thermal energy to the pyrolysis material. This in turn can have ramifications on the cost of the pyrolysis process [27, 29, 30, 38, 39].

The term lignocellulosic biomass can include a wide variety of materials with each composed of a number of constituents. Guedes et al. [40] list 162 types studied during biomass pyrolysis experiments which include plant matter such as leaves, bark, trunk wood, fruit derives material, shells/husks, straws/grasses and refuse derived wood. The most commonly examined examples in literature were rice husks, palm shell, jatropha curcas cake, rapeseed and pine wood with these dry fibrous materials being readily available in many parts of the world and amongst the most suitable for pyrolysis [40]. Regardless of the biomass material the major constituents are water, extractives, hemicellulose, cellulose, lignin and inorganic species (which are often associated with ash deposits). Variations in the proportions of these constituents accounts for the suitability of a particular material for use with pyrolysis as well as the yield and the characteristics of the products [38]. In general bio-oil yields are best for woody biomass followed by energy crops and then agricultural residues [29]. Van Loo et al. [10] compared thermogravimetric analysis of four woody biomass samples (spruce, birch, beech and acacia). These showed a similar trend for devolatilisation, however there was variation in the amount of hemicellulose and cellulose which led to differences in the devolatilisation profile. Hard woods contain a greater proportion of hemicellulose than softwoods although for an average dry wood sample, hemicellulose is likely to account for 20-35 wt.%,

cellulose for 40-45 wt.% and lignin 15-30 wt.% [10, 41]. Bridgwater et al. [27] also highlight that different biomass feedstocks will lead to a variation in the organic yield from pyrolysis at a specific temperature.

For any biomass sample as well as the intrinsic composition, there are also a number of key process parameter which will have a significant effect on the yield and selectivity of the pyrolysis products. The main factors which are discussed in literature are heating rate, residence time, pyrolysis temperature, particle size, reactor type and the interactions of ash/char with pyrolysis vapours [27, 30, 40].

2.2.2.1 Heating rate

Heating rate is a key property for the production of high yields of bio-oil. The aim is to increase the temperature of a sample from the resting temperature where the material is stable through to the temperature at which reactions which favour liquid compounds are most favoured whilst spending minimal time at intermediate temperatures where char formation reactions are operating favourably. The resulting vapours then required stabilising as rapidly as possible to inhibit secondary reactions which may lead to further coke formation. This is usually achieved by removal of the vapours away from the heat source. During pyrolysis, the processes which are happening such as heat transfer, mass transfer, chemical reactions and phase change are very rapid, in the order of seconds or below. Rapid heating rates introduce control over these fast processes [27]. As well as rapid heating of a reactor it is also necessary to introduce rapid heat transfer from the reactor to the sample itself. One method to achieve this is to use small particle sizes to minimise the time necessary for the heat to conduct through the particle [40]. There are also reactor designs which are more suited to rapid heat transfer such as ablative heating, and fluidised bed reactors which minimise the time taken to raise the temperature of a sample by heating transfer using solid-solid contact rather than relying on heat transfer through gas-solid contact which is a much slower process. Fast pyrolysis uses heating rates in the region of $10°Cs^{-1}$ to $1000°Cs^{-1}$ to achieve high bio-oil volumes of around 65 wt.% to 80 wt% (dry basis). For biomass these usually use temperatures of around 500°C or sometimes marginally higher for different feedstocks [29]. Guedes et al. [40] highlight that whilst heating rate often leads to a significant increase in oil yield this effect often became negligible at high heating rates which varied depending on feedstock. They also found that for some studies such as those of Morali et al. [42] and Sensoz et al. [43], oil yield remained relatively constant or reduced as heating rates increased. This shows that the effect of changing heating rate is

not an independent factor and may lead to the introduction or inhibition of secondary processes.

Biomass is a poor conductor of heat which means that particle size reduction is associated with increased heat transfer in fluidised bed reactors leading to increased oil yields. The same effect is not as clearly observed in fixed bed reactors where heat transfer to particles is reduced by low gas-solid heat transfer rates. In this case Bridgwater et al. [44] recommend particle sizes of 2 mm or lower in a fixed bed reactor. Research by Akhtar et al. [45] challenge this statement and indicate that particle sizes which gave the maximum oil yields for one feedstock could vary widely from another. In general, particle size of between 0.2-2 mm appear to give the highest oil yields from a list of feedstocks examined by Guedes et al. and Akhtar et al. but it appears to depend both upon the reactor design and the biomass sample. Particle sizes outside this range were also observed to be optimal in some cases. In general, there is agreement that reduction of particle size is beneficial to oil yields however this is limited for each feedstock and reactor design. Reducing size below a certain point may be detrimental to oil yields and increases the energy in milling which will also reduce overall efficiency [40, 45].

2.2.2.2 Vapour Residence time

Vapour residence time becomes a critical factor with regards to increasing oil yields. In general, residence time reflects the purpose for which pyrolysis is being utilised with low heating rates and long residence times leading to increased solid carbonaceous material whilst high heating rates and short residence times lead to high oil yield [29]. Conditions require optimising to produce high oil yields which are also high quality. To maximise oil yields, biomass must be heated for a long enough period to allow for decomposition reactions to be completed, however the longer vapours are held at pyrolysis temperatures and conditions the more susceptible they are to secondary reactions such as thermal cracking, repolymerisation, recondensation and char formation leading to increased char and gas yields [38]. In this way a very short residence time may reduce the loss of vapours to secondary reactions but may not allow for complete biomass particle decomposition [45]. Bridgwater et al. [27] recommend very short hot zone residence times (<2s) to discourage secondary reactions however Akhtar et al. [45] highlight that whilst this leads to high oil yields it is not the optimal conditions for increasing bio-oil quality. Their consideration is that longer residence time at elevated temperatures may lead to loss of oil yield through secondary reactions, however, it also allows for deoxygenation of bio-oils which is not achievable at extremely short residence

times. In an ideal reactor the residence time, particle size, temperature of pyrolysis should be optimised to both to give elevated oil yields as well as oils with beneficial characteristics. Use of inert gases to remove tar compounds away from the pyrolysis zone are viewed as beneficial to encourage these high oil yield and high quality oils. Guedes et al. [40] examine the use of nitrogen as a low cost and readily available inert gas for pyrolysis. They found that in many cases the increase in flow rate of the inert gas increased oil yields with greater removal of vapours away from the high temperature pyrolysis zone leading to reduction in secondary reactions leading to coke or gas formation. This effect was limited, however, with modest increases in inert gas flow improving yield but larger increases leading to no quantifiable increase in yield. Some studies showed that if inert gas flow was too high it could lead to reduction in oil yields by hindering product condensation and forcing biomass particles out of the pyrolysis zone of the reactor [46, 47].

2.2.2.3 Pyrolysis temperature

The temperature at which pyrolysis is most effective for production of bio-oil is dependent on the feedstock which is being utilised. In general, the optimum temperature is approximately 500°C [27, 29]. Table 2.2 gives the optimum pyrolysis temperatures in order to maximise liquid yield from a wide range of biomass sources examined by Guedes et al. [40]. The range is from 450°C with rice husks through to 600°C with olive bagasse and a mean of 486°C for this range of samples. Once these temperatures are exceeded the liquid yield may remain steady and then start to decrease as temperatures increase further.

Table 2.2: Various biomass resources evaluated by Guedes et al. [40] showing the variation in the temperature of maximum liquid yield and the maximum yield obtained during different literature studies.

Biomass sample	Optimum temperature (°C)	Maximum liquid yield (wt.%)	Literature reference
Rice Husk	450	70	[48]
Palm waste	500	72	[49]
Neem de-oiled cake	400	40	[50]
Olive Bagasse	600	46	[51]
Sugar cane bagasse	475	56	[52]
Cassava rhizome	472	63	[53]
Jatropha seed shell cake	470	48	[54]
Pistachio shell	550	21	[55]
Poplar	455	69	[56]

The temperature needs to be balanced to meet several factors, it needs to be high enough to cause sufficient decomposition of the material however as the temperature increases, secondary reactions are encouraged leading to loss of liquid yield with increased coke and non-condensing gases formed [45]. It should also be considered that as temperatures rise further they may also encourage deoxygenation reactions which may be beneficial to the quality of the oil although they will likely also lead to reductions in yield.

2.2.2.4 Char and ash metal species

The char material which is the primary solid product from pyrolysis contains a range of inorganic species which would be present in an ash formed during combustion of a material and these species are concentrated by removal of volatile matter from the biomass material. These species include alkali and alkaline-earth metals such as potassium, sodium, calcium and magnesium which are key nutrients obtained by plants from soil and water where they are valuable to the development of healthy plants. These species are actively used by the plants for key processes and reactions and as such are often accumulated in particular parts of a plant such as the leaves or fruit. In this way these species can, to a limited extent, be avoided by careful harvesting of biomass in a particular season, through the selection of parts of the plant with low levels of these species such as trunk wood or through biomass pre-treatment such as washing [10, 57, 58]. The most active of the species are potassium and calcium and these can accumulate in the char obtained during pyrolysis and can lead to secondary vapour reactions with the char acting as a natural catalyst [27, 38]. These reactions usually lead to increased yields of both coke deposition as well as cracking to non-condensing gases. It is of primary importance to limit the exposure of the vapours to the char to reduce these secondary reactions. The fine char species are also able to pass into oil collection systems and thereby introduce further instability into bio-oils. Beyond introducing instability into the bio-oil, these fine char particles may be problematic for use of the oil with increased corrosion and deposition on engines a common effect of these inorganic species. Hot vapour filtration is a potential method to reduce the quantity of fine char material in a bio-oil but it is has only limited efficacy [27]. Inorganic species such as transition metals, alkali and alkaline-earth metals may also detrimentally impact catalyst used for bio-oil upgrading with deactivation caused by clogging of pores and reduction of surface area [59].

2.2.3 Biomass pyrolysis

The three major constituents of lignocellulosic biomass which are decomposed during pyrolysis and give rise to bio-oil yields and compositions are cellulose, hemicellulose and lignin. The decomposition of each of the constituents gives rise to different compounds and it is therefore important to understand the reactions which are occurring so that upgrading strategies can be applied to the compounds which are forming during biomass devolatilisation.
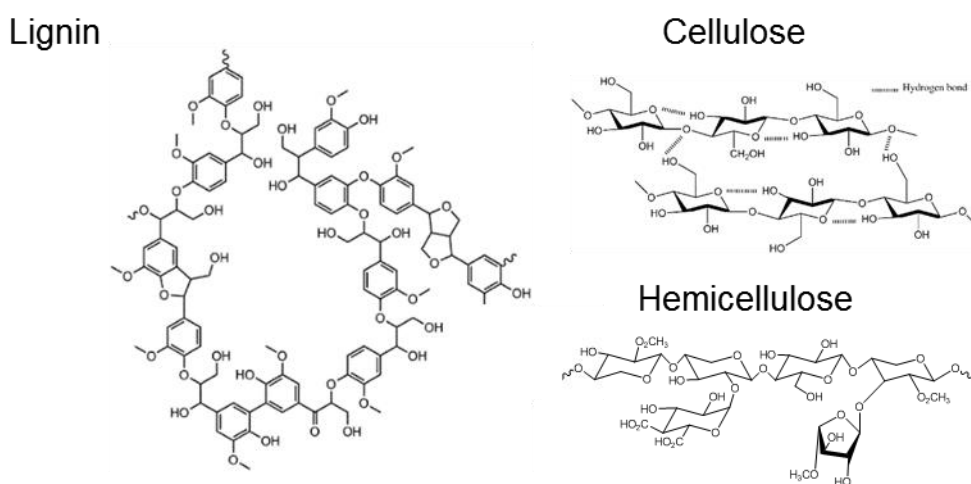
Figure 2.3: Example structures for cellulose, hemicellulose and lignin given by Talmadge et al. [41].

Figure 2.3 shows three example structures of cellulose, hemicellulose and lignin which are given by Talmadge et al. [41] These components of lignocellulosic biomass are made up of repeating and recognisable building blocks however the final structure will contain a high degree of variability. Cellulose is a crystalline polymer with variation presenting itself chiefly in terms of polymer chain length. Hemicellulose is very similar to cellulose in terms of chemical formula, being formed from sugar subunits, however unlike cellulose it is amorphous and branched. Lignin is also made up of repeated building blocks although not sugars as is the case with cellulose and hemicellulose and is an amorphous polymeric material which includes an extremely high level of structural complexity [58, 60].

The high proportion of oxygen atoms in the biomass material is very clear in Figure 2.3 and this oxygen content is particularly for cellulose and hemicellulose. The composition of the bio-oil, formed by pyrolysis, will be highly dependent on the composition of the biomass material which is used but will also be affected by the reaction pathways which predominate the pyrolysis

process. These pathways are different for the cellulose, hemicellulose and lignin [41].

Table 2.3 shows the variation in lignocellulosic content that was measured for a range of different biomass samples. The hardwoods and softwoods contained a greater proportion of cellulose than either the hazelnut shell or the wheat straw. There was some variation between the mean softwood and the mean hardwood analysed however this variation was lower than that measured between a representative hardwood, beech, and the mean hardwood. Wheat straw had a much lower lignin content than the wood and the shell samples whilst the shell sample had the lowest cellulose content.

Table 2.3: Variations in lignocellulosic content for different biomass samples measured by Demirbas et al. [61].

	Biomass content (wt.%)		
	Cellulose	Hemicellulose	Lignin
Spruce wood	51	21	28
Softwood (Mean)	46	24	28
Beech wood	46	32	22
Hardwood (Mean)	45	31	43
Hazelnut shell	26	30	43
Wheat straw	39	29	19

2.2.3.1   Cellulose

Cellulose is the simplest of the three major structural components of lignocellulosic biomass. It consists of single glucose units linked together through a glucosidic bond to form a cellobiose unit (two glucose units in opposite orientation). Many thousand cellobiose units (>10,000) combine end-to-end to produce a single long cellulose polymer (see Figure 2.4) [32, 41, 62].
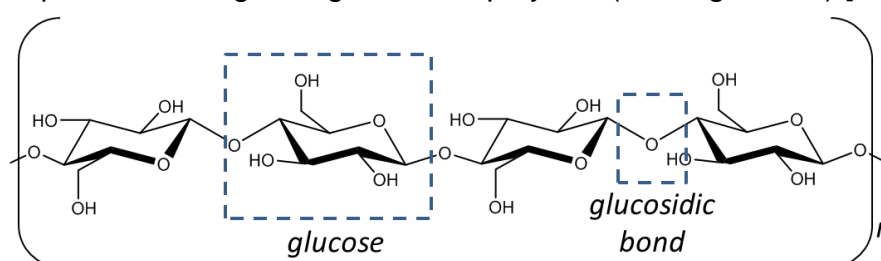
Figure 2.4: Diagram of glucose units linked together to form a linear polymer chain which is cellulose [33].

These long cellulose polymers can then form tightly bound bundles using intermolecular forces such as hydrogen bonding to form microfibrils suitable for plant cell walls [33].

Pyrolysis of cellulose is a complex process which has been modelled by a number of different researchers with varying levels of complexity [63-66]. The basic methodologies are similar but later models account for more of the products of pyrolysis. Figure 2.5 shows a simplified reaction scheme for the pyrolysis of cellulose similar to that proposed by Piskorz et al. [65, 67, 68]. During heating of cellulose, the glucosidic bond is the point at which cleavage is most readily achieved. The initial stages of pyrolysis of cellulose involves the breaking of the long cellulose polymer into much shorter sections. This reduction in the degree of polymerisation (DP) is not accompanied by the release of volatiles but is in competition with a low temperature char formation reaction which produces water and carbon dioxide gas. The low molecular weight cellulose units are able to follow two main reaction pathways. One pathway involves the fragmentation of the cellulose molecular ring to produce hydroxyacetaldehyde and other low molecular weight compounds. The other main pathway involves a breaking and reformation of the glucosidic bond (transglucosylation). This pathway is responsible for the formation of laevoglucose type compounds as well as other sugar derivatives. These products may undergo secondary reactions such as char formation or vaporisation reactions if not removed from the pyrolysis environment [67].
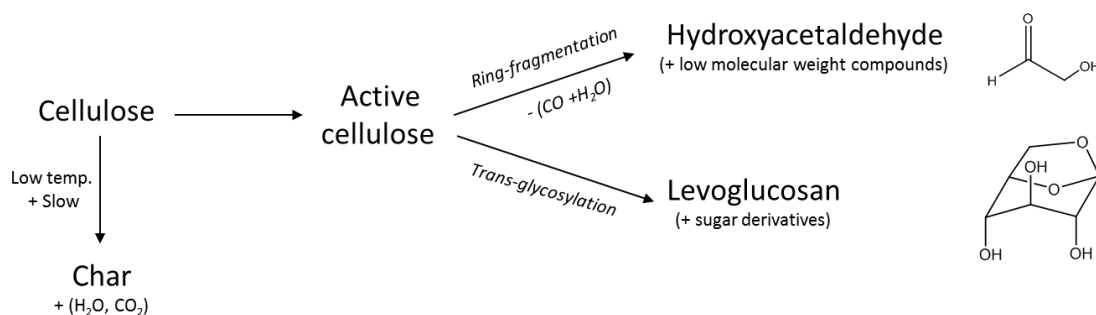
Figure 2.5: Simple cellulose pyrolysis pathway similar to that proposed by Piskorz et al. [65, 67, 68].

Cellulose begins to decompose at around 300°C and decomposition is completed before around 430°C although this will depend on both the structure of the cellulose as well as interactions with hemicellulose and lignin [62, 69].

2.2.3.2   Hemicellulose

Hemicellulose is a polymeric material which is composed from a number of different sugar molecules in such a way as to produce short strands with branching in the order of around 150-200 sugar units (Figure 2.6). The backbone of the hemicellulose molecule is commonly composed of xylobiose which is a molecule composed from two xylose molecules (Figure 2.7). The main constituent sugars which make up hemicellulose are glucose, galactose, mannose, xylose, arabinose and glucuronic acid (Figure 2.8) which contrasts to cellulose which is composed of repeated units of glucose alone [32, 41, 62].
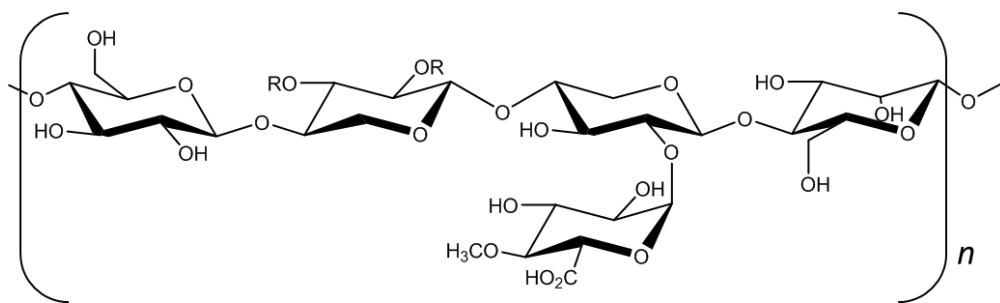
Figure 2.6: Diagram of a generic hemicellulose molecule – a branched strand.

Xylobiose
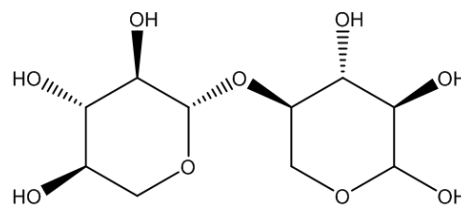
Figure 2.7: The polysaccharide xylobiose, formed from two xylose saccharide molecules, is the major constituent of the hemicellulose backbone.

glucose   galactose   mannose

xylose   arabinose   glucuronic acid
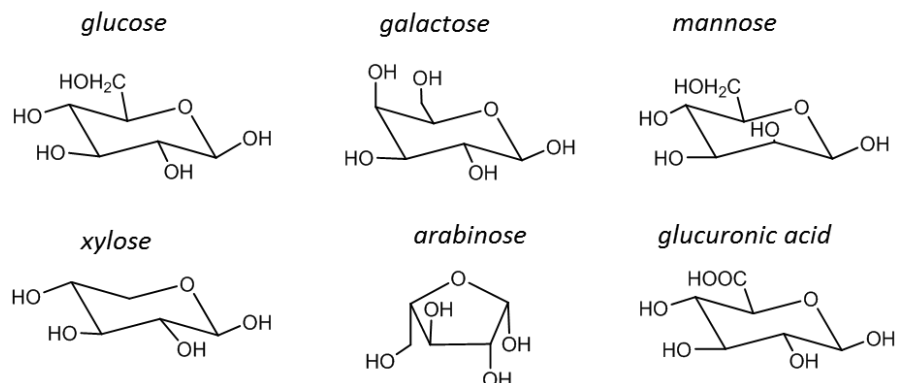
Figure 2.8: Monosaccharides of which hemicellulose is composed.

Decomposition of hemicellulose will often occur between 200°C and 260°C which is lower than that for cellulose. The varied structure of hemicellulose makes study into decomposition of the material more challenging than for cellulose with methods often focusing on model saccharide decomposition [67, 70, 71] although experimental studies have also been completed [72]. Patwardhan et al. [72] studied the decomposition of hemicellulose which had been extracted from switchgrass and compared the resulting products with those from cellulose. They found three major classes of compounds from the hemicellulose. The first class of compounds were low molecular weight compounds, containing carbon, hydrogen and oxygen, mostly in the molecular size range C_1-C_3. These compounds included, CO, CO_2, formic acid, acetic acid, acetaldehyde and acetol. These low molecular weight compounds are likely to have been formed by ring scission as was the case with the low molecular weight compounds produced from cellulose. The second group of compounds included furan and pyran rings which are likely to have been formed by a combination of depolymerisation, dehydration and rearrangement reactions. The third group included anhydrosugars which would likely have been formed through depolymerisation and rearrangement pathways although in contrast to cellulose this did not lead to levoglucosan as a major product as was the case during rearrangement of cellulose derived feedstocks. Competition would be present for each of these reaction pathways and char formation was also higher than was observed when cellulose was the feedstock [33, 67, 72]. Hemicellulose composition can vary significantly between feedstock and this variation leads to differences in pyrolysis products observed although common products such as anhydrosugars and furfuran are observed [33].

2.2.3.3 Lignin

Lignin is an aromatic framework which adds rigidity to biomass and is therefore present in different proportions depending on the purpose of a plant material. The three-dimensional lignin framework is mainly composed of three basic compounds, p-coumaryl alcohol, coniferyl alcohol and sinapyl alcohol (see Figure 2.9). Each of these compounds contains an aromatic ring, a propyl alcohol group and a phenyl group which can be linked together at a number of different points which leads to very complex structures. The type of compound which makes up the lignin can vary substantially depending on the type of biomass material with grasses, softwoods and hardwoods containing widely differing proportions of the three main compounds [32, 33]. The structure of

these building block units often referred to as phenylpropane units (ppu) contains some oxygen however this is significantly lower as a proportion than for the sugar compounds which compose cellulose and hemicellulose.
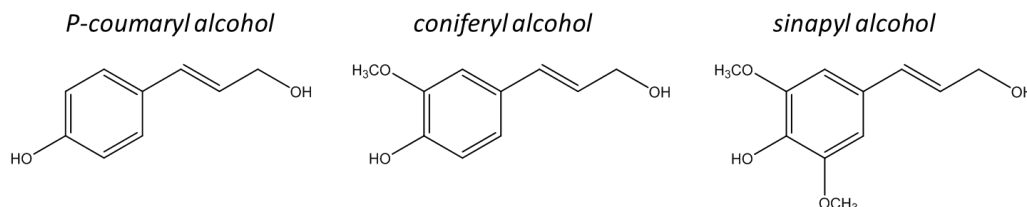
Figure 2.9: Lignin is a complex structure constructed from three primary molecules, p-coumaryl alcohol, coniferyl alcohol and sinapyl alcohol [32, 33, 62].

The structure of lignin is more complex than that of cellulose and hemicellulose and decomposition occurs over a greater temperature range. Figure 2.10 shows a number of processes which have been observed to occur in pyrolysis of lignin by Anca-Couce [67] with the temperatures or temperature ranges at which they occur detailed.
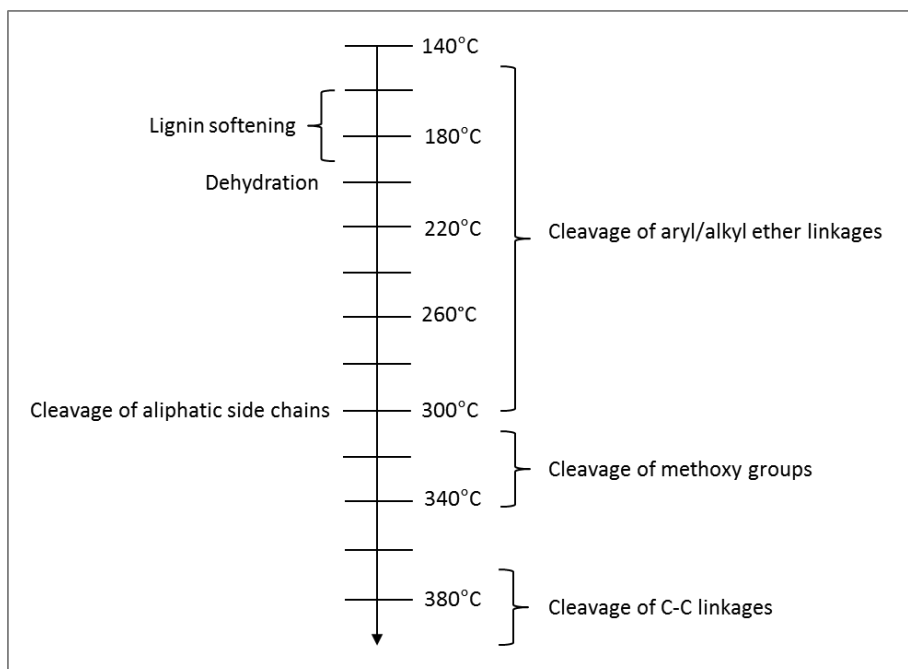
Figure 2.10: Temperatures at which lignin decomposition processes occur during thermal degradation [67].

Although the structure of lignin is very complex and varied, there are three main types of bonding between the basic lignin subunits. 60-70% of the linkages are ether (C-O-C) bonds which break at relatively low temperatures and lead to phenolic products [73] and 30-40% are carbon-carbon bonds which require a much greater energy input to break. A small proportion may be ester bonds, but this tends to be constrained to herbaceous lignin material. Side chains such as methoxy groups and aliphatic side chains can also be broken and these are broken at temperatures intermediate to those required to break the two major unit linkage bonds [33]. Zhou et al. [74] have studied the decomposition of biomass and proposed a mechanism to explain the general process which leads to pyrolysis products (Figure 2.11). As with cellulose and hemicellulose the initial process is the breaking up of the matrix into smaller units often referred to as pyrolytic lignin [75]. In the case of lignin there is also an intermediate process where the rigid framework becomes softened and liquefied prior to the cleavage reactions. The cleavage of lignin is considered to be dominated by free radical reaction mechanisms which can explain the presence of a number of lignin pyrolysis products [58, 76].
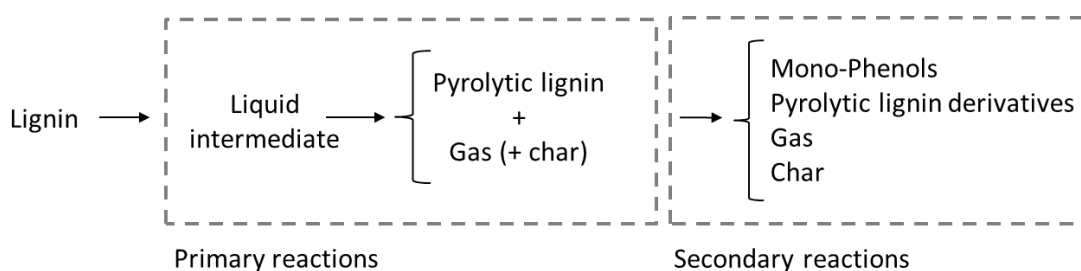
Figure 2.11: Lignin decomposition mechanism proposed by Zhou et al. [67, 74].

2.2.3.4 Combined lignocellulosic pyrolysis

When biomass undergoes pyrolysis the three components are not reacting in isolation and this adds levels of complexity to the reaction pathways which are followed [77]. Whilst the three components are produced over different temperature ranges there is significant overlap between volatile release from cellulose, hemicellulose and lignin allowing for interactions of the vapours (see Figure 2.12).
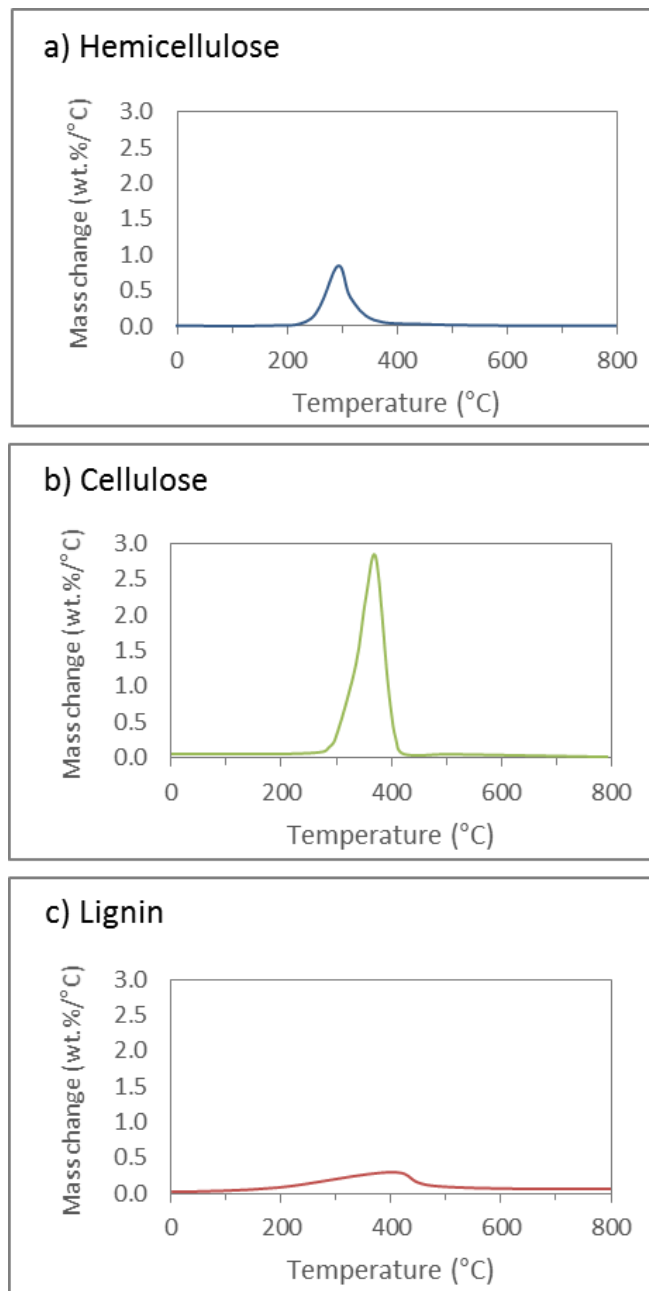
Figure 2.12: Temperature ranges for devolatilisation of the three main constituents of lignocellulosic biomass. a) Hemicellulose, b) cellulose and c) lignin [30, 62, 67, 69, 78].

Collard et al. [78] explain that both chemical interactions and physical effects such as mass and heat transfer are critical during pyrolysis. This ensures that whilst individual decomposition of the three components of lignocellulosic biomass may be relatively well understood it is still challenging to account for the actual yield. Hosoya et al. [79, 80] examined the differences in the compounds which were measured when comparing pyrolysis of biomass components separately or together under the same conditions. They found that

addition of cellulose to lignin was particularly influential with guaiacol type compounds removed with the formation of catechols, cresols and phenols instead. These conversions appear to be due to hydrogen donation reactions between cellulose and lignin. There were also effects observed on sugar derived compounds such as levoglucosan with stabilisation of C-H bonds by the presence of π-electron densities which are prevalent in lignin derived compounds.
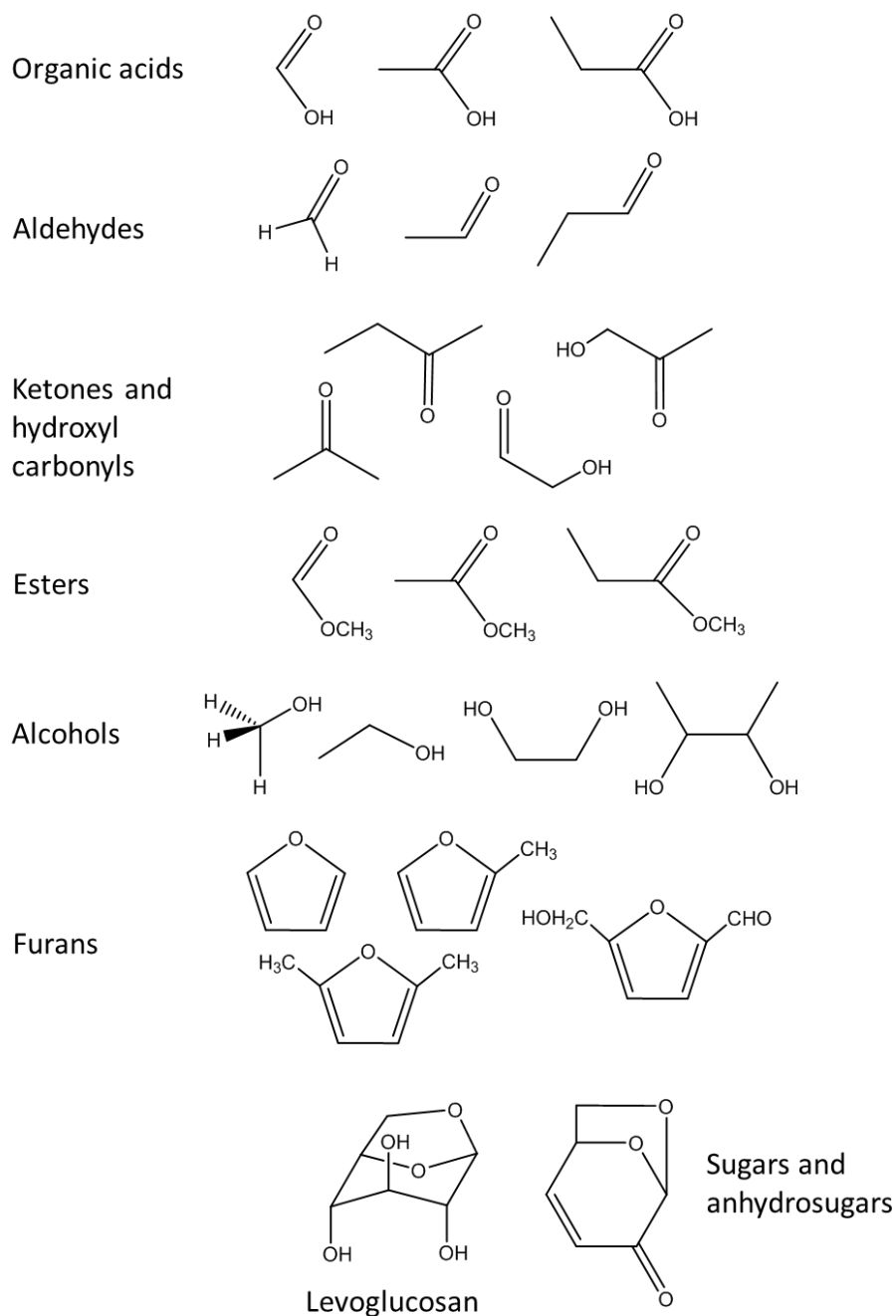
Figure 2.13: Compounds obtained from pyrolysis of cellulose and hemicellulose.

The complex interactions of hemicellulose, cellulose and lignin make it challenging to predict the precise outcome of pyrolysis, by examining the constituent products. Despite the multitude of reaction pathways and physical interactions it is still possible to identify a wide range of compounds which are present in bio-oil and to understand the component form which they were derived in many cases. Figure 2.13 shows a number of compounds typically observed in bio-oils which Talmadge et al. [41] identify as derived from cellulose and hemicellulose. These are categorised into a number of functional groups with oxygen accounting for a vast majority of the functionality and a high proportion of the compound molecular mass.
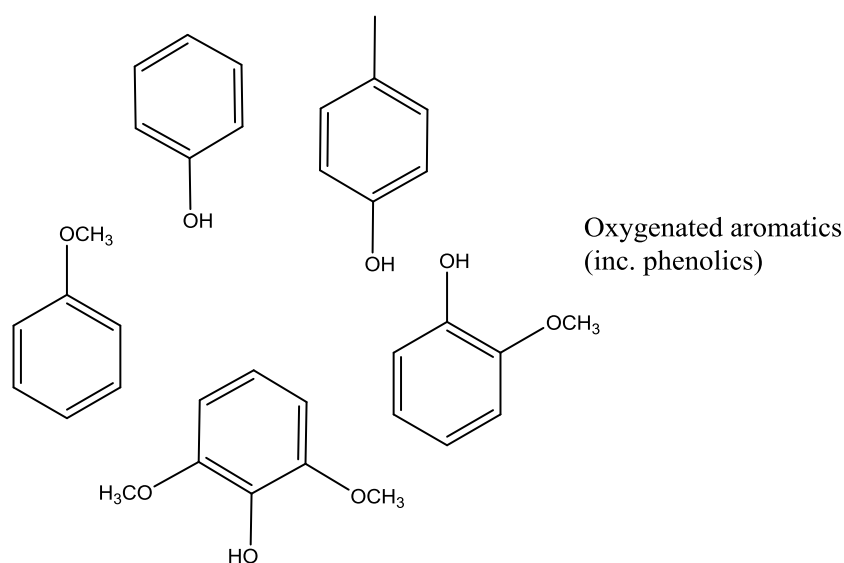
Figure 2.14: Compounds derived from pyrolysis of lignin (41).

Figure 2.14 shows some of the products which are regularly observed as derived from lignin during pyrolysis of biomass to bio-oils [41]. These also contain oxygenated functional groups and all the compounds listed contain aromatic nature although fragmentation and loss of side chains from lignin is likely to account for non-aromatic compounds to some extent [33, 67].

Wang et al. [62] made a list of bio-oil compounds which are typically present in bio-oil (see Table 2.4) drawing on several studies [81-84] which used a range of biomass materials and varying pyrolysis and analysis methodologies to determine the oil composition. The compounds which were determined contain a range of functional groups which often contained oxygen. These compounds vary significantly. Variations in compounds include, molecular size, pH range, aromatic nature and boiling point. Although these are commonly observed

compounds the number of compounds which are present can be extremely large (many hundreds of compounds) [33].

Table 2.4: Compounds observed during pyrolysis of bio-oil, adapted from Wang et al. [62].

Compounds	Standard compounds
Acids	Acetic acid, formic acid, propanoic acid, methyl-1-propanoic acid, butanoic acid, methyl butanoic acid, pentanoic acid, glycolic acid
Esters	Methyl acetate, methyl formate, methyl propionate, butyrolactone, dimethyl pentanedioate
Alcohols	Butane-2,3-diol, methanol, ethanol, 2-propene-1-ol, isobutanol, ethylene glycol
Ketones	Acetone, 2-butanone, 2,3-butanedione, cyclopentanone, methyl-cyclopentanone, 2-pentamone, cyclohexanone, 3-hexanone, methylcyclohexanone, cyclopentanedione
Aldehydes	2-butenal, glyoxal, formaldehyde, acetaldehyde, 2-propenal, 2-methyl-2-butenal, pentenal, benzaldehyde
Other oxygenates	Glycolaldehyde, 1-hydroxyl-2-propanone, methyl-2-oxopropanoate, 1-hydroxyl-2-butanone
Sugar derivatives	Levoglucosan
	Glucose, fructose, D-xylose, D-arabinose
Furans (+ derivatives)	Furan, methylfuran, dimethyl-furan
	Furfural
	2-furanone, 4-methyl-2-furanone, furfuryl alcohol, 2-acetalfuran,
Alkenes and alkanes	Hexane, methyl-propene, alkylated cyclohexene
Single unit aromatics	Toluene, xylene, ethylbenzene, naphthalene
Phenols	Phenol, methyl-phenol, dimethyl-phenol
Anisoles	Anisole, methyl-anisole, ethyl-anisole
Catechols	Catechol, methyl-catechol, ethylcatechol, methoxycatechol
Guaiacols	Guaiacol, methyl-guiaicol, ethyl-guiaicol eugenol
Syringols	Syringol, methyl-syringol, ethyl-syringol, propyl-syringol, 4-propenyl-syringol
Others	Vanillin, vanillic acid, sinapaldehyde, syringaldehyde, acetosyringone
High-molecular-weight	Dimer, trimer and oligomer of cellulose, hemicellulose and lignin pyrolysis products

2.3 Pyrolysis of Plastics

Pyrolysis is a method which may be used to convert waste polymers into useful or valuable products. This allows for efficient use of materials as well as energy [85, 86]. In the UK there are seven categories which are used to identify plastics (see Table 2.5) [87].

Table 2.5: Categories used for identification of common plastics [87].

PETE 1	PET	polyethylene terephthalate
HDPE 2	HDPE	high-density polyethylene
V 3	PVC	polyvinyl chloride
LDPE 4	LDPE	low-density polyethylene
PP 5	PP	polypropylene
PS 6	PS	polystyrene
OTHER 7	Other	Other plastic types

2.3.1 Polyethylene

HDPE and LDPE are both polyethylene (PE) polymers (see Figure 2.15) with the difference consisting in the different amounts of branching and crosslinking which is present. LDPE has the greater degree of branching and crosslinking which hinders the polymer chains from packing as tightly together therefore leading to a lower density material. These differences also change other physical characteristics of the polymeric material.
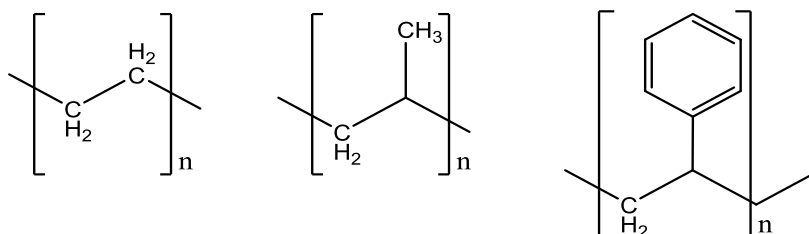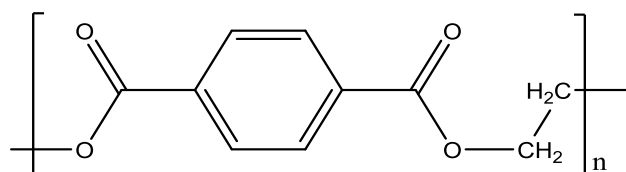
Figure 2.15: Chemical structure for polyethylene, polypropylene, polystyrene and polyethylene terephthalate.

Williams and Williams [88] examined pyrolysis of LDPE using a fluidised bed reactor for temperatures between 500°C and 700°C. At 500°C the gas yield was 10.8 wt.% and the oil (oil and wax) yield 89.2 wt.%, when the temperature was increased the gas yield increased to 24.2 wt.% at 600°C and 71.4 wt.% at

700 °C. This was accompanied by a comparable decrease in the oil yield. The gas composition was mainly alkene gases (ethene, propene and butene) although lesser quantities of hydrogen, and alkanes (ethane, propane, butane) were also measured. Increasing temperature increased the proportion of the hydrocarbon gases especially the alkenes. Gas chromatography analysis of the liquid showed a clear peak (triplet) for each molecular size composed of an alkene peak flanked by an alkadiene peak and an n-alkane peak.

Research by Sogancioglu et al. [89] examining recycled HPDE and LDPE found similar liquid yields to Williams et al. [90] at 500°C. As they increased the reactor temperature there was a more limited shift from liquid products to gas products although the liquid yield was at the highest at 300°C. As the temperature was increased from 300-700°C the yield of char also decreased from 2.24 - 2.14% in the HDPE sample and from 10.12 - 6.44% in the LDPE sample. These are recycled materials and the char is much lower in the pyrolysis products of virgin polymers [85].

Research by Aguado et al. [91] attempted to establish a kinetic mechanism for HDPE pyrolysis using a conical spouted bed reactor and proposed the scheme outlined in Figure 2.16. Initially HDPE is decomposed to form waxes which can then undergo secondary reactions to account for three products observed from HDPE pyrolysis, liquids, gases and aromatics. The aromatics may then continue to react to produce char. Williams et al. [90] did not observe aromatic compounds until temperatures were 600°C or above with increasing aromatic yield as temperatures increased further.
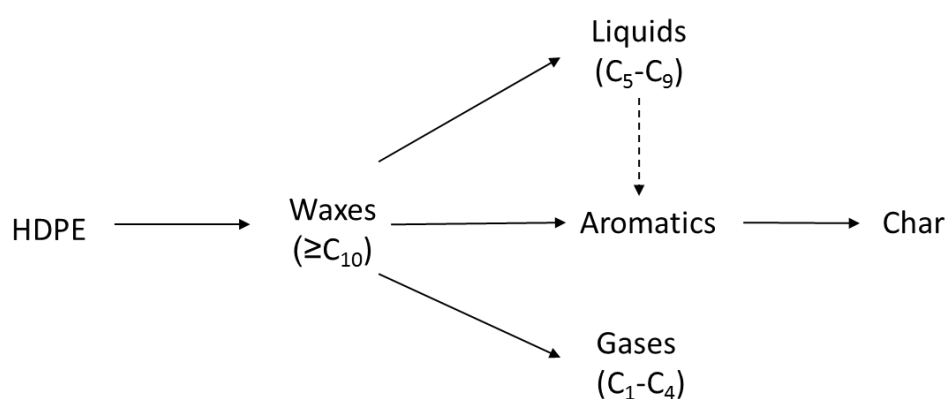
Figure 2.16: Kinetic scheme proposed by Aguado et al. [91] to account for HDPE pyrolysis, dotted arrows represent other potential routes proposed by Onwudili et al. [92] and Westerhout et al. [93]

2.3.2 Polypropylene

Encinar et al. [85] analysed the pyrolysis of virgin PP in a nitrogen atmosphere with heating of the material from room temperature through to 800°C with heating rates ranging from 5°Cmin^{-1} to 20°Cmin^{-1}. The yield of pyrolysis products at the intermediate rate (10°Cmin^{-1}) gave a char at 0.1 wt.%, liquid at 82.7 wt.% and gas at 17.2 wt.%. The gaseous products were mainly alkenes and alkanes with a greater selectivity towards alkene gases though not as much so as for PE this was also observed by Williams et al. [90]. Demirbas [94] analysed pyrolysis of PP as part of a study into pyrolysis of municipal waste between temperatures of 400° and 600°C. At 400°C the oil products were mostly composed of linear hydrocarbons (alkane – 30.4 wt.%, alkene – 44.7 wt.%) with some aromatic compounds (naphthenes – 21.5 wt.%, aromatics – 1.4 wt.%). At 600°C the linear hydrocarbon yield has decreased slightly (alkane – 29.6 wt.%, alkene – 35.5 wt.%) with an increase in aromatic compounds (naphthenes – 23.5 wt.%, aromatics – 10.2 wt.%). Both PE and PP are understood to decompose via random chain scission mechanisms which lead to a wide range of products (gas and liquid) [94].

2.3.3 Polystyrene

By contrast PS is understood to decompose both by random chain scission as well as end-chain scission [94]. Onwudili et al. [92] analysed pyrolysis of PS in a closed batch reactor over a range of temperatures. At 300°C there was little degradation of the starting material present whereas at 350°C all of the sample was degraded to a liquid. GC analysis of the oil determined that all the compounds were aromatic in nature or linear compounds were below detection limits. The compounds included, toluene, xylene, benzene, ethylbenzene as well as further alkylated benzene and naphthalene. There was no observance of the monomer styrene as may be expected from a sample of polystyrene however it is probable than the unstable styrene molecule was hydrogenated to ethyl benzene in the closed batch reactor which is both sealed and pressurised which is not the case for many pyrolysis reactors.

Pyrolysis of PS by Demirbas [94] at 400°C determined styrene yield as 58.0 wt.%, C_2-C_4 hydrocarbons at 3.4 wt.%, C_5-C_8 hydrocarbons at 19 wt.%, methane at 7.5 wt.%, toluene at 6.8 wt.% and benzene at 5.3 wt.%. Increasing temperature to 475°C increased the styrene yield slightly but beyond this temperature it decreased rapidly again. The C_5-C_8 compounds decreased as temperatures were raised above 375°C whereas the C_2-C_4 gaseous compound

increased over the same temperature range. These findings are consistent with the findings of Scott et al. [95] where a monomer yield greater than 75% was obtained from pyrolysis of styrene with aromatic compounds of between 83-88%. This links to findings from Kiran et al. [86] which connected the high liquid yields from pyrolysis of polystyrene with the control obtained through intermolecular forces in contrast to the random scission for PE.

2.3.4 PET

PET as a material is comparable to lignin in that it contains both aromatic rings as well as oxygenated groups. This combination makes pyrolysis both potentially valuable but also challenging. Grause et al. [96] examined using catalytic processes to convert high purity PET into benzene. They show in earlier research [97] that PET starts by cleaving to produce terephthalic acid and other products. In the presence of water this can produce ethylene glycol which can further decompose into carbon dioxide and hydrogen (see Figure 2.17 - a). At higher temperatures PET can undergo intramolecular reactions leading to terephthalic acid and benzoic acid vinyl ester (b). These initial steps are possible without a catalyst however decarboxylation (d) of these products to produce benzene is not efficient without a catalyst such as CaO. Use of high temperatures may be used to drive decarboxylation but this will lead to uncontrolled side reactions and increase gas yield with a reduction in liquid yield [98].
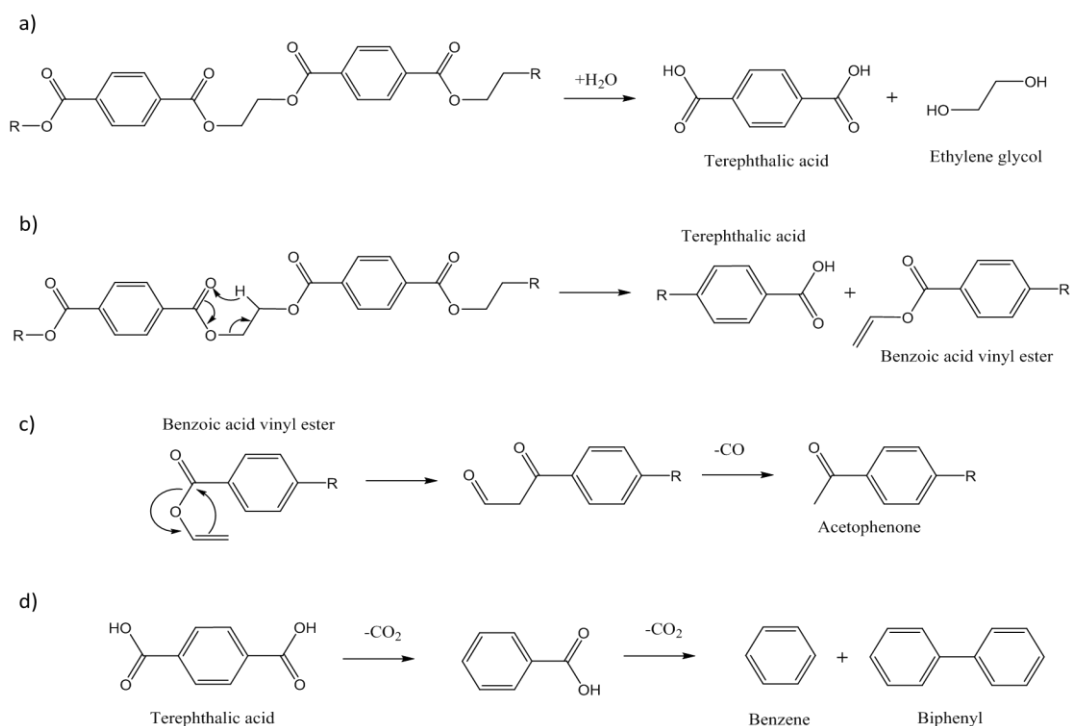
Figure 2.17: Various mechanisms which may feature during thermal pyrolysis of PET [96, 99, 100].

For non-catalytic pyrolysis of PET, the major liquid products are benzoic acid and terephthalic acid. The other products are generally composed of aromatic and aliphatic oxygenated compounds. The gaseous products are mainly carbon dioxide and carbon monoxide [98]. Williams et al. [90] determined the yields of pyrolysis products from PET, with heating rate at 25°Cmin^{-1} to 700°C, with gas at 34.0 wt.% oil at 41.3 wt.% and char at 15.6 wt.%.

2.4 Upgrading of bio-oils

Pyrolysis of biomass can be controlled to a limited degree by utilising process conditions such as heating rate, temperature, inert gas flow etc. However, this only gives limited control by managing the energy available to pyrolysis reactions and by controlling the way in which the products of those reactions interact. This has serious shortcomings when trying to optimise to products of pyrolysis meaning that pyrolysis oils often reflect the composition of the starting material. In biomass this means that bio-oils are highly oxygenated leading to poor properties such as instability and low pH leading to corrosiveness [38, 101].

There are alternative ways to control the pyrolysis process allowing for upgrading [59]. The main pathways for upgrading revolve around catalysis [59] which allows for alternative reaction mechanisms by stabilising intermediate chemical species. The other method is to introduce new chemical species which can react with the compounds in the pyrolysis oil to produce differently composed oils. This approach may coincide with catalytic upgrading or may be used separately. One example of a chemical species being used alongside a catalyst might be hydrodeoxygenation where pressurised H$_2$ gas is used alongside solid catalysts to remove oxygen in the form of water [102]. A catalyst does not always need to be involved as may be the case in co-pyrolysis. Research by Lu et al. [103] compares pyrolysis of two different materials together, in this case PE and biomass, with the material pyrolysed separately. They found that synergistic effects could produce greater oil yields than could be achieved by separate pyrolysis. Li et al. [104] investigated synergistic effects of catalytic co-pyrolysis between cellulose and LDPE and found Improved aromatic selectivity with reduced coke deposition. This contrasts with hydrodeoxygenation where one specific reaction pathway was targeted, in this case complex interactions between catalyst and two different sets of compounds can lead to improvements against separate pyrolysis.

2.4.1 Bio-oil characteristics

The composition of bio-oils can vary highly depending on the composition of feedstocks and the processing conditions. Yet it is important to understand the characteristics which would be expected from a bio-oil so as to ascertain the suitability for utilisation of the oil and to target upgrading to improve the necessary characteristics. Table 2.6 outlines values given by Mortensen et al. [105] which could reasonably be expected for a bio-oil sample with comparison against a typical crude petroleum oil sample.

Table 2.6: Comparison between bio-oil and crude petroleum oil [105].

		Bio-oil	Crude Oil
Moisture	Water [wt%]	15-30	0.1
Acidity	pH	2.8-3.8	-
Density	ρ [kg/l]	1.05-1.25	0.86
Viscosity	$\mu_{50°C}$ [cP]	40-100	180
Energy density	HHV [MJ/kg]	16-19	44
	C [wt%]	55-65	83-86
	O [wt%]	28-40	<1
Elemental composition	H [wt%]	5-7	11-14
	S [wt%]	<0.05	<4
	N [wt%]	<0.4	<1
Ash composition	Ash [wt%]	<0.2	0.1

For some of the properties there is limited variation between values for the two oils yet with others there is a significant difference. The properties of particular note are, moisture, acidity, oxygen content and energy density. For these properties there are two major factors which would need to be corrected to improve the oil characteristics.

The high moisture content increases the pH of bio-oil by diluting the acidic compounds whilst at the same time reducing the viscosity and the energy density [38]. However, the most important factor effecting bio-oil is the high oxygen content which not only reduces energy density but also causes low volatility, low pH and high viscosity, as well as instability and corrosivity which is due to the acidic nature of the oils. The oxygen containing groups include organic acids which have low pH values but also contain groups which will react together at room temperature and pressure which leads to the instability observed during storage. There can also be serious immiscibility issues with existing petroleum infrastructure which is also due to oxygenated compounds in the oil [41]. Reductions in oxygen levels lead to improvements in the quality

of bio-oil to a limited extent, however, this needs to be extensive to allow for combination with and utilisation alongside petroleum based fuels [62].

2.4.2 Fuel characteristics

If bio-oils are to be used for transport fuel purposes, there are specifications which need to be met. Table 2.7 shows the specifications which are required for gasoline fuels in the European Union. These include standards for oxygen content as well as limited proportions of certain oxygenate compounds. A bio-oil may not meet this specification directly but may instead require blending with petroleum derived oils to meet these standards, however, this introduces a further set of challenges [16, 41, 106].

Table 2.7: Fuel specifications for highway gasoline in the EU [107].

Parameter	Unit	Limits	
		Minimum	Maximum
Research octane number		95	—
Motor octane number		85	—
Vapour pressure, summer period4	kPa	—	60
Distillation:			
Percentage evaporated at 100 °C	% v/v	46	—
Percentage evaporated at 150 °C	% v/v	75	—
Hydrocarbon analysis			
Olefins	% v/v	—	18
Aromatics	% v/v	—	35
Benzene	% v/v	—	1
Oxygen content	% m/m	—	3.7
Oxygenates			
Methanol	% v/v	—	3
Ethanol (stabilising agents may be necessary)	% v/v	—	10
Iso-propyl alcohol	% v/v	—	12
Tert-butyl alcohol	% v/v	—	15
Iso-butyl alcohol	% v/v	—	15
Ethers (≥five carbon atoms per molecule)	% v/v	—	22
Other oxygenates	% v/v	—	15
Sulphur content	mgkg^{-1}	—	10
Lead content	gL^{-1}	—	0.005

There are also standards for the direct utilisation of bio-oils within industrial burners and boilers. These standards are not as rigorous as those for transport use but still require pH, viscosity, energy density and water content to meet prescribed levels. These do not require oxygen content to be measured, however, the properties which are measured are directly affected by the oxygen content [38].

2.4.3 Upgrading methodology

There are many different methodologies which may be used for upgrading of pyrolysis oils. Figure 2.18 outlines a number of steps which may be included in an upgrading methodology depending on the required products. The route which is being used in this research is outlined in red and involves online upgrading of pyrolysis vapours as they pass through the reactor prior to product collection through condensation.
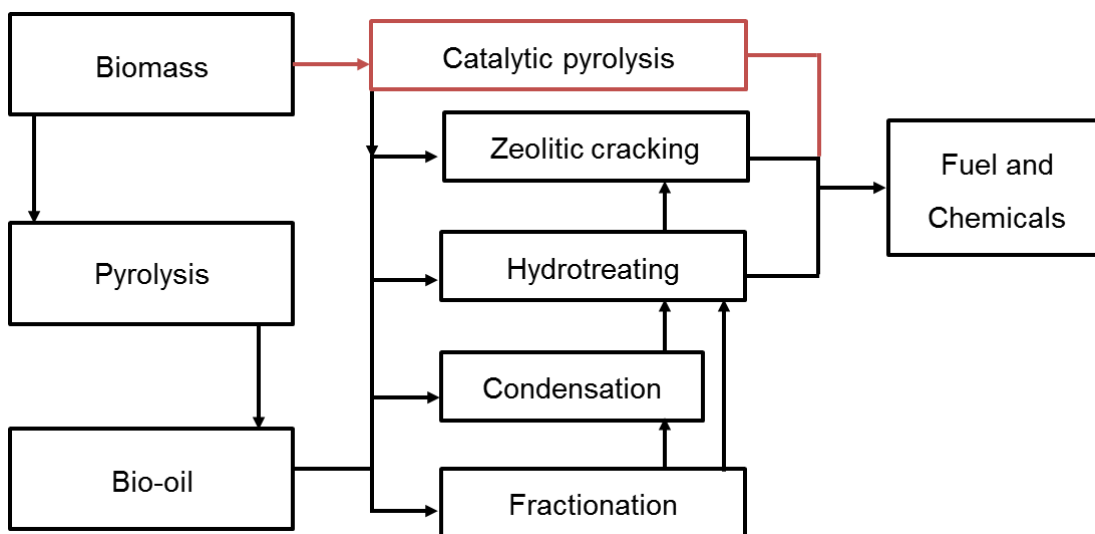
Figure 2.18: Routes which may be used for the pyrolysis and upgrading of biomass to produce fuels or chemicals [59, 62].

There are two main upgrading processes which remove oxygen, these are hydroprocessing and zeolitic cracking [108].

i) Decarboxylation is a process which utilises carbon in the pyrolysis feed to remove oxygen as carbon dioxide. This is often accompanied by some degree of decarbonylation (removal of carbon monoxide) and coke formation which further deplete the carbon in the sample which is no longer available for oil formation. There is usually hydro-

deoxygenation which will occur in conjunction with the decarboxylation.

ii)   Hydro-deoxygenation uses hydrogen to remove the oxygen from the oil. This may be achieved through utilisation of hydrogen in the sample but this this reduces the hydrogen content of the sample leading to increased coke formation. Often hydrogen gas is added at high pressure (10-20 MPa) in the presence of a catalyst and this efficiently removes the oxygen. The hydrogen is very costly and bio-oil can severely degrade the expensive catalysts leading to further expense meaning this is not cost competitive with existing petroleum fuels [109].

The main focus of this research will be on zeolitic cracking although hydro-deoxygenation will also be present to a smaller extent with hydrogen donation through co-pyrolysis of polymers. Zeolitic upgrading may be online, offline or a combination of the two options. The advantages of each option are as follows.

1. Offline catalytic upgrading using zeolites cracking or hydroprocessing of pyrolysis oils is possible, but the additional condensation and vaporisation step increases the formation of PAH compounds and coke deposition.

2. Catalytic pyrolysis involves upgrading of pyrolysis vapours before they condense which removes the issues associated with offline upgrading however the disadvantage is that the catalysts are in close proximity to the sample leading to increased deactivation by species present in the pyrolysis vapours. There is a limit as to how far the oil can be upgraded through this approach.

3. Catalytic pyrolysis with further offline upgrading is a combination of options 1 and 2. This means that the pyrolysis oils are upgraded using robust catalysts such that they are more suitable for further upgrading using more expensive catalysts with removal of oxygen ensuring that a lower hydrogen input is required and improved miscibility with existing petroleum feedstocks might allow for co-refining which would further reduce process costs.

2.4.4 Hydroprocessing

Hydroprocessing is a term denoting several processes which use hydrogen gas to chemically alter compounds, examples of this include hydrocracking, hydrodeoxygenation (HDO), hydrotreating and hydrogenation [16, 30, 62, 105, 110-112]. Whilst each process might utilise different conditions (pressure, temperature) catalysts or equipment, to achieve varied results, they all apply the same fundamental method, Hydrogen is added to a compound or set of compounds; the hydrogen reacts with the compound(s) directly or in the presence of a catalyst; this leads to new compounds. Common applications of these processes in the petroleum refinery industry include cracking large molecules into smaller molecules, increasing saturation of unsaturated hydrocarbons and removal of oxygen atoms in the form of water (H_2O). The degree to which each of these processes happen depends on the function of the catalyst and the process conditions. Talmadge et al. [41] considered the potential of hydrodeoxygenation of bio-oil to produce gasoline and diesel fuel. The recommendation of the authors was that whilst the removal of oxygen through the application of hydrogen is beneficial for fuel production it is achieved at a relatively high financial cost. The strategy which was deemed most beneficial was to use hydroprocessing to reduce the oxygen content of the bio-oil to around 7 wt.% and then to utilise existing petroleum refinery infrastructure for additional upgrading, assuming certain criteria were met. The criteria which were needed for successful operation in the refinery included, reducing the acidity of the oil, ensuring complete miscibility with hydrocarbon feedstocks and ensuring the bio-oil was of high enough volatility to pass through fractional distillation equipment (b.p <540°C). The strategy of mild hydrotreating followed by refinery upgrading meant that a lower quantity of hydrogen was needed for this process whilst minimising the hydrogenation of aromatic molecules which consumes hydrogen whilst not improving the oil.

2.4.5 Zeolite reactions

Fluid catalytic cracking (FCC) is a key process during the petroleum refining process. The major component of a FCC catalyst is zeolitic material which acts as a molecular sieve providing selective catalysis since its introduction in the 1960s [113]. Zeolites are porous crystalline lattice structures, generally composed from silicon, aluminium and oxygen, in a tetrahedral geometry. The silicon atoms may form a tetrahedral geometry with the oxygen atoms without carrying a net charge but the aluminium-oxygen formations have a net negative charge which requires balancing using a counter-ion to add stability [114].

Zeolites can be naturally occurring but many synthetic types have been discovered including ZSM-5 which is highly regarded in literature [115]. During zeolite synthesis sodium (Na^+) is often used to balance the negative charge such that ZSM-5 often refers to Na-ZSM-5. The acidity of a zeolite is related to the ratio of silicon and aluminium as this is the major cause of acid sites in the material and by changing this ratio the effect of the catalyst may be modified [116]. Whilst many synthetic zeolites are formed with sodium as the counter-ion it is common for ion-exchange to be used to change this. In the case of ZSM-5, hydrogen is commonly exchanged for sodium to give H-ZSM-5. There are usually two main methods of operation for zeolite type catalysts. They can act as proton donators, which is due to acid sites on the surfaces of the zeolite, and they can also control reactions of species through steric control, which is mainly due to pore volume effects [115].

2.4.5.1   Acid sites

Within a zeolite material there are three main types of acid site these are Brönsted acid sites, terminal hydroxyl sites and Lewis acid sites. These acidic sites form where there are defects in the crystalline structure and by necessity are at the surface of the material to enable interaction with the reactants.
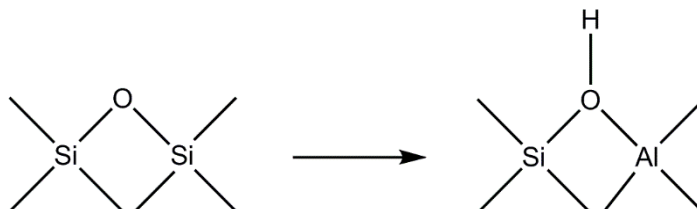
Figure 2.19: Brönsted acid site - hydroxyl bridging acid site formation from a silicon-oxygen bridge.

A Brönsted acid site is a strong acid site which forms where a silicon-oxygen-silicon bridge is altered through the exchange of one silicon atom for an aluminium atom. This produces an uneven charge on the bridging oxygen which will then gain stabilisation as a hydroxide group. The hydroxide bridge may lose this proton relatively easily with stabilisation of the negative charge on the oxygen (see Figure 2.19) [116, 117].
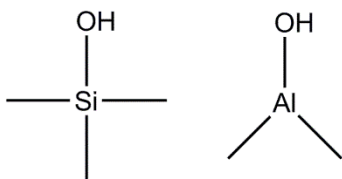
Figure 2.20: Terminal hydroxyl sites supported on both silicon and aluminium.

The edges of zeolite crystals often have terminal hydroxyl groups such as the silanol group (Si-OH). Damage to the crystal structure using high temperatures or strong acids can lead to defects, which enable the formation of hydroxyl groups on both silicon and aluminium (seeFigure 2.20).
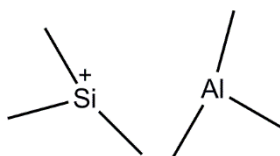
Figure 2.21: Lewis acid site caused by steam damage to zeolite.

Lewis acid sites can be formed by delamination of the zeolite framework on external surfaces (see Figure 2.21). These acid sites are much weaker than Brönsted acid sites. However, a Lewis acid site positioned near a Brönsted acid site may help withdraw electrons from the bridging OH which in the Brönsted acid site and lead to a superacidic Brönsted acid site [118].

2.4.5.2 Steric effects

Steric effects are also extremely important in solid acid catalysts. A major factor which makes zeolites so effective is that they are both catalytically active but also very selective. The selectivity is due in large part to the ability of zeolites to constrain reactions by restricting products to those which can be produced and diffuse through the geometric limitations of pores [119]. Zeolites can be described as microporous because they have pores which are smaller than 2 nm. Some zeolites have extremely small pores for which only gas molecules such as carbon dioxide can pass through. For others, such as ZSM-5, the pores are medium sized allowing for hydrocarbon rings of up to 10 carbon atoms able to diffuse. This has the effect of selectively producing compounds such as p-xylene, benzene and toluene with compounds such as methylated

naphthalenes becoming too large to pass through pores rapidly although these may pass through slowly or at high temperatures (above 600°C). Whilst reactions may be constrained within pores (internal active sites) it is also possible for reactions to take place on the surface of a zeolite catalyst (external active sites). These external reactions are not constrained in the same way as compounds which react within the pores, however, most of the reactive sites will only be available in the internal framework of the zeolite. Bhatia [120] suggests that internal sites may be around 100 times higher than the external sites, therefore many of the reactions will occur internally. Shape selectivity can be improved by reducing the number of active sites on the external surface of the catalyst. Conversely coke deposition may limit diffusion through the pores and thereby improve the overall effect due to external sites through limiting access to the internal sites [30, 113]. The size and shape of catalyst and enzyme active sites can produce selectivity effects which control or template the products which may be produced during a reaction. These size and shape effects can apply in several different ways which may be referred to as shape selectivity. Bhatia [120] describes three types of shape selectivity which are observed during reactions within the restrictive pores of zeolites.

- Reactant selectivity – selectivity is controlled by the types of reactants which are readily available within the pores i.e. those which are the optimal size and shape to diffuse freely.
- Product selectivity – selectivity is governed by products which are able to diffuse from the pores after formation. If products are too large they may be converted into smaller or less hindered products through equilibrium processes and may then pass from the pores as a product or if this is not possible the large product will block the pore causing catalyst deactivation.
- Transition state hindrance – in this case the products and reactants may be able to diffuse freely through the pore but the transition state which would be needed to produce the product is not possible or is restricted by the necessary space availability. Shape selectivity therefore generally favours mechanisms which require smaller transition states.

2.4.5.3   Zeolite reactions and product selectivity

Mortensen et al. [105] outlined a number of key reactions which take place during HDO and zeolite cracking of bio-oil through catalytic pyrolysis. The rate of a reaction is dependent on the availability of the reactants. In the presence of high pressure hydrogen gas, as is the case during hydroprocessing, the

hydrocracking (d), hydrodeoxygenation (e) and hydrogenation (f) reactions shown in Figure 2.22 will be enhanced. These reactions are also possible during zeolite cracking processes, but the limited availability of hydrogen will be a rate limiting factor. The catalyst is key to promoting the effectiveness of these reactions by adsorbing hydrogen and presenting it to the reactants during the reaction. Cracking (a), decarbonylation (b) and decarboxylation (c) are not dependent on the arrival of a secondary reactant as the reaction is directed by interaction with an active site in the catalyst.

In a zeolite, cracking (a) is directed by acid sites of which there are two main types, Brönsted acid sites function through donation of a proton (H^+), whereas, Lewis acid sites accept electrons which can be seen as a removal of H^- from the reactant. Both processes have the effect of producing a positively charged carbon atom within the hydrocarbon. This charge is unstable and rearrangement of the ion can occur to produce greater stability with stability greatest on a tertiary carbon (a three carbon branch). It is least stable on the end carbon in a linear hydrocarbon. The cracking reaction will then usually occur through beta-scission with longer hydrocarbon chains more reactive than short chains due to charge stabilisation being lower on a small molecule. 4 or 5 carbon chains are not able to stabilise the positive charge and can transfer it to a larger hydrocarbon. The positive charge continues to pass between molecules propagating the scission until the charge terminates through chain collision. During catalytic cracking hydrogen transfer is also possible with two alkenes able to transfer a hydride (H^-) such that one of the alkenes becomes an alkane and the other becomes a cyclic-alkenes such as aromatics. Alkenes and naphthalenes can also transfer hydrides to produce an alkane and an aromatic [121].
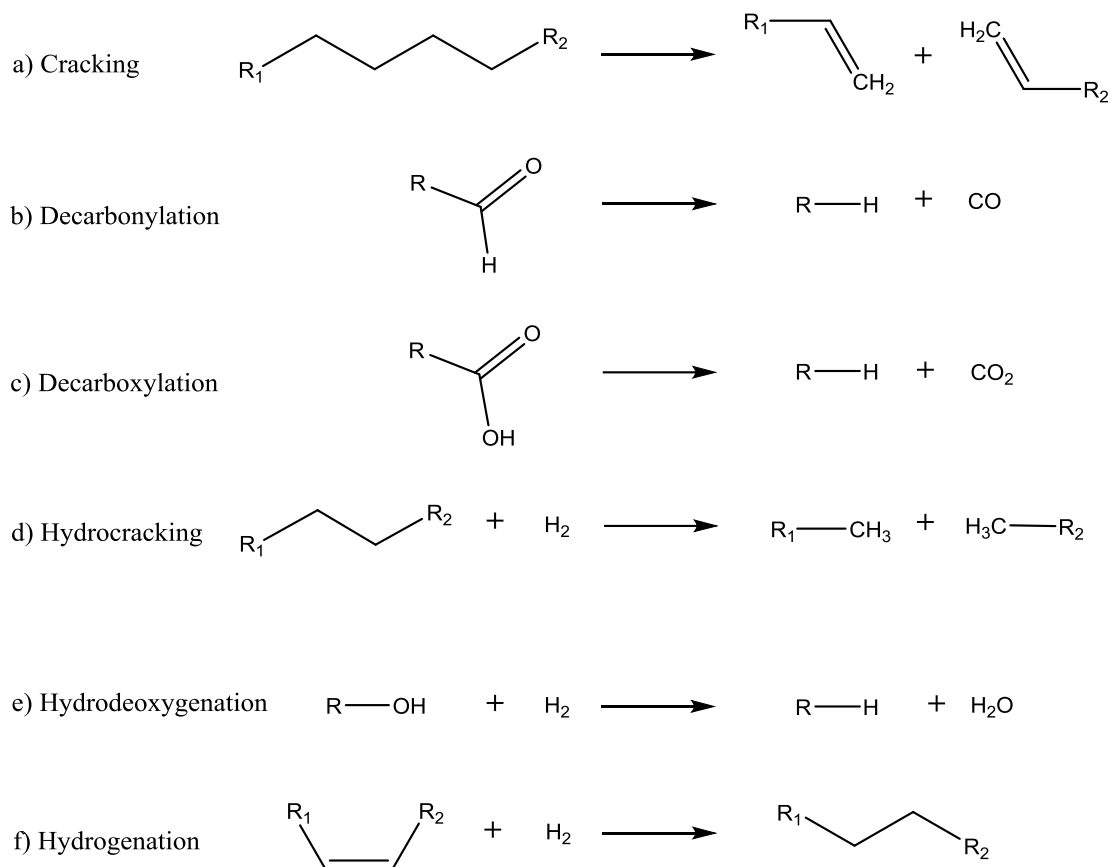
Figure 2.22: Key reactions identified by Mortensen et al. [105] for zeolite cracking and HDO.

A major purpose for zeolite cracking is the removal of oxygen atoms from bio-oils and this is accomplished through three main reactions decarbonylation (b), decarboxylation (c) and hydrodeoxygenation (e) which remove oxygen as carbon monoxide, carbon dioxide and water respectively. Carbon dioxide and carbon monoxide are non-condensing gases and don't participate in further reactions. Water is a condensing gas and has the potential to participate in further reactions such as steam reforming.
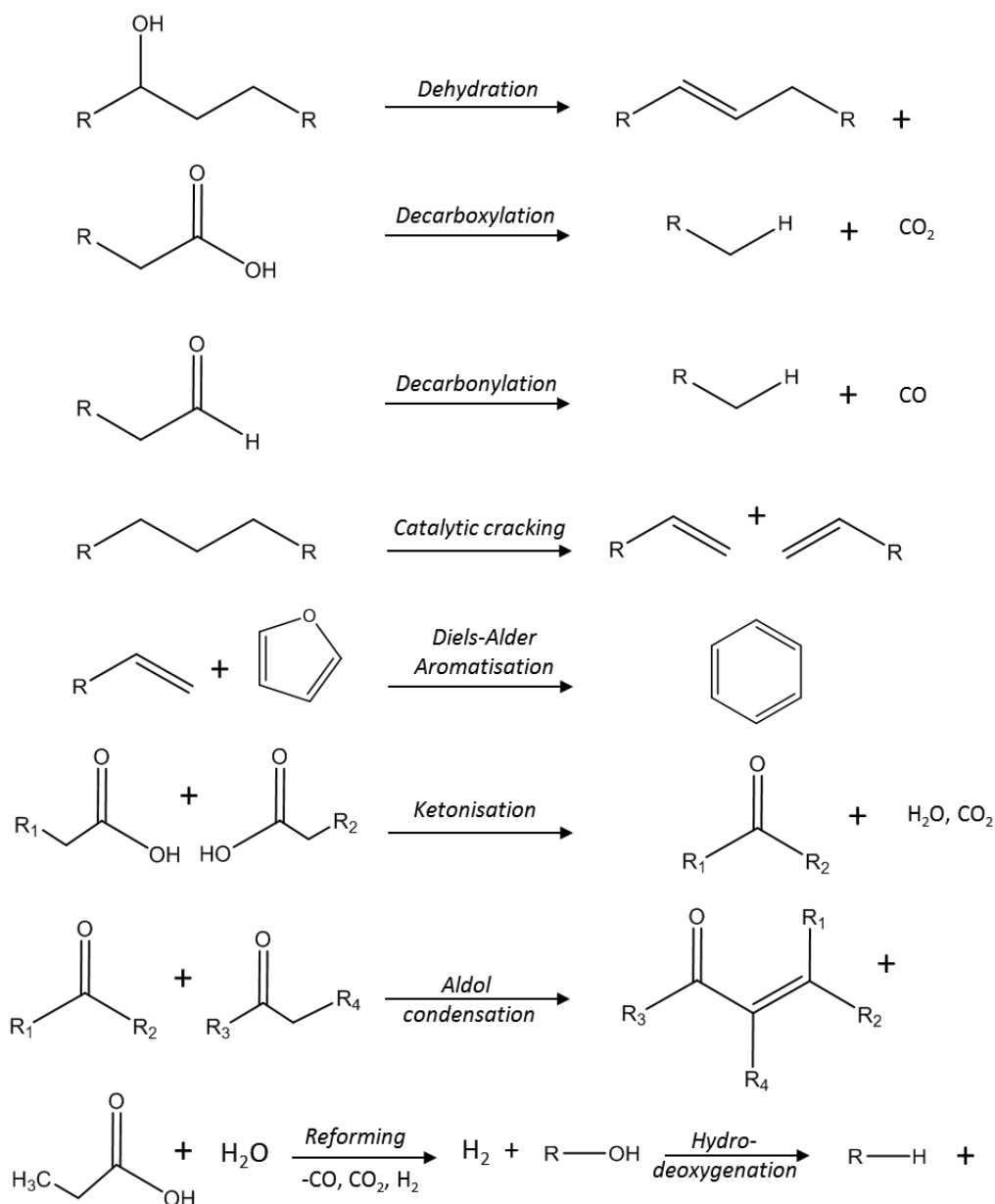
Figure 2.23: Various reactions which are involved during catalytic pyrolysis of biomass as identified by Wang et al. and Pham et al. [33, 122].

Wang et al. [33] include further reactions during their analysis of catalytic pyrolysis which includes catalytic effects from inorganic species in the biomass itself whereas Mortensen et al. [105] focused solely on zeolite catalysis. As with the zeolite reactions the major products are carbon dioxide, carbon monoxide and water although for Mortensen et al. the production of water depended on hydrogen gas availability whereas these reactions produce water through other pathways. Formation of aromatics were possible through catalytic cracking reactions but could also be produced by Diels-Alder type aromatisation of alkenes with furan derived compounds.
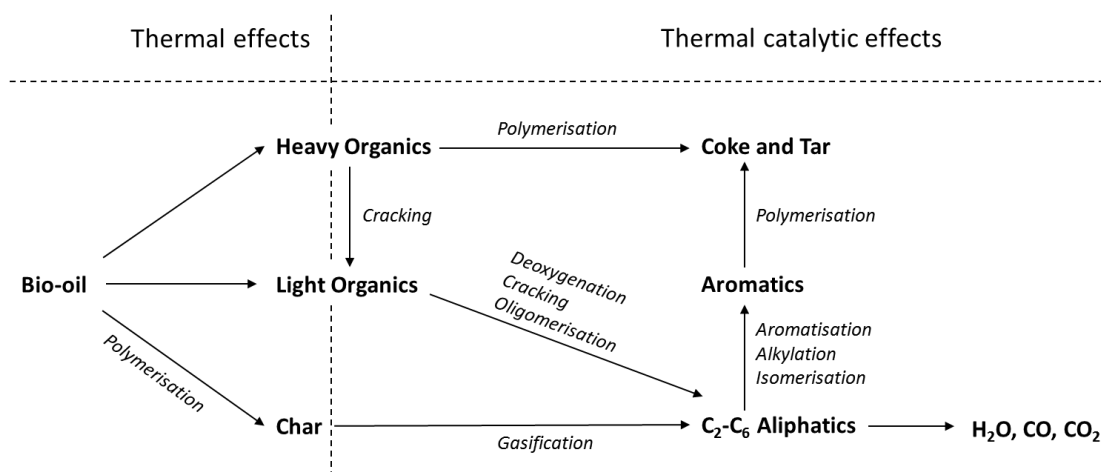
Figure 2.24: Pathway for the catalytic upgrading of bio-oil over acidic zeolite catalysts with thermal effects (TE) and thermo-catalytic effects (TCE) partitioned, proposed by Adjaye et al. [123-125].

Rezaei et al. [123] examined catalytic pyrolysis of bio-oil using zeolite catalysts with the aim of producing green aromatic compounds. Figure 2.24 shows a scheme giving an overview of bio-oil upgrading with the focus being on the relationships between different products. Rezaei argue that catalytic cracking may be an economically feasible alternative to HDO, however, there are issues which need to be overcome. Zeolites have three main drawbacks; they can cause high coke formation which produces catalyst deactivation; they can cause increased formation of polycyclic aromatic hydrocarbons (PAHs), with medium pore sized zeolites forming these predominately on external surfaces [120]; and low liquid yields with liquid compounds converted to coke, gases and PAHs. The scheme (Figure 2.24) is divided into two regions with initial thermal effects responsible for breaking down of the bio-oil with thermal catalytic effects responsible for many of the reaction pathways which lead to specific product types such as short chain aliphatics, aromatics, coke and tar.

Figure 2.25 which is adapted from Wang et al. [33] examines the pathways which lead from cellulose, hemicellulose and lignin through to liquid products. The scheme starts by identifying key compounds produced by the components of lignocellulosic biomass. It then identifies key reactions, such as those in Figure 2.23 and how these combine to produce catalytically upgraded bio-oil. It is clear that whilst primary reactions produce highly oxygenated compounds form each component, the secondary reactions, which are directed by catalysts, produce both non-oxygenated aromatics and aliphatics as well as coke.
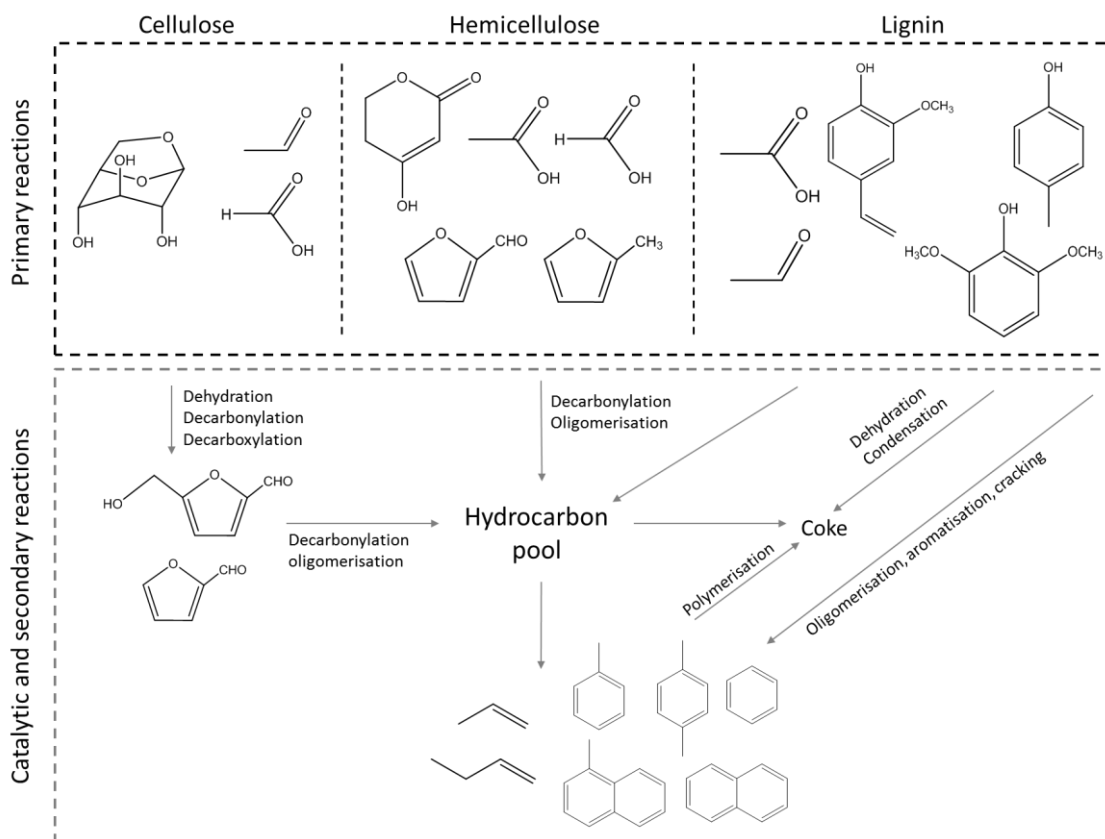
Figure 2.25: Complex combinations of biomass compounds and various reaction mechanisms can lead to a number of different products (adapted from Wang et al. [33]).

2.4.6 ZSM-5

ZSM-5 is a zeolite type catalyst which has been recognised as a suitable catalyst for both petroleum FCC as well as for biomass catalytic pyrolysis [59, 126, 127]. It is composed of a three-dimensional structure which contains two different channel system. There are linear channels which are eliptical in shape and there are zigzag channels which are circular with both channels approximately 0.55 nm in diameter. Pattiya [59] compared a number of studies analysisng pyrolysis of biomass using different catalaysts, this included a section on ZSM-5. The findings indicate that ZSM-5 is an effective catalyst for biomass catalytic pyrolysis. Liquid yields were reduced when the catalyst was used and this was accompanied by increased in permanent gases and light hydrocarbon gases inclucing carbon dioxide, carbon monoxide, methane and hydrogen gas. Whilst this is not a beneficial effect, however, it was also accompanied by deoxygenation of the liquid yield with water, carbon dioxide and carbon monoxide the main routes of removal of oxygen. The oils which had been catalytically upgraded had lower content of oxygenated compounds,

higher content of hydrocarbon compounds and molecular weight range of compounds reduced.

Research by Williams and Horne [128] compared Na-ZSM-5 with H-ZSM-5, zeolite-Y and alumina during pyrolysis in a fluidsed bed reactor and found that whilst the ZSM-5 catalysts gave similar results to each other they both gave better results than the zeolite Y and alumina in terms of hydrocarbon yield, oxygen content and coke deposition. Both ZSM-5 catalysts did contain increased quantities of PAH compounds which are both damaging to health and presursors to coke and tar formation. Both zeolite Y and alumina have greater pore sizes than ZSM-5 and this is likely to be the reason for the higher coking of the catalyst. Zhao et al. [129] found that Na-ZSM-5 was superior than H-ZSM-5 for catalytic pyrolysis of lignin as it was less acidic and led to a lower deposition of coke and a reduction in oxygenates. In ZSM-5 the pores are too small for formation of PAHs within the pores, rather they are produced on the external surfaces which may include entrances to pores [120]. French and Czernik [106] found that ZSM-5 based catalysts were more effective for in-situ deoxygenation of pyrolysis vapours, from model biomass compounds, than other catalysts with larger pores, including zeolite Y.

Bridgwater et al. [27] listed research organisations which have been examining catalytic upgrading of pyrolysis products using zeolite cracking since 2000. Integrated catalytic pyrolysis was identified at 12 organisations for which 6 used ZSM-5 catalysts, 3 used zeolite Y catalyts. 9 organisations used close coupled, decoupled or other vapour upgrading processes, of these 8 used ZSM-5 type catalysts and 1 utilised zeolite Y. This shows that ZSM-5 has become established as the main catalyst for upgrading of biomass pyrolysis vapours in research worldwide. ZSM-5 is stable, non-toxic, product selective and active which accounts for many of the advantages of using it.

Liu et al. and Taarning et al. [30, 130] reviewed the use of ZSM-5 for upgrading of biomass pyrolysis vapours. They noted that whilst a large number of microporous materials had been examined for catalytic pyrolysis the most effective for production of aromatic compounds was ZSM-5. This is due to the catalyst being highly acidic, with the largest possible molecules which may fit within pores equivalent to tri-methyl-benzene. There were numerous reactions identified during biomass pyrolysis with ZSM-5 and these included: fragmentation of compounds – Cracking and disproporitonation; buiding up fo compounds – polymerisation, oligomerization, alkylation; removal of oxygen – deoxygenation and decarboxylation; rearrangement – cyclisation, isomerisation and addition of functionality such as aromatisation [125].

Deoxygenation occurs through different processes during ZSM-5 catalysed pyrolysis of biomass [30]. Diebold et al. [131] reported the water, carbon dioxide and carbon dioxide which was released during deoxygenation using ZSM-5 with the conclusion that both functional group and reaction conditions affected the product. Simple hydroxy groups like methanol converted to water (100%) whereas dimethylphenol converted to water (80%), carbon monoxide (17%) and to a lesser extent carbon dioxide (3%). In contrast Furfural produced less water (18%), with the main product carbon monoxide (80%). These results indicate that whilst there is variation in mechanism for different oxygenated compounds, leading to different deoxygenation products, generally ZSM-5 removes oxygen through dehydration. Carbonylation also occurs and this is more significant than carboxylation [127]. This is problematic as it increases the carbon/ hydrogen ratio of the remaining mixture leading to a shortage of hydrogen. If the oxygen was expelled as carbon dioxide or carbon monoxide this would improve the C/H ratio and lead to a greater viability for hydrocarbon products. This may also reduce the deposition of carbon rich – coke on the catalysts [130]. The major action of ZSM-5 is through acidic sites particularly Brönsted acid sites and if these are removed or neutralised the reactivity and selectivity is severely reduced [132].

2.4.7 Metal impregnated zeolites

Zeolites are porous materials which contain charged elements within their structure which introduces the possibility of adapting the function of the catalyst by exchanging the sodium ion within the zeolite for another metal [30]. In newly synthesised ZSM-5 the pores are populated with bulky organic molecules [120]. The process of producing an acid zeolite involves removal of these bulky organics to replace them with smaller cations such as sodium (Na^+). These can in turn be replaced through various techniques to produce proton or metal cationised ZSM-5. This metal exchange can lead to interchange between Brönsted and Lewis acid sites although this may also be accomplished through hydration or dehydration. Bhatia [120] has produced an in depth publication detailing synthesis, modification and functionality of zeolites such as ZSM-5 which contains methodologies which may be used for metal impregnation into zeolites. There are seven basic methods which are suggested (as listed below). Mullen et al. [133] use methods 1,2 and 5 for synthesis of gallium containing ZSM-5 catalysts and these are often the most suitable and accessible for transition metals.

1. Ion Exchange
2. Impregnation (incipient wetness)
3. Co-deposition
4. Gaseous adsorption
5. Introduction during zeolite synthesis (hydrothermal synthesis)
6. Adsorption of metal vapour
7. Co-mulling

Ion exchange involves mixing a metal in a cationic form such as in a salt with the zeolite and allowing ion exchange to occur spontaneously either in solid state or in an aqueous solution. This will often involve elevated temperatures and is most suitable for larger pore sizes and where low metal concentrations are required. This method is well suited to noble metal exchange [120].

Impregnation or incipient wetness involves producing a metal complex which is water soluble such as $Co(NO_3)2.6H_2O$. This is dissolved in a solvent and mixed with the zeolite. Stirring and heating causes the complex to pass into the catalyst as the solvent is slowly removed. Once dry, the zeolite is calcinated which degrades the metal complex, driving off the organic portion and leaving the metal deposited onto the zeolite. This is suitable for zeolites, such as ZSM-5, where exchange capacity is low and where higher concentrations of metal are needed. Wet impregnation and ion exchange are commonly used to exchange metals onto zeolites, with Incipient wetness impregnation more often used for ZSM-5 [114, 126, 134-136].

The effect of metal impregnation onto ZSM-5 for catalytic upgrading of pyrolysis vapours is described by Liu et al. [30]. Different metals can cause variations in the yields of catalytic pyrolysis and the composition of the products. In some cases it was possible to identify a particular reaction pathway which was responsible for the alteration but this was not always the case. Table 2.8 lists a range of metal compounds, identified in literature, which have been impregnated onto ZSM-5 and used as a catalyst for upgrading of pyrolysis vapours or model compounds representative of this, such as furfural. The metal compounds which were most regularly examined were those which consistently appeared to introduce useful alterations to the oils collected. Those which are highlighted in bold, copper, cobalt, iron, gallium, magnesium, and zinc were the most prominent both in regularity of use and in terms of efficacy. These will be examined further for their bio-oil upgrading potential.

Table 2.8: Selected metals used for impregnation of ZSM-5 for upgrading of pyrolysis vapours and petroleum derivatives.

Metal	References
Ce	[126]
Co	[59, 106, 123, 135-141]
Cu	[126, 134, 135, 137, 142-144]
Fe	[126, 137, 138, 142, 145-147]
Ga	[59, 102, 106, 123, 133-135, 137, 139, 147-153]
Mg	[126, 134, 137, 143, 147]
Mo	[139, 140]
Ni	[59, 106, 123, 126, 134-137, 139, 140, 142-144, 147, 154, 155]
Pd	[137, 139]
Pt	[59, 135]
Sn	[126, 134, 143]
Zn	[126, 137, 144, 148, 149, 156, 157]

2.4.7.1   Cobalt

Iliopoulou et al. [136, 141] studied the wet impregnation of cobalt metal onto commercially available ZSM-5 at 1 wt.%, 5 wt.%, and 10 wt.%. Through comparison to unmodified ZSM-5 to assess the effectiveness of the cobalt. The effect of cobalt addition led to a reduction in the bio-oil yield but with a reduced oxygen content in the liquids. The aromatic selectivity was also improved with coke formation remaining relatively unchanged. Both carboxylation and carbonylation reactions were increased which accounts for the oxygen content reduction in the oils and the water content was only slightly increased. This was accompanied by an apparent increase in hydrogen as well as volatile hydrocarbons (C_1-C_6). Zheng et al. [137] studied catalytic pyrolysis using a number of transition metals (Co, Cu, Ga, Mg, Ni and Zn). and compared this against unmodified H-ZSM-5 Elemental analysis of the upgraded bio-oils was used to determine the oxygen content (by difference). Elemental analysis of volatile mixtures such as bio-oils may be affected by evaporation of species so care should be taken when considering these values. The metal impregnated ZSM-5 catalysts used during this study by Zheng et al. [137] outperformed the HZSM-5 catalyst by producing liquids with lower oxygen content by >2 wt.%. These metal impregnated catalysts also produced lower oxygen content (>16 wt.% lower) in liquids when compared to non-catalytic pyrolysis. Cobalt was the 4th most effective metal catalyst from those examined however the best four oxygen content values were within 0.8 wt.% so it is inconclusive which was

the most effective considering the methodology. Cobalt was determined to be median amongst the metals for liquid yield and aromatic selectivity [137]. Vichaphund et al. [139] examined catalytic upgrading of pyrolysis vapours from Jatropha to produce aromatic compounds and found that cobalt impregnated ZSM-5 was not quite as effective as other metal impregnated ZSM-5 catalysts (Ni, Mo, Ga and Pd) for aromatic selectivity. Pattiya et al. [59] identify cobalt as an important metal for production of catalysts for steam reforming to produce hydrogen gas. This may lead to enhanced H-transfer and hydrogenation reactions which may account for the reduced aromatic selectivity.

2.4.7.2   Copper

Veses et al. [134, 143] investigated the upgrading of raw bio-oil using metal impregnated ZSM-5 including copper. They found that whilst bio-oil yields were not adversely affected there was a reduction in the oxygen content of the oils. There was a reduction from 32 wt.% down to 21 wt.% with Cu-ZSM-5 with all the ZSM-5 investigated ranging from 22-20 wt.% (H, Mg, Ni, Ga, Sn, Cu). This was accompanied by a reduction in phenols, acids and furans and an increase in aromatics and PAH compounds. The yield of carbon dioxide and carbon monoxide shifted significantly compared to the non-catalytic experiment with carbonylation increasing and carboxylation decreasing when using Cu-ZSM-5. Zheng et al. [137] also observed an oxygen reduction during catalytic pyrolysis using Cu-ZSM-5 and aromatic selectivity similar to that of H-ZSM-5.   Both Stanton et al. [135] and Miskolczi et al. [126] found that copper impregnation led to a reduction in acidity of the catalyst, however, this did not appear to adversely affect the catalyst function. As the activity in zeolites is usually related to the acidity of the ZSM-5 this implies that the copper metal is acting as a catalytic species relatively independently of the acid sites. Stanton et al. [135] found that whilst copper did not lead to greater liquid yields or greater deoxygenation than other metal-ZSM-5 catalysts, the addition of a hydrogen atmosphere caused a significant reduction in the proportion of oxygenated compounds. Whilst hydrogen increased deoxygenation with each of the metals examined (Cu, Ga, Ni, Co and Pt) this was greater than gallium and cobalt although surpassed by platinum and nickel. The deoxygenation in the presence of hydrogen was greater for all the metal impregnated ZSM-5 than unmodified ZSM-5.

2.4.7.3   Iron

Zhang et al. [147] and Zhang et al. [145] both examined catalytic pyrolysis of biomass using iron modified ZSM-5. Both studies found that the use of Fe-ZSM-5 led to a slight reduction in bio-oil yield which was accompanied by a consistent

increase in gaseous yield. The increase in gas yield was due to an increase in light alkenes, carbon monoxide and carbon dioxide. This produced an upgraded bio-oil which had excellent aromatic selectivity with a reduction of oxygenated compounds. Zhang et al. [146] also examined Fe-ZSM-5 catalysts researching catalytic pyrolysis of rice husks with different iron loading on ZSM-5. The chemical composition of bio-oils upgraded using Fe-ZSM-5 when compared to ZSM-5, had a reduced proportion of oxygenates, including phenol, and an increased proportion of hydrocarbons. As the loading was increased from 0.5 wt.% through to 8 wt% the proportion of hydrocarbons increased further as phenol decreased. The increase in iron loading increased benzene and toluene yield whilst reducing that of bi- and tri-substituted aromatics whilst also increasing the yield of naphthalenes and naphthalene derivatives as well as PAHs.

2.4.7.4   Gallium

Cheng et al. [102] examined a number of different gallium containing ZSM-5 and alumina silicate catalysts for furan conversion to aromatics. These including ion exchange impregnation, incipient wetness impregnation, synthesis of MFI with structural gallium and impregnation onto SiO_2 also using incipient wetness impregnation. The Zeolite formed with gallium within the structure were less catalytically active than ZSM-5 with lower aromatic selectivity and increase coke formation. The gallium impregnated silicon dioxide catalyst had poor activity and also produced high coke yields and bi-cyclic aromatic compounds such as indene and naphthalenes. Measurement of the acidic nature of the materials revealed that both of these catalysts lacked Brönsted acid sites which are necessary to convert allene produced during decarbonylation of furan, into alkenes for subsequent conversion into aromatics. Impregnation of ZSM-5 through ion exchange and wet impregnation both yielded catalysts with similar activity with increased aromatic selectivity compared to unmodified ZSM-5. The results show that addition of gallium to ZSM-5 increased the rate of decarbonylation and the subsequent aromatisation from alkenes. When the Brönsted acid sites in the gallium impregnated catalysts were absent the conversion of furan to aromatics was reduced with evidence that both decarbonylation of furan and aromatisation of alkenes are promoted by gallium whilst the acid sites are involved with allene conversion to alkenes even when gallium was not present.
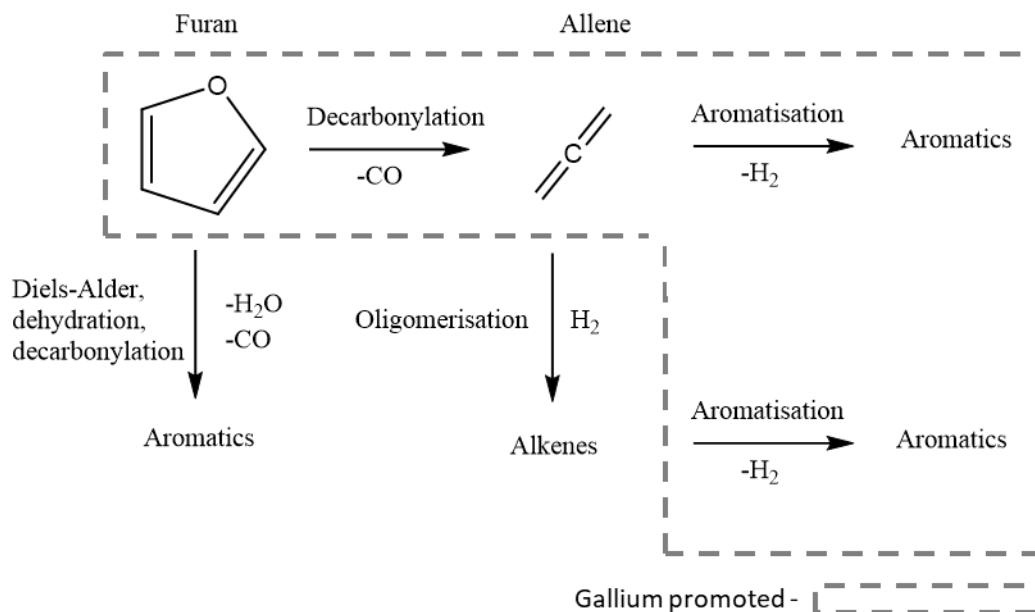
Figure 2.26: Selected reactions promoted through gallium impregnated conversion of furan to aromatics, adapted from Cheng et al. [102]. Reactions contained within the dashed box are promoted by gallium.

As well as promoting formation of aromatics Zheng et al. [137] also recognise the deoxygenation action of Ga-ZSM-5 during in-situ catalytic pyrolysis of biomass. From six metals (Co, Cu, Ga, Mg, Ni and Zn) impregnated onto ZSM-5, Ga-ZSM-5 produced the oil with the lowest oxygen content, although there were three other metals with oxygen contents within 0.8 wt.% of the value obtaine for Ga-ZSM-5. Veses et al. [134] found that the proportion of carbon monoxide increased when gallium was deposited onto H-ZSM-5 with a 1 wt.% decrease in oxygen content of the oils. In this case all the metals used to modify ZSM-5 (Cu, Ga, Mg, Ni and Sn) gave oxygen contents within a 1 wt.% range.

Zheng et al. [137] found that gallium also produced the highest oil yield of the metal impregnated catalysts with a higher liquid yield even than H-ZSM-5. Choi et al. also [152] produced greater liquid yields for Ga-ZSM-5 over H-ZSM-5 using ex-situ upgrading of biomass upgrading. However, the reverse was found when comparing ZSM-5 to Ga-ZSM-5 as with Zhang et al. [147] and Li et al. [149]. Stanton et al. [135] found that Ga-ZSM-5 was the only metal impregnated catalyst that produced more liquid yield that ZSM-5 in an inert atmosphere, however, if hydrogen was introduced the liquid yield decreased for Ga-ZSM-5. It appears that liquid yield is affected by complex interactions and is therefore, dependent on the type of biomass utilised (furan / H_2 availability), metal loading, reactor design (ex-situ/ in-situ) and possibly other factors. Pattiya et al. [59] cite several studies which have found gallium impregnation improved the aromatic

selectivity of biomass pyrolysis. This was particularly evident for benzene, toluene and xylene (BTX) yields which in some cases were twice that of H-ZSM-5 [153].

2.4.7.5 Magnesium

Zheng et al. [137] examined aromatic production using catalytic pyrolysis of biomass with transition metal impregnated ZSM-5. During impregnation magnesium experienced a significant decrease in Brönsted acidity similar to that experienced with copper. The effect of this was that during pyrolysis, there was a lower aromatic yield and increased coke and PAH formation.

Zhang et al. [147] studied catalytic pyrolysis using ZSM-5 impregnated with cheap transition metals (Fe, Ni, Ga and Mg). Magnesium had the lowest selective with regards to BTX and the highest oxygen content remaining in the bio-oil after upgrading. All the metal impregnated ZSM-5 catalysts performed more effectively than ZSM-5 and the non-catalytic reference. The deoxygenation using magnesium appeared to be predominately through carboxylation, rather than carbonylation with higher output of CO_2 than CO. This effect was also found by Veses et al. [134] who examined different metal impregnated ZSM-5 (Mg, Ni, Cu, Ga and Sn). They found that magnesium produced the equally lowest oxygen content in a bio-oil with the result for all the metal catalysts within a 1 wt.% range but that phenol and acid functional groups were higher than those measured for the other metals. The magnesium in this case gave amongst the highest aromatic selectivity and the lowest PAH content. Both Veses et al. [134] and Zheng et al. [137] observed loss of strong acid sites. Zheng et al. [137] inferred that this contributed to higher PAH and coke through increase pore blockage whereas Veses et al. [134] record that loss of acid sites reduced cracking and esterification reactions producing lower coke yield.

The major difference between the two studies was the metal loading of the catalyst. Veses et al. [134] used 1 wt.% magnesium loading, whilst Zheng et al. [137] used 5 wt.%. The magnesium at a lower loading reduced the acidity and so reduced coke and PAH formation whereas the higher metal loading also reduced the acidity but potentially also caused substantially greater pore blockage leading to an increase in coke and PAH formation.

2.4.7.6 Nickel

Nickel is a metal which is associated with steam reforming and when impregnated into ZSM-5, high H_2 yield confirms that these types of dehydrogenation reactions are occurring [59, 134, 136, 137]. Iliopoulou et al.

[136] found that Ni-ZSM-5 caused deoxygenation with an almost linear decrease in oxygen content as metal loading was increased from 1 wt.% through 5 wt.% to 10 wt.%. The increase in metal loading also caused an increase in H_2 and CO_2 gas production. Zheng et al. [137] found that Ni-ZSM-5 led to dehydrogenation, oligomerisation and cyclisation as well as deoxygenation at a similar level to gallium, zinc and cobalt. Nickel metal appeared to affect the size selectivity of the ZSM-5 by partially blocking channels which combined with carbon deposition led to reduced access to pore catalytic sites. This causes a reduction in mono-aromatic compounds particularly p-xylene and an increase in naphthalenes. Both Stanton et al. [135] and Zhang et al. [147] found that nickel gave lower liquid yields than unmodified ZSM-5 and lower when compared to other metal catalysts (Mg, Ga, Cu, Co, Fe) with only iron giving a lower liquid yield. Veses et al. [134] found that of the metals compared (Mg, Ni, Cu, Ga, Sn), nickel gave the highest aromatic selectivity but also the equal highest polyaromatic yield with gallium. Vichaphund [139] found that nickel gave the second highest aromatic selectivity after gallium and greater than that from cobalt, palladium and molybdenum. This difference may be due to Veses et al. [134] upgrading bio-oils using these catalysts post pyrolysis whereas Vichaphund [139] was examining their use during pyrolysis. This is likely to have an effect on the types of compounds passing across the catalysts with a greater coke deposition expected during post-pyrolysis upgrading. Both studies also used different biomass feedstocks to produce the bio-oil which may also account for variations.

2.4.7.7 Zinc

Zinc impregnation in ZSM-5 is complex with Niu et al. [157] indicating that at least two different species are possible depending on crystal size. Zheng et al. [137] examined zinc impregnated ZSM-5 for catalytic pyrolysis of ZSM-5 alongside other metals (Mg, Cu, Ga, Ni and Co). Zn-ZSM-5 produced the second highest liquid yield from these metals behind gallium and was amongst the four lowest oils in terms of oxygen content. The Zn-ZSM-5 catalyst were found to be highly aromatic specific particularly with regards to mono-aromatics. However, Fermoso et al. [158] found that impregnated zinc species often present as ZnO and this can cause significant blocking of pores, leading to coke and deactivation. The impregnation of zinc however was also associated with deoxygenation and increased aromatic formation.

2.5 Co-pyrolysis

Catalytic pyrolysis can be used to improve the quality of bio-oil, but, it has a drawback. Due to the low H/C ratio of biomass, once oxygen has been removed via hydrodeoxygenation, carbonylation and carboxylation, liquid yields are significantly reduced and coke deposition is high [159]. The H/C ratio is useful to determine if hydrocarbon mixtures can produce viable hydrocarbon compounds however it does not account for the detrimental effect heteroatoms such as oxygen and nitrogen might have on the formation of hydrocarbon compounds by removal of necessary hydrogen atoms. For this the (H/C_{eff}) ratio can be used as it uses a calculation to make allowance for the number of hydrogen atoms which are unavailable to the carbon due to removal of these heteroatoms such as through hydrodeoxygenation [160]. For effective formation of hydrocarbon compounds an (H/C_{eff}) ratio of between 1 and 2 is suitable. Catalysts may promote carbonylation and carboxylation mechanisms in such a way as to increase the removal of oxygen through the use of carbon atoms and therefore increase the (H/C_{eff}) ratio.

$$H/C_{effective} = (H - 2O - 3N - 2S) / C$$

One clear solution is to add more hydrogen to the pyrolysis mixture, as is the case with commercial hydrodeoxygenation, however, hydrogen is expensive to produce and energy intensive to manufacture. This reduces the economic and ecologic feasibility of this approach, although it is effective. Hydrogen may also be introduced through the co-pyrolysis of a material which is rich in hydrogen (i.e. has a high (H/C_{eff}) ratio) [160]. Waste plastic is a commonly cited material to be used in co-pyrolysis with biomass [115, 161-165]. It has a higher (H/C_{eff}) ratio than biomass because it does not contain such a high proportion of heteroatoms. Waste polymers are low cost materials and utilisation may bring a value to this commodity where previously disposal was costly and ecologically problematic [19]. Co-pyrolysis has the potential to convert this material into a useful product which could be both economically and ecologically beneficial. If this technology is simple, economical and effective then it would be suitable for rapid uptake and utilisation [163]. It may also improve the operation and viability of biomass pyrolysis, with co-pyrolysis of biomass alongside polymers leading to increased oil stability through radical interactions, particularly those which reduce the phenol content of oils [166]. The polymers most often researched for this purpose were polyethylene, polypropylene, polyethylene terephthalate and polystyrene [115].

2.5.1 Biomass and polyethylene

Li et al. [104, 167] examined co-pyrolysis of LDPE and cellulose both with and without a catalyst (ZSM-5). The non-catalytic experiments suggested that the oils compounds produced from co-pyrolysis were similar to those present in individual pyrolysis oils. This compares to research undertaken by Bhattacharya et al. [168] who found that PS, PP and HDPE also interacted in a similar way with pine in a screw auger pyrolysis experiment. Xue et al. [169] examined tandem pyrolysis of PE alongside model biomass constituents, cellulose, xylan and lignin. Whilst there was no major change in the types of compounds, there were significant shifts in the proportions of compounds produced. Co-pyrolysis of cellulose and PE increased the yield of furans and anhydrosugars by 45%; xylan increased furans, anhydrosugars and acetic acid; and lignin with PE created significantly higher proportions of phenolic compounds. This increase in phenolic compounds indicates that the PE radicals were promoting lignin depolymerisation. There was also a marked decrease in char, carbon monoxide and carbon dioxide from these experiments. An increase in short chain alkanes and alkenes from the co-pyrolysis of the PE with biomass indicates that not only the compounds from biomass but also those from the polyethylene were becoming altered during co-pyrolysis. In this case the biomass was enhancing depolymerisation of the polyethylene with longer chain hydrocarbons becoming cracked into shorter chain molecules.

When H-ZSM-5 was utilised alongside the co-pyrolysis there was an increase in aromatic hydrocarbons accompanied by a decrease in ethylene and propylene selectivity. The removal of alkenes from the pyrolysis products without a corresponding increase in alkanes indicates that aromatic formation was most likely a product of the Diels-Alder reaction such as in Figure 2.27. The Diels-Alder reaction involves the combining of two unsaturated bonds (C=C) to produce a ring structure. This results in a reduction in the number of unsaturated functional groups and an increase in the number of cyclic compounds. This is also possible between unsaturated bonds within ring structures and will result in polycyclic structure. As well as aromatic production, the co-pyrolysis of biomass and PE together produced higher hydrocarbon products with lower coke on the catalyst than during pyrolysis of the two samples separately.
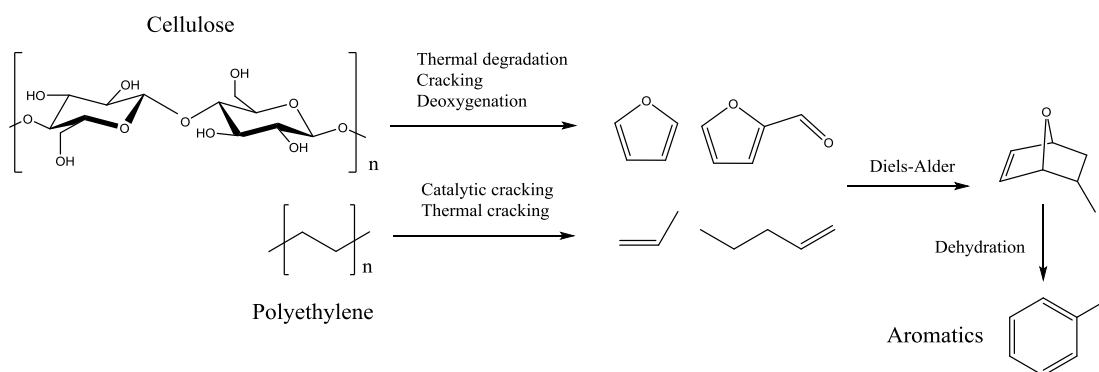
Figure 2.27: Proposed process for catalytic co-pyrolysis between cellulose and PE [115, 167, 169-171].

Li et al. [104, 167] found that ZSM-5 significantly affected the products of co-pyrolysis also observing a reduction in coke and an increase in aliphatic and aromatic products. This aromatic formation was attributed mainly to furan formation from ZSM-5 interaction with cellulose, leading to Diels-Alder reactions together with the alkene products from catalytic cracking of PE.

2.5.2 Biomass and polypropylene

Li et al. [167] compared LDPE and PP co-pyrolysis with cellulose. The aromatic and olefin yield from individually pyrolysed PP was higher than that for LDPE. During co-pyrolysis with cellulose, the aromatic yield is increased to a greater extent for LDPE than for PP such that the aromatic yield is higher in LDPE and cellulose co-pyrolysis. This was accompanied by a slight reduction in coke in each case. Ohja et al. [172] examined co-pyrolysis of PP and cellulose at different, mixing ratios using Py-GC/MS and Py-FTIR. The mixtures produced a significantly higher proportion of alcohol compounds than was predicted from experiments using the individually pyrolysed samples. This indicates that vapour phase extraction of hydroxyl radicals is induced by the presence of PP derivatives leading to alcohol products upon recombination with the PP radicals. Sajdak and Muzyka [165] examined co-pyrolysis of PP with different wood samples with synergy observed during analysis of the pyrolysis products. A mixture of biomass and PP (30% PP), led to a reduction of liquid yield with a comparable increase in solid and gas yield. The yield of CO and CO_2 were increased during co-pyrolysis with the overall effect that the oxygen content of the liquid decreased whilst the oxygen content of the gases increased.

2.5.3 Biomass and polystyrene

PS varies from the other polyolefin polymers (LDPE, HDPE, PP) in that it contains an aromatic group within the structure of the polymer. Li et al. [167] compared pyrolysis and co-pyrolysis of LDPE, PP and PS with cellulose. At 550°C PS produced the greatest aromatic yield at 80% of the carbon compared to 28% for LDPE and 35% for PP. PS also produced a much lower yield of alkanes and alkenes. Catalytic co-pyrolysis of the polyolefins produced aromatic compounds mainly through Diels-Alder reactions between furan and small alkene compounds, however this is limited in PS where there are fewer alkene compounds available. Zhang et al. [115] propose a different mechanism for PS which involves the PS polymer dissociating to produce the monomer material styrene which is itself a mono-aromatic compound. This styrene may then react with allene compounds, produced from the deoxygenation of furan derivatives, to produce two-ringed indane, and subsequently naphthalene compounds (Figure 2.28). This compares to reaction networks proposed by Cheng et al. [170], for production of aromatic compounds, from furan derivatives, over ZSM-5 catalyst. The formation of allene compounds is increased at elevated temperatures so increased temperature will also increase the proportion of bi-cyclic aromatics.
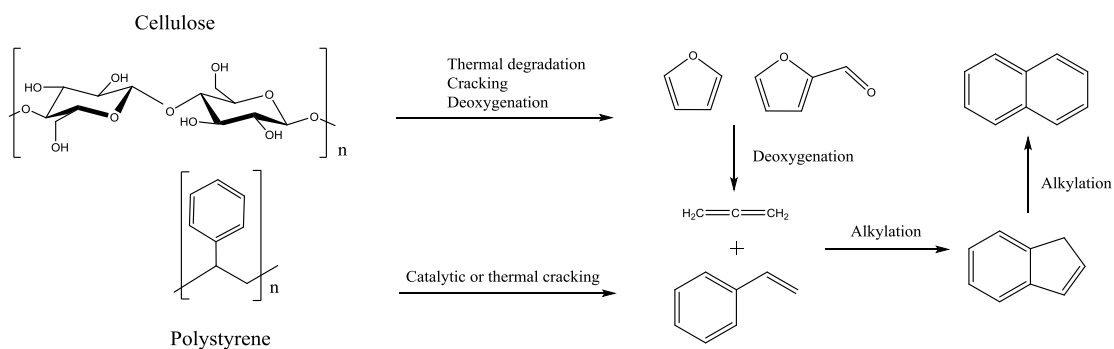
Figure 2.28: Co-pyrolysis of cellulose with polystyrene with ZSM-5 catalyst [167, 171].

Abnisa et al. [173] found that during co-pyrolysis of palm shells with PS the maximum liquid yield was achieved at temperatures between 500° and 600°C with liquid yield increasing at the proportion of PS in the mixture increases. This compares with results from Rutkowski and Kubacki [174] which found that cellulose produced 45.5 wt.% liquid yield compared to 94.8 wt.% for PS when pyrolysed individually. The relatively higher liquid yield from PS is reflected in the liquid yield from co-pyrolysis with different mixing ratios.

2.5.4 Biomass and polyethylene terephthalate

Pyrolysis of biomass with PET is not as thoroughly researched as other common waste polymers despite high usage and collection of the material. There are three main reason for this which are: high recycling rates of PET; high oxygen content of PET which may cause it to create poor liquid fuels; high formation of benzoic acid and terephthalic acid which are acids and can also cause deposition and clogging during pyrolysis processes. Dorado et al. [171] examined the origin of compounds produced during co-pyrolysis of cellulose and PET. The major product of pyrolysis was carbon oxides with about 75% of the carbon oxides sourced from the cellulose. The carbon monoxide yield was a slightly higher than that for carbon dioxide with cellulose providing 90% of the carbon monoxide and around 50% of the carbon dioxide. The experiment produced a greater alkene yield than aromatic yield with both cellulose and PET involved in alkene and aromatic synthesis. Dorado et al. [175] in separate research found that when PET was catalytically (H-ZSM-5) co-pyrolysed with Lignin, xylan, cellulose and switchgrass the yield of carbon which made up toluene, ethyl-benzene, xylene, naphthalene and methyl-naphthalene was increased compared to individual pyrolysis. Chen et al. [176] found synergistic effects during thermal co-pyrolysis studied through TGA of paulownia wood and PET. Synergy between PET and the biomass led to an increased degradation of PET at temperatures below 500°C whilst as the temperature increased beyond this point char yield was increased. The synergy was also observed as a change in weight loss during co-pyrolysis and temperatures at which decomposition occurs shifted slightly in co-pyrolysis samples.

2.5.5 Interaction of biomass and plastics overview

Zhang et al. [115] produced a simplified reaction scheme for catalytic co-pyrolysis of plastics with lignocellulosic biomass which is displayed in Figure 2.29. Both biomass and polymers crack to produce small compounds which may then react together to produce non-oxygenated aromatic compounds. The major interaction between polymers and lignocellulosic biomass appears to be between short chain alkenes and furan derivatives from cellulose and hemi-cellulose.
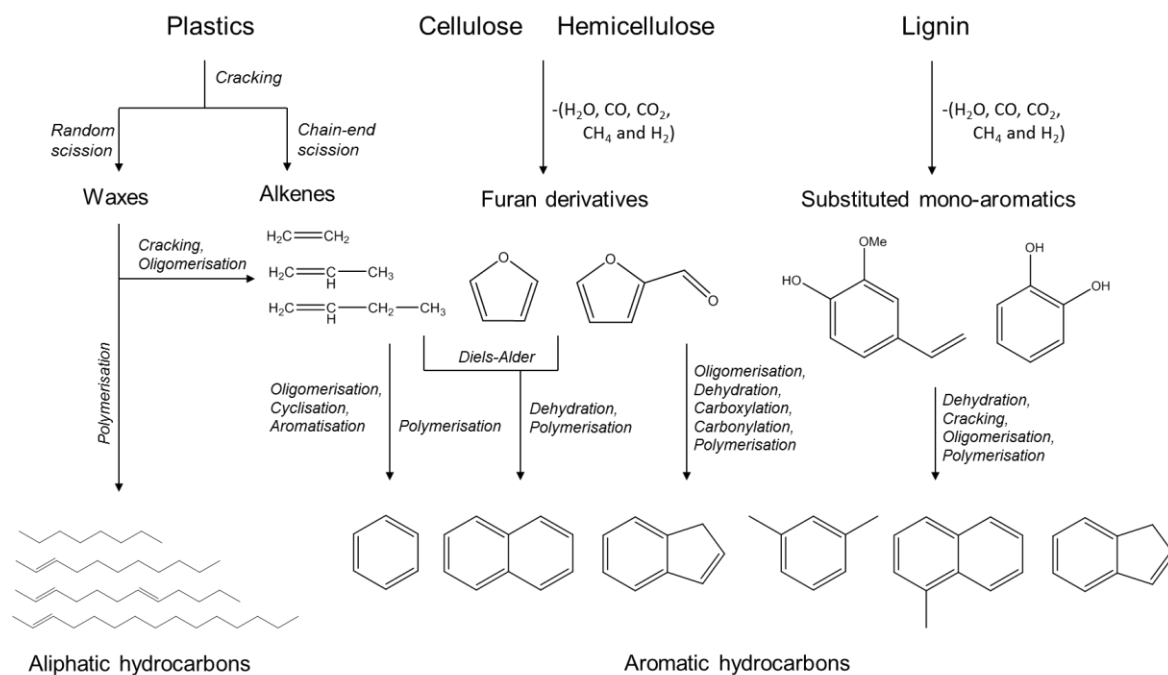
Figure 2.29: Overview of reactions participating in catalytic pyrolysis of biomass and polymers to produce aliphatic and aromatic hydrocarbons, adapted from Zhang et al. [115].

Abnisa et al. [164] explain that synergy is observed between biomass and polymers yet at this time knowledge of the mechanism is poorly understood this is in agreement with Zhou et al. [177]. Johannes et al. [178] found that synergy during co-pyrolysis can be both positive as well as negative and this may change depending on the conditions. Heating rate, temperatures and mixing of pyrolysis samples may all affect the synergy effect as well as solvents, catalysts and hydrogen sources. Onäl et al. [179] examined co-pyrolysis of HDPE and almond with an emphasis on synergy. The properties of the oils produced during co-pyrolysis improved with regards to use as a transport fuel. The positive synergy in this case was mainly attributed to hydrogen transfer from polymer decomposition, leading to a reduction in oxygenated compounds. However, the exact mechanisms are challenging to elucidate though due the wide array of chemical species involved during the process.

2.5.6 Metal impregnated ZSM-5 and co-pyrolysis

There is only very limited literature relating to catalytic co-pyrolysis of biomass and polymers with much of the research focusing on H-ZSM-5 with a little on H-Y (H-Y zeolite), FCC catalysts (fluidic catalytic catalysts (used)) and alumina

silicates [115]. Unsurprisingly there is also very little focusing on modified ZSM-5 catalytic co-pyrolysis.

Zhou et al. [180] examined the effect of boron impregnation (0.5-3 wt.%) on the effectiveness of utilising ZSM-5 for catalytic co-pyrolysis of biomass and cellulose for production of valuable monoaromatic hydrocarbons, particularly focusing on p-xylene. As an important precursor in the production of terephthalic acid and pharmaceutical products, p-xylene is more valuable than the meta- or ortho- isomers of xylene. It has been clearly demonstrated by Breen et al. [181] that simple impregnation of boron into ZSM-5 can be used to control the shape selectivity of products through pore restriction with the resulting product yield from alkylation of toluene achieving greater than 99% p-xylene selectivity using boric acid impregnated into ZSM-5 (10 wt.% boron) [182]. Zhou et al. [180] used TPD (Temperature programmed desorption) using NH_3 to study the effect of boron impregnation on acid sites in the ZSM-5 and identified that the addition of boron reduced the intensity of the strong, Brönsted acid sites, leaving the weaker Lewis acid sites relatively unaffected. This reduction in Brönsted acidity was considered to be due to the boron binding preferentially at these sites in the ZSM-5. The reduction in strong acid sites was suggested as the main reason for an increased monoaromatic yield and olefin selectivity whilst minimising the formation of PAH (polyaromatic hydrocarbons) compounds. Catalytic fast pyrolysis of cellulose was undertaken using a Curie-point pyrolyzer (590°C, 60s) with helium used to carry the vapours to a GC for quantification for hydrocarbon compounds and non-condensing gases by FID and TCD. The impregnation of boron was found to be most effective at 1 wt.% loading with an increase in the selective formation of p-xylene increasing from 48% to 75%. This increase in p-xylene selectivity indicates templating within the ZSM-5 pore where the p-xylene is the least sterically hindered form.

Lin et al. [183] studied phosphorus impregnation into ZSM-5 for catalytic co-pyrolysis of biomass and HDPE. The catalysts were prepared by wet impregnation of HZSM-5 with Ammonium phosphate dibasic ((NH_4)$_2$$HPO_4$) with different loading between 0 wt.% and 10 wt.% produced and these confirmed using XRF (X-ray fluorescence) spectrometry. The addition of phosphorus reduced both the strong acid and weak acid sites during NH_3-TPD analysis with this reduction attributed to phosphorus reacting with bridging hydroxyl groups in the ZSM-5. The prepared P-ZSM-5 was used for catalytic pyrolysis of wood plastic composites, formed from extrusion of finely milled poplar wood with HDPE (1:1 wt.%), using pyroprobe equipment (550°C, 30s) combined with online GC-MS for product analysis. The peaks in the MS chromatogram were

identified using the NIST compound library and literature for H-ZSM-5 and different loadings of P-ZSM-5. In the case of H-ZSM-5 69% of the peak area was composed of aromatic compounds and 2% of light aliphatic compounds (C_4-C_{12}). In contrast the P-ZSM-5 was composed of 57% aromatics and 4% light aliphatics at 2 wt.% loading and 34% and 15% respectively at 5 wt.% loading. The authors attribute this shift from aromatic compounds through to light aliphatic compounds during phosphorus impregnation to the reduction in acidity in the catalyst. As well as an increase in light aliphatics there was also an increase in oxygenated compounds identified in the MS results with an increase from 22% (peak area) in H-ZSM-5 to 32% and 42% at 2 wt.% and 5 wt.% phosphorus respectively.

Yao et al. [184] also utilised phosphorus for impregnation of ZSM-5 and examined the combined effect of phosphorus with nickel on the co-pyrolysis of biomass and LDPE. Their research aimed to use phosphorus to enhance the conversion of alkanes to alkenes which may then be available for further reactions such as aromatic formation such as through Diels-alder reactions. Their research used pyroprobe equipment (550°C, 60s) combined with online gas chromatography (TCD and FID) and in-situ ZSM-5 at a ratio of catalyst to feedstock at 15:1 (by weight) to pyrolyse pine wood sawdust and LDPE powder. The phosphorus catalyst was produced by wet impregnation of the zeolite with Ammonium phosphate dibasic ((NH_4)$_2$$HPO_4$) as with Lin et al. [183]. The nickel/phosphorus catalysts were produced by further impregnation with nickel nitrate solution (Ni(NO_3)$_2$). The impregnation of both nickel and phosphorus did not affect the structure of the ZSM-5 (XRD) but reduced the Brönsted acidity of the zeolite (NH_3-TPD). This reduction in Brönsted acidity occurred in the phosphorus impregnated catalyst and was further reduced in the nickel/phosphorus zeolite. For ZSM-5 ~30% of the carbon yield was in aromatic compounds which increased to ~33% for P-ZSM-5 (1.5 wt.%) and ~38% for Ni/P-ZSM-5 (1.9/2.0 wt.%). This increase in aromatic yield was accompanied by a similar reduction in char and coke yields. For both modified catalysts the alkane yield was reduced by a similar proportion compared to ZSM-5 yet the alkene yield was increased more in the P-ZSM-5. This indicates that some of the extra alkene compounds produced during the Ni/P-ZSM-5 catalysis have been converted to aromatic compounds. This is in part thought to be due to reactions between LDPE derived alkenes and biomass derived furans through Diels-alder reaction mechanisms to produce aromatics. The reduction in char and coke formation was attributed to the reduction in strong Brönsted acid sites which have been linked to coke formation through dehydration of oxygenated compounds derived from biomass [106, 185].

The impregnation of ZSM-5 with gallium was studied by Li et al. [186] for catalytic co-pyrolysis as a pathway for production of petrochemical feedstocks. Several gallium impregnated catalysts were produced using the wet impregnation with gallium nitrate $(Ga(NO_3)_3)$ or including the gallium within the structure of alumina silicate and MFI zeolites synthesised with Ga_2O_3 included in the synthesis gel mixture. Catalytic co-pyrolysis of pine sawdust and LDPE powder was conducted in using a pyroprobe microreactor linked through helium transfer line to GC using TCD and FID for quantitative analysis. The sample was heated at $20°Cms^{-1}$ to 550°C with the temperature held for 60s. Analysis of the catalysts found that the inclusion of gallium within the structure of the catalysts led to significant reduction in Brönsted acidity as bridging silanol groups with gallium (Si-O-Ga) rather aluminium (Si-O-Al) are more covalent [187, 188]. The gallium impregnation of ZSM-5 is mostly expected to remain external to pores and restrict the pore openings. Although some is gallium ions are likely to inhabit the active acid sites, a large proportion of the gallium is likely to be located on the external surfaces of the catalyst in the form of gallium oxide (Ga_2O_3) particles [189, 190]. This acts to restrict catalytic reactions to the internal surfaces which increases the effect of templating catalytic reactions. Li et al. [186] found that gallium wet impregnation on ZSM-5 lead to improved monoaromatic and p-xylene selectivity during biomass and LDPE co-pyrolysis. Monoaromatic carbon yield (C%) increased from ~23% through to 27% on addition of gallium at 5 wt.% loading and p-xylene selectivity increasing from ~2.5% through to ~4%. This is accompanied by a moderate reduction in polyaromatic formation (~2%) and a slight reduction in coke and char (~1%). This confirms the supposition that internal pore reactions are favoured over reactions on external surfaces as PAH formation is hindered inside the pores of ZSM-5 due to size restrictions.

Xiang et al. [191] studied cobalt impregnation for catalytic co-pyrolysis of biomass (rice straw, cellulose and lignin) and LDPE through TGA. Cobalt impregnation of ZSM-5 was completed using cobalt nitrate hexahydrate $(Co(NO_3)_2 \cdot 6H_2O)$. Powdered rice straw and LDPE (mixing ratio 4:1) were heated in the TGA from room temperature to 600°C at $30°Cmin^{-1}$ under a nitrogen atmosphere. The catalyst was used in-situ by mixing with the feedstock at 25 wt.% prior to heating. The results of the kinetic analysis showed synergy between the biomass and the polymer material with a reduction in activation energy whilst using the catalyst. This compared to research by Zhang et al. [192] who used unmodified ZSM-5 and concluded that co-pyrolysis of biomass and PE showed synergy in the form of reduced activation energy and this was increased through application of the catalyst. The interaction between cellulose

and LDPE appeared to be the strongest with that between lignin and LDPE relatively unaffected by co-pyrolysis.

It is noteworthy that each of these studies examined catalytic co-pyrolysis of PE with biomass with pyroprobe reactors combined with GC used for a majority of the analysis of pyrolysis products. Catalysis is in-situ and ratios of catalyst to feedstock of between 10 and 20 (by weight) are utilized to ensure adequate conversion in the short time period prior to online analysis. There is much less literature relating to co-pyrolysis of biomass and PS and an absence of literature on metal-impregnated catalytic co-pyrolysis of biomass and PS. The understanding of catalyst action is focused on surface area, pore volume and acidity of active sites to a high degree, whereas the interaction of metal atoms with reactive species during pyrolysis is much more challenging to measure and is far less extensively understood.

2.6 Compounds suitable for chemical feedstocks

Zhang et al. [115] compare the compounds which are produced selectively during catalytic co-pyrolysis and highlight that in many cases the compounds produced are valuable both for fuel use as well as for chemical synthesis. Petrochemicals are often sources from petroleum with some of the main target compounds including, benzene, toluene and xylene (BTX) as well as light olefins. These compounds are primary building blocks which may be used to synthesise other useful compounds particularly for producing solvents, plastics pharmaceutical and clothing (fibres). Zhou et al. [180] highlight the potential for biomass and cellulose to be converted into these valuable compounds using modified ZSM-5 to control co-pyrolysis and promote selectivity towards valuable aromatic products. Talmadge et al. [41] highlight the importance of removing oxygenated species in order to produce both fuels and valuable chemicals. This is often accomplished through expensive hydroprocessing however polymer donation of hydrogen may be a lower cost method to allow for selective production of valuable and useful products. As well as BTX, ethylbenzene and styrene are also compounds which are subject to high demand. This means they are more valuable as chemical feedstocks than as fuel components where separation is economically viable [193-196].

2.7 Summary of literature review

The literature available for this research field is extensive and useful, however, there are a number of key limitations.

i) Due to the complexity of pyrolysis for biomass and polymers a high proportion of the research focuses on the results of pyrolysis rather than the underlying mechanisms. Modelling has been utilised to explore the interactions and mechanisms which drive pyrolysis with general pathways proposed, accounting for the products of lignin, cellulose and hemi-cellulose with reasonable accuracy. The sheer scale of the challenge, however, leaves much remaining to be elucidated.

ii) The action of ZSM-5 catalysts has been understood in detail as these materials have been utilised in FCC processes for many decades. The utilisation of these catalysts for pyrolysis has benefited from much of this research however, as with the study of pyrolysis itself, the complexity has left much understood through general effects rather than through detailed analysis of mechanisms. This is also the case with metal loaded ZSM-5 catalyst with most studies showing the effect of the catalyst on the products rather than studying the underlying mechanisms involved. These studies into product yields and compositions are valuable, however, a more in-depth understanding would add greatly to this research field.

iii) Catalytic co-pyrolysis often uses ZSM-5 with limited research into metal-impregnated ZSM-5 catalysts. Those metal-impregnated catalysts which have been utilised in literature were focused on biomass and polyethylene with other plastics not closely examined.

iv) A particular problem across literature is the limited scale of research and the variations between each methodology. Wide variations exist in the literature with regards to polymer type, biomass type, sample mixing ratio, reactor type, reactor conditions, catalyst type, catalyst yield, analytical equipment and analytical output format to name a few of the multitude of variations. This makes comparison between research challenging and reduces the significance of any small variations observed as these could simply be due to variations in methodology.

The goal of this research was to provide a set of results which use consistent methodology and samples for pyrolysis, co-pyrolysis and catalytic co-pyrolysis such that variations between each may be clearly compared. This included determination of pyrolysis product yields (char, gas, liquid, oil), with detailed analysis of the oils and gases to observe the changes to the products caused by changes to variables. This research also examined a wide range of metal

impregnated catalysts, where in literature many projects are limited in scope. Catalytic co-pyrolysis for a sample composed of biomass and PS with metal-impregnated ZSM-5 is absent in literature so this was investigated. The co-pyrolysis experiments examined a wider range of mixture ratios compared to those examined in literature which are often limited to 1:1 mixture of biomass and polymer.

Chapter 3: Experimental

3.1 Introduction

There are four main sections which compose the experimental part of this research:

- The first section, presented in chapter 4, involved the preparation of a two-stage pyrolysis reactor. The reactor and methodology were initially tested to ensure that results could be obtained with suitable repeatability and all pyrolysis products were collected ensuring mass balances approaching 100%. The test experiments also allowed for establishment of analytical methodologies although these were further developed throughout the research. Once the reactor was prepared fully, the initial experimental section examined catalytic and non-catalytic pyrolysis of biomass, using both unmodified and metal-impregnated ZSM-5.
- The second section used TGA-MS to study the devolatilisation process for biomass and polymers. This was completed for both individual samples, as well as mixed samples of biomass and polymers to model devolatilisation during co-pyrolysis.
- The third section used the two-stage reactor to study the catalytic co-pyrolysis of biomass with polymers using a range of mixing ratios using unmodified ZSM-5.
- The fourth section studied the catalytic co-pyrolysis of biomass with PS, with a particular focus on the combined effect of both metal impregnated ZSM-5 and the mixing ratio of the pyrolysis sample.

3.2 Biomass and waste plastic samples

Six samples were used for all of the experiments. The six sample materials were as follows, biomass (BMS), high-density polyethylene (HDPE), low-density polyethylene (LDPE), polypropylene (PP), polyethylene terephthalate (PET) and polystyrene (PS). The samples were selected with the aim of elucidating real-world situations, so a mixture of recycled and virgin material was used.

The biomass sample used was a mixed source wood pellet supplied by Liverpool Wood Pellets [197], a company which manufactures wood pellets from UK sourced virgin wood, these pellets are equivalent to those which would be used in a domestic heating system.

The polymer materials were from two different sources. The virgin materials, LDPE and PET were sourced from Sigma-Aldrich Limited [198, 199]. The LDPE

was a pure pelletised material whereas the PET contained 30% glass reinforcement material. Reinforcement is used with PET products particularly with regards to improving electrical properties or for improving performance and endurance of mechanical components. The reinforcement can increase stiffness, toughness and chemical resistance. However, these improved properties increase difficulty for recycling the polymer. Pyrolysis provides a potential method for PET utilisation with the reinforcement material remaining in the char formed during pyrolysis whilst the volatiles are collected separately. The PP, HDPE and PS polymers were also in pellet form but were produced from recycled polymers and were provided by Regain Polymers Limited, Castleford, UK (now ImerPlast UK Ltd.) [200].

Figure 3.1 shows photographs of the materials as they were received, before they were prepared for analysis or pyrolysis experiments. Each of the materials is in a homogenous, pelletised form. It is possible to assume that the polymers are similar to each other, particularly when considering the chemical composition. However, there are both physical and chemical differences between each polymer which can be observed in the pellet structure and the response of each material to compression. There are also variations in colouration which are likely to be partially due to dyes within the recycled materials.

Figure 3.1: Photographs of the samples used during pyrolysis.

3.3   Sample preparation

The biomass and plastics (HDPE, LDPE, PP, PET and PS) samples were received in pellet form and were then prepared for pyrolysis or material

analysis. The biomass pellets were approximately 10mm x 5mm x 5mm in a densely packed cylindrical form and were prepared for the pyrolysis experiments using a cutting mill to produce a homogenous woodchip which was passed through a multiple sieve system to collect a sample between 2.8mm and 1.0mm in size. The polymer materials were received as pellets and were approximately 3 mm^3 and were used for fixed bed pyrolysis without further reduction processing. Proximate and ultimate analysis requires a finely ground homogenous sample to ensure measurements are precise and representative of the entire sample so for these methods the samples were prepared by grinding at low temperatures in a Freezer Mill 6770 using liquid nitrogen (-196°C) to enable the reduction of the material to lower than 90 μm. TGA analysis was initially undertaken at Leeds University to gain insight on the thermal degradation of the samples prior to starting experiments using the pyrolysis reactor. Further analysis was conducted at Tsinghua University, Beijing, China as part of a researcher exchange scheme, using TGA in conjunction with mass spectrometry equipment to examine in detail the thermal degradation of biomass and polymer samples during pyrolysis and co-pyrolysis. Samples which were used for TGA-MS studies at Tsinghua University were prepared by grinding using a mechanical mill to lower than 250 μM.

3.4   Proximate and Ultimate Analysis

Proximate and ultimate analysis was used to determine the composition of the pyrolysis samples. The proximate analysis uses a furnace to devolatilise and combust samples according to set standards to determine the comparative proportion of char, ash, volatile gases and moisture which are formed by thermal decomposition of the samples under standard test conditions. The procedure used followed standards which were developed for use with biomass, but the same methodology was also used for the polymers to maintain consistency between treatment of the samples. The procedure requires samples to be milled to smaller than 1000 μM after which three methods were used for the analysis.

Moisture content was determined according to standard BS EN 14774-3:2009 [201]. This involves heating the sample for 2 hours in a furnace at a fixed temperature of 105°C. A pre-dried and pre-weighed glass vessel with a lid was used for this method in accordance with the standard. The lid was heated in the oven with the vessel throughout the procedure as was then placed onto the vessel immediately on removal from the furnace to prevent moisture returning to the sample during cooling. The weight of the vessel and remaining sample was determined using a balance and the moisture content determined as the

change in sample mass between the original sample and the sample after the drying process.

Volatile content was determined using the standard BS EN 15148:2009 [202]. A pre-dried sample was heated in a furnace fixed at 900°C for 7 mins in a pre-dried and pre-weighed silica crucible with lid which remained on the vessel throughout the procedure. Once the sample was removed from the furnace it was allowed to cool before being weighed on a balance. The mass change between the initial sample and the sample post-heating is due to loss of volatiles from the sample.

Ash content was measured in accordance with the standard BS EN 14775:2009 [203]. Each sample was heated in a furnace in an inert shallow flat-based silica dish with the temperature of the furnace ramping from room temperature through to 250°C at a heating rate of approximately 5°Cmin^{-1}. After this temperature was reached the furnace remained at 250°C for 60 mins before a further heating stage from 250°C through to 550°C at a rate of 10°Cmin^{-1}. This temperature was held for 120 mins although if the material was not fully decomposed to ash during this time period a longer time period the sample should be held at this temperature for longer to ensure complete ash formation. This was not needed for these samples. This was undertaken in a furnace with adequate oxygen supply for all carbon material to be completely combusted.

Ultimate analysis was undertaken using carbon, hydrogen, nitrogen and sulphur analysis (CHNS) according to the standard BS EN 15104:2011 [204] using a Thermo EA-2000. This involves combusting a known quantity of sample, in a tin capsule, in the presence of a predetermined quantity of an oxidising agent, in this case vanadium pentoxide (V_2O_5). The combustion at 1000°C causes oxidation of all present carbon, nitrogen and sulphur atoms into CO_2, NO_2 and SO_2. The NO_2 is reduced to N_2 in a secondary reaction step and the three gases are separated through a gas chromatograph (GC) column and pass across a thermal conductivity detector (TCD) using an inert carrier gas (Helium) at which point they are quantified. Standards are analysed alongside the unknown samples to confirm that the analysis is providing accurate values. In this case repeated measurement of oatmeal and BBOT (2,5-Bis(5-tert-butyl-benzoxazol-2-yl)thiophene) were used as standards alongside an empty tin capsule and blank samples with barley flour was analysed after every eighth unknown sample to confirm that the values remained consistent. Approximately 3 mg of sample was used in each capsule measured to 2 decimal places.

The oxygen content may be calculated by difference however it is more accurate to measure the oxygen separately using CHNS-O analysis which has been calibrated to quantify the oxygen accurately. In this case silver foil capsules are used and the combustion at 1000°C releases volatiles which react with a nickel carbon catalyst to produce carbon monoxide from all present oxygen. The CO and N_2 are then carried by the inert carrier gas, helium, separated by GC and quantified using a TCD. Standards of acetanilide, benzoic acid and aspartic acid are used to calibrate the process to determine accurate oxygen values. For both methods duplicate analysis of samples was used.

3.4.1 Biomass composition

For all of the experiments a single homogenised batch of biomass was used. The biomass material was chosen to be a high quality, consistent and homogeneous material such that variation between experiments would be minimised whilst still representing a real-world biomass source as might be available to a commercial pyrolysis operator. The material contains a relatively low ash and moisture content which ensures that detrimental effects due to these species are limited.

The ash content of a biomass source can contain a wide range of metals including alkali metals, potassium and sodium; alkaline-earth metals, calcium and magnesium; as well as heavy metals including the transition metals copper, and nickel. These elements are accumulated by plants as they grow by bio-accumulation with the soil being a primary source of nutrients and contaminants. These species may be advantageous for plant growth for example potassium which is a vital nutrient for plant development, but can also have an influential catalytic effects during pyrolysis [10, 27, 58, 205]. The composition of the biomass sample was ascertained by proximate and ultimate analysis and the results of this are provided in Table 3.1, however Thermogravimetric analysis (TGA) was also used to provide further elucidation of the manner in which the material undergoes devolatilisation in an oxygen free atmosphere comparable with pyrolysis.

The TGA was undertaken using a TA TGA Q5000 IR with the sample heated from room temperature through to 1000°C at a ramping rate of 10°Cmin^{-1} in a nitrogen atmosphere flowing at a rate of 50mLmin^{-1}. The prepared sample (~25mg) was placed in a pre-weighed and tared platinum pan which remains inert through to high temperatures. A data point was collected every 0.1s during heating. The weight change and differential weight change give key information about the devolatilisation process.

Table 3.1: The composition of the biomass sample, as determined by proximate and ultimate analysis.

Biomass	As received	Dry	Dry ash-free
Proximate Analysis			
Moisture (wt%)	7.77	-	-
Volatile (wt%)	86.43	93.70	93.32
Fixed Carbon (wt%)	5.50	5.97	6.68
Ash (wt%)	0.30	0.33	-
Ultimate Analysis			
C (wt%)	46.07	49.95	50.11
H (wt%)	4.97	5.39	5.40
N (wt%)	0.12	0.13	0.13
S (wt%)	0.00	0.00	0.00
O[a] (wt%)	44.67	48.43	48.59
GCV[b] (MJKg^{-1})	18.10	19.65	19.72

[a] Determined by direct oxygen analysis

[b] Predicted from Friedl et al. 2005 [206]

The composition may be defined according to three basis. The first, 'as received' (ar), determines to what extent a component (volatiles, moisture, hydrogen etc.) of the sample contributes to the total weight of a sample which is being examined. The second, 'dry basis' (d) determines to what extent a component contributes to the proportion of the sample which is not composed of moisture. This allows samples which contain varying levels of moisture to be compared. The third, 'dry ash-free' (daf) shows the value for the portion of the sample not composed of ash or moisture. This allows the composition of the reactive hydrocarbon part of the sample to be examined, unaffected by the ash and moisture in the sample.

The gross calorific value (GCV) is the total energy contained within a sample without taking into account any energy which would be needed to remove moisture through evaporation. This is often determined using a bomb calorimeter however Friedl et al. [206] developed an empirical equation which could be used to accurately predict the calorific values of biomass samples using the carbon, hydrogen and nitrogen content of the samples. The standard error between predicted values and measured values using this method is approximately 2% of the GCV.

Table 3.1 shows that the sample contains approximately 8 wt.% moisture. This moisture will pass out of the sample during devolatilisation and in doing so will create fissures within the biomass particles. This moisture having passed out of the sample will travel through the reactor and into the condenser, therefore,

any bio-oil collected will contain this moisture. Under the conditions used during proximate analysis [201-203], 86 wt.% (ar) of the sample will become volatiles and pass from the reactor into the condensers. The conditions are different in the case of proximate analysis and the pyrolysis reactor [26, 27, 30, 40] which will affect the volatiles yield. Both the heating rate and maximum temperature are significantly lower in the two-stage pyrolysis reactor than in the proximate furnace. Guedes et al. [40] compared a large number of bio-oil production experiments and found that in general a higher heating rate and higher maximum temperature will both lead to more volatiles and therefore less fixed carbon. However, as temperatures rise above 500°C the increased formation of coke and gas can reverse this trend. These volatiles will leave the pyrolysis sample and pass over the catalyst in the second stage of the catalytic pyrolysis experiments.

The ash content is low at just 0.3 wt.% (ar). Phyllis 2 [207] is a database which contains composition values for a wide range of biomass samples which have been accumulated from researchers investigating biomass. Comparison of the ash content measured during this study with samples entered into the Phyllis 2 database showed strong correlation to untreated and oven-dried pine wood (46 samples (ar), range: 0.07-5.74 wt.%), median: 0.41 wt.%, and mean: 0.62 wt.%) [9, 208]. The fixed carbon value 5.5 wt.% indicates that any char collected is predominately composed of carbon and would therefore have a potential use for combustion to produce process heat.

Elemental analysis of the biomass sample puts carbon at 46 wt.% (ar), hydrogen at 5 wt.% (ar) and oxygen at 45 wt.% (ar) with a low proportion of nitrogen (0.12 wt.%). This provides all the elements necessary for hydrocarbon bio-oil production however if the high oxygen concentration present in the sample is transferred to the bio-oil which would be expected this is likely to produce oils with high proportions of oxygenated compounds.
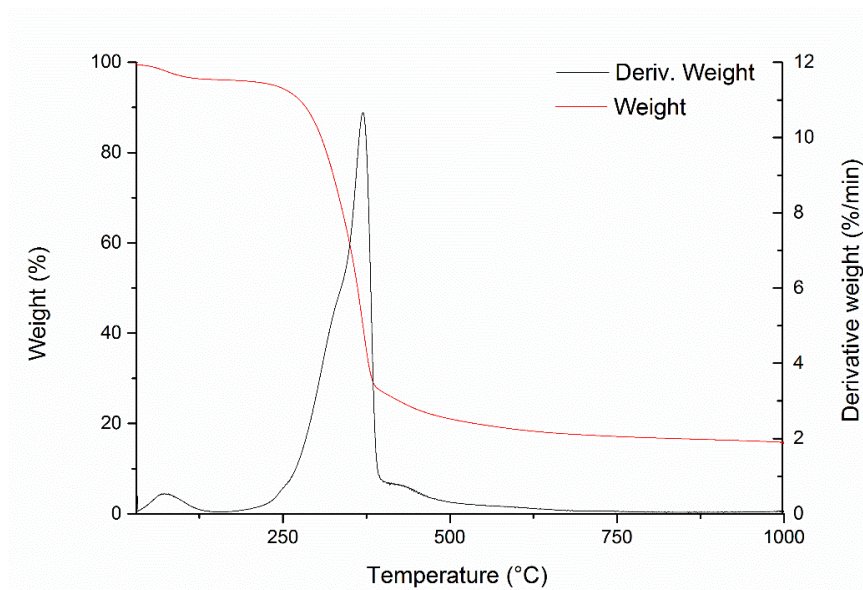
Figure 3.2: TGA and DTG showing devolatilisation of biomass sample heated from room temperature to 1000°C at 10°C/ min in a nitrogen atmosphere.

As well as elemental composition the TGA and DTG graphs give further information about the biomass sample by observing the devolatilisation of different components of the biomass. In contrast to the proximate analysis, the TGA method follows a much closer heating profile to that which was used during the pyrolysis experiments. Initially (below 100°C) a weight loss is observed which is associated with drying of the sample. At approximately 250°C the sample begins to reduce in weight and this continues until approximately 400°C. After this point further weight loss is observed but this is much more limited in scope. Most of the weight change is concluded by around 500°C although there is a slight continued weight loss as temperatures increase through to 1000ºC.

These are four main thermochemical processes which contribute to this weight loss. Studies of lignocellulosic biomass decomposition have found that the shape and position of the major peak during biomass devolatilisation is due to thermal decomposition of cellulose. A shoulder feature is also observed on the front face of the cellulose peak and this is due to thermal degradation of hemi-cellulose which is similar in composition to cellulose, but which degrades at a slightly lower temperature. At around 400°C the main peak has declined but there is still a continued region of weight loss, this is due to lignin decomposition which occurs over a broader temperature range than either hemi-cellulose or cellulose. However, the lignin peak is mostly hidden by the other two features [34, 35, 67, 69, 209].

As temperatures increase above 500°C there is ongoing decomposition of fixed carbon within the char, however, without the presence of oxygen to bring about char combustion this is a much more limited weight loss than the with the other materials. Once a temperature of 500°C is reached there remains approximately 20 wt.% of the original material which indicates that pyrolysis experiments using a similar heating profile are likely to also produce around 20 wt.% char yield.

3.4.2 Composition of plastics

The composition of the polymers also needs to be evaluated to ensure that any difference between them are accounted for during the research. The proximate and ultimate analysis for all the plastic samples is shown in Table 3.2 including biomass for comparison.

Table 3.2: Proximate and ultimate analysis of biomass and plastic samples used for pyrolysis experiments – oxygen values directly measured with value by difference in brackets.

	Basis	Units	Biomass	HDPE	LDPE	PET	PP	PS
Moisture	a.r.	wt%	7.8	0.0	0.0	0.0	0.0	0.0
Ash	dry	wt%	0.3	4.1	0.3	42.7	0.8	1.6
Volatile	daf	wt%	93.3	98.1	100.0	94.6	100.0	100.0
Fixed Carbon [a]	daf	wt%	6.7	1.9	0.0	5.4	0.0	0.0
GCV [b]	dry	MJkg^{-1}	19.6	47.5	51.2	16.4	46.2	47.5
Elemental								
C	daf	wt%	50.1	82.5	83.3	69.0	81.0	87.8
H	daf	wt%	5.4	13.1	12.6	5.0	11.4	9.5
O	daf	wt%	48.6	1.8	0.7	32.7	0.6	0.0
N	daf	wt%	0.1	0.1	0.1	0.0	0.1	0.0

a - determined by difference   b - predicted from Friedl et al. 2005

HDPE and LDPE have very similar chemical compositions with the difference lying in branching of polymer chains leading to differing mechanical properties [89]. However, in this case, the HDPE is a recycled material whereas the LDPE is virgin, the comparison between them might elucidate whether using recycled

materials for pyrolysis causes issues. When the elemental composition is compared there is very little difference with the more branched LDPE containing a marginally greater ratio of carbon to hydrogen as would be expected from the chemical structure.

The recycled HDPE contains twice as much oxygen as the virgin LDPE which might be a drawback for fuel production although this is far lower than in the biomass sample. The LDPE contains only a small amount of ash and no moisture was determined during proximate analysis. This is expected in a virgin material and the volatiles analysis indicated 100% conversion to the volatile phase which could potentially lead to high oil yields. The HDPE had a much higher ash content than the LDPE (4.1 wt.%). This ash might be inert and therefore the only detriment would be to conversion efficiencies alternatively it may contain material which can act as a natural catalyst or contain toxic and harmful substances in which case scale-up of pyrolysis would need to be carefully considered. The composition of the ash will not be dealt with further here as it is outside the envelope of this research.

The PET contains 30 wt.% ground glass reinforcement which is reflected in the high ash content although the ash content is greater than 30 wt.% which suggests a relatively high ash content even without the reinforcement material. This is likely to lead to a large reduction in oil yields however, pyrolysis presents an opportunity to isolate the glass material from the PET material which may be utilised for other purposes. The oxygen content for PET is also at 32.7 wt.% which matches with the chemical structure of PET ($C_{10}H_8O_4$) containing four oxygen atoms per monomer unit which would give 33 wt.% oxygen. This high oxygen content in the sample is likely to be expressed in the oxygen content of the pyrolysis oils.

The PP was very similar to the LDPE and had ash, fixed carbon and oxygen content which were all low. The PS is the only sample for which no oxygen was measured in the elemental analysis although the ash content was greater than with the virgin polyolefins (LDPE & PP) which is unsurprising considering the PS is a recycled material. Despite the PS being from a recycled source there was still a considerably lower ash content than for either PET or biomass. As with LDPE, the PS produced 100 wt.% volatiles if the ash and moisture is overlooked. This gives the potential for high oil yields during pyrolysis.

3.5   Reactor experiments

The pyrolysis experiments used a two-stage fixed bed reactor with independent temperature control for each reactor stage and controlled nitrogen gas flow

through the reactor. The nitrogen gas flow entered the reactor at the top and passed down through the first stage, which contained the pyrolysis material in a steel container, and then through the second stage, which contained a catalyst bed laid onto quartz wool which was supported by a steel grid, and out through the lower part of the reactor, through a three stage condensing system, and finally into a gas bag. The diameter of the reactor was 40 mm with a vertical height of 470 mm giving a volume of approximately 0.59 L with a 200 mLmin^{-1} flow of nitrogen used for the experiments. For each experiment 2.0g of pyrolysis sample and 4.0 g of catalyst were placed into the reactor and the inert nitrogen gas flow was initiated. The flow at the outlet of the condenser system was measured to ascertain that the inlet flow matched the outlet flow, therefore ensuring that there were no leaks.

The reactor was heated according to the following procedure. Firstly, the second stage which contained the catalyst was heated at 50°Cmin^{-1} up to the operation temperature, usually 500°C. Once this temperature was reached, and was stabilised, the first stage containing the pyrolysis sample was heated at 10°Cmin^{-1} up to the operating temperature, usually 500°C. The heating time was 50 minutes with the temperature held for 20 mins and then the heating was switched off to allow the temperature to fall for 20 mins to ensure pyrolysis is no longer progressing once the condensing and gas collection systems are dismantled for analysis. The gas from pyrolysis was collected during this 90-minute period.

During pyrolysis the gases passed through a three-stage condenser system which was composed of three glass vessels cooled by dry ice. Any gases which were non-condensing passed through the condensers and into the gas bag where they were collected for analysis. At the end of the reactor operation the gas bag was sealed followed by the condenser system using rubber bungs and Parafilm^{TM} to ensure a full seal. At this point the condensers were brought up to room temperature to remove external condensation, which would hinder accurate weighing of the liquid yield, using cold water and dried externally using paper towel. The change in weight of the condenser system before and after pyrolysis was used to determine the liquid yield from pyrolysis. The non-condensing gas was collected in a 25L Tedlar^{TM} bag which had both an inlet valve and an injection port for later analysis.

Before each experiment, both the catalyst and pyrolysis sample were carefully weighed as well as each of the parts of the reactor including the vessel containing the pyrolysis sample and the grid and quartz wool holding the catalyst. The condenser system was weighed independently before and after

the experiment, liquid and solid yields could be determined from the change in mass of the reactor and condensers with gas yield determined using gas chromatography (GC).
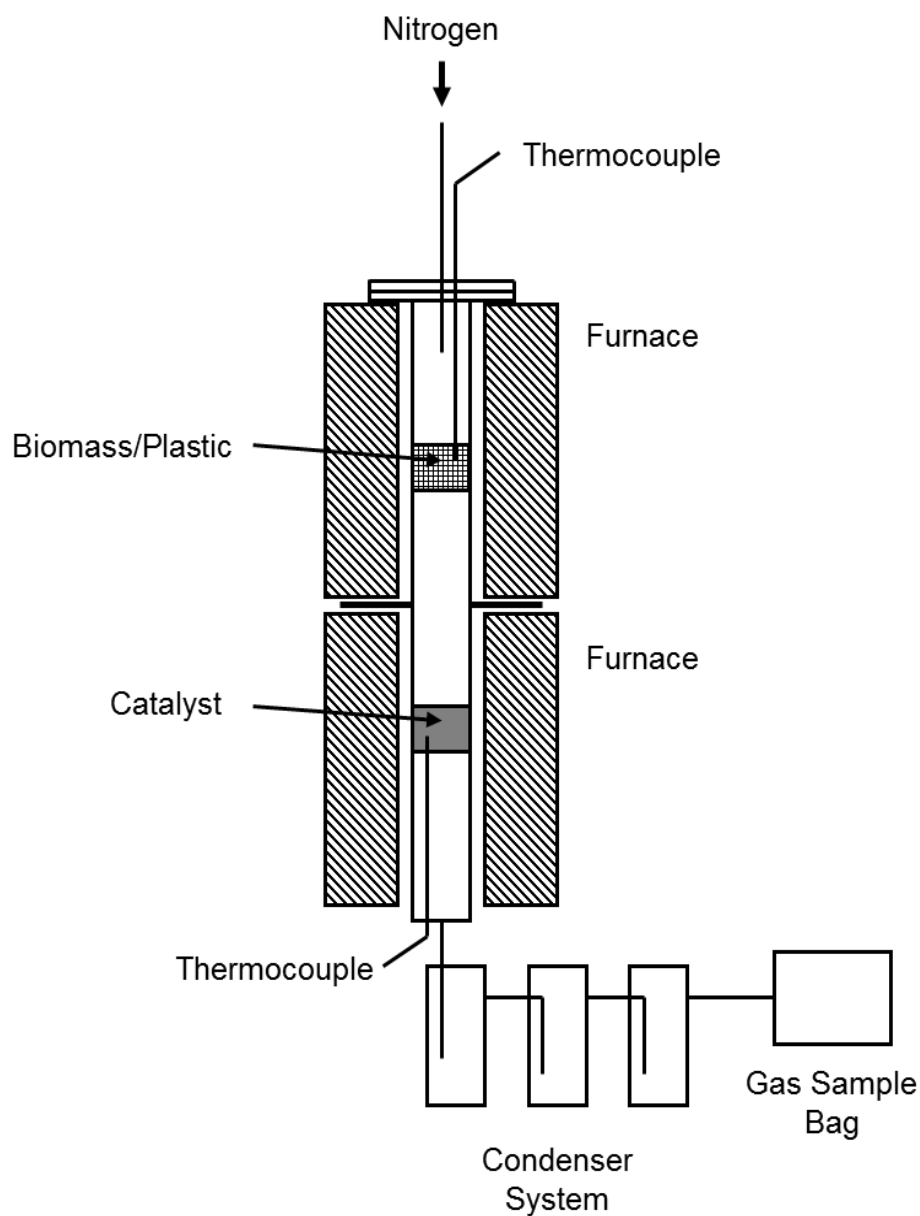
Figure 3.3: Diagram of the two-stage, fixed bed pyrolysis reactor.

Figure 3.3 is a diagram of the two-stage pyrolysis reactor with a photograph of the equipment in Figure 3.4 with each of the main components labelled (a-g).
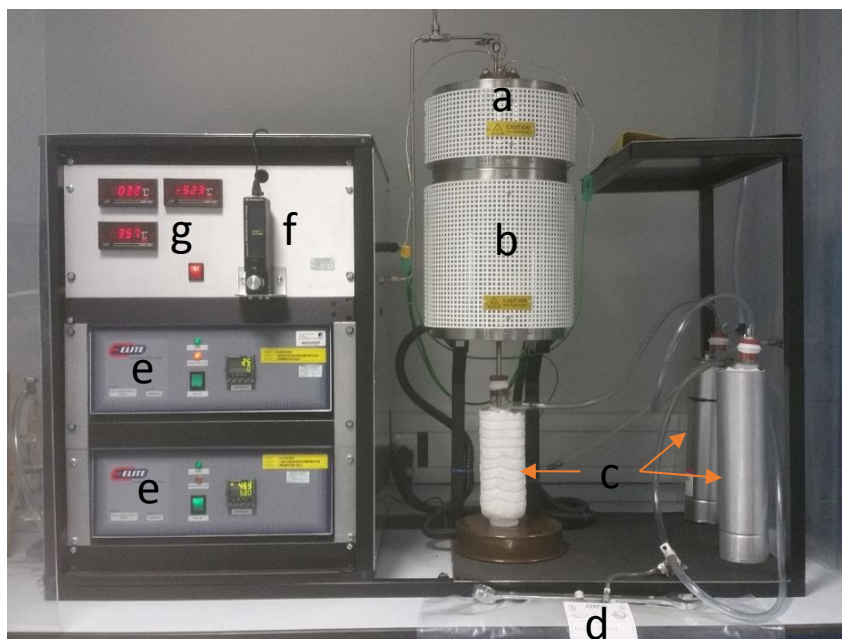
Figure 3.4: Photograph of the 2-stage pyrolysis reactor used for the pyrolysis experiments: (a) pyrolysis reactor, (b) catalysis reactor, (c) condensers, (d) gas collection bag, (e) reactor temperature control equipment, (f) gas flow meter and (g) thermocouple temperature displays.

3.6   Gas analysis

Gas was collected during the pyrolysis experiments during sample heating using a 25 L Tedlar® gas bag. This gas was analysed offline using three GC instruments which were configured and calibrated for quantitative analysis of key compounds. The first instrument, a Varian CP-3380 analysed the permanent gases (H_2, O_2, N_2 and CO) with using argon as the carrier gas and a 2 m x 2 mm column packed with a 60-80 mesh molecular sieve and a thermal conductivity detector (TCD). The second instrument was also a Varian CP-3380 but with a HayeSep column and was configured to measure carbon dioxide also using a TCD. The third instrument was used to determine hydrocarbon gases (C_1-C_4), used nitrogen as a carrier gas and a 2 m x 2 mm stainless steel column packed with Hysesp, 80-100 mesh using a flame ionisation detector (FID). Calibration was achieved using known standards these were used to calculate response factors (RF) for each gas. The results indicate relative proportion of each gas. From these values two assumptions can be used to calculate the weight of each gas produced during the experiment. Firstly, that the nitrogen flowrate in the reactor was constant and recorded accurately, secondly that 1 mole of gas at standard temperature and pressure has a volume of 22.4 L in accordance with the ideal gas law. Each gas sample was injected three times with the average used to calculate the gas yield.

3.7 Liquid yield collection

From each experiment the pyrolysis oil was removed from the condenser system using 10 ml of solvent, dichloromethane (DCM) or methanol depending on the pyrolysis sample and therefore the proportion of moisture in the liquid yield. The liquid was transferred to dark borosilicate glass vials to reduce the possibility of light triggered side reactions occurring prior to offline analysis. Pyrolysis oils from biomass samples contain a high proportion of water and polar oxygenated compounds which have low solubility in dichloromethane, methanol is more polar than DCM and is able to dissolve both the water and these polar compounds. In the case of polymer pyrolysis products these produce more non-polar compounds and much less water and are therefore less soluble in methanol. When methanol was used to collect these samples the non-polar compounds precipitate out of solution which presents challenges for analysis. It was found through experimentation using mixed biomass and polymer samples that where the sample contained 50 wt.% biomass or greater the liquid product would dissolve fully in methanol without phase separation or precipitation. In mixtures where biomass content was below 50 wt.%, complete solubility was achieved in DCM but phase separation and precipitation was often observed with methanol. Table 3.3 shows the solvent which was used for experiments based on the mixing ratio of the pyrolysis sample. This ensures that each set of experiments conducted with the same mixing ratio uses the same solvent whilst there is variation at different mixing ratios to ensure that liquid products are not being missed by offline analysis through phase separation or precipitation of compounds.

Table 3.3: Solvent choice for extraction and analysis of pyrolysis liquid for experiments. Dependent on the mixing ratio of the pyrolysis sample.

		Plastic			
		100%	50%	20%	0%
Biomass	100%				Methanol
	80%			Methanol	
	50%		DCM		
	0%	DCM			

Prior to water or oil analysis the sample had to be divided into two homogenous and even parts. The lining of the GC-MS column, which was used for oil analysis, is susceptible to damage if excess water is passed through so it was necessary to dry the liquid sample prior to injection. In contrast the Karl-Fischer

water titration requires that water is not removed in order to ensure values are accurate. This separation was accomplished through pipette transfer. The sample was agitated before and during transfer to ensure a homogenous sample with the pipette sample drawn from upper, middle and lower parts of the vial to ensure that any separation based on density should not result in differences in the separated samples.

3.7.1 Repeatability of experiments

Due to the scale of the research and the necessity to undertake a large number of experiments to establish the products of pyrolysis for a range of factors prior to examining the novel catalytic co-pyrolysis part of the research, it was not possible to repeat all experiments. Repeats were undertaken when anomalies were observed in the results or mass balance values. It is important for good repeatability during experiments to ensure that values which are measured during each experiment do not vary to a high degree and to understand the degree of confidence which can be attributed to values which are similar. Before the research was started the equipment was tested and methodologies examined and improved to ensure that mass balance values close to 100 wt.% could be achieved consistently and the mass of each contributing product was determined such that a standard deviation between values could be calculated. Table 3.4 shows the product yields which were determined using the established equipment. The lowest deviation was observed in the weight of char measured after pyrolysis with the largest deviation present in the mass balance value. This is expected as the mass balance is calculated using the other measured values, each of these values carry their own deviation.

Table 3.4: Values measured during repeated pyrolysis of 2g of the biomass sample with 2g of ZSM-5 and sand at 500°C with mean and standard deviation calculated to show the repeatability of experiments using the reactor and condenser equipment.

	ZSM-5 Exp 1	ZSM-5 Exp 2	ZSM-5 Exp 3	ZSM-5 Exp 4	Mean	Standard deviation (s)
Mass balance (wt.%)	96.7	99.2	101.7	98.8	99.1	2.05
Char (wt.%)	25.0	25.5	25.5	25.0	25.3	0.29
Liquid (wt.%)	49.0	49.5	51.5	51.0	50.3	1.19
Gas (wt.%)	25.5	23.0	24.5	25.0	24.5	1.08
	Sand Exp 1	Sand Exp 2	Sand Exp 3			
Mass balance (wt.%)	99.0	96.6	100.1	-	98.6	1.79
Char (wt.%)	26.5	25.5	25.5	-	25.8	0.58
Liquid (wt.%)	53.0	50.0	52.6	-	51.9	1.63
Gas (wt.%)	19.0	18.5	21.0	-	19.5	1.32

3.8   Oil analysis

3.8.1 GC-MS procedure

The sample which was prepared for GC-MS analysis required drying prior to analysis to protect the GC-MS equipment. The sample was dried by using a flash column prepared with 6g of anhydrous sodium sulphate. Sodium sulphate has a high drying capacity and does not interact with functional groups such as alcohols, phenols, ketones, aldehydes and esters. The sample was applied to the flash column and allowed to pass through using gravity, once the sample passed onto the column it was washed with 2 x 2.5mL of the solvent. The dried sample was loaded into a sample vial and 2µL injected into the GC-MS column using an auto-sampler. Each sample was analysed in the GC-MS using two methods which were optimized to maximize the separation of compounds whilst ensuring elucidation of a wide a range of compounds. Both methodologies were calibrated using known compounds with one optimized to elucidate aromatic compounds and one to elucidate oxygenated compounds. The aromatic methodology was used for all of the peak areas with the oxygenated methodology used to elucidate compounds which were not clearly elucidated using the aromatic methodology.

The GC-MS equipment was a Varian CP-3800 GC with Saturn 2200 MS containing a 30m x 0.25mm VF-5 MS column which combines selective separation of aromatic compounds with inert handling of polar and semi-polar compounds such as phenol. The GC temperature was increased step-wise during the procedure to increase the separation of the compounds whilst ensuring all suitable compounds could be eluted during the procedure.

The resulting chromatogram was matched against the calibration to identify key compounds with other compound peaks identified through matching against the National Institute of Science and Technology (NIST) compound library. This library contains mass spectrum data consisting of ionization peak position (m/z) and relative peak heights for a large number of compounds. Separate calibration was performed for both the DCM and methanol solvents with four-point calibration performed for both aromatic and oxygenated compounds. Calibration was performed with four increments, 100ppm, 80ppm, 40ppm and 20ppm.

3.8.2 Calibration of GC-MS

The resulting chromatogram was matched against the calibration to identify key compounds with other compound peaks identified through matching against the NIST compound library. Separate calibration was performed for both the DCM and methanol solvents with four-point calibration performed for both aromatic and oxygenated compounds. Calibration was performed using four increments, 100ppm, 80ppm, 40ppm and 20ppm. Quantitative analysis was possible for the calibrated compounds, however, any compounds identified only through library matching may only be evaluated as semi-quantitative. Combining of calibrated and non-calibrated results would result in distortion of the results, therefore because a significant proportion of the pyrolysis oils could not reasonably be analysed with full calibration, the oil analysis utilised only the non-calibrated values which are labelled accordingly as relative abundance (area%).

The calibration of the equipment gives important information about the elution of compounds through the GC column and the response of these compounds as they pass through the detector. The calibration was used initially to establish the retention times and ion pattern for known compounds such that it is possible to identify these with confidence in the oils which were to be analysed. Figure 3.5 shows a chromatogram for oxygenated compounds (see Table 3.5) used to calibrate the GC-MS equipment using DCM as the solvent. The temperature profile of the procedure was adjusted to ensure that compounds could be distinguished and so that a wide range of compounds present in oil samples would elute during the analysis. The compounds with lower boiling points generally elute before those with higher boiling points with polar compounds also eluting faster generally due to the relatively non-polar nature of the stationary phase. It can be observed that the response factors are different for each compound which means that fully qualitative analysis is not possible unless each compound in the oil sample has been calibrated. However, it is possible to undertake semi-quantitative analysis where there is a linear relationship between compound concentration and MS response. The values obtained will not be absolute values but a difference between two samples should be evident in the values in the resulting chromatogram. Known standards were used to calibrate the GC-MS equipment with retention times and response factors determined for each of the solvents used (methanol or DCM) (see Table 3.7 and Table 3.8).
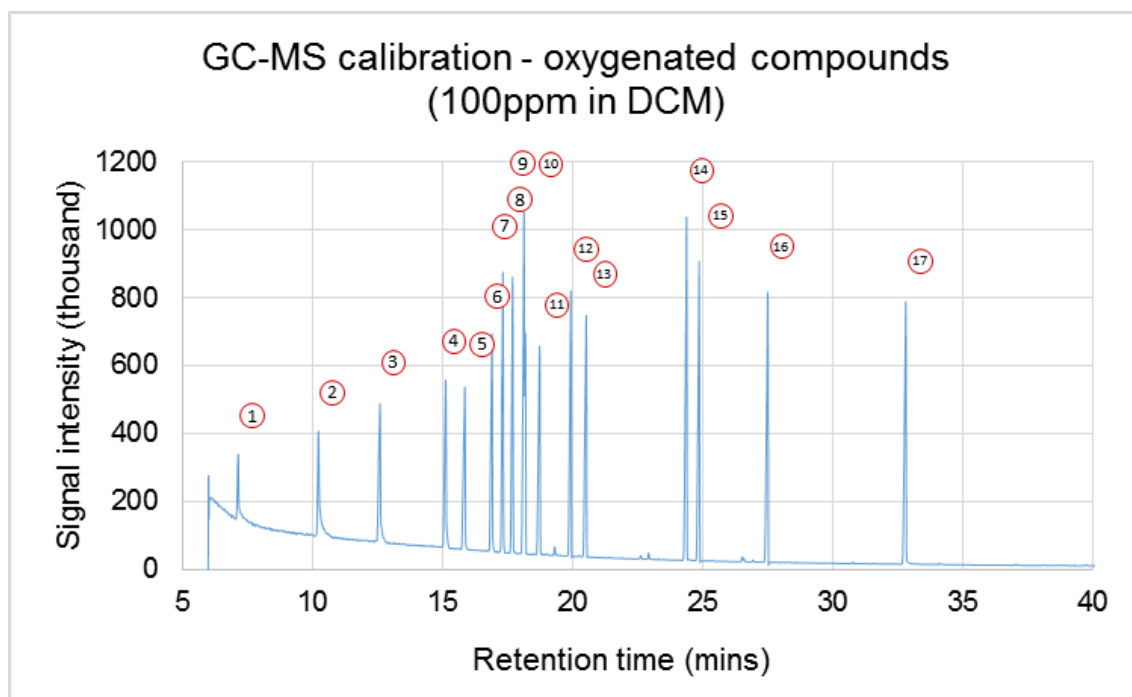
Figure 3.5: Initial calibration run for oxygenated compounds in DCM labelled against known standards in Table 3.5.

Table 3.5: Compounds which were used for initial calibration with the resulting peaks shown in Figure 3.5 with boiling point of each compound listed.

	RT / mins	Oxygenated Calibration	b.p. (°C)
1	7.34	Furfural	162
2	10.38	Anisole	154
3	12.73	Phenol	182
4	15.25	o-cresol	202
5	15.98	p-cresol	202
6	17.02	2,6-dimethylphenol	203
7	17.45	3,5-dimethylanisole	193
8	17.82	2,3-dimethylanisole	195
9	18.25	3,4-dimethylanisole	201
10	18.27	2,4-dimethylphenol	212
11	18.84	4-ethylphenol	219
12	20.05	4-Isopropylphenol	213
13	20.64	2,4,6-trimethylphenol	220
14	24.49	2-methoxy-4-propylphenol	250
15	24.98	Biphenyl	255
16	27.61	Acenaphthene	278
17	32.90	4-phenylphenol	305

The calibration is also important as it allows for the library matching of unknown compounds to be evaluated. Library matching of known compounds was able to correctly identify the correct compound in a clear majority of cases. Where the library matching did not identify the correct compound, a similar compound was instead identified i.e. p-cresol was sometimes identified as a different isomer. There was one set of compounds which was particularly challenging for matching against the library, identifying the molecular size of linear aliphatic compounds. To identify the carbon number of these compounds known standards were injected for C_9-C_{14} linear aliphatic compounds with the resulting retention times matching exactly with regular repeated peaks present in the LDPE and HDPE pyrolysis oil chromatogram. This allowed the retention time for the aliphatic compounds from C_{15}-C_{31} to be estimated using the regular repeating peak pattern. When the compounds which were identified through library matching were compared to those obtained through known sample injection the molecular size in terms of carbon number gave high correlation with increasing retention time, adding confidence to the results of library matching.
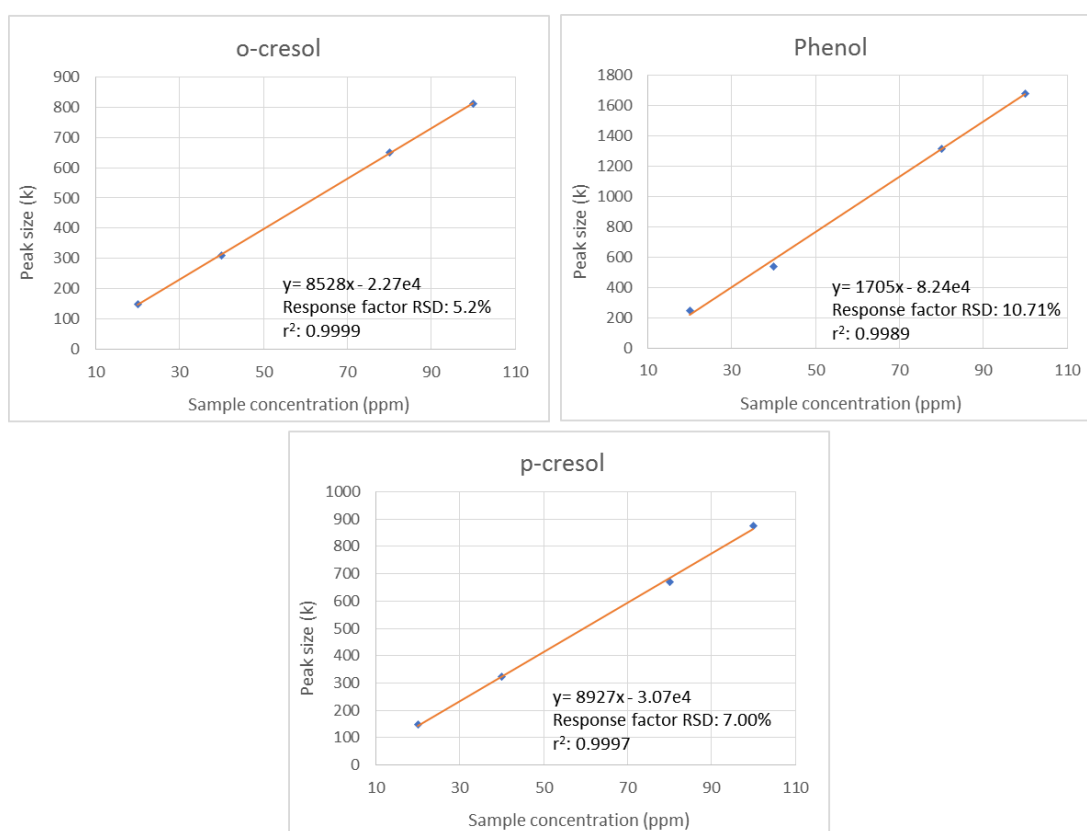
Figure 3.6: Calibration profile for o-cresol, phenol and p-cresol with linear fitting for standards at 20, 40, 80 and 100ppm.

Figure 3.6 gives three of the calibration profiles produced using four-point calibration of known compounds. The response between 20ppm and 100ppm is linear with excellent calibration fitting. This confirms that within these concentrations the response factor is relatively linear ensuring that semi-quantitive analysis may be used with confidence that an increased value is due to an increased concentration of a species, though not an absolute value. These are three examples but are representative of the other calibrated compounds.

Table 3.6: The proportion of the GC-MS signal which was due to calibrated compounds and the estimated proportion of oil yield the GC-MS signal represents if mean or median response factors are applied to the whole signal.

Sample	Proportion of relative abundance accounted for by calibrated compounds (area%)	Estimated mass of oil detected by GC-MS using mean or median response factors for calibrated compounds (wt.%)	
		Mean (rf)	Median (rf)
LDPE	17.8	72.8	65.8
Biomass (ZSM-5)	48.0	43.0	46.1
Biomass (Sand)	7.3	82.3	76.8
BMS: PS, 4:1 (ZSM-5)	10.8	78.3	82.5

Table 3.6 shows the proportion of the oil signal (area%) which was due to compounds which had been calibrated. The mean and median response factors for the calibrated compounds were then applied across the remainder of the signal to estimate the proportion of the oil yield which was being analysed during GC-MS. This estimate is very limited as there is a high likelihood that response factors for the non-calibrated compounds will differ from the calibrated compounds. However, it does give an indication that whilst the GC-MS is unable to detect and measure all the compounds in the oil sample, a large proportion of the compounds in the oil may be accounted for, possibly as much as 82 wt.% in some cases. These values must be treated with caution however, due to the uncertainty involved in the calculation. If the calibrated compounds were the only compounds examined during the oil analysis is it probable that these would not give a representative consideration of the oil samples as these calibrated compounds together are only a limited proportion of the relative abundance signal. An analysis which focused on these alone would ignore a large part of the oil sample.

Table 3.7: Known standards used for calibration of GC-MS (Methanol as solvent).

	RT / mins	Aromatic compounds		RT / mins	Oxygenated Calibration
1	2.04	Benzene	1	3.84	Furfural
2	2.89	Toluene	2	6.16	Anisole
3/4	4.64	p/m-Xylene	3	6.68	3-Methylpyrazole
5	5.23	o-Xylene	4	7.19	Solketal
6	5.25	Styrene	5	8.86	Phenol
7	9.44	p-Methylstyrene	6	11.85	o-Cresol
8	10.71	Limonene	7/8	12.86	p/m-Cresol
9	16.08	1,2-Dihydronaphthalene	9	13.09	Guiaicol
10	16.87	Naphthalene	10	14.02	2,6-Dimethylphenol
11	20.94	2-Methylnaphthalene	11	14.47	3,5-Dimethylanisole
12	24.26	2-Ethylnaphthalene	12	14.92	2,3-Dimethylanisole
13	25.67	2,6-Dimethylnaphthalene	13	15.46	3,4-Dimethylanisole
14	25.67	1,4-Dimethylnaphthalene	14	15.64	2,4-Dimethylphenol
15	27.03	Acenaphthene	15	16.36	4-Ethylphenol
16	35.36	Phenanthrene	16	17.39	Catechol
17	38.16	o-Terphenyl	17	17.79	2,4,6-Trimethylphenol
18	43.50	Pyrene	18	18.60	4-Isopropylphenol
19	44.42	m-Terphenyl	19	23.35	2-Methoxy-4-propylphenol
			20	23.89	Biphenyl
			21	29.81	Furoin
			22	33.83	4-Phenylphenol

Table 3.8: Known standards used for calibration of GC-MS (DCM as solvent).

	RT / mins	Aromatic compounds		RT / mins	Oxygenated Calibration
1	4.55	Toluene	1	6.99	Furfural
2	6.91	1,2-Dimethylcyclohexane	2	10.00	Anisole
3	8.29	Ethyl-Benzene	3/4	10.96	Solketal/3-Methylpyrazole
4	8.76	p-Xylene	5	12.44	Phenol
5	8.84	o-Xylene	6	15.18	p-Cresol
6	9.93	m-Xylene	7	15.64	o-Cresol
7	9.94	Styrene	8	16.20	Guaiacol
8	16.85	p-Methylstyrene	9	16.48	m-Cresol
9	19.00	Limonene	10	17.48	2,6-Dimethylphenol
10	26.84	Naphthalene	11	17.99	3,5-Dimethylanisole
11	30.72	2-Methylnaphthalene	12	18.48	2,3-Dimethylanisole
12	33.61	2-Ethylnaphthalene	13	19.06	3,4-Dimethylanisole
13	33.93	2,6-Dimethylnaphthalene	14	19.22	2,4-Dimethylphenol
14	34.82	1,4-DimethylNaphthalene	15	10.02	4-Ethylphenol
15	35.96	Acenaphthene	16	21.68	2,4,6-Trimethylphenol
16	42.86	Phenanthrene	17	22.64	4-Isopropylphenol
17	44.99	o-Terphenyl	18	28.51	2-Methoxy-4-propylphenol
18	49.39	Pyrene	19	29.14	Biphenyl
19	50.054	m-Terphenyl	20	33.26	Furoin
20	50.72	p-Terphenyl			
21	62.08	1,3,5-Triphenylbenzene			

3.8.3 GC-MS data collection

The GC-MS data was collected and analysed using the following methodology. From the chromatogram a peak list was created for every peak with a count greater than 5% of the highest peak. For each recorded peak the retention time and peak area were determined, and the peak was matched against the NIST library to identify the most probable compound. The ionic fragmentation pattern was examined at the front and rear edges as well as at the point of maximum height to identify if a peak was due to one compound or whether the peak was due to more than one compound which had eluted at the same retention time. The calibration was used to confirm the presence and identity of calibrated compounds and where more than one compound eluted at the same retention time the secondary oxygenated method was examined as the variation in methodology would usually lead to improved separation for certain compounds not separated clearly using the aromatic methodology.

The identity and area of each peak was used to semi-quantitatively characterise the types of compounds which were present in each pyrolysis oil sample such that samples could be compared and variations which had developed between the samples identified. The compounds were grouped into separate categories which were non-exclusive, with each category accounting for 100% of the total peak area. The categories were aromatic compounds, oxygenated compounds, cyclic compounds and molecular size measured based on the number of carbon atoms.

The aromatic compounds were determined as all compounds which contained at least one aromatic ring. The aim of this category was to compare the proportion of aromatic compounds and aliphatic compounds. This category was further sub-divided into primary aromatics (mono-aromatic, no oxygen), phenolics (mono-aromatic, oxygen), naphthalenes, indene derivatives, aliphatics and polyaromatic hydrocarbons (PAHs). The oxygenated category divided compounds between those which contained oxygen and those which did not. The cyclic category divided compounds by the number of cyclic rings which made up the compound i.e. unicyclic (1-ring), bicyclic (2-rings), tricyclic (3-rings), quadcyclic (4-rings) and linear (0-rings). The molecular size was determined by the number of carbon atoms which made up the compound with C_5-C_{12} designated as gasoline range and $\geq C_{13}$ treated as non-optimal for gasoline. These categories overlap one another but by examining each of them it is possible to observe the characteristics of the compounds in an oil and to observe how these are varied through use of a catalyst of through co-pyrolysis.

Table 3.9: Oil analysis was repeated for biomass pyrolysed with ZSM-5 (4g) including mean values and standard deviation (s) for four measured criteria. The experiments span the period May 2016-March 2018.

	Sample 1	Sample 2	Sample 3	Mean	Standard deviation (s)
Mass balance (wt.%)	101.4	105.2	101.2	102.6	2.3
Aromatic (Area %)	99.3	97.0	94.9	97.1	1.8
Oxygenated (Area %)	35.2	36.2	33.9	35.1	1.1
C_5-C_{12} (Area %)	96.9	98.6	95.4	97.0	1.6
Unicyclic (Area %)	82.8	78.4	78.4	79.9	2.6

Table 3.10: Oil analysis was also repeated for biomass pyrolysed without a catalyst (sand - 4g) four measured criteria. The experiments span the period May 2016-March 2018.

	Sample 1	Sample 2	Sample 3	Mean	Standard deviation (s)
Mass balance (wt.%)	99.6	105.2	95.5	100.1	4.9
Aromatic (Area %)	64.0	62.9	61.4	62.8	1.3
Oxygenated (Area %)	99.8	96.7	99.6	98.7	1.7
C_5-C_{12} (Area %)	98.2	98.4	99.9	98.8	0.9
Unicyclic (Area %)	88.7	84.4	85.8	86.3	2.2

Table 3.10Table 3.9 and Table 3.10 show the values obtained from repeated GC-MS analysis of oils from pyrolysis of biomass with and without a catalyst. These experiments were repeated during the duration of the project to ensure that experimental results were not varying due to changes in equipment as the project was undertaken across a long-time span (3 years). The deviation is around ~1.5% for aromatic, oxygenated and gasoline range compounds and is slightly higher for the unicyclic values ~2.5% for both data sets. Because these were measured across the duration of the project these standard deviations are likely to be larger than for the datasets collected across a few weeks or months.

3.9 Water content in liquid analysis

The water content from each pyrolysis oil collected was analysed by Karl-Fischer volumetric titration. Due to differences in solubility between pyrolysis

liquids from biomass and polymers the solvent used for liquid analysis (methanol and dichloromethane) was varied to ensure that all of the compounds were dissolved homogenously solution. For each solvent a methodology was developed to ensure accurate results. Karl-Fischer titration uses two components which are each composed from a number of chemicals. The solution which is to be titrated contains the sample and Hydranal – ketosolver (1-methoxy-2-propanol and ethanol) to which Hydranal – Composite 5K (2-(2-Ethoxyethoxy)ethanol, Iodine, sulphur dioxide, Imidazole, 2-methylimidazole and 1H-imidazole monohydriodide) is added during titration. In the reaction cell the ethanol reacts with the sulphurous acid to form an ester which is neutralised by the imidazole base. Water will then react with the alkyl sulphurous ester, base and iodine to produce alkyl sulphate. The end point is determined through a potentiometric method with each mole of water removing a mole of iodine which is regenerated continuously at the anode, consuming electrons. Once the water is consumed there is an excess of Iodine which provides a drop in voltage which marks the end point [210].

3.9.1 Water content analysis with methanol as the solvent

For water analysis with methanol as the solvent produce a calibration graph using known concentrations of methanol and water between 5% and 30% (wt.%) plotted against the values obtained by the instrument for each concentration (see Figure 3.7). The resulting fit is linear and can be used to determine the water content of the oil sample in the solvent. Karl-Fischer titration uses chemicals which react with water, so it is important to be able to confirm that these reactants have not become diluted through interaction with environmental moisture during storage of the equipment. Known standards of water and methanol were produced and these were injected into the KFT before each analysis to confirm that the calibrated results were still valid.

The oil sample in solvent was injected into the KFT and the mass of the injected sample recorded, the water concentration was measured by the equipment. Each sample was analysed in duplicate. The water concentration which was measured was as a proportion of a diluted sample. This was then converted to a water concentration (wt.%) as a proportion of the liquid pyrolysis sample to give the water and oil content of the liquid.
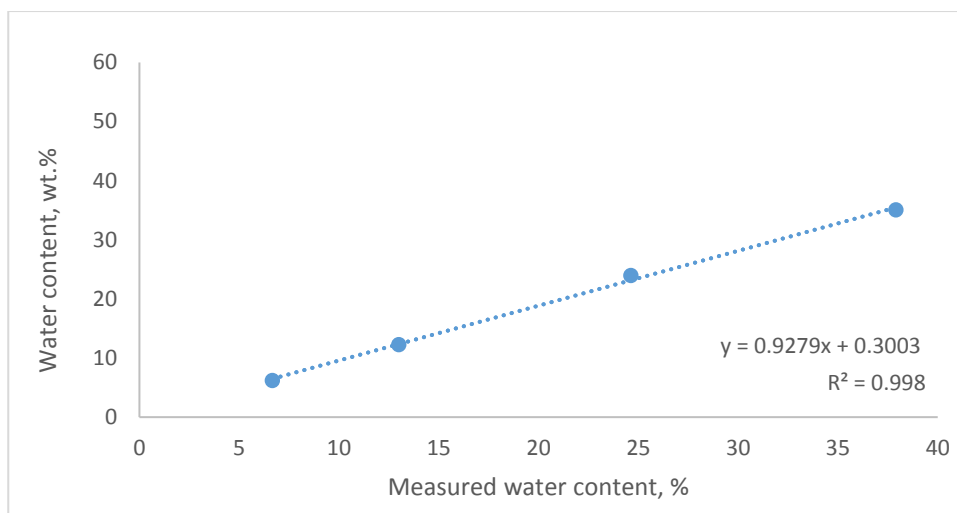
Figure 3.7: Calibration for water content in methanol solvent using known standards.

3.9.2 Water content analysis with DCM as the solvent

For the samples where DCM was the solvent a 1:1 (vol%) mixture of methanol and DCM was used as the solvent. Water does not readily dissolve into the pure DCM and as such water may phase separate which would give incorrect readings. A 1:1 mixture of methanol and DCM will dissolve water providing the moisture content is 10% or lower. As with the methanol a calibration graph was produced (see Figure 3.8), and standards were used before each analysis cycle to ensure the values determined for known standards matched the calibration trend line. As with the methanol the sample and solvent mass was used to calculate the mass of water in the liquid produced during pyrolysis.
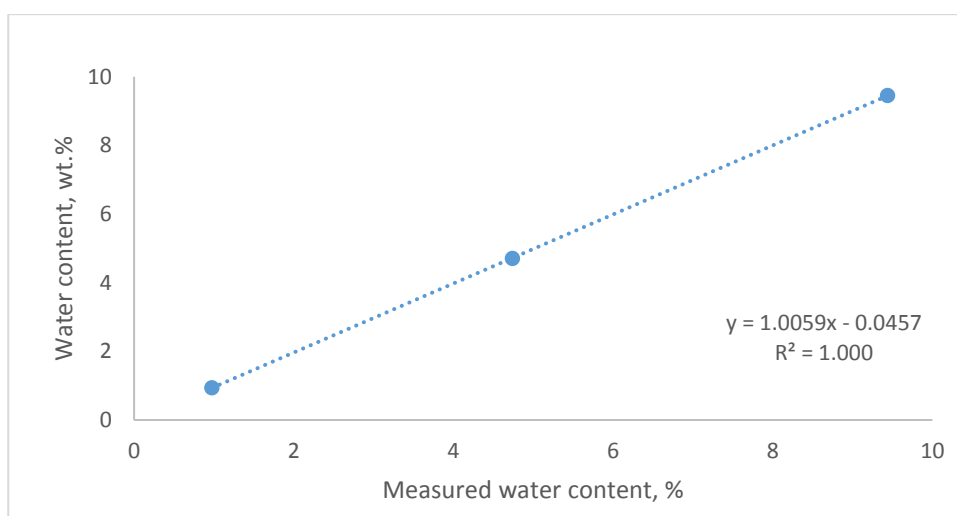
Figure 3.8: Calibration for water content in methanol and DCM (1:1) using known standards.

3.9.3 Effect of solvent on oil analysis

The difference in polarity of methanol and DCM introduces the possibility that some compounds will preferentially dissolve in water rather than in the solvent and this could in turn cause variation between characteristic results obtained through GC-MS analysis. In order to account for variation caused by using different solvents some samples were analysed by both methanol and DCM where full solubility could be achieved for both solvents. This was possible in the case of the 4:1 mixture (by weight) of biomass and PS and the 1:1 mixing of biomass and PET.

Table 3.11: Mass and oil results for co-pyrolysis of biomass and PS (4:1) with both methanol and DCM as the solvent.

	DCM	Methanol	Mean	Standard deviation (s)
Mass balance	100.7	100.3	100.5	0.31
Char (wt.%)	21.4	21.9	21.6	0.36
Liquid (wt.%)	59.2	59.3	59.3	0.07
Gas (wt.%)	21.9	22.2	22.0	0.22
Water (wt.%)	26.0	25.3	25.7	0.47
Oil (wt.%)	33.2	34.0	33.6	0.54
Aromatic (Area %)	100.0	100.0	100.0	0.00
Oxygenated (Area %)	12.5	12.6	12.5	0.11
C_5-C_{12} (Area %)	83.3	82.9	83.1	0.31

Table 3.12: Mass and oil results for co-pyrolysis of biomass and PET (1:1) with both methanol and DCM as the solvent.

	DCM	Methanol	Mean	Standard deviation (s)
Mass balance	93.0	100.9	97.0	5.61
Char (wt.%)	37.5	34.5	36.0	2.12
Liquid (wt.%)	33.0	35.5	34.3	1.77
Gas (wt.%)	22.5	25.0	23.8	1.77
Water (wt.%)	23.3	24.9	24.1	1.13
Oil (wt.%)	9.7	10.6	10.2	0.64
Aromatic (Area %)	100.0	100.0	100.0	0.00
Oxygenated (Area %)	19.7	20.6	20.2	0.65
C_5-C_{12} (Area %)	89.2	88.6	88.9	0.44

Table 3.11 shows the results for two experiments using biomass and PS which were undertaken within 3 days of each other. The deviations between each experiment is very small for each criterion analysed. The deviation for biomass and PET (Table 3.12) was much larger which in part was due to deposition of terephthalic acid derivatives onto the thermocouples of the reactor but also due to the experiments being undertaken with a year between. The deviations measured across the three year of experiments undertaken for the project were slightly larger, so it appears that the deviation is related in some part to the time period between experiments. The experiments were undertaken in sets and it is likely that the deviation in each set is smaller than the deviation across the whole dataset. When considering the significance of variation between GC-MS data the values from Table 3.11 and Table 3.12 will be used as this gives the broadest deviation and covers the whole period over which experiments were undertaken.

3.10 Thermogravimetric analysis- mass spectrometry (TGA-MS)

TGA-MS of biomass and polymers was undertaken at Tsinghua University to examine the thermal devolatilisation process which is occurring during pyrolysis and co-pyrolysis. This involved heating samples individually and then repeating the same heating process using a mixture composed from the biomass and polymer. A Q600 thermograviametric analyzer produced by TA instruments was used for this analysis with an online Hiden HPR20 Mass spectrometry module connected via a heated capillary transfer line. The instrument and alumina pans were tared before the MS was calibrated to ensure that the signal from both the Faraday and Secondary electron multiplier detectors (MSE) was equivalent. This was accomplished using the isotope signal detected from the argon carrier gas at 20 m/z. The signal multiplier was adjusted to ensure both detectors gave equal signal output. The Faraday detector is most effectively used to detect high concentration products during devolatilisation this was used to measure the flow of the argon carrier gas during the experiment to allow for the concentration of the other compounds to be calculated. The MSE detector was used to measure the low concentration compounds carbon monoxide, carbon dioxide, water and hydrogen.

During each experiment the prepared samples were loaded into a pre-tared pan which was placed into the heating cell. Argon gas was passed through the heating cell at 500 mLmin^{-1}. The balance was allowed thirty minutes to stabilize

before heating was initiated with the temperature increased from room temperature through to 800°C at a heating rate of 10 °Cmin^{-1}. For each experiment a sample of approximately 3mg was used. The MS unit was programmed to scan for five pre-determined species (see Table 3.13).

Table 3.13: The species which were detected using online MS during devolatilisation of biomass and polymer samples during TGA-MS analysis.

Detector	Compound	m/z
MSE	Hydrogen	2
MSE	Water	18
MSE	Carbon monoxide	28
MSE	Carbon dioxide	44
Faraday	Argon	40

3.11 ZSM-5 catalyst

3.11.1 Unmodified ZSM-5

A single batch of ZSM-5 catalyst was used throughout the pyrolysis experiments both as the unmodified and for synthesis of the metal impregnated catalysts. This ZSM-5 had a silica/alumina molar ratio of 38 which determines the acidity, activity and stability of the catalyst. These properties as may also be affected by changes to the structure through modification, damage, poisoning or coke deposition. This may occur during experiments using the catalyst but may also be accomplished through application of heat and active species such as steam or sodium hydroxide to modify the functionality of the catalyst. The counter-ion which is present in ZSM-5 is sodium which remains from the synthesis procedure however this can be exchanged for hydrogen or other metals to alter the function of the material [59, 136, 211].

3.11.2 Metal impregnated ZSM-5

Metal impregnated ZSM-5 catalysts were produced using a wet impregnation methodology to produce cobalt, copper, gallium, iron, magnesium, nickel and zinc – ZSM-5. Metal nitrate hydrates containing each metal were used as they allow for the metal to be dissolved into deionized water and then to diffuse into the porous ZSM-5 material. The mass of metal was calculated from the metal nitrate such that 5 wt.% of metal was added to each batch of ZSM-5. The metal salts used for each metal were cobalt (II) nitrate hexahydrate ($Co(NO_3)_2 \cdot 6H_2O$),

copper (II) nitrate trihydrate ($Cu(NO_3)_2 \cdot 3H_2O$), gallium (III) nitrate nonahydrate ($Ga(NO_3)_3 \cdot 9H_2O$), iron (III) nitrate nonahydrate ($Fe(NO_3)_3 \cdot 9H_2O$), magnesium (II) nitrate hexahydrate ($Mg(NO_3)_2 \cdot 6H_2O$), nickel (II) nitrate hexahydrate ($Ni(NO_3)_2 \cdot 6H_2O$) and zinc (II) nitrate hexahydrate ($Zn(NO_3)_2 \cdot 6H_2O$) respectively. Each metal salt was added into deionized water and heated to 30°C to aid dissolution. The ZSM-5 was added to the solution the mixture heated gradually from room temperature through to 80°C. The increase in temperature increases the rate of diffusion of the metal complexes into the pores of the zeolite as well as gradually reducing the water content thereby concentrating the solution which also aids further diffusion. Once sufficient water was evaporated from the zeolite, the mixture was placed in a drying oven at 110°C for 10 hours. At this point the metal is still present as a nitrate complex which was removed through calcination at 500°C for 5 hours. The nitrate complex is removed by calcination as ammonia and nitrogen gas leaving the metal on the internal and external surfaces of the zeolite [212]. The catalyst was then reduced at 800°C for 1 hour in a 5% hydrogen (95% nitrogen) gas to reduce any oxides formed during the calcination process.

3.12 X-Ray powder diffraction (XRD)

The unmodified ZSM-5 and the metal impregnated ZSM-5 catalysts were analysed using X-ray powder diffraction to study any structural changes caused by metal impregnation. The samples were initially dried at 100°C for one hour after which they were ground to a fine powder. Each sample was individually prepared for analysis by packing into a sample holder with excess material removed using a glass slide producing a firmly packed, smooth surface for diffraction. The XRD instrument was a Bruker D8 which utilised a monochromatic CuKα radiation source with a wavelength of 1.54056 Å. Diffraction of the x-ray beam was measured for 2Θ values between 10º and 80º with the   change in angle at $2°min^{-1}$.

The resulting signal corrected to remove background effects with peaks identified and compared against a reference library to determine the closest match from known powder diffraction patterns.

3.13 Temperature programmed oxidation

Temperature programmed oxidation (TPO) was used to analyse the carbon deposition on the catalyst during pyrolysis. Samples of approximately 15 mg were collected from the catalysts used for pyrolysis experiments. Care was taken to ensure that the sample was representative of the entire catalyst sample with the colouration and size at approximately the mid-point of the sample

where variation in size and colour existed. The sample was placed in a pre-tared alumina pan and heated at a steady rate of $15^{\circ}Cmin^{-1}$ from room temperature through to 800 $^{\circ}$C. The instrument used was a Shimadzu – TGA 50 with an airflow through the heating cell of 50 $mLmin^{-1}$, providing oxygen for oxidation of the carbon deposits on the catalyst. The weight of the vessel was recorded throughout the heating cycle. The change in mass of the sample was determined as a weight percentage with the temperature range of the weight change also determined through plotting of derivative weight change. A clear change in colour was observed for all used samples during the analysis with grey/black colouration returning to a bright white after TPO.

The powder X-ray diffraction (XRD) of ZSM-5 and metal-impregnated ZSM-5 (5 wt.%) are plotted together in Figure 3.9. Comparison of these XRD patterns against databases found that the strongest match was with ZSM-5 (Orthorhombic, $Al_2O_{111}Si_{54}$). The XRD pattern for ZSM-5 is shown in Figure 3.10 and this compares very closely with the patterns for both the modified and unmodified ZSM-5 samples (Figure 3.9) used in these experiments [213].
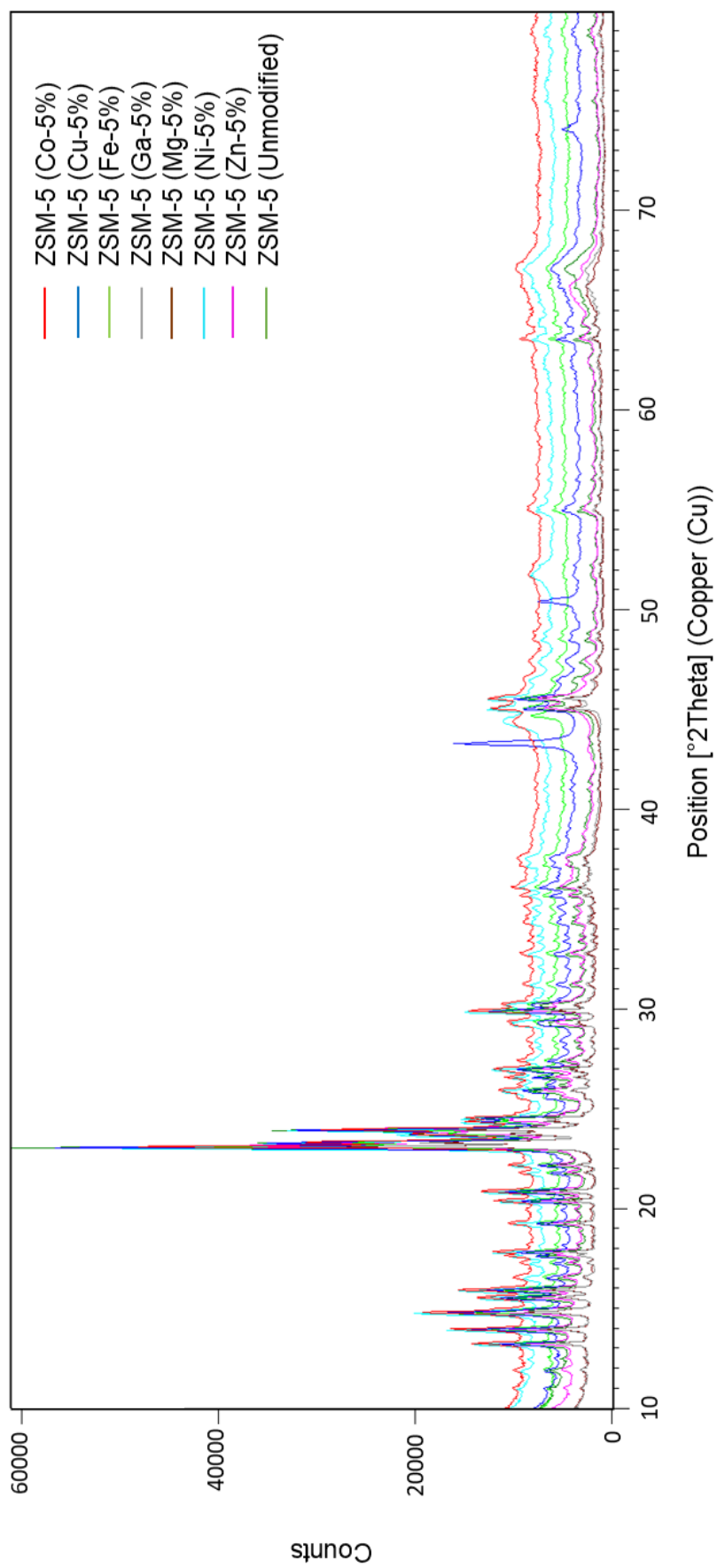
Figure 3.9: XRD analysis of unmodified ZSM-5 and metal impregnated ZSM-5.
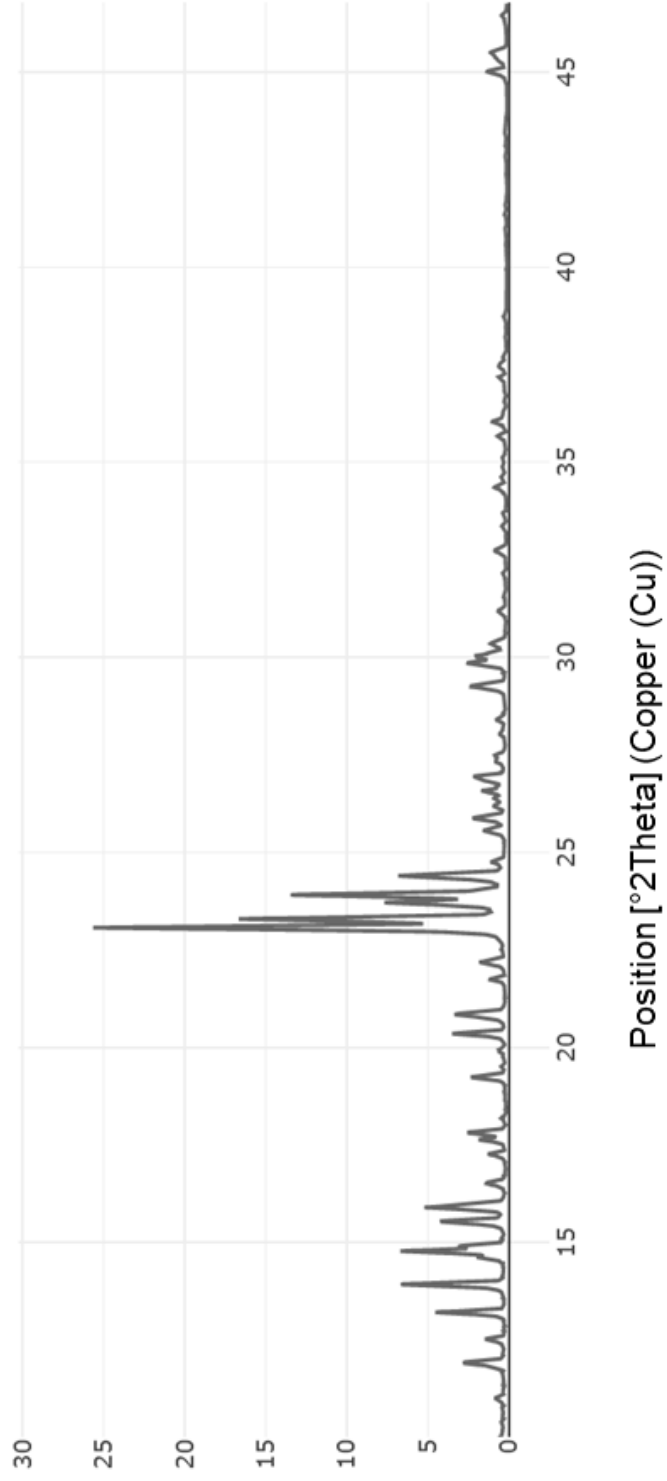
Figure 3.10: ZSM-5 (MFI) template free XRD powder diffraction pattern from International zeolite association database of zeolite structures (202).

Comparison of these figures confirms that the initial material is ZSM-5 as expected and that the addition of metal to the zeolite material by the wet impregnation method does not change this basic structure of this material. Despite the structure remaining close to ZSM-5 there are also clear changes observed in the impregnated samples, particularly in the region $2\theta > 40°$. This is especially evident in the region around $45°$ where peaks present in the unmodified ZSM-5 become altered both in shape and position and this is particularly clear with copper, nickel, cobalt and iron (see Figure 3.11). For Mg and Zn there is no clear change in the 45° region but there is a peak at 67° with a shift both in shape and position. Due to these alterations occurring at approximately the same points it is possible that this is due to metal interaction with a similar part of the ZSM-5 structure in each case. The metal which had the smallest impact on the ZSM-5 pattern was gallium which produced a minor change in the peaks at 45° and 67° but these are only changes in shape rather than peak position. This is in keeping with other research which suggests that gallium can become uniformly distributed within a ZSM-5 material without clear alteration of the original structure [134, 214-216]. Vichaphund et al. [139] observed subtle changes to the structure caused by impregnation of metal to ZSM-5 by wet impregnation. These changes were thought to be caused by partial loss of crystallinity rather than major structural alteration. Another observation from their research was that impregnation of palladium metal could give strong peaks such as those seen with the case of copper impregnated ZSM-5. Copper nanoparticles have been studied using XRD and produced a strong peak at 43°, and two weaker peaks at approximately 51° and 74° [217]. These fit very closely with the non-ZSM-5 peaks in the copper XRD pattern so it is likely that copper nanoparticles have formed on the surfaces of the ZSM-5 catalyst. It is possible that these copper nanoparticles were produced during the reduction process applied to the metal impregnated catalysts.

111
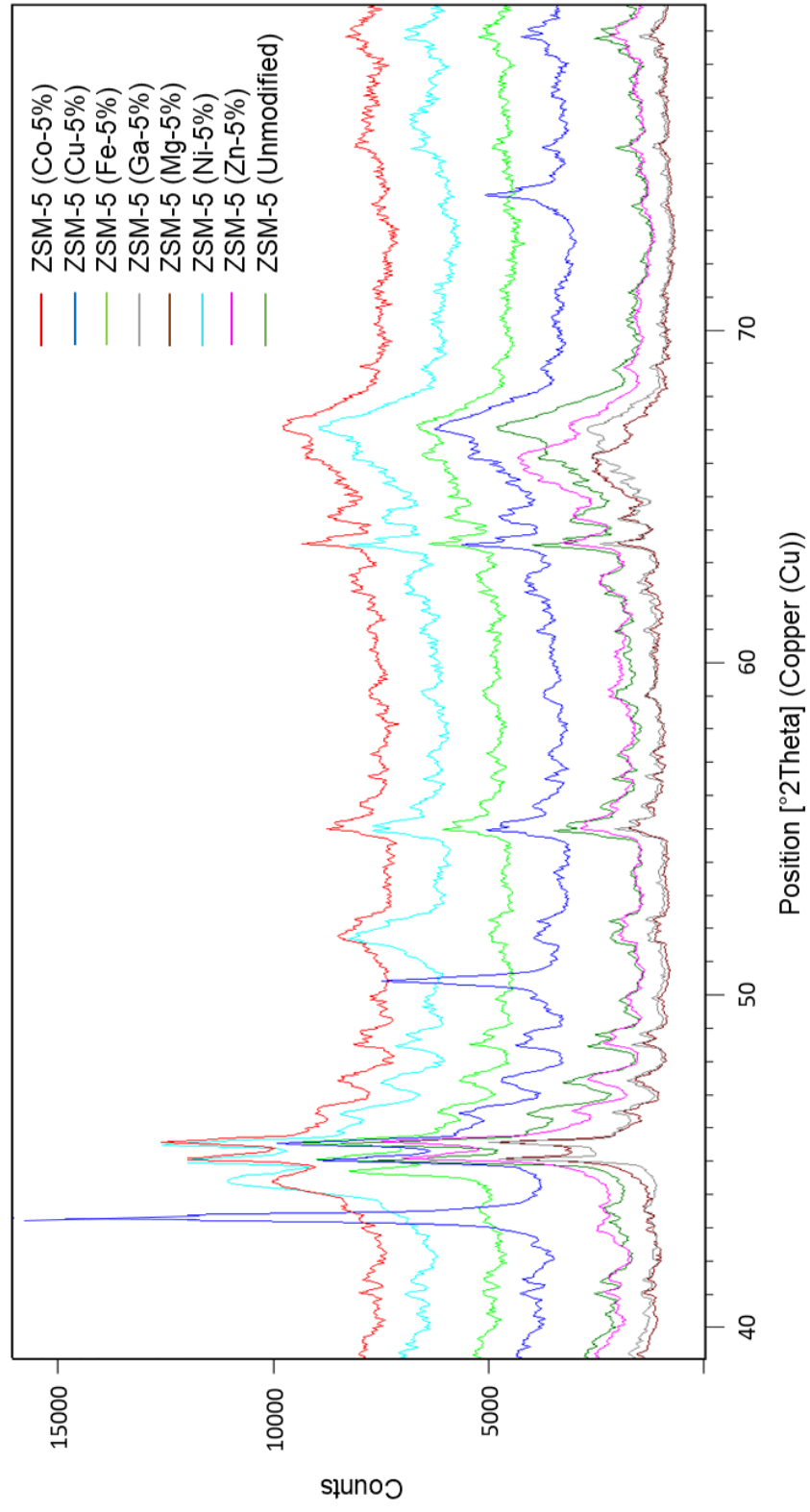
Figure 3.11: XRD analysis of metal impregnated ZSM-5 between 40° and 80°.

Several studies have examined the application of variations of wet impregnation for the loading of metals onto ZSM-5 materials with different loading ratios and for different catalytic purposes [126, 134, 149, 215, 216]. In nearly every case the loading of metals led to a reduced surface area compared to the original catalyst material and the greater the metal loading wt.% the higher the reduction in surface area that was observed. The size of the effect was different between loadings of different metals, however there was no consistent pattern as to which metal caused the greater reduction in surface area. Other factors such as initial catalyst surface area, Si/Al ratio, catalyst structure and metal loading proportion had a bigger impact on the surface are than the type of metal used [126, 134, 139, 158, 215, 216].

Table 3.14: BET Surface area and pore volume of non-modified ZSM-5 and metal impregnated ZSM-5.

Sample	Specific surface area (m^2/g)	Pore Volume (cm^3/g)
ZSM-5	282	0.26
5% - Cu – ZSM-5	268	0.25
5% - Co – ZSM-5	264	0.23
5% - Fe – ZSM-5	278	0.25
5% - Ga – ZSM-5	269	0.23
5% - Ni – ZSM-5	275	0.25
5% - Mg – ZSM-5	224	0.21
5% - Zn – ZSM-5	241	0.22

The surface area measurements (see Table 3.14) showed similar results to other studies using metal impregnated ZSM-5. The loading of metal onto the catalyst lead to reduced surface area, both regarding specific surface area and pore volume. The metals with the biggest reduction in surface area were magnesium and zinc and this might be due to effects observed by Fermoso et al. [158] who found that zinc oxide (ZnO) and magnesium oxide (MgO) led to partial blockage of pores in ZSM-5. The research by Fermoso et al. used a higher metal loading (10 wt.%) but the same partial blockage may still be possible. Although specific surface area is an important factor for catalyst activity it is important to note that the addition of metal atoms to a catalyst can also improve selectivity by restricting the interactions of compounds with the active surfaces of the catalyst. Al-khattaf et al. [218] highlight in their research that metal and metal oxide depositions on the external surface of H-ZSM-5 could improve selectivity by ensuring that more of the catalytic activity was

undertaken within the internal pores thereby increasing selectivity towards the sterically less hindered p-xylene.

3.14 Scanning electron microscopy

Scanning electron microscopy (SEM) was also used to provide image of the carbon deposition onto the external surface of the catalysts. Conductive carbon tape was applied to the aluminium pin stub and this was used to remove the carbon deposit off the surface of ZSM-5 catalyst which has been used for pyrolysis. The pins were then sputter coated in 10nm of iridium [219] to reduce charging caused by the electron beam and therefore to increase the resolution and clarity of the image. The samples were loaded into the equipment which was used for imaging was a Hitachi SU8230 [220], a high performance cold field emission (CFE) SEM with an Oxford Instruments Aztec Energy EDX system and X-Max SDD detector. This instrument is capable of ultra-high resolution images at low kV. The sample cell was evacuated to give a vacuum and imaging of the samples was conducted at several points in the sample which were representative of the whole sample and at a range of magnifications (x20K-50K). The electron energy used was 2.0kV and secondary electron (SE) scanning was used to produce the image.

Chapter 4: Pyrolysis of biomass with metal impregnated ZSM-5 catalysts

4.1 Introduction

Chapter 4 examines the effect of using a commercial ZSM-5 catalyst on the yield and composition of pyrolysis products from the pyrolysis-catalysis of biomass (objectives 1 and 2). This work then examined the influence of ZSM-5 impregnated with 5 wt.% of different metals on the yield and composition of the product oils and gases during pyrolysis in the two-stage, fixed-bed reactor (objective 3 and 4). The metals examined were, copper, cobalt, gallium, iron, magnesium, nickel and zinc. Initially, the effect of the ZSM-5, which had not been modified, was compared to a catalyst free pyrolysis process. In this case an equal mass of sand was used to the catalyst in the catalytic experiments to ensure the flow through the reactor was similarly congested to the catalytic experiments. Temperature programmed oxidation was used to analyse the coke deposition on the unmodified and metal impregnated ZSM-5 catalysts used during pyrolysis experiments (objective 11).

4.2 Pyrolysis of biomass with and without ZSM-5 Catalyst

The first experiments examine the effect that ZSM-5 catalyst has on the pyrolysis yields when compared to pyrolysis without a catalyst bed. This was undertaken by comparison with sand which is mostly composed of silica dioxide and as such is not widely different in elemental composition to the alumina silicate, ZSM-5 catalyst. This ensures that pyrolysis vapours pass through the reactor in a similar time period for both cases with surface interactions also occurring, ensuring that any differences in yield and oil composition are due to active catalyst effects rather than differences in other variables such as reactor residence time.

4.2.1 Pyrolysis yields with ZSM-5 and sand

Table 4.1 shows the product yields from pyrolysis of biomass at 500°C with and without the unmodified ZSM-5 catalyst. The mass balance is the total yield of char, liquid, gas collected including the mass of any residue, which is deposited on the reactor during the pyrolysis experiment. The liquid yield is made up of a combination of oil (hydrocarbon) and water, with the water fraction measured using Karl-Fischer titration to determine the mass fraction of the total liquid which was due to water.

Table 4.1: Pyrolysis yields (char, oil, gas and mass balance) for biomass pyrolysed at 500°C with and without ZSM-5.

	Char (wt.%)	Liquid (wt.%)	Gas (wt.%)	Water (wt.%)	Oil (wt.%)	Mass balance (wt.%)
ZSM-5	25.1	48.3	26.6	34.4	13.9	101.4
Sand	25.1	56.3	15.6	23.7	32.6	99.6

Thermal decomposition of the biomass in the case where a catalyst was not present in the second stage of the reactor produced approximately 25 wt.% char 56 wt.% liquid and 16 wt.% gas with a small residue deposited on the surface of the reactor and sand (catalyst substitute) . Variations to heating rate and maximum temperature can produce measurable changes to the liquid yield proportion from pyrolysis yield so for all further experiments these were kept constant [40]. This ensures that any changes in yield can be directly attributed to variation of sample and catalyst rather than other factors.

Research by Olazar et al. [221] examining pyrolysis of wood sawdust with catalytic upgrading by H-ZSM-5, over a range of temperatures, found that at 500°C the addition of the catalyst reduced the liquid yield by approximately 5 wt.% whilst at the same time increasing the gaseous yield by approximately 8 wt.% with a slight decrease in the proportion of char also observed when the catalyst was used. A similar trend is observed in this experimental data which used Na-ZSM-5 rather than H-ZSM-5, although research suggests the variation between these two catalysts has limited effect on pyrolysis results [128, 129]. In this case, the liquid yield decreasing by 8 wt.% and the gas increasing by 11 wt.% when a catalyst was used during pyrolysis.

In this process the intention was to produce liquid hydrocarbons or valuable chemical feedstock compounds as a priority, but it is important that both the char and gaseous products may be utilised, to increase process efficiency. These products may be combusted to produce process heat to drive the pyrolysis process or they may be used for other purposes for example bio-char which is becoming increasingly important as an agricultural soil amendment [222]. Whilst these products have use and value it is the bio-oil which is the primary product and increasing the yield of oil from the process is most advantageous.

The effect of adding an ex-situ catalyst has little or no effect on the char yield from pyrolysis which is as would be expected considering that no interaction is possible between the sample and the catalyst. Deposition of coke on catalysts is likely to increase the yield of solid products during pyrolysis, although this mass change would be measured in the residue mass rather than the char mass. The main change observed was in the proportions of liquid and gas yield with interactions over or through the porous catalyst leading to increased gas yield and a reduced liquid yield. In this case, the gas yield in the catalytic example reached almost twice the proportion compared to the non-catalytic system.

Yildiz et al. [223], established a bubbling fluidised bed reactor which was used to produce bio-oil with the aim of the experiments to study the regeneration of an in-situ ZSM-5 catalyst. The liquid was collected using an ESP (Electrostatic precipitator) followed by a glass condenser with a cotton fibre also used to filter any other liquid prior to gas analysis. The biomass material was a pine material of particle size between 1-2mm and with moisture and ash of 7.52 wt.% and 0.33 wt.% on and as received basis. The Ultimate analysis was, C: 47.1, H: 5.9, O: 46.4 and N: 0.04 (wt.%) on a dry basis which is very similar to the material size and composition used in this experiment [223]. The analysis included water analysis by Karl-Fischer titration and it was found that at 500°C the water yield was 18.7 wt.% (MB - 94.6%) for the non-catalytic reactions and 23.4 wt.% (MB – 96.3%) for the reactions using ZSM-5 catalyst.

The sample used by Yildiz et al. [223] was equivalent to that which was used in this research and very similar analytical methods were used which allows for comparison between the results. There were differences in the type of reactor used and the way in which the catalyst interacted with the sample which has the potential to introduce differences between results. Despite the differences in equipment, however, very similar trends were observed for both experiments with an increased yield of water when ZSM-5 was introduced.

Yildiz et al. found that the organic fraction (oil) was larger for the non-catalytic pyrolysis with the addition of the catalyst leading to a reduction in organic yield from 33 wt.% down to 22 wt.%. In comparison, this research found that the organic fraction reduced from 35 wt.% to 14 wt.% which is a greater change. This difference in scale is likely due to the difference in catalyst loading with this research using a catalyst to sample ratio which was double that of Yildiz et al.
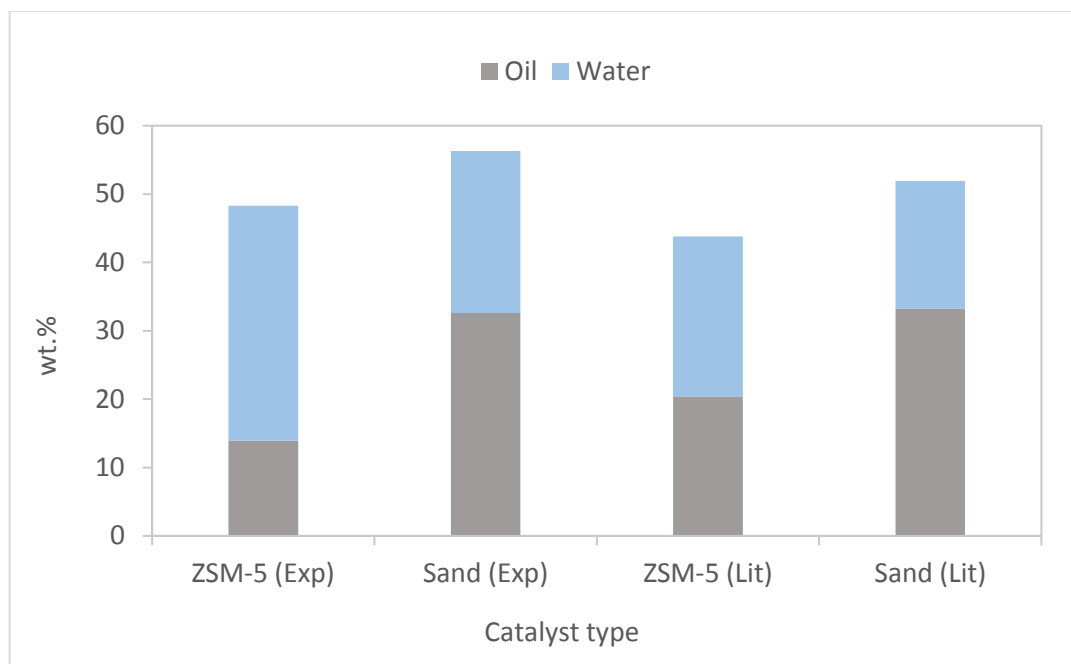
Figure 4.1: The liquid yield for pyrolysis experiments for biomass and ZSM-5 at 500°C with oil and water composition of the liquid determined by Karl-Fischer titration. Experimental data compared to results from literature [223].

As was observed from Yildiz et al. [223] and other literature sources [33] pyrolysis oil from biomass will usually contain a proportion of water and there are two major sources of this water. Primarily, biomass material naturally contains water and this can be removed by drying the sample prior to pyrolysis which can take considerable energy [10, 224, 225]. As well as this water which is already present in the material, deoxygenation reactions which occur on solid acid catalysts, produce CO_2, CO and H_2O as oxygen is removed from the compounds which make up the volatiles [33, 40, 41, 106]. Porous zeolites may absorb some moisture from the atmosphere which may pass from the catalyst into the condensers during heating of the catalyst. Due to the relatively high catalyst loadings used for these experiments this may contribute to the moisture content of oils, although this was minimised by drying the ZSM-5 prior to use.

Guedes et al. [40] examined correlation coefficients for a number of non-catalytic biomass pyrolysis studies and observed that moisture content of the bio-oil was closely related to the moisture content of the biomass resource although dehydration reactions also contributed to the water content of oils. In contrast to this, Figure 2.22 several reactions which are observed during catalytic pyrolysis of biomass alongside a solid acid catalyst such as ZSM-5. Oxygenated compounds, derived from the biomass volatiles [105] may react to produce non-oxygenated hydrocarbons with the removal of oxygen in the

gaseous phase as CO_2, CO and H_2O. The selectivity of each reaction pathway is dependent on the composition of the biomass, the catalyst as well as the conditions in the reactor [40].

The water (H_2O) will be produced in the gaseous phase as temperatures in the reactor are greater than 100°C and will then condense along with the bio-oils as they pass through the condenser system. The carbon dioxide and carbon monoxide are non-condensing gases, so are straightforward to remove from the liquid products, passing through the condensers and into the gas collection bag. Figure 4.1 shows the amount of liquid produced by pyrolysis of material either with sand or with ZSM-5 in a two stage fixed bed reactor at 500°C compared to results collected using a sample with a similar composition in a continuous feed, bubbling fluidised bed reactor with in-situ catalysis from literature also at 500°C [223]. The water content from both sets of research is a high proportion of the total liquid sample, although greater in the catalytic experiments.

As well as liquid yield it is important to examine the gaseous yield to gain an insight into what reactions are occurring to produce the changes observed in the liquid yield. Figure 4.2 examines the yield of all the gas components measured, whereas Figure 4.3 focusses on the gas components which do not contain oxygen. The gases measured using GC were CO, CO_2, CH_4, H_2 as well as hydrocarbon gases (ethane, ethene, propane, propene, butane, butene and butadiene). For both figures the nitrogen content has not been plotted although this is the major constituent of the gas yield. This is because it was used as the inert carrier gas as was not produced during pyrolysis.
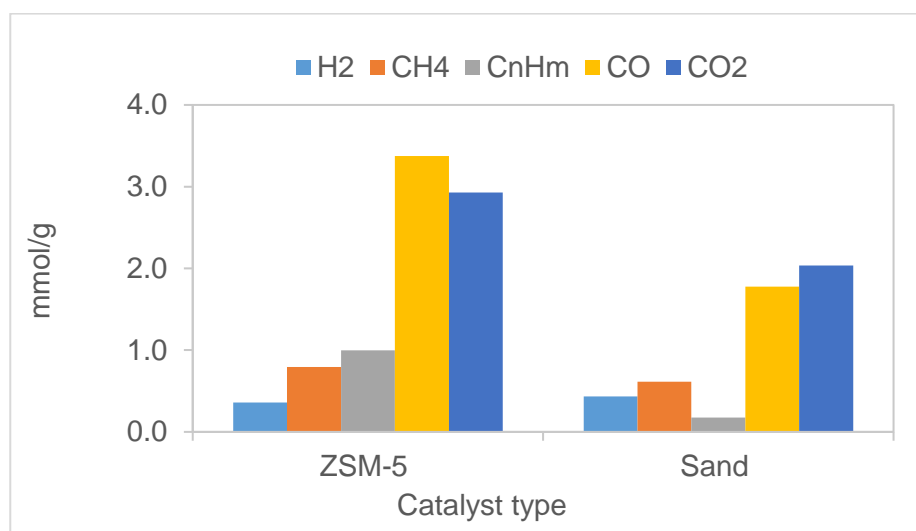
Figure 4.2: The composition of the gas collected during pyrolysis at 500°C (without nitrogen) with and without ZSM-5 catalyst.

Table 4.1 shows that using the catalyst increased the gas yield whilst decreasing the liquid yield. This also decreased the oil yield both in mass as well as in proportion, as water content increased in the catalytic pyrolysis liquid. The addition of ZSM-5 increased each of the measured gas compounds other than hydrogen which decreased by 7%. The methane increased by 29% and the hydrocarbon gases by 463% whilst of the two oxygen containing compounds carbon monoxide increased by 90% and the carbon dioxide by 44%. The large increase in small hydrocarbon molecules is due to the catalytic cracking reactions which are strongly promoted by ZSM-5. These produce hydrocarbons to a much greater extent than through thermal (non-catalytic) cracking. The carbon atom is the major energy carrier in a fuel so an increase in hydrocarbon gases leads to a smaller proportion of carbon atoms in the oil, this is detrimental to the total energy contained in the oil. However, these hydrocarbon gases are energy rich and do have the potential to be used as a fuel or to provide process heat via combustion. The increase in oxygen containing gases also reduces the oil yield but it achieves one of the key aims, producing oil with a lower oxygen content. In an ideal situation carbon dioxide is preferable to carbon monoxide as for each carbon atom removed from the oil, two oxygen atoms can be removed from the oil.

Figure 4.3 examines the hydrocarbon compounds in greater detail and it can be seen that each of the hydrocarbon gases increases, with ethane/ethene increasing by 327%, propane/propene by 852% and butane/butene/butadiene by 448%. This change in hydrocarbon gas yield clearly indicates that there are reactions occurring to produce these short chain hydrocarbons with an apparent selectivity towards C_3 yield. The most likely cause of these results are increased cracking reactions over the ZSM-5 catalyst (Figure 2.23). The ratio of unsaturated to saturated hydrocarbons in the non-catalytic experiment was ~2:1 whereas in the catalytic experiment this increased to ~7:1. Cracking reactions produce short chain unsaturated hydrocarbons from saturated hydrocarbons, so this would suggest that cracking reactions are involved in this increase in unsaturated hydrocarbons.
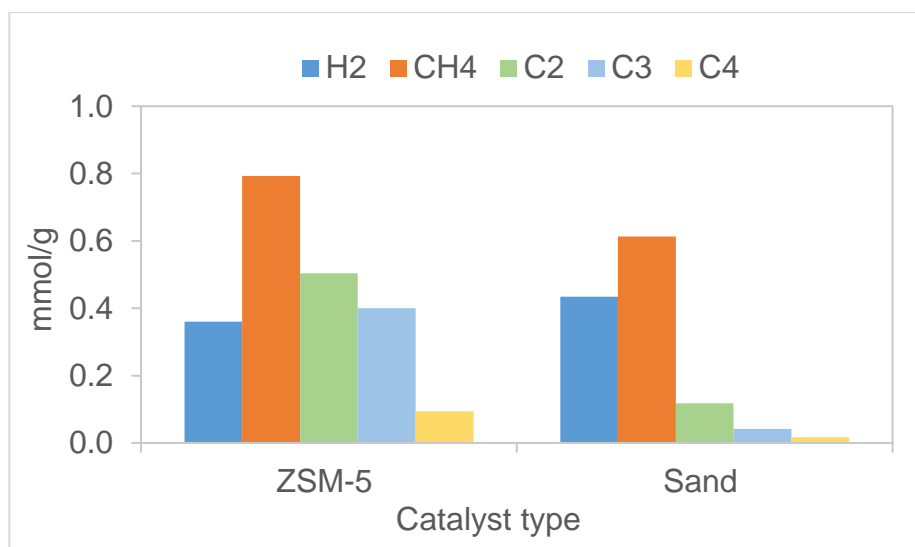
Figure 4.3: The composition of the non-oxygen containing fraction of the gases collected during pyrolysis with and without ZSM-5 catalyst.

4.2.2 Pyrolysis oil compositions with and without ZSM-5 catalyst

The yields of the products produced by the various samples during pyrolysis are important, however, it is also important to consider the composition of the liquid that is produced. These pyrolysis liquids contain water as well as a wide range of hydrocarbon compounds which together comprise the oil and are crucial to understanding the properties of the liquid. Figure 4.4 and Figure 4.5 show the GC-MS chromatogram recorded for biomass pyrolysed without catalyst and with catalyst respectively. Detailed analysis of the chromatograph data can be used to determine the types of compounds which comprise the oils from each sample and each catalyst. However, it is immediately clear from the chromatogram that there is a difference between these oils. The oil samples collected during both catalytic and non-catalytic pyrolysis of biomass are very complex with many peaks which denote different compounds. However, there are fewer large peaks in the catalytic pyrolysis oils which is due to the catalyst acting to control the products which are being formed.
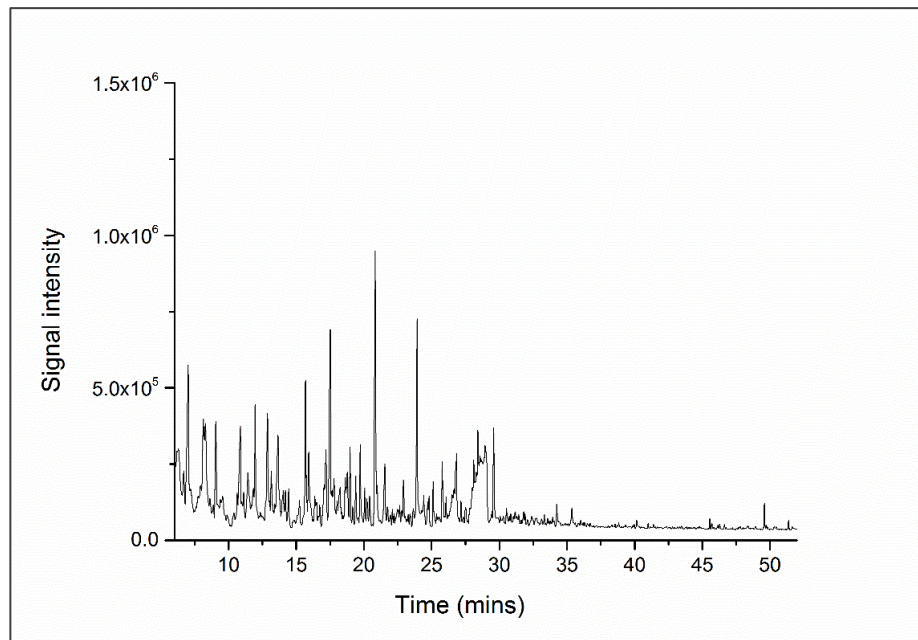
Figure 4.4: GC-MS chromatogram for bio-oil without catalyst (Sand).
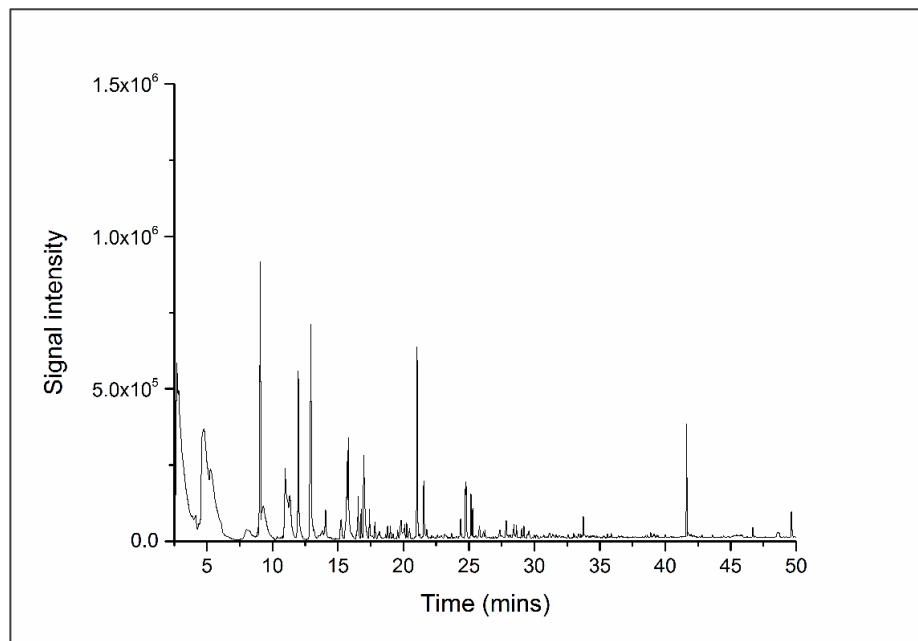
Figure 4.5: GC-MS chromatogram for bio-oil with ZSM-5 catalyst.

The chromatogram for the oil which was produced with a catalyst (Figure 4.5) appears to contain fewer peaks and a lower peak area which indicates that the catalyst introduced greater selectivity to the compounds in the oil whilst reducing the oil yield. The decrease oil yield has already been determined using measurement of liquid yield and Karl-Fischer titration in Table 4.1. Further detail will be obtained through semi-quantitative analysis of the pyrolysis oil using library matching of compounds detected by GC-MS.

The pyrolysis oils are composed from a complex mixture of compounds with each compound peak given a relative proportion (%) determined as the peak area for each compound divided by the total area for all the compounds identified. This can be used to characterise the types of compounds which together compose the oil. The results are semi-quantitative but allow for the composition of pyrolysis oils obtained from different sample sand catalysts to be compared. Differences in the types of compounds which compose a sample should be observed as a change in relative signal. However, these values are not absolute values and should not be treated as such. Table 4.2 shows the proportion of the compounds (area %) from the oil which can be categorised according to four different criteria. Each criterion is non-exclusive, such that a compound will be defined according to each criteria with each accounting for 100% of peak area. For example: a single compound may be aromatic (contain an aromatic ring), oxygenated (contain an oxygen atom), uni-cyclic (contain one cyclic ring feature) and defined by a molecular size between C_5-C_{12}.

Table 4.2: Proportion of compounds identified in bio-oil which contained an aromatic feature, oxygen, cyclic features or are within the gasoline fuel range C_5-C_{12}, with and without ZSM-5 catalyst.

	Sand	ZSM-5
Aromatic (%)	64.4	99.4
Aliphatic (%)	35.6	0.6
Oxygenated (%)	99.8	37.3
Non-oxygenated (%)	0.2	62.7
C_5-C_{12} (%)	98.2	97.2
$\geq C_{13}$ (%)	1.8	2.8
Uni-cyclic (%)	88.9	83.6
Bi-cyclic (%)	0.7	13.6
Tri-cyclic (%)	0.0	2.7
Quad-cyclic (%)	0.0	0.1
Linear (%)	10.4	0.0

4.2.2.1 Aromatic compounds

One of the key functional features in hydrocarbon compounds is the presence of highly stable aromatic rings [104, 157, 218, 226-229]. Aromatic compounds are desirable both for chemical and fuel production and are an important part of most fuel blends due to some of its useful properties such as increasing octane number in a fuel which can have implications on the ignition characteristics. Aromatic compounds are produced in oil refineries through catalytic reactions both to produce valuable materials but also to provide hydrogen which is important for other upgrading reactions (see Figure 4.6). Each fuel is a complex mixture of compounds and the addition of aromatic compounds may be used to improve ignition and combustion behaviour with the blend profile adjusted to provide a fuel which best meets the required purpose [41, 230-233].
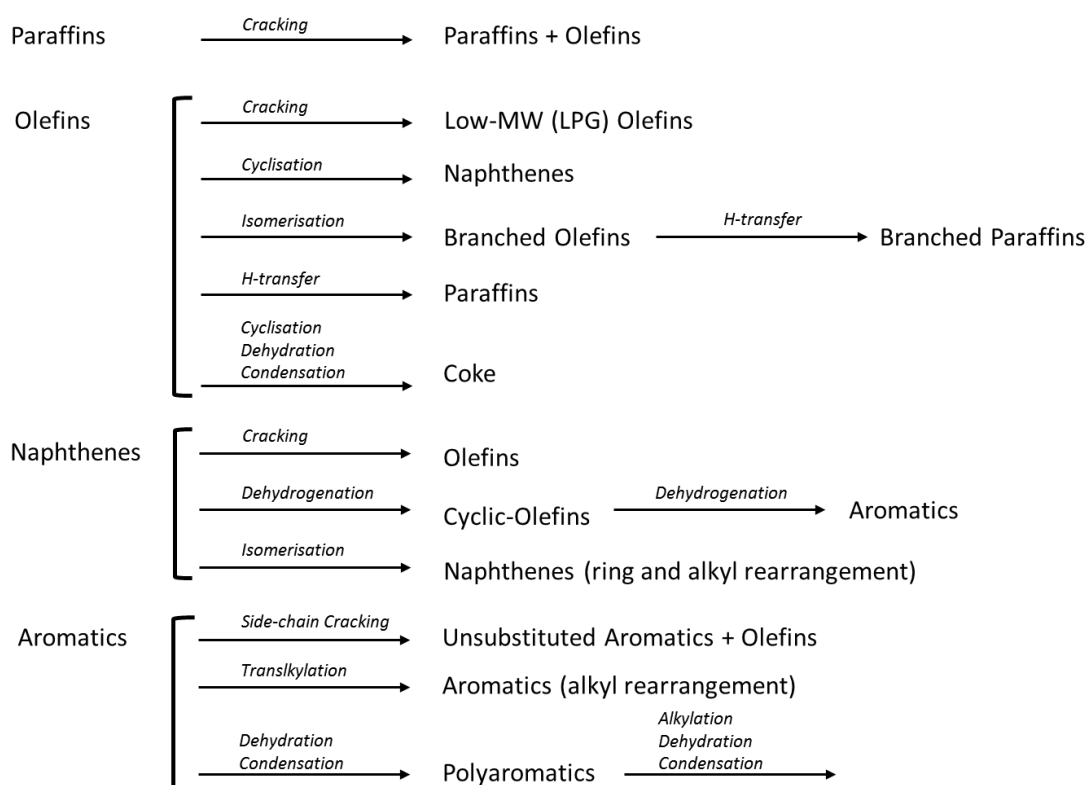
Figure 4.6: Summary of Fluid catalytic cracking reactions from Talmadge et al. [41].

Figure 4.6 is a summary of reactions which are commonly observed during the fluid catalytic cracking of the 4 main hydrocarbon constituents which make up a crude feedstock, paraffins (alkanes), olefins (alkenes), naphthenes

(cyclo-alkanes) and Aromatics. These reaction pathways can also interconvert between these compound types [41].

The removal of linear hydrocarbons (linear aliphatics) during pyrolysis is most often due to three effects. Cracking of both paraffins and olefins to produce greater quantities of low molecular weight hydrocarbons as was observed in the gas analysis. Coke deposition may also remove linear aliphatic hydrocarbons through cyclisation, dehydration and condensation. Aliphatics may also be involved in reaction pathways which produce naphthenes and aromatics through cyclisation and dehydrogenation reactions. Liu et al. [58] propose that non-cyclic products derived from cellulose and hemi-cellulose are likely to form aromatic and poly-aromatic compounds through Diels-Alder reaction pathways with lignin derived aromatics more likely to follow the hydrogen abstraction acetylene addition (HACA) mechanism which was studied by Shukla et al. [234] (see Figure 4.7). There are other mechanisms which are not listen here but which can also produce aromatic and polyaromatic compounds.
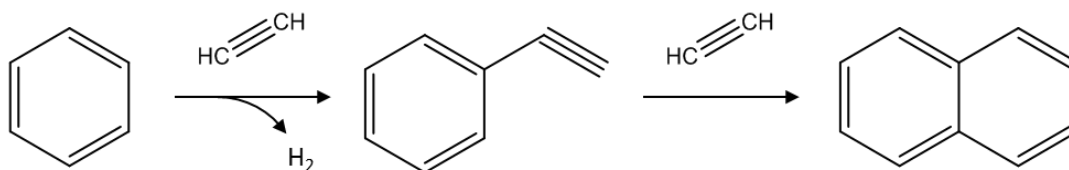
Figure 4.7: HACA mechanism proposed by Li et al. [58].

The process of producing aromatics releases hydrogen so are referred to as dehydrogenation reactions and this hydrogen becomes available for reactions such as those in Figure 2.22. which remove oxygen in the form of water. The hydrogen yield decreased when the ZSM-5 catalyst was used which is counter-intuitive considering the aromatic compound proportion increased which should have led to greater hydrogen yield. The hydrogen must therefore have been utilised, which may account for part of the increase of water in the pyrolysis products, which was large. In this way increasing aromatic yield may be beneficial in its own right but might also provide a pathway towards oxygen removal [39, 41, 235].

Figure 4.8 shows the types of compounds which were measured using GC-MS analysis of the oils from pyrolysis of biomass with and without the ZSM-5 catalyst. The proportion of compounds which contained aromatic rings increased from 64% to 99% through addition of the ZSM-5 catalyst. This is a

substantial change although at the same time the oil yield has also decreased from ~35 wt.% to ~14 wt.% such that the overall mass of aromatic containing compounds would be reduced if the semi-quantitive value for aromatics is applied to the oil yield.

Beyond determining whether a compound contains an aromatic ring it is also of value to evaluate the type of aromatic containing compounds which is in the oil. Figure 4.8 shows the relative proportions of different aromatic compounds which were identified in the pyrolysis oil. Primary aromatics, those with a single aromatic ring and which do not contain oxygen, are the most valuable of the aromatic species for fuel use. Phenolic compounds are similar to primary aromatics, although they contain oxygen which causes these compounds to be more reactive and acidic. These phenolic compounds may be converted into primary aromatic compounds through dehydration reactions [33]. Indene and naphthalene derivatives are aromatic compounds with two-ring features and are suitable for fuel use at a limited scale. PAH compounds contain two or more aromatic rings which in many cases would include naphthalene and indene compounds, however, it is useful to separate them in this case as Naphthalene and indene compounds, whilst not ideal compounds, are more suitable for fuel use than larger poly-aromatic compounds.
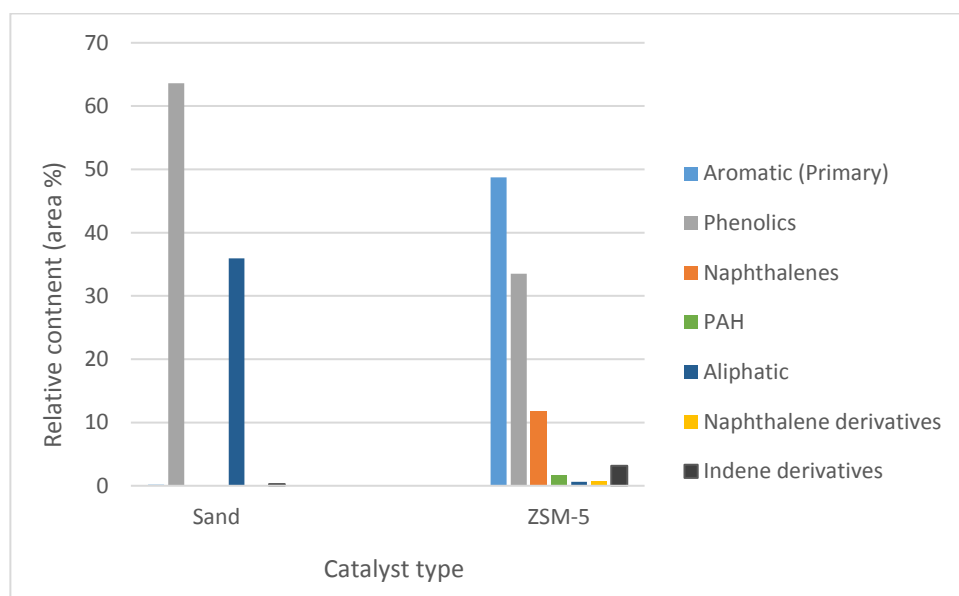
Figure 4.8: Oil composition categorised by compound type for raw and ZSM-5 upgraded biomass.

When no catalyst was used in biomass pyrolysis the majority of compounds were of the phenolic (64%) and aliphatic (36%) types. The aliphatic compounds

included acids, esters, ketones, furans and sugars. These results are similar to those obtained by Zhang et al. [146] during pyrolysis of rice husks although they observed a lower phenolic proportion (40%). When Zhang et al. introduced ZSM-5 catalyst to the process they observed a reduction of phenolic compounds to around 30% and a small reduction in the other aliphatic compounds. Sugar compounds which were present in the non-catalytic pyrolysis oil were completely removed in the catalytic pyrolysis oil and this too was observed during these experiments.

The broad feature in Figure 4.4 between 28-30 minutes is caused by sugar compounds and in Figure 4.5 which is the chromatogram from the ZSM-5 catalysed pyrolysis oil, this feature is no longer present. Zhang et al. [146] also observed an increase in hydrocarbon compounds (without oxygen) from 0% in the non-catalytic process through to around 40% when ZSM-5 was introduced with both primary (uni-cyclic) and secondary (bi-cyclic) aromatics identified. This increase is also observed in this research with a shift from 0% primary aromatics in the non-catalytic process to over 60% in the catalytic process and a shift from 0% naphthalenes to over 10%.

4.2.2.2 Compound molecular size

Another key feature particularly for produce fuel is the effect of compound molecular size which can have a strong effect on the way in which fuels perform as it is one of the main factors in fuel vaporisation temperatures and behaviours [41]. In a petroleum refinery compounds are separated by distillation which utilises phase change temperatures such as boiling range. Boiling point of a compound correlates closely with molecular carbon number so it is possible to differentiate compounds according to the number of carbon atoms which make up the compound. The range of compounds which are used for fuel can vary depending on the required use with light compounds (C_3-C_4) often utilised for LPG (Liquefied petroleum gas); Naphthas (C_5-C_{10}), predominately going to gasoline purposes; middle distillates span a larger range (C_{10}-C_{20}). This range can be subdivided into two sub categories with C_{10}-C_{14} useful for kerosene or gasoline production and the upper range C_{14}-C_{20} being more suitable for use as diesel fuel or as a heating oil [41]. There are increased difficulties with utilising biomass derived oils for aviation fuels due to increased rigour towards standards and testing to ensure safety [236]. This research is using the range between C_5 and C_{12} to encapsulate the compounds most suitable for gasoline utilisation, although this is a compromise with a proportion of compounds

between the ranges or C_4-C_{12} used for this value across literature (see Table 4.3).

Table 4.3: Compound molecular size ranges assigned to different fuel usages across literature.

LPG	Gasoline	Kerosene	Diesel	Reference
3-4	5-10	10-14	14-20	[41]
-	5-12	-	-	[237]
-	8-12	-	-	[238]
-	8-10	-	-	[94]
-	5-12	13-22		[148]
-	-	8-16	-	[115]
-	4-10	-	-	[239]
-	4-10	-	-	[232]
-	-	-	10-24	[240]
3-4	4-12	8-18		[11]

Examination of the compounds recorded in the pyrolysis oil produced from biomass with and without ZSM-5 catalyst (Table 4.2) shows that there is only a small difference between the proportion of compounds identified in the gasoline fuel range (C_5-C_{10}) with compounds identified in the fuel range at near to 100% of the total relative abundance. This shows that pyrolysis oils from biomass are likely to be suitable for production of hydrocarbon fuels with use as a gasoline fuel more preferable than for diesel fuel if the molecular size is the major consideration. The addition of the catalyst leads to a small decrease in fuel range compounds although this effect is within the standard deviation determined from repeated experiments.

ZSM-5 catalysts can cause compound size to increase as well as decrease. The primary reactions with relation to size selectivity are olefin cracking, to produce smaller MW olefins (C_3-C_4), and dehydrogenation to produce aromatic compounds, which can lead to larger molecular weight compounds. The change in fuel range compounds is likely to depend on a combination of these two reactions. Talmadge et al. suggest that ZSM-5 leads towards C_5-C_{10} selectivity within a crude oil refinery process, however in this case where the oil yield was already matching the fuel range to a high degree, the ratio of catalyst to feedstock may need to be optimised to increase this further. Optimisation of is particularly important in this regard as to produce a 1-unit increase in octane number through the use of upgrading catalysts in the refining process produces a 2% decrease in gasoline yield [41].

4.2.2.3　　Cyclic and linear compounds

Hydrocarbon fuels are composed of a number of types of compounds including paraffins and naphthenes which are naturally occurring and olefins and primary aromatics (uni-cyclic) which are often produced through catalytic reactions. In general, catalytic reforming seeks to upgrade paraffins by converting them to primary aromatics and naphthenes and then to take these naphthenes which can be further processed to produce primary aromatics. The primary aromatic is the preferred product because it has a high octane number and produces hydrogen for use in further reactions as well. There are also issues with combustion of polycyclic aromatic hydrocarbons (PAH) which are hydrocarbons that consist of 2 or more fused aromatic ring features and are problematic compounds for soot, coke and tar formation as well as being toxic in their own right [39, 41, 59, 230, 241].

Analysis from the non-catalytic pyrolysis experiment identified the majority of pyrolysis products as uni-cyclic in nature (89%) with some linear compounds (10%) and a very small proportion of bi-cyclic naphthalene compounds (<1% of identified compounds). In this regard the non-catalytic pyrolysis oils appear suitable for fuel use with a minimal formation of PAH compounds. The addition of the ZSM-5 catalyst to pyrolysis of biomass, alters this by removing the linear compounds and increasing the proportion of PAH formed. This includes an increased formation of compounds containing one, two and three membered rings. The uni-cyclic compounds are still the major product identified however the proportion of bi-cyclic compounds has increased significantly. Catalytic reforming would be a potential method for improving this oil by converting some of these PAH compounds into primary aromatic compounds but this would require further energy input and increase the cost of processing these oils [41].

4.2.2.4　　Oxygen containing compounds

The oxygen containing compounds within fuels can lead to properties which are poor for fuel use including low pH values, low boiling points, high viscosity and low oil stability [27, 123]. It is therefore, important for a successful upgrading system to remove oxygen from the oil. It has been observed that both the water yields as well as the carbon dioxide and carbon monoxide yields increased significantly when the ZSM-5 catalyst was used, and this suggests that, during pyrolysis, oxygen was removed from the compounds which comprise the oil. Analysis of the oil by GC-MS indicates that this is indeed the case. In the non-catalytic pyrolysis process 100% of compounds which were identified contained

oxygen, in contrast to this when the ZSM-5 catalyst was used only 37% of the compounds identified contained oxygen. This is a large reduction however if these oils are to be successfully integrated into current refinery infrastructures the oxygenated compounds should reasonably be below 10% and hydro processing to reduce oxygen content to this level can add significant cost to the process. Therefore, a reduction in the proportion of oxygenates can lead to large cost savings for upgrading as well as improving fuel mixing and handling properties [41]. Oxygen content is not directly measured in during many testing procedures however indirect effects of oxygen content such as energy density and pH are measured, for which a high oxygen content will cause non-compliance [38]. Testing regimes such as that implemented in the EU set a maximum oxygen content for gasoline at 3.7 wt.% [107] although most bio-oils are above this value blending of biomass derived fuels with petroleum derived fuels may be possible to reduce the oxygen content however this would be dependent on miscibility of the two fuels.

In an ideal situation pyrolysis oil derived from biomass for use as a gasoline fuel would contain aromatic compounds in the range of C_5-C_{12}, with low or no oxygen containing compounds. Fuel standards such as the EU standard will often have maximum aromatic content which is lower than that for biomass, however blending of biomass can ensure than the maximum aromatic content is not exceeded. In this way the biomass derived oils may be used to increase the octane number of petroleum derived fuels. Figure 4.9 and Figure 4.10 show the molecular size distribution defined according to carbon atoms of the bio-oil compounds determined by GC-MS. The compounds which are both non-oxygenated and aromatic are the most suited to fuel use and are highlighted in orange.

The effect of utilising a catalyst is an increase in compounds which meet the desired properties. However, there is also a shift of the distribution with a tighter size distribution to the C_7-C_8 region. This highlights the templating effect ZSM-5 can have on molecule sizes through restriction of reactions which may occur within the regularly sized pores [39, 59]. Whilst many of the changes observed in the bio-oils through use of the ZSM-5 catalyst may be desirable, there are also drawbacks including an increased number of compounds which are beyond than the C_5-C_{12} fuel range, and these include PAH compounds. It is important to consider all aspects of a particular compound rather than focussing too closely on one aspect or another. The PAH compounds may appear as an improvement due to their low oxygen content but are detrimental to the fuel and are undesirable due to coke formation and toxicity.
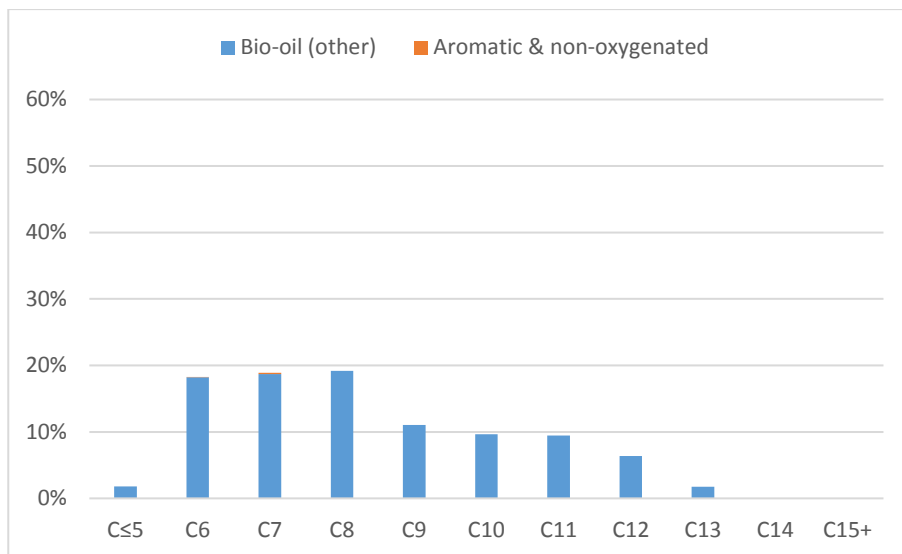
Figure 4.9: The size distribution of compounds in biomass non-catalytic pyrolysis oil (defined by number of carbon atoms), with compounds which are both aromatic and non-oxygenated highlighted (orange).
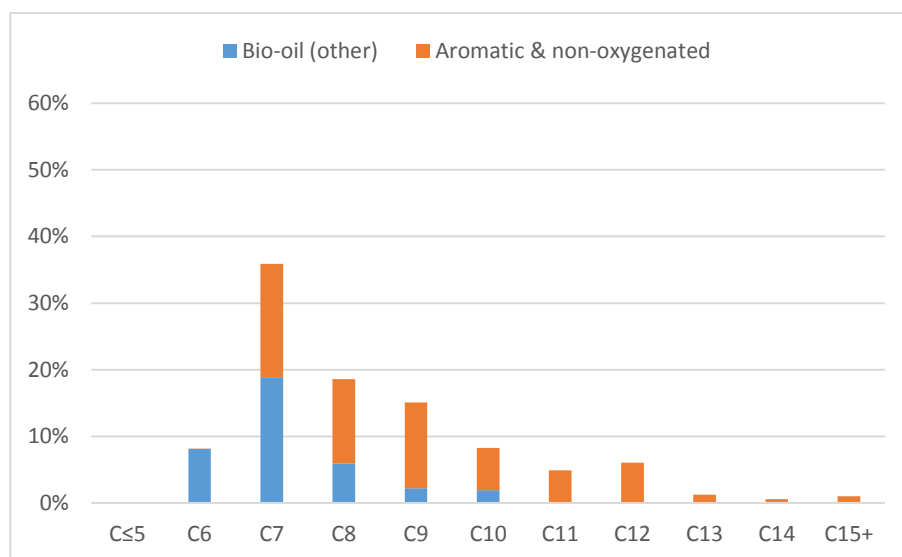
Figure 4.10: The size distribution of compounds in biomass catalytic pyrolysis oil (defined by number of carbon atoms), with compounds which are both aromatic and non-oxygenated highlighted (orange).

4.3 Pyrolysis of biomass with metal impregnated ZSM-5 Catalyst

Introducing a catalyst to the pyrolysis process had a significant impact on the yields and the composition of the products. There are a multitude of catalysts which could be explored for improvement of bio-oil properties. One relatively simple method for modifying ZSM-5 is by addition of metal atoms to the porous catalyst which can act as a co-agent in catalytic processes. In this research seven metals which showed promising results in literature were examined (Cu, Co, Ni, Ga, Fe, Mg and Zn) each at 5 wt.% loading [30, 58, 59, 134, 135, 137, 242]. The results from these experiments will be compared against those from the unmodified ZSM-5

4.3.1 Product yields of biomass with metal impregnated ZSM-5 Catalyst

Table 4.4 shows the product yields during pyrolysis of biomass with the metal impregnated catalysts. The yields of char were relatively unaffected by pyrolysis with the different metal catalysts whereas the liquid and gas yields showed significant variation. The highest liquid yield was produced using the copper impregnated ZSM-5 at ~51 wt.% with the lowest liquid yield from the nickel catalyst at ~35 wt.%. In comparison the unmodified ZSM-5 catalyst produced a liquid yield of ~48 wt.% and the sand at ~56 wt.%. Therefore, if the target is to maximise liquid yield then all of the metal catalyst are inferior to pyrolysis without catalyst and only three of the seven metal-impregnated catalysts had a greater liquid yield than the unmodified ZSM-5. This result compares to research by Zheng et al. [137] which found that metal modification of ZSM-5 increased gaseous yields at the expense of liquid yields. The gas yield for ZSM-5 was 27 wt.% which was exceeded by the cobalt, nickel, iron and zinc impregnated ZSM-5 which all had lower liquid yields than unmodified ZSM-5. The three metal catalysts which produced greater liquid yield than ZSM-5, copper, gallium and magnesium, had lower gas yields.

The oil yield for biomass without a catalyst was ~33 wt.% and the use of a catalyst reduced this to ~14wt.%. The oil yield as with the liquid yield is different for each metal zeolite catalyst and a high liquid yield does not always produce a high oil yield. The highest oil yield was obtained for copper (25 wt.%) and the lowest for magnesium whereas cobalt had the second lowest liquid yield and magnesium (~14 wt.%) which produced the second highest liquid yield. The addition of the metals to ZSM-5 improves the oil yield for all of the metals except magnesium, with copper and zinc providing the largest increases. Magnesium,

132

nickel and gallium are all within the standard deviation value for liquid yield (1.2 wt.%) determined in the experimental methodology chapter so these should be considered as equivalent to ZSM-5 rather than increased values.

Table 4.4: Yields from pyrolysis of biomass at 500°C with metal impregnated ZSM-5 catalysts.

	Char (wt.%)	Liquid (wt.%)	Gas (wt.%)	Water (wt.%)	Oil (wt.%)	Mass Balance (wt.%)
ZSM-5 (Cu-5%)	25.1	51.3	24.1	26.6	24.7	97.4
ZSM-5 (Co-5%)	27.0	39.7	29.6	19.4	20.3	94.7
ZSM-5 (Ni-5%)	26.6	34.9	41.7	20.5	14.4	95.9
ZSM-5 (Ga-5%)	25.3	49.0	25.8	34.9	14.0	99.5
ZSM-5 (Fe-5%)	24.5	43.6	27.9	27.6	16.1	102.0
ZSM-5 (Mg-5%)	24.5	51.0	26.5	37.1	13.8	102.2
ZSM-5 (Zn-5%)	24.9	48.3	29.3	25.0	23.3	102.5
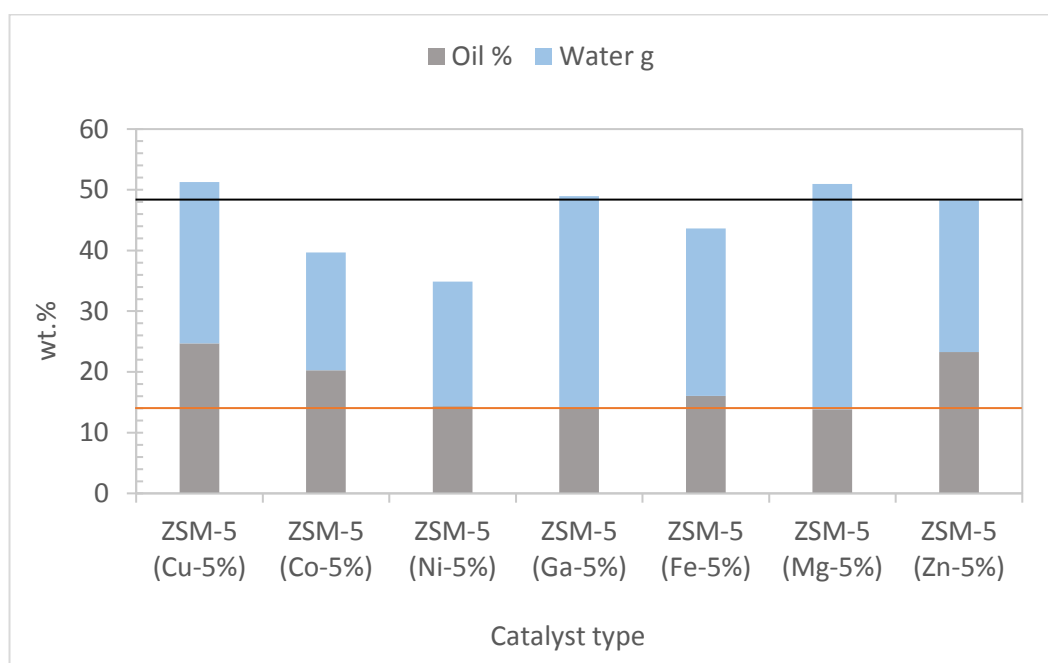
Figure 4.11: The liquid yield for metal impregnated ZSM-5 catalysts at 500°C compared against the oil yield for unmodified ZSM-5 (orange line) and total liquid yield for ZSM-5 (black line).

Figure 4.11 shows the liquid yield of each metal/ZSM-5 catalyst with the liquid yield plotted as a combination of the oil yield and the water yield. This shows clearly that a higher liquid yield does not always imply a higher oil yield. This is because of deoxygenation and coke formation. Deoxygenation using dehydration reduces the oil yield but produces water which remains a liquid product, whereas deoxygenation through carbon oxides formation reduces both the oil and liquid yield as it produces a gaseous product. Coke formation also reduces both the oil yield and the liquid yield as it produces a solid product. Cobalt and nickel show a particular reduction in liquid yield which appears to indicate a lower water content than for many of the other metal catalysts. This may indicate that water not being produced or is being used to produce hydrogen gas (see Table 4.13). In this way the nickel impregnated ZSM-5 catalyst may be more suitable for promotion of gasification rather than pyrolysis.

An increase in water yield reduces the quantity of oil produced but also acts to upgrade the oils. Water is a product of dehydration reactions which remove oxygen from bio-oil compounds and condensation reactions which may produce aromatic compounds. However, it may also act as reactant in the formation of carbon dioxide from carbon monoxide or steam reforming reactions which produce carbon monoxide both yielding hydrogen gas as a product. Figure 4.12 outlines a number of key reactions for which hydrogen and water are important reactants and products. Many of the key reactions which remove oxygen from the oil compounds utilise water at some point [39, 242].
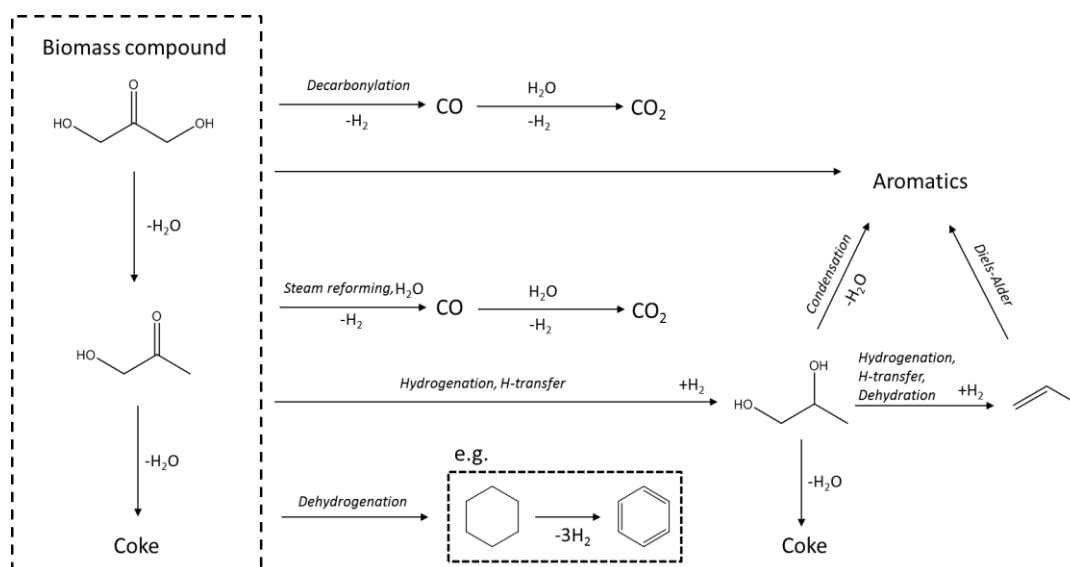
Figure 4.12: Key reaction pathways involving hydrogen and water during catalytic upgrading of oxygenated biomass derived feedstock proposed by Huber et al. [39].

Figure 4.13 shows the composition of the gases which were collected during the pyrolysis experiments. It is immediately clear that the reductions in liquid yield for nickel and cobalt which resulted in reduced water yield were likely to be due to formation of hydrogen gas. The yield of hydrogen gas for both these catalysts is significantly higher than for the other catalysts with nickel producing ~10 mmolg^{-1} and cobalt ~ 5mmolg^{-1}. For the other catalysts the hydrogen gas yield is below 2mmolg^{-1}. In contrast to this the unmodified ZSM-5 produced 0.36 mmolg^{-1}. Iliopoulou et al. [136] examined flash pyrolysis of biomass with metal impregnated catalysts and observed large increases in hydrogen yield for cobalt and nickel with the nickel hydrogen yield more than twice that of the cobalt as in this case.

As well as these extremely large increases for nickel and cobalt, the other metal catalysts also increased hydrogen yield in the order magnesium (0.4 mmolg^{-1}) << gallium (1.2 mmolg^{-1}) < copper (1.3 mmolg^{-1}) < iron (1.3 mmolg^{-1}) < zinc (1.4 mmolg^{-1}). Nickel also had an increased output for both carbon monoxide (5.7 mmolg^{-1}) and carbon dioxide (4.3 mmolg^{-1}) compared to unmodified ZSM-5 (CO-3.4 mmolg^{-1}, CO_2–2.9 mmolg^{-1}). The other metals had carbon monoxide and carbon dioxide values which were marginally higher or lower than those for ZSM-5. In terms of hydrocarbon gases (C_nC_m) output decreased for all the metal impregnated catalysts compared to ZSM-5 but copper, cobalt and nickel decreased by a greater amount.
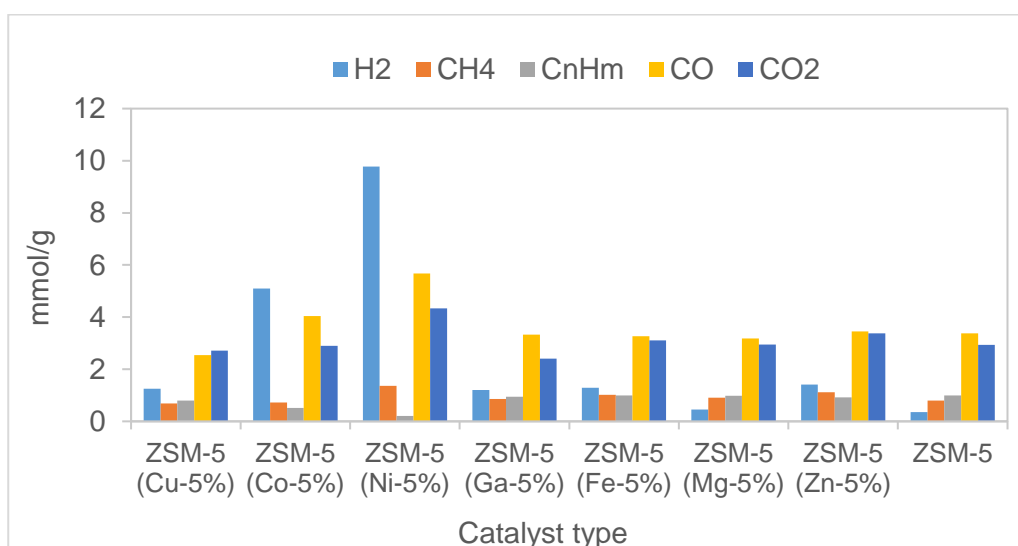
Figure 4.13: The composition of the gas collected during pyrolysis (without nitrogen) using metal impregnated ZSM-5.

Figure 4.14 gives a more detailed view of the non-oxygen containing gases. The yield of methane increased from 0.8 mmolg^{-1} in unmodified ZSM-5 to 1.4 mmolg^{-1} in nickel, 1.1 mmolg^{-1} in zinc and 1.0 mmolg^{-1} in iron with a small reduction for copper and cobalt. The hydrocarbon gases other than methane reduce slightly on addition of a catalyst however the selectivity remained the same for each with $CH_4 > C_2 > C_3 > C_4$ as was the case with ZSM-5.
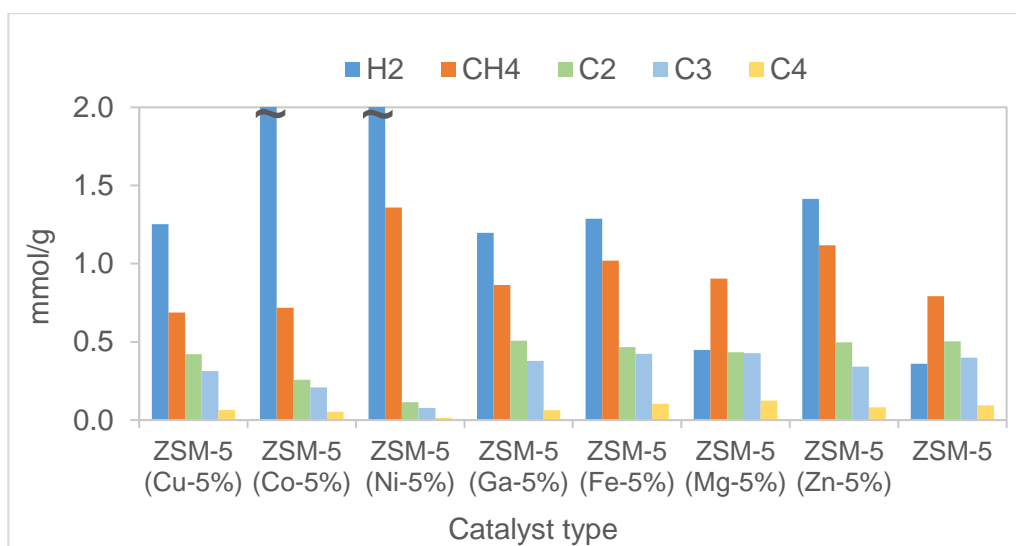
Figure 4.14: The composition of the non-oxygen containing gases collected during pyrolysis with metal impregnated ZSM-5 catalyst.

4.3.2 Pyrolysis oil composition with metal impregnated ZSM-5 catalysts

The use of a catalyst may change both the composition of the oil as well as the yield and this, therefore, needs to be considered to understand if the use of a catalyst is beneficial for production of gasoline range fuels. Table 4.5 reports the types of compounds present in the bio-oil produced from catalytic pyrolysis using the metal impregnated catalysts. When unmodified ZSM-5 was used as the catalyst 99.4% of the compounds determined by GC-MS contained at least one aromatic ring, 62.7% of compounds were non-oxygenated, 97.2% of compounds were within the gasoline fuel range and in terms of cyclic nature 83.6% unicyclic, 13.6 bi-cyclic, 2.7% tri-cyclic, 0.1% quad-cyclic and 0% linear. The pyrolysis yield data suggested that oil yields remained equivalent to ZSM-5 or were improved so any improvement in the composition of the oil would yield an overall advantageous effect as a combination of both yield and composition.

Table 4.5: Proportion of compounds in bio-oil which were aromatic, oxygenated, cyclic or in the gasoline fuel range (C_5-C_{12}), for catalytic pyrolysis using metal impregnated ZSM-5.

	ZSM-5 (Cu-5%)	ZSM-5 (Co-5%)	ZSM-5 (Ni-5%)	ZSM-5 (Ga-5%)	ZSM-5 (Fe-5%)	ZSM-5 (Mg-5%)	ZSM-5 (Zn-5%)	ZSM-5
Aromatic (%)	100.0	96.3	91.6	100.0	100.0	97.3	95.0	99.4
Aliphatic (%)	0.0	3.7	8.4	0.0	0.0	2.7	5.0	0.6
Oxygenated (%)	34.5	34.0	67.3	26.0	47.1	50.4	41.8	37.3
Non-oxygenated (%)	65.5	66.0	32.7	74.0	52.9	49.6	58.2	62.7
C_5-C_{12} (%)	100.0	99.1	99.3	99.4	99.5	100.0	98.6	97.2
$\geq C_{13}$ (%)	0.0	0.9	0.7	0.6	0.5	0.0	1.4	2.8
Uni-cyclic (%)	83.4	87.0	79.7	79.3	80.7	81.9	76.7	83.6
Bi-cyclic (%)	16.6	12.3	11.8	20.6	19.3	18.1	23.3	13.6
Tri-cyclic (%)	0.0	0.3	0.0	0.0	0.0	0.0	0.0	2.7
Quad-cyclic (%)	0.0	0.3	0.1	0.0	0.0	0.0	0.0	0.1
Linear (%)	0.0	0.0	8.4	0.0	0.0	0.0	0.0	0

4.3.2.1 Aromatic compounds

The increased production of aromatic compounds is beneficial for a number of reasons. These compounds can be valuable as they may be used as building blocks in the production of chemicals [149, 243]. The formation of aromatic compounds from aliphatics may lead to the release of hydrogen gas during aromatization / dehydrogenation reactions which is can for further catalytic upgrading reactions such as dehydration. Aromatic compounds also have higher octane numbers than non-aromatic equivalents, this may enable pyrolysis oils from biomass to be blended into petroleum oils to increase octane numbers important for high performance fuels [41].

The introduction of the unmodified ZSM-5 catalyst to pyrolysis of biomass increased the aromatic compounds which were identified form 65% of the total compounds to over 99%. The metal modified catalyst also produced similar proportions of aromatic compounds ranging between 92-100%.

Veses et al. [134] studied the upgrading of bio-oil using 1 wt.% metal impregnated ZSM-5 catalysts (Ga, Cu, Ni, Mg and Sn) and found that the aromatic fraction (phenols, primary aromatics and PAHs) determined by semi-quantitative GC-MS analysis increased from ~59% in the raw bio-oil to between 74% and 79% in the metal impregnated catalysts. Stanton et al. [135] used Py-

GC-MS to analyse the effect of ~3 wt.% metal impregnated ZSM-5 catalysts (Cu, Ga, Ni, Co) on for the upgrading of pine pyrolysis vapours in an inert atmosphere and found that aromatic (primary aromatics + phenols) ranged between 74% (cobalt) and 84% (gallium) although each was lower than the 92% recorded for un-modified ZSM-5.

These studies suggest that whilst there are variations observed between the metal modified catalysts these are smaller than those observed between a non-catalytic system and a catalytic system. In each case the use of a ZSM-5 catalyst increased the aromatics content compared to a non-catalytic system. Veses et al. [134] examined upgrading of bio-oils which had been obtained using non-catalytic pyrolysis as a second stage (offline). This produced lower aromatics content than in the case of Stanton et al. [135] and this research where upgrading was combined as part of the pyrolysis process (online). It must be noted that Veses et al. [134] used a lower metal loading on the ZSM-5 catalyst (1 wt.%) than either Stanton et al. (3 wt.%) or this research (5 wt.%).

The catalysts which gave the highest aromatic content in this research was iron, gallium and copper which all recorded 100% aromatic compounds (which was an increase compared to unmodified ZSM-5). Nickel, magnesium, zinc and cobalt all decreased compared to ZSM-5, with the biggest decrease observed for nickel. In contrast to this the nickel catalyst used by Stanton et al. [135] performed more effectively with regards to 82% aromatic content than cobalt (74%) and copper (81%) and in the results from Veses et al. [134] nickel and magnesium produced a slightly higher aromatic yield than gallium and copper [134]. This variation between experiments highlights that the reaction pathways for formation of aromatic compounds is complex. Figure 2.24 highlights some of the key pathways proposed by Adjaye et al. [124, 125]. The pathway which leads to the formation of aromatic compounds involves a number of catalytic reactions including deoxygenation (decarbonylation, decarboxylation and dehydration), cracking (breaking of larger hydrocarbon compounds into smaller units) and oligomerisation (combining of small hydrocarbon units into a larger molecule). The resulting aliphatic compounds may then undergo aromatisation, alkylation and isomerisation to produce aromatic compounds. The resulting aromatic compounds may then be converted into coke and tar through polymerisation reactions [123]. Surface effects will also be crucial in the formation of aromatics with internal surfaces templating primary aromatic compounds whilst external surfaces may produce PAH compounds. The ratio of internal to external surfaces will depend on catalyst loading amongst other factor [120].

Research by Cheng et al. [102] examining gallium impregnated ZSM-5 catalysts suggested that whilst the metal atoms could replace protons within the material and encouraged decarbonylation of furan molecules leading to aromatisation of alkenes (olefins) this was hindered if Brønsted acid sites were unavailable. The temperature at which the reactions operated most effectively was also relatively unchanged in the presence or absence of the gallium atoms which suggests that the mechanism is not altered by the addition of the metal atom. It was proposed that the metal works in conjunction with the acid sites to promote aromatic formation. In addition to this, research by Zheng et al. [137] indicated that the relationship between acid sites and transition metal atoms was complex with the possibility of co-operation between Lewis acid sites, Brønsted acid sites and metal atoms as well as competition between them. This is further complicated by the introduction of the metal atoms leading to both increases and decreases in the strength of these acid sites within a material. Steric effects may also be introduced during metal impregnation with a potential reduction in internal surface, external surfaces or pore blocking. They also found that metals including nickel and copper could promote the formation of coke with the further effect of changing or reducing surface areas and pore volumes leading to deactivation of the catalyst and this was particularly prevalent where the metal loading was greater.

Therefore, the function of a catalyst is dependent both on the conditions of pyrolysis as well as the particular condition of the catalyst used [16, 134, 244]. In general, the metal impregnated catalysts encouraged formation of aromatic compounds although it must be noted that metal impregnation may lead to increased or reduced efficacy compared to an unmodified ZSM-5.
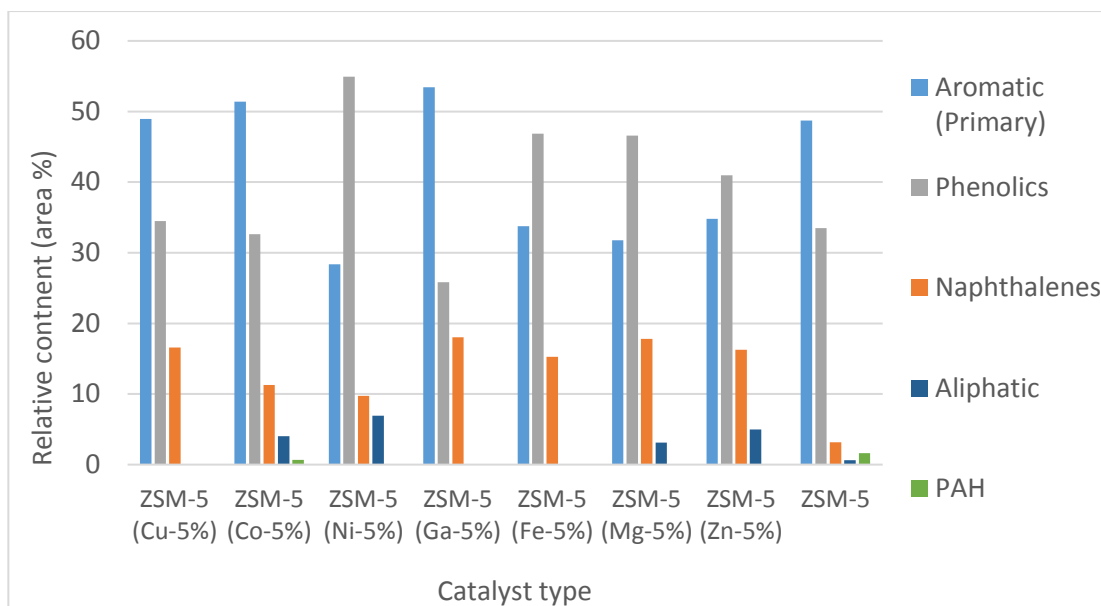
Figure 4.15: Oil composition categorised by compound type for different metal impregnated ZSM-5 catalysts.

Figure 4.15 compares the types of compounds within the bio-oil derived using metal impregnated ZSM-5 and this can be compared to that for unmodified ZSM-5 for which primary aromatics accounted 49%, phenolics 33% and naphthalenes 12%. When we compare the aromatic these values to the metal impregnated catalysts there are three which increase primary aromatic compounds and these are gallium (53%), cobalt (51%) and copper (49%). From these three catalysts, gallium also reduces the proportion of phenolics (26%) and produces an increased yield of non-oxygenated naphthalene compounds (15%). Cobalt increases the phenolic and decreases the naphthalene compounds and copper conversely, decreases the phenolic and increases the naphthalene compounds. Iron, magnesium and zinc all reduced the primary aromatic yield with an increased phenolic yield compared to unmodified ZSM-5, whilst nickel was the least effective catalyst according to these criteria with a large increase in phenolic compounds and a large decrease in the proportion of primary aromatic compounds.

This large decrease in nickel primary aromatics was not suggested by literature although Zheng et al. [137] showed that nickel-ZSM-5 was slightly less effective for 1-ring aromatic production than the other metal-ZSM-5 catalysts examined. They also highlighted that nickel impregnated on ZSM-5 is particularly selective for benzene production whilst less selective for toluene. This may account for the increased hydrogen production which is could be due to aromatisation reactions although it is also possible that steam reforming reactions are the cause of this high hydrogen yield. Benzene is more volatile (b.p. 80ºC) than the

other compounds measured such as toluene (b.p. 110ºC) and is more readily lost as a vapour prior to offline GC-MS analysis. It is possible therefore that the primary aromatic yield for nickel ZSM-5 should be higher than that measured.

The increase in aromatic compounds observed for gallium has been observed in literature [135, 137] as with Stanton et al. [135] identifying higher hydrocarbon oil yield as well as increased 1-ring aromatic selectivity compared to ZSM-5 and this was elevated beyond values for copper, nickel and cobalt. The high aromatic yields for gallium are not new observations with several studies utilising gallium to increase aromatic formation as part of a bifunctional catalyst involving a solid acid catalyst and gallium metal [59, 102, 153]. Cheng et al. [102] studied a number of different methods for inclusion of gallium into ZSM-5 framework and several methods were suitable for increasing aromatic production. It was found that if gallium was incorporated into the ZSM-5 structure through displacement of silicon or aluminium atoms this did not lead to improved aromatic yield, however, where the gallium metal atoms displaced protons within the catalyst pores the interaction between strong acid sites and a metal led to increased aromatic yield. The exact catalytic mechanism is not yet known but it is believed to function through promotion of decarbonylation of furan and aromatization of alkenes (olefins) which are also key steps in the deoxygenation of bio-oil compounds.

4.3.2.2   Compound molecular size (C_5-C_{12})

The compounds identified in pyrolysis oils with unmodified ZSM-5 catalyst which were in the gasoline fuel range (C_5-C_{12}) comprised 97.2% of the identified compounds and the metal impregnated catalysts increased this further with a range from 98.5% with zinc and increasing to nearly 100% with magnesium and copper. This is an improvement for fuel use, however, the unmodified ZSM-5 was already effective in regards to gasoline range hydrocarbon selectivity [41]. Rezaei et al. [123] examined the effect of pore size on the formation of coke within solid acid catalysts and concluded that for some model compounds a smaller pore size allowed small species to pass through the catalyst and undergo selective catalysis whilst inhibiting formation of large PAHs. They also discovered that for other compounds a small pore aperture hindered large species entering the catalyst pores which led to an increase in thermal coke formation rather than templated catalytic reactions. With bio-oils being composed of such complex combinations of compounds it is likely that both of these effects are occurring, although, in this case it appears as though the addition of metal to the ZSM-5 catalyst, which is understood to cause restriction

of pore apertures, may be favouring the formation of smaller liquid hydrocarbons through selective templating. The addition of metal to ZSM-5 catalysts to produce bifunctional catalysts has been shown to assist aromatic formation via favouring of dehydrogenation reactions as well as by reducing the number of Brønsted acid sites and at the same time causing more Lewis acid sites to form [123, 155].

4.3.2.3   Cyclic and linear compounds

The ZSM-5 which had not been modified led to 83.6% unicyclic, 13.6% bi-cyclic, 2.8% PAHs (tri-/quad-cyclic) and 0% linear compounds. Zheng et al. [137] researched the effect of 1% loading of Zn, Mg, Ga, Ni, Co, and Cu on ZSM-5, for catalytic pyrolysis of pine to produce bio-oil and these results can be compared to those from Zhang et al. [146] for various loadings (0-8%) of Fe-modified ZSM-5 during pyrolysis of risk husks.

Zheng et al. [137] found that the impregnation of 1 wt.% zinc to ZSM-5 increased the uni-cyclic aromatic yield whilst reducing the yield of bi-cyclic compounds and PAHs. When magnesium was impregnated onto ZSM-5 a minor decrease in unicyclic compounds was observed which was offset by an increase in bi-cyclic compounds. In this research, at 5 wt.% loading, the same result was also observed that the uni-cyclic compounds decreased slightly, and the bicyclic compounds also slightly increased with PAH compounds decreasing in each case.

When using gallium, Zheng et al. [137] found an increase for both uni-cyclic and bi-cyclic aromatics which is different to this research which found an increase in bi-cyclic compounds but not a decrease in the uni-cyclic compounds as with Zheng et al.

For both nickel and cobalt, results matched for both sets of research, with increases in the uni-cyclic proportion, however, in this research nickel produced a moderate amount of linear hydrocarbon compounds which were not included in the dataset used by Zheng et al. which focused on aromatic hydrocarbons. Copper impregnated ZSM-5 made little change for either research when compared to ZSM-5.

Iron with ZSM-5 was researched by Zhang et al. [146] and they found an increased bi-cyclic yield and a decreased uni-cyclic yield. This included an increase in benzene and toluene which was offset by a decrease in xylenes, ethylbenzenes and 1,2,4-trimethylbenzene and also a decrease in PAH as was observed for each of the other metal impregnated ZSM-5 catalysts.

The differences between the results from this research and literature values were small and may equally be due to differences in equipment and catalyst loadings rather than variations caused by the individual metal used. This is particularly likely considering the complex connection between pore size and compound size selectivity and the surface altering effect of introducing metal atoms into porous materials [137, 143, 146].

4.3.2.4   Oxygen containing compounds

The proportion of compounds in the oil produced from the unmodified ZSM-5 which contained oxygen was 37.3% and by comparison with Table 4.5 there are three catalysts which contain lower proportions of oxygenated compounds. These were copper (34.5%), cobalt (34.0%) and gallium (25.8%) of which gallium had the lowest value by a significant margin. The other catalysts all led to increased oxygenated content with nickel having the highest proportion of oxygenated compounds at 67%. Deoxygenation has three main routes for oxygen removal which are decarbonylation, decarboxylation and dehydration. Reactions involving Gallium impregnated ZSM-5 have been found to promote decarbonylation reactions [102], thereby leading to reduced oxygen content in bio-oils and this can be seen in Table 4.5 where the carbon monoxide gas emissions are elevated compared to many of the other metal based catalysts where carbon dioxide is higher [41, 134, 143]. The exception to this trend is for cobalt and nickel which produced higher carbon monoxide, carbon dioxide and hydrogen yields and decreased water yield compared to gallium, although these are probably due to steam reforming and water gas shift reactions rather than decarbonylation.

$$C_nH_m + nH_2O \rightleftharpoons (n + m/2)\,H_2 + nCO - \textit{Steam reforming}$$

$$CO + H_2O \rightleftharpoons H_2 + CO_2 - \textit{Water-gas shift}$$
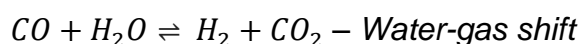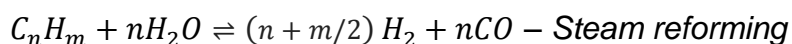
As well as observing the reactions which are promoted by a certain catalyst it is also important to understand the availability of compounds which will readily undergo a particular reaction [58]. The nickel catalyst produced the highest proportion of hydrogen gas of the metal catalysts by a significant margin. This hydrogen in turn may be used through a hydrodeoxygenation reaction to remove oxygen from the oil. However, this does not appear to have occurred with the water measured in the oil from the nickel loaded catalyst particularly low and the hydrogen remaining in the gas phase. In contrast to this the carbon monoxide and carbon dioxide content were increased, suggesting that more

oxygen was removed through decarbonylation and decarboxylation rather than hydrodeoxygenation. This is in contrast to experiments by Zheng et al. [137] and where nickel based ZSM-5 has led to oxygenated compounds reducing. Stanton et al. [135] found that metal (Co, Ga, Cu, Ni, Pt) impregnated ZSM-5, in an inert atmosphere, did not lead to reduced oxygenated compounds compared to unmodified ZSM-5 whereas Veses et al. [143] observed that metal (Sn, Cu, Ni, Mg) impregnated ZSM-5 did increase deoxygenation and found that this effect was greatest with magnesium, in this research magnesium produced one of the highest proportion of oxygenated compounds (50%). Due to the variation between studies it is likely that the deoxygenation potential of metal relies on several factors. One factor of particular importance may involve catalyst loading. Veses et al. used a 1 wt.% loading for which magnesium was an effective catalyst for oxygen removal however in this study 5 wt.% loading was used and it is possible that blockage of pores at the higher metal loading may be responsible for this reduced deoxygenation [158]. This effect was observed by Zheng et al. who also found high proportions of oxygenated compounds in magnesium impregnated ZSM-5 at 5 wt.% loading [137].

Figure 4.16 shows the molecular size distribution profiles for the compounds identified in oils produced during catalytic pyrolysis using the metal impregnated ZSM-5. As with the unmodified ZSM-5, C_7-C_8 was the mode molecular compound size. Copper, cobalt and gallium appear to be the most suitable for gasoline fuel use with the highest proportion of oxygen free aromatic compounds in the range C_8-C_{12}. The nickel catalyst is clearly the least effective of the catalysts measured here for fuel purposes.
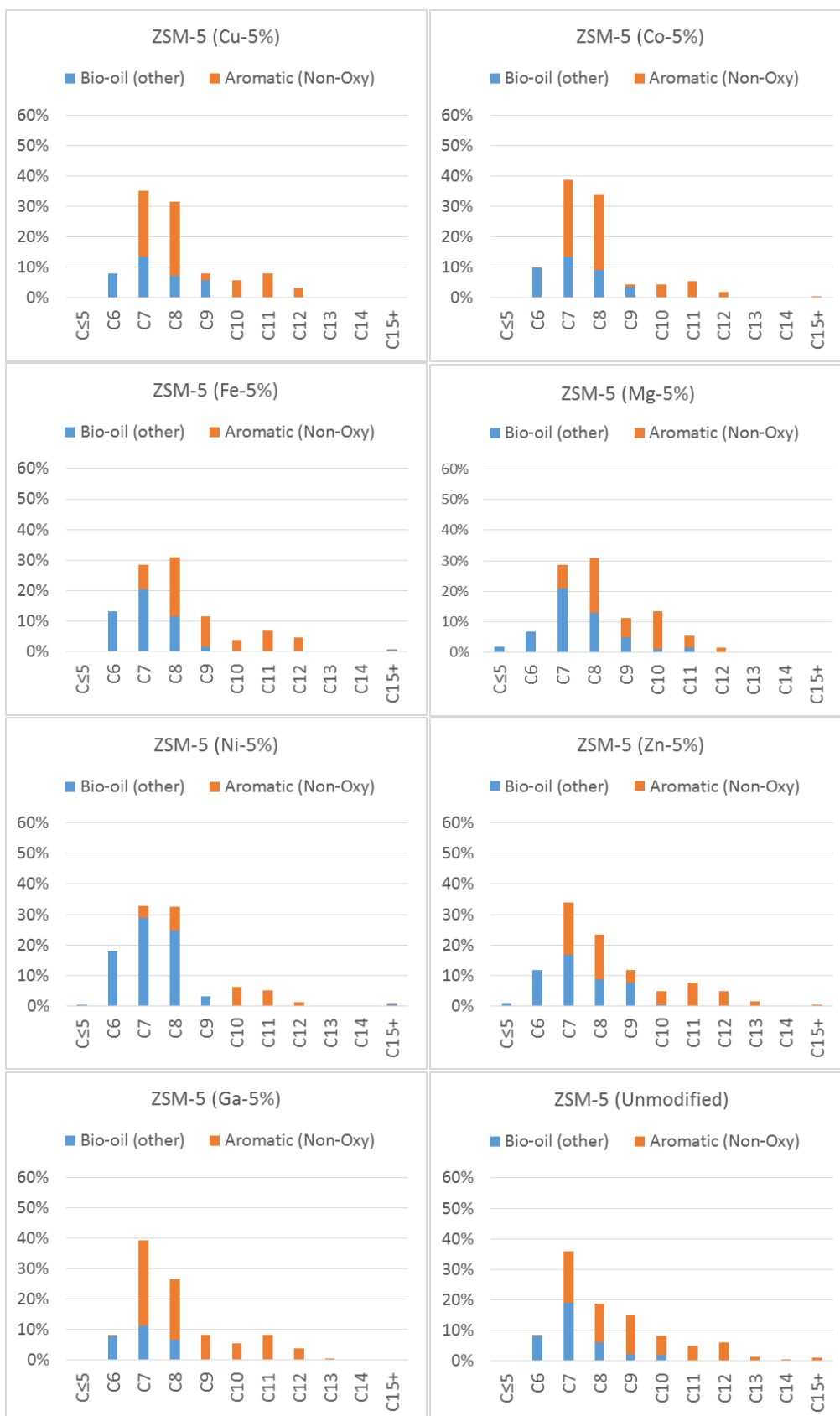
Figure 4.16: The compounds identified during metal impregnated catalytic pyrolysis of biomass were plotted according to molecular size with compounds which were both oxygenate and aromatic (1 or 2 rings) highlighted in orange.

4.4 Coke deposition on metal impregnated catalysts

Bayraktar and Kugler [245] examined coke deposition on FCC catalysts using TPD techniques and used the results to analyse the type of coke which was deposited over a range of temperatures. Habib et al. [246] identified four types of coke deposition on catalysts and these were used to classify the coke deposits identified by Bayraktar and Kugler.

The four coke types identified were:

- Catalytic coke formed during acid catalysed cracking reactions.
- Metal-contaminated coke formed through interactions with metal species present in the catalyst.
- Conradson coke or graphitic coke.
- Cat-to-oil coke which is due to hydrocarbon compounds which have become absorbed or adsorbed onto the catalyst surfaces.
-

Bayraktar and Kugler observed that cat-to-oil coke was removed from the catalyst during heating in an oxidising atmosphere in the lower temperature ranges between approximately 200-400°C. The metal contaminated coke was desorbed between 300-600°C. Catalytic coke was desorbed between 400-700°C and graphitic coke which represented a much smaller peak between 500-700°C. This was achieved through deconvolution of a poorly resolved broad peak fitted against Gaussian profiles. In this case the first derivative of the TPO plot against temperature gave two clear regions of weight change.

Gayubo et al. [247] identified two regions of coke deposition as 'thermal coke' at lower temperatures and 'catalytic coke'. The lower temperature thermal coke was related as that which deposits on the surface of the catalyst matrix whereas the catalytic coke was formed and deposited on the internal surfaces of the catalyst.

Table 4.6: TPO results showing coke deposition on metal impregnated catalysts used for pyrolysis of biomass at 500°C.

	Temp 1st Δ (°C)	1st Δ (wt.%)	Temp 2nd Δ (°C)	2nd Δ (wt.%)	Total Δ (wt.%)
Sand	-	-	-	-	-0.2
ZSM-5	100-400	0.8	400-700	2.3	3.1
ZSM-5 (Cu-5%)	100-400	0.9	400-700	1.3	2.2
ZSM-5 (Co-5%)	100-400	0.7	400-700	1.0	1.7
ZSM-5 (Ni-5%)	100-400	1.2	400-700	2.6	3.8
ZSM-5 (Ga-5%)	100-400	0.9	400-700	1.0	2.0
ZSM-5 (Fe-5%)	100-400	1.8	400-700	2.8	4.7
ZSM-5 (Mg-5%)	100-400	3.6	400-700	1.1	4.7
ZSM-5 (Zn-5%)	100-400	0.8	400-700	2.6	3.4

Table 4.6 identifies the weight loss which was associated with each metal impregnated catalyst during temperature programmed oxidation experiments with the weight change categorised by region, where separate regions of weight loss was observed. The catalysts which experienced the highest coke deposition were nickel, magnesium and iron which were the three poorest catalysts in terms of deoxygenation. The three catalysts with the lowest coke deposition was on the copper, cobalt and gallium catalysts which were also the most effective catalysts for deoxygenation. Zinc which was the catalyst which was in the middle for deoxygenation was also in the middle for coke deposition. This establishes a strong correlation between coke deposition and ability for a catalyst to remove oxygen from pyrolysis vapours. If this correlation is to be tested using the unmodified ZSM-5 we may compare it to the zinc impregnated ZSM-5 with the oxygenated compounds in the zinc catalyst at 41.8% and the oxygenated compounds in the ZSM-5 at 37.3%. This would suggest that the coke deposition for ZSM-5 should be slightly lower than that of zinc. This is indeed correct. The sand which was used to take the place of the catalyst in a non-catalytic system had negligible coke deposition although it darkened in colour during pyrolysis. This is not surprising as the zeolites have far greater surface area, on which coke may deposit, due to their porous nature. In terms of the temperature at which the coke was oxidised, one catalyst was significantly different from the others and this was the magnesium impregnated ZSM-5 which had a far greater extent of low temperature coke. The magnesium

catalyst also had the lowest surface area, and this may indicates that reduction in pore volume or blockage of pores caused thermal coke deposition on external surfaces and reduction in deoxygenation reactions. For the other catalysts the coke oxidation was greater in the high temperature region which would be expected if this represents internal coke deposition as the internal surface of ZSM-5 is greater than the external surface [120]. The low temperature oxidation could be due to compound adsorption referred to as cat-to-oil coke. This might indicate that this is not coke formation through the action of catalytic activity, producing coke, but is rather due to trapping of volatile compounds within the porous material. This may indicate that loading metal into the catalyst has obstructed the pores of the ZSM-5.

It is unclear whether it is increased coke deposition which reduced the deoxygenation potential of the catalysts or whether the changes in the reactions such as polymerisation are favoured by a particular catalyst lead to coke deposition instead of deoxygenation. It is also possible that increased coke deposition is caused by blockages in the ZSM-5 pores which then undermines the ability of the catalyst to undertake deoxygenation reactions. However, this fails to explain why the three most effective catalysts improved as it would only account for deterioration. Potentially interactions between gallium, copper and cobalt and acid sites lead to a reduction in acidity and therefore a reduction in coke deposition. Both Stanton et al. [135] and Miskolczi et al. [126] observed a reduction in acidity of zeolites impregnated with copper whilst deoxygenation was not hindered. In this case the copper atoms appear to act independently from the acid sites whereas with gallium the interaction between acid sites and metal atoms would appear to be crucial to the effectiveness of the catalyst [102].

4.5 Metal impregnated catalysts – summary

4.5.1 Cobalt-5% (ZSM-5)

The cobalt catalyst caused a reduction in liquid yield compared to unmodified ZSM-5, however, this liquid had a much lower water content, resulting in an increase in oil yield from 13.9 wt.% to 20.3 wt.%. There were also improvements in the measurable criteria of the oil with proportion of identified oxygenated compounds reducing slightly (3.3%), the C_5-C_{12} proportion increasing slightly (1.9%) and unicyclic proportion increasing (3.4%). The proportions of primary aromatics increased very slightly whilst phenolic content remained unchanged. There was a large increase in hydrogen gas yield and a smaller increase in both carbon monoxide and carbon dioxide yield.

4.5.2 Copper-5% (ZSM-5)

The addition of copper increased the liquid yield of the catalyst and the oil yield with an increase from 13.9 wt.% to 24.7 wt.% compared to the unmodified ZSM-5. This increase in oil yield was accompanied by an improvement in oil characteristic with oxygenated compounds reducing (2.8%) and the C_5-C_{12} proportion increasing (2.8%). The unicyclic proportion remained relatively unchanged but bi-cyclic selectivity increased by 3%. The aromatic compounds remained relatively unchanged other than an increase in naphthalene compounds.

4.5.3 Iron-5% (ZSM-5)

Iron had reduced liquid yield but an improved oil yield from 13.9 wt.% (ZSM-5) up to 16.1 wt.%. There was an improvement in the proportion of compounds in the range C_5-C_{12} however the other characteristics deteriorated with oxygenated compounds increasing from 37.1% (ZSM-5) to 47.1% which includes an increase in phenolic compounds from 33.5% to 48.8%. There was also an increase in bicyclic compounds, mainly naphthalenes increasing from 13.6% (ZSM-5) to 19.3%. These effects together reduce the primary aromatic compounds from 48.7% (ZSM-5) to 33.8%

4.5.4   Gallium-5% (ZSM-5)

Gallium impregnation had very little effect on the yield of liquid or oil compared to ZSM-5, however, there was a substantive change to the amount of oxygen containing compounds identified. The compounds containing oxygen accounted for 37.1% of those identified in the ZSM-5 and this reduced to 26.0% in the gallium impregnated catalyst. This included an increase in primary aromatic compounds from 48.7% to 53.5% and a reduction in phenolic compounds from 33.5% to 25.8%. There was also an increase in bi-cyclic compounds from 13.6% to 20.6% of which naphthalene comprised the majority.

4.5.5 Magnesium-5% (ZSM-5)

Magnesium increased the liquid yield slightly however this was accompanied by a very small reduction in oil yield, although within standard deviation. The proportion of compounds, C_5-C_{12} increased to 100% whilst the proportion which contained oxygen also increased from 37.1% to 50.4%. The yield of water suggests a relatively high removal of oxygen in the form of water however the high proportion of oxygenated compounds in the oil may suggest that these oxygen free compounds are those which are contributing to the high coke

deposition on the catalyst. The addition of magnesium reduced the unicyclic proportion of the oil only a small amount, however, this reduction caused primary aromatics to reduce from 48.7% to 31.8% and phenolics to increase from 33.5% to 46.6%. There was also an increase in naphthalene compounds from 13.6% to 17.8%.

4.5.6 Nickel-5% (ZSM-5)

Nickel had a reduced liquid yield, but the oil yield was equivalent to that of the unmodified ZSM-5. It produced the greatest increase in in gas yield of the metal impregnated catalysts increasing from 26.6 wt.% to 41.7 wt.%. The proportion of aromatic compounds identified decreased from 99.4% (ZSM-5) to 91.6% and of the compounds phenolics accounted for 54.9% and primary aromatics only 28.4%. This is the main reason for the oxygenated compounds increasing to 67.3% from 37.3% in the unmodified ZSM-5. This was the highest oxygenated content of the metal impregnated catalysts. The C_5-C_{12} proportion increased 2% to 99.3% and there was a 4% reduction in unicyclic compounds with 8.4% linear compounds identified. The PAH compounds including naphthalene were reduced to 11.9%.

4.5.7 Zinc-5% (ZSM-5)

The zinc impregnated catalyst produced a high oil yield of 23.3 wt.% which is significantly higher than that for the unmodified ZSM-5 at 13.9 wt.%. Unfortunately, this was accompanied by an increase in oxygenated compounds from 37.3% to 41.8%. Zinc produced the highest selectivity towards bi-cyclic compounds including naphthalene at 23.3% which reduced the proportion of unicyclic aromatics with primary aromatics at 34.8% and phenolics at 41.0%.

4.6 Metal impregnated catalysts - overview

There were three metal catalysts which saw large increases in oil yield. These were cobalt, copper and zinc, of these cobalt (34%) had the lowest proportion of oxygenated compounds identified followed by copper (35%) and with zinc (42%) which increased the amount of oxygen containing compounds above that of the unmodified ZSM-5. Gallium, whilst producing similar oil yields to the unmodified ZSM-5 catalyst, reduced the oxygenated compounds proportion identified to the lowest of the catalysts examined (26%) and produced the highest proportion of primary aromatic compounds (54%). Cobalt and copper also produced high proportions of primary aromatic compounds at 51% and 49% respectively. All of the catalysts produced oil yields which were equivalent

to that of the unmodified ZSM-5 or greater although some of the catalysts also increased the proportion of oxygenated compounds. The catalysts for which the highest proportion of oxygenated compounds was identified also had the greatest coke deposition on the catalysts post pyrolysis. The catalysts with the lowest coke deposition were also those which produced the lowest proportions of oxygenated compounds.

4.7 Conclusion

The experiments using the two-stage fixed-bed reactor for pyrolysis of biomass shows clearly that introduction of a ZSM-5 catalyst has a large impact on both yields and composition of the bio-oil (objectives 1 and 2). The introduction of a catalyst reduced the liquid yield however, there was a significant increase in formation of deoxygenated compounds, carbon monoxide, carbon dioxide and water. This increase in deoxygenated products is observed in the semi-quantitive GC-MS analysis with a reduction in the proportion of compounds identified which contain oxygen reducing from 100% of peak area in the non-catalytic oils, to 37% in the catalytic experiment. This produces a large loss in oil yield due to the efficiency inherent in removing oxygen from the oil through the formation of carbon oxides and water although the oils produced would be greatly improved such that it might be possible to consider further upgrading of the liquid. Water would need to be removed from the sample as it contributes a higher proportion of the yield than would be suitable for fuel production. The ZSM-5 catalyst also produced an increase in light hydrocarbon gas formation through catalytic cracking. This was evidenced by the predominance of alkene hydrocarbons over alkane products which is a key indicator of catalytic cracking. These cracking reactions further reduces the oil yield, but it may be possible to valorise the gaseous products as they contain energy carrying molecules. The design of the two-stage fixed-bed reactor would make it challenging to valorise the gas products because the gases are diluted by nitrogen carrier gases. This reactor is designed for research whereas in a commercial reactor care would be needed to design a process which provided products in a form by which they could be readily utilised. ZSM-5 use also increased the proportion of compounds identified which were PAHs which would reduce the suitability of the products for fuel use however this was also accompanied by an increase in primary aromatic compounds which are suitable for fuel use and potentially could be valuable for formation of chemicals. These primary aromatic compounds (toluene, xylene, ethylbenzene) are part of a varied and complex mixture which increases the complexity of separating

compounds required for production of valuable building block compounds and may make this uneconomical in practice.

Use of the metal impregnated ZSM-5 catalysts brought about limited improvement beyond that of the unmodified ZSM-5 catalyst (objectives 3 and 4). For some of the metal impregnated catalysts there was a slight increase in oil yield but in most cases this increased oil yield corresponded to reduced production of deoxygenating products. In these cases, GC-MS analysis identified greater proportions of oxygenated compounds in the oils. Although none of the metal-impregnated catalysts excelled both for increased oil yield and increased deoxygenation there was observable variation in the function of the catalysts. Gallium impregnated ZSM-5 reduced oxygen content through hydrodeoxygenation to a higher degree than the unmodified ZSM-5. In contrast nickel impregnated ZSM-5 produced higher yields of carbon oxides compared to unmodified ZSM-5 but had a highly reduced water yield comparatively. The net effect of these differences was a much higher proportion of oxygenated compounds identified in the oils from nickel impregnated ZSM-5 than in the unmodified ZSM-5. It must also be observed that a high liquid yield did not equate to a high oil yield in every case. The formation of water may give a high liquid yield which may mask a reduction in oil yield. The converse effect is also possible as with nickel impregnated ZSM-5 which had a lower liquid yield than the unmodified ZSM-5 but still had a similar oil yield once the water content was considered.

Coke deposition was analysed for the modified and unmodified ZSM-5 catalyst as well as the non-catalytic system (objective 11). Coke deposition was much higher for the ZSM-5 catalysts than the non-catalytic system which is both due to the difference in surface area as well as reactions on the ZSM-5 which produce coke directly. The coke deposition varied between the catalysts which with though those which produced more coke than the unmodified ZSM-5 generally also less effective at reducing oxygen content in the oils. It is not clear whether the formation of coke causes a reduction in deoxygenation in a catalyst or whether this is due to competing reactions promoted by the catalysts which do not produce deoxygenation products and instead enhance coke formation. It is possible that both effects could be contributing to this coke formation.

Chapter 5: Devolatilisation of biomass with plastics

5.1 Introduction

Chapter 5 examines the non-catalytic thermal degradation of the biomass and plastic samples using TGA-MS analysis for both individual samples and for 1:1 mixtures (by weight) of the biomass with the plastics. This chapter examined both the weight change observed during thermal degradation as well as measuring the output of products (Carbon monoxide, carbon dioxide, water and hydrogen) during this degradation process. The differences between the profiles observed during thermal decomposition individually and in conjunction may be used to identify changes to the decomposition and devolatilisation of the samples caused by interactions between the samples as they are decomposed (objective 8).

5.2 Devolatilisation of biomass and plastics

The decomposition of biomass and plastics during pyrolysis can be studied by examining the devolatilisation process [69, 248, 249]. Thermogravimetric analysis (TGA) can be used to study the devolatilisation process, determining the effect of temperature on the change in mass of a sample. The TGA profile which is obtained may give valuable information about the temperatures at which the devolatilisation occurs and the proportion of the sample which is converted from a solid to a gaseous state. Comparison between single samples and those which are combined together may show how the samples are interacting together during devolatilisation. The interactions or synergy between the two substances may lead to changes in rates of decomposition or change the amount and type of products obtained. These effects may result in positive or detrimental changes to a pyrolysis process which is conditional on a number of factors. For pyrolysis a beneficial effect might include, increased yield of a desired product or improvement in volatile composition for a specific purpose, such as for use as a fuel. TGA does not provide direct information about product composition so it is often linked with a second analytical process to elucidate the product composition. Gas chromatography (GC), mass spectrometry (MS) and Fourier-transform infrared spectroscopy (FTIR) are routinely used to provide online analysis about species or functional groups present in a gas sample. For this research online MS was used as it allowed for quantitative monitoring of five key devolatilisation compounds at 12 second intervals. This research was undertaken at Tsinghua University as part of a research secondment. This provided the opportunity to utilise the high-performance GC-

MS equipment which Tsinghua made available. It also provided the occasion to work alongside researchers with an expertise in this field with support given for analysis of the data collected.

5.3 TG and DTG for single samples

TGA involves heating a sample at a steady heating rate whilst measuring and recording the weight of the sample which is being heated. An argon atmosphere was used to provide the conditions for pyrolysis to occur. Differential thermogravimetric analysis (DTG) utilises the differential of the TGA weight change profile against temperature to determine the rate of change in weight at each temperature. This gives vital information about the temperature at which devolatilisation is most rapid.

TG and DTG can be used to determine the temperature at which devolatilisation is occurring. Devolatilisation occurs over a temperature range, and whilst it may be possible to simply measure the temperature range over which weight change occurs, it is also possible to identify characteristic temperatures which may be used to compare between different samples. Two commonly used characteristic temperatures are T_{ID} and T_{MWL}.

Temperature of initial decomposition (T_{ID}) can be obtained from the TGA graph and relates to the point at which the first major weight loss is observed (post drying). The gradient of the TG weight change profile before and after devolatilisation can be used to characterise the temperature of initial decomposition. The temperature at the intersect of the two gradients gives the characteristic temperature, T_{ID}.

Another characteristic temperature is obtained from the DTG graph and is the temperature at the point of maximum weight loss (T_{MWL}). In biomass or single plastic devolatilisation there is often one peak only, although for biomass this peak may be broadened because it is composed of 3 main constituents, cellulose, hemicellulose and lignin. In biomass, cellulose decomposition is often the cause of the peak of maximum weight loss. Characteristic temperatures are useful to compare between samples, however, devolatilisation is a complex mixture of chemical and physical processes which may not be summarised by a single temperature. The profile of the DTG curve can also give key information about the structure of the material being heated such as the number of different components which make up the material, this is particularly key for biomass.

5.3.1.1   TG and DTG for biomass

Figure 5.1 shows the TG and DTG profiles of biomass heated in an inert atmosphere. The TG profile for biomass is relatively broad because it is composed of three major components. The first component which is clearly observed during biomass decomposition is hemicellulose, which starts to break down between 200°C and 260°C causing a 'shoulder' feature on the DTG plot [67, 70, 71]. Cellulose is semi-crystalline and decomposes across a relatively narrow temperature range, between approximately 300°C and 430°C, producing the sharpest peak in the devolatilisation profile [62, 69]. Lignin is a diverse and structurally unsystematic material which breaks down over a wider temperature range (140-500°C) than either hemicellulose or cellulose [67, 78]. Due to the broad temperature range during devolatilisation of lignin the peak profile is shallow which means it is often masked behind cellulose and hemicellulose in TGA and DTG graphs. The lignin is observed in Figure 5.1 as the tailing part of the DTG peak once cellulose has completed decomposition.
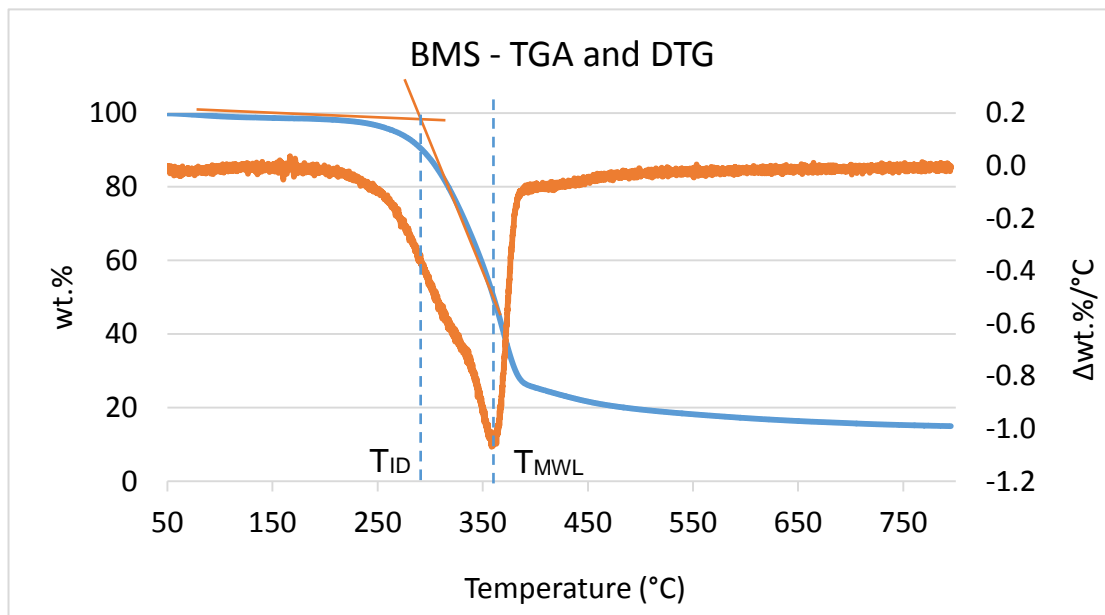
Figure 5.1: TG (blue) and DTG (orange) profile during devolatilisation of biomass sample in an argon atmosphere.

The biomass sample used in Figure 5.1 devolatilises between approximately 200-400°C, with peak weight loss at 360°C. The moisture content which is measured as the weight change below 100°C is around 1.1% wt. The material remaining after devolatilisation has occurred gives the weight of char which is 15%. The char is composed of a combination of ash and fixed carbon and is dependent on the final temperature of devolatilisation as well as heating rate. The char content observed from the same biomass sample used during

pyrolysis reactions in a fixed bed reactor was 25 wt.% of the sample. The TGA experiment reached a maximum temperature of 800°C which is 300°C above that of the fixed bed reactor experiment which explains why the char content was lower. The volatiles yield was increased from 75 wt.% to 85 wt.% as temperature was increased from 500°C in fixed bed experiments to 800°C in the TGA experiments. This TGA data suggests that a pyrolysis temperature greater than 400°C would be necessary to ensure devolatilisation is maximised. Any further increase in temperature would increase the volatiles content slightly but significantly more energy would be required to accomplish this marginal gain in volatile yield.

5.3.1.2   TGA and DTG for HDPE

The biomass sample started devolatilising at around 200°C and this continued until over 400°C. In comparison the HDPE sample decomposed over a much narrower temperature range between 400°C and 510°C (see Figure 5.2). This tight symmetrical profile indicates that there is only one major component to the material despite the HDPE being of recycled origin. There is a small feature at the start of devolatilisation peak around 410°C but this could be due to chemical additives such as dyes or even another plastic material which was not separated fully pre-recycling. Interestingly, this peak matches the temperature profile of the PS sample, but this might equally belong to another material. Temperatures above 500°C continue to increase the volatile yield but much of the possible weight loss has been completed by this temperature. The char remaining after decomposition was ~3 wt.% which is above that of the LDPE although the HDPE was a recycled material and the LDPE virgin material.
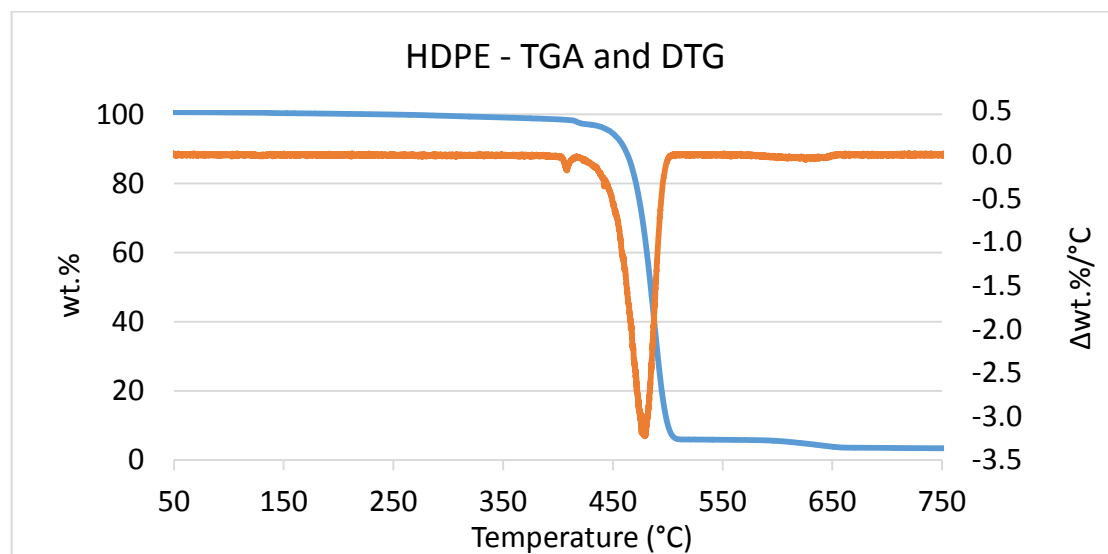
Figure 5.2: TGA and DTG during devolatilisation of HDPE sample.

5.3.1.3   TGA and DTG for LDPE

Unsurprisingly, LDPE also exhibited a similar profile to that for HDPE (see Figure 5.3) with devolatilisation commencing at a slightly lower temperature and finishing at a slightly lower temperature also. The char remaining after devolatilisation in the TGA was marginally lower than that for HDPE for which a greater proportion of ash was measured during proximate analysis. The char remaining after TGA of LDPE was 2.8 wt.% which is greater than would be expected from proximate analysis which determined ash to be 0.3 wt.% and fixed carbon at 0 wt.%. The main variable which is changed between proximate analysis and the TGA experiment is heating rate and the gaseous atmosphere in the reaction chamber. The proximate analysis uses a high heating rate and an oxidising atmosphere whereas the TGA was undertaken at a steady low heating rate and an inert atmosphere. This has the effect of increasing the proportion of char present after devolatilisation. Whilst both HDPE and LDPE produced similar proportions of char during the TGA experiment the ratio of fixed carbon to ash was greater for LDPE meaning that this char material would have a higher calorific value. The variation in ash content is most likely due to HDPE being a recycled material which has increased the inorganic content. The DTG maximum weight loss peak is at an almost identical temperature and magnitude for both LDPE and HDPE which indicated that both materials devolatilise in a very similar manner.
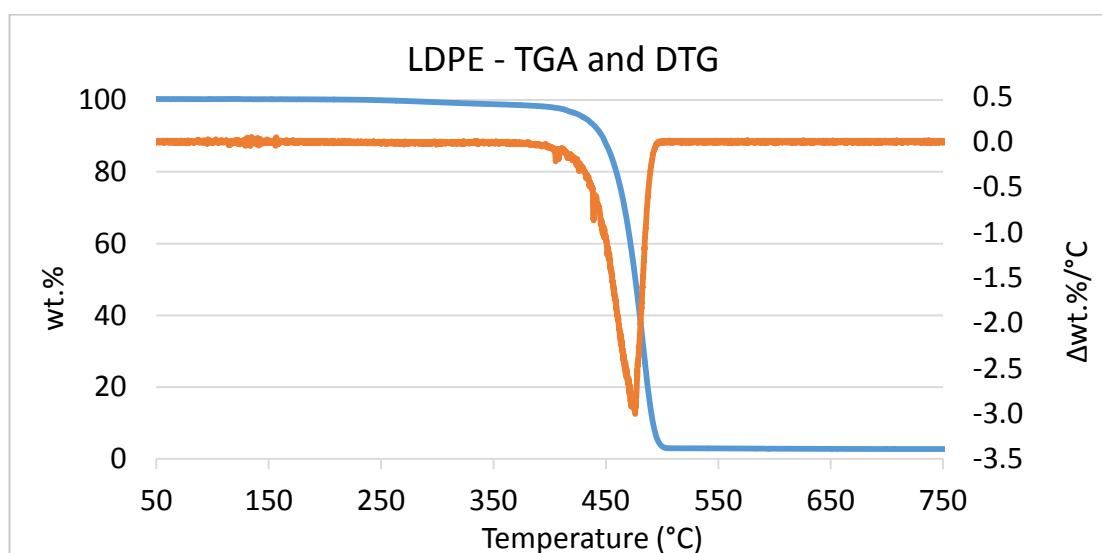
Figure 5.3: TGA and DTG during devolatilisation of LDPE sample.

5.3.1.4   TGA and DTG for PP

For each of the polyolefins, LDPE, HDPE and PP (see Figure 5.4) the same shape of TGA profile is observed which is consistent with the fact that each decomposes through the same radical chain scission mechanisms [94]. The initial curve at the start to devolatilisation is exponential in profile and the contrasts with the end of devolatilisation where there is an abrupt almost right-angle shape where it must be concluded that all carbon chains available for scission have been broken. The DTG profile of the polyolefin samples match that for HDPE recorded by Oyedun et al. [249]. The profiles observed in biomass, PS and PET are distinctly different from those of the polyolefin samples. At 457°C, the temperature of maximum weight loss is slightly lower for PP than for HDPE and LDPE for which this temperature is 478°C and 476°C. However, despite the difference in peak temperature for PP it appears to decompose in a very similar manner to both HDPE and LDPE with a close correlation in the rate of devolatilisation at the temperature of peak weight loss.
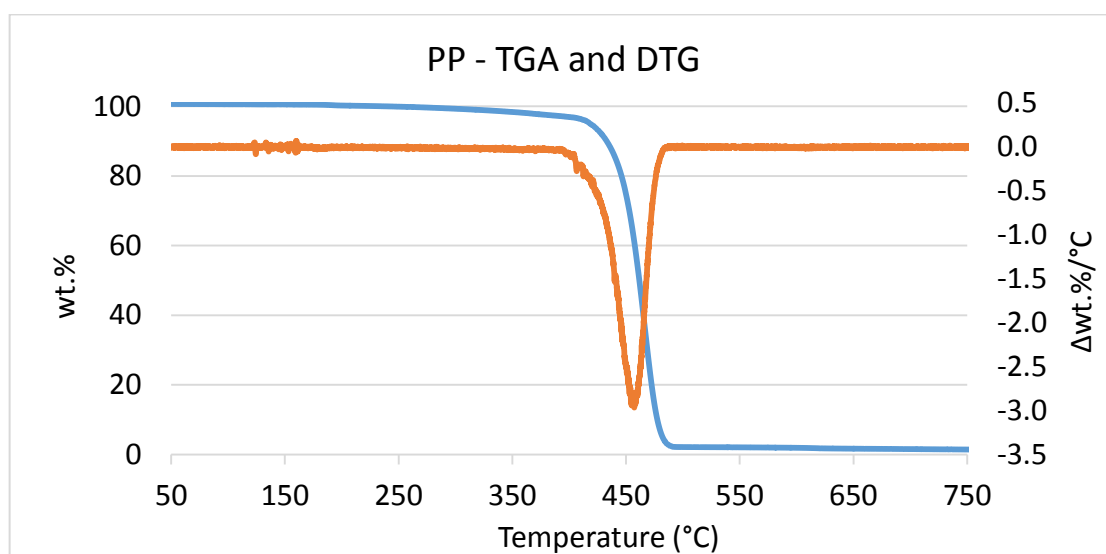
Figure 5.4: TGA and DTG during devolatilisation of PP sample.

The physical characteristics of the plastic pellets was quite varied. The LDPE pellet were clear and pliable and could be readily milled to produce a fine powder. The HDPE pellets were more dense and tougher and milling was more challenging to produce a powder. The PP pellets were resistant to impact and therefore the most challenging to mill. The pellets required a much longer time to grind into a fine powder for analysis than either the HDPE or LDPE which were comparatively more brittle. The difference in the material properties,

however, was not reflected in the TGA studies where the DTG profiles are very similar.

5.3.1.5 TGA and DTG for PS
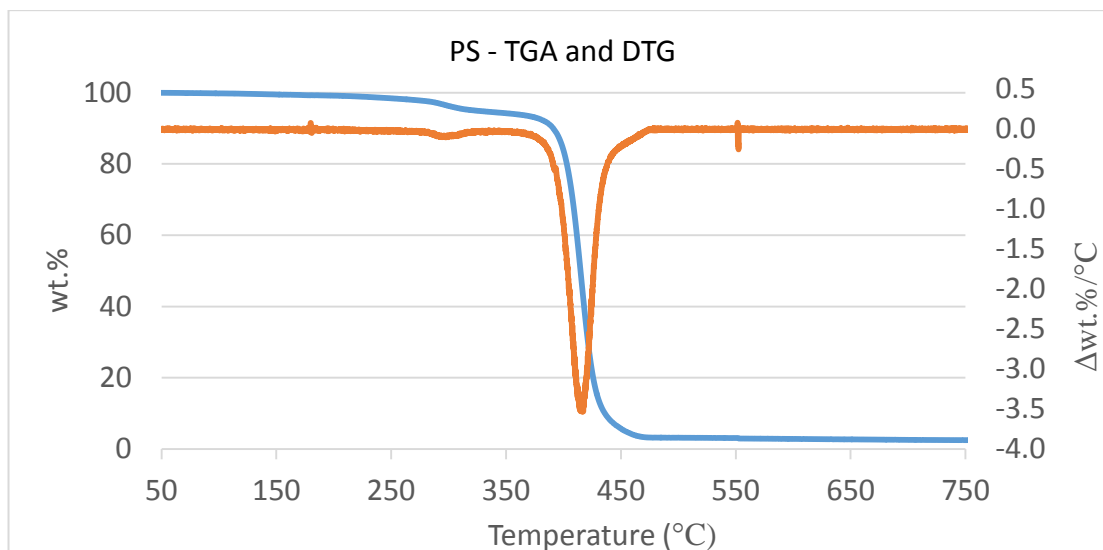
Figure 5.5: TGA and DTG during devolatilisation of PS sample.

The polystyrene used was a recycled material and as with the HDPE a small peak is observed at 300°C, which does not appear to be from the PS material (see Figure 5.5). Again, this could be a dye or other additive used with the polystyrene for its original purpose or potentially product contamination during recycling. The profile of main peak of the polystyrene however is the sharpest of those examined but with broadening at the base of the peak. This is particularly clear at the end of devolatilisation where an abrupt end to decomposition which was observed with the polyolefins is replaced with a much gentler decline in the PS. The major point of comparison however, is the temperature of devolatilisation which is lower than that for the polyolefins by around 30-40°C. This brings it closer to that for biomass which is between 250-400°C. The maximum weight loss was greater than that for the polyolefin samples.

5.3.1.6 TGA and DTG for PET

The profile for PET (see Figure 5.6) is far broader than the other plastics with a nearly symmetrical shape which matches with research by Al-Salem et al. [250]. It also starts to decompose at a lower temperature of around 323°C and finishing before 500°C. This overlaps with the devolatilisation profile for

biomass. The reinforcement material means that the final char material makes up greater than 40 wt.% of the original sample mass but even taking this into account the peak mass change is lower than for the other plastics. This is likely due to the broad devolatilisation peak meaning that the weight change occurs over a larger temperature range than for the other polymers. Although the sample contains inert reinforcement material, the devolatilisation profile is very similar to non-reinforced PET in literature [250-252].
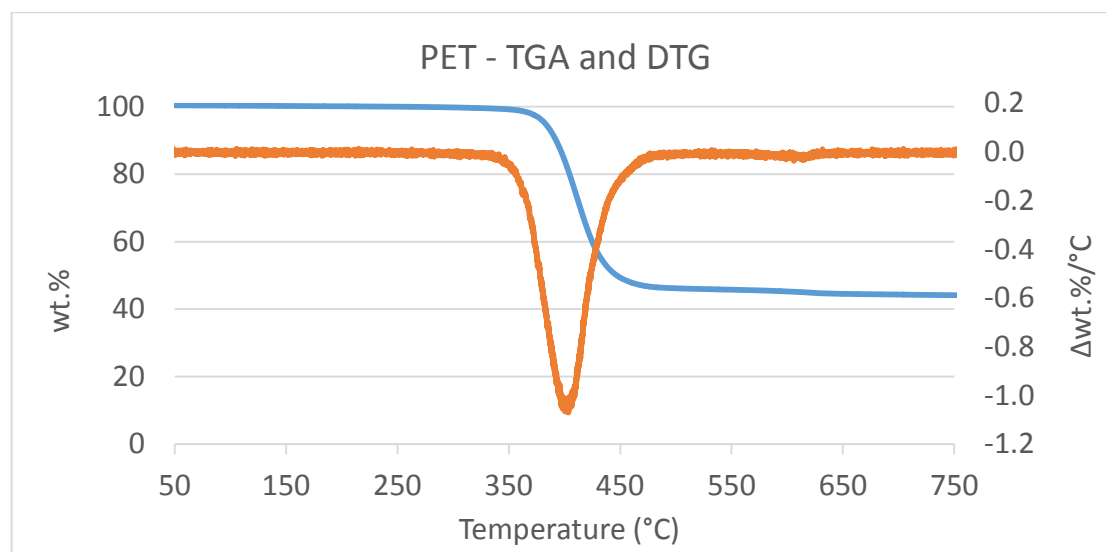
Figure 5.6: TGA and DTG during devolatilisation of PET sample.

5.3.1.7 Peak temperatures during single sample devolatilisation

Table 5.1 lists the temperatures over which devolatilisation occurs for each of the samples and compares them to temperatures recorded in literature. In general, there was agreement between the results from the TGA and literature however the TGA devolatilisation was lower than the literature for the recycled polymers HDPE and PS. The temperature range over which biomass was devolatilised was the lowest of the samples with the weight loss starting around 200°C and concluded by 400°C. The plastics devolatilised at higher temperatures with PET the lowest, PS the next lowest and the polyolefins at the highest temperatures. PP weight loss began at a higher temperature than either LDPE or HDPE but the peak weight loss temperature for PP was lower than either HDPE or LDPE.

Table 5.1: Temperatures of devolatilisation for individual pyrolysis samples during TG and DTG, compared against literature values.

	Measured (°C)			Literature (°C)			
	T_{onset}	T_{peak}	T_{end}	T_{onset}	T_{peak}	T_{end}	ref
Biomass	201	360	394	250/200	350/360	380/400	[103, 252]
HDPE	404	478	507	451/400	505/483	528/510	[177, 252]
LDPE	382	476	503	383/398	492/478	515/505	[160, 177]
PP	392	457	491	375/317	486/452	512/487	[160, 177]
PS	360	416	478	372/360	437/425	506/475	[252, 253]
PET	323	402	480	320/350	400/400	490/480	[250, 254]

Table 5.2 lists some of the key parameters of the devolatilisation of the samples including char, moisture and volatiles yield as well as the temperature and the rate at peak weigh loss. The rate at peak weight loss (DTG_{Max}) can be used to compare the rate of devolatilisation with a low temperature range of devolatilisation giving a sharp DTG peak with a high rate.

Table 5.2: Key properties measured during TG and DTG analysis of individual pyrolysis samples.

	T_{peak}	Rate at DTG_{Max}	Moisture	Volatiles	Char
Unit	°C	Δwt.%/°C	wt.%	wt.%	wt.%
Biomass	360	1.1	1.1	83.9	15.0
HDPE	478	3.2	0.1	97.1	2.8
LDPE	476	3.0	0.1	97.5	2.5
PP	457	3.0	0.1	99.2	0.7
PS	416	3.5	0.3	97.2	2.5
PET	402	1.1	0.2	56.0	43.8

Biomass had the lowest rate of devolatilisation with weight loss spread over a 160°C temperature range with cellulose the main contributor to the peak weight loss peak. PET was the second lowest rate even if the reinforcement material is accounted for. After this the polyolefin samples were relatively close together with PS having the highest peak weigh loss rate.

As well as the broadness of the peak another factor on the rate of weight change is the proportion of the sample which is converted from a solid sample into the volatiles. In this case PET had the lowest volatiles yield with a 44 wt.% char yield which is a combination of ash (including reinforcement), fixed carbon and potentially desublimation of benzoic acid and terephthalic acid derivatives [99]. The biomass sample had a relatively low moisture content here which may be due to drying during the milling process where friction generated heat in the mill would be able to dry the fine powder sample produced for the TGA analysis. There is still a char content of 15 wt.% however if devolatilisation were concluded at 500°C this would be higher at around 20 wt.%. All of the plastics had low char and high volatiles content between 97-99 wt.%. This would allow for efficient production of pyrolysis oils and gases however the weight loss does not distinguish between gas or liquid product yield.

5.3.2 MS profiles during devolatilisation of single samples

Mass spectrometry combined with TGA may be able to give further insight into the processes which are happening during devolatilisation by measuring the quantity of four compounds produced as the TGA experiment progresses using the argon carrier gas as an internal standard. The compounds measured were hydrogen, water, carbon dioxide and carbon dioxide. These are often produced during devolatilisation and therefore the rate of their production may give insight into the devolatilisation process.

5.3.2.1   MS profile during devolatilisation of biomass

Figure 5.7 shows the MS signal measured during devolatilisation of biomass for each of the five compounds. At temperatures below 100°C the major product is water which is due to drying of the sample. At around 250°C, the sample begins to decompose which is indicated by an increase in water, carbon dioxide and carbon monoxide. This signal peaks around 350°C before returning towards the baseline at around 400°C. There is a small residual signal slightly above 400°C which matches the tailing end of lignin decomposition observed on the DTG profile. During decomposition of cellulose and hemicellulose the major product is water with carbon dioxide and carbon monoxide approximately equal in yield at a lower level. During lignin decomposition water is still the highest yield product but it is a similar level to that of the carbon oxides. These three compounds are all acting to remove oxygen from the biomass sample thereby potentially reducing the oxygen content of the bio-oil. The signal from methane is quite unclear but there is a slight increase around the temperature of peak compound measurement for the three main gases. The hydrogen signal shows a small peak at this maximum yield temperature and then reduces before

increasing steadily once the temperature exceeds 500°C and is the main compound measured after 600°C. This profile of the three main compounds matches that from the DTG plot with the shoulder feature due to hemicellulose visible. This confirms that with biomass these gases are released over a similar temperature profile to devolatilisation and are therefore likely to be involved in this process.
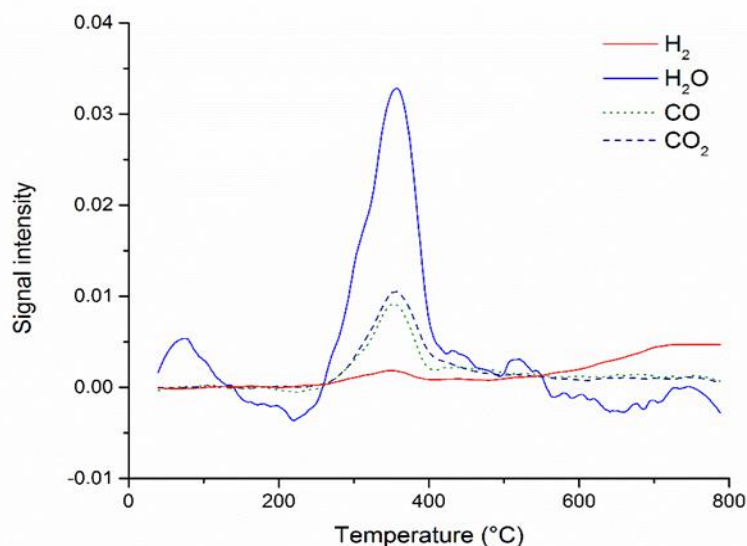
Figure 5.7 : MS profile during devolatilisation of biomass.

5.3.2.2 MS profile during devolatilisation of HDPE

In contrast to biomass the plastics (excluding PET) contain a much lower oxygen content and this is likely to be reflected in the quantity of oxygen containing compounds in the MS plot. As with biomass there is an initial period of water production at around 100°C after which point there is very little activity until after 400°C where there is an increase in each of the compounds being measured. Once again, the water is the strongest signal which matches pyrolysis experiments where water makes up a bigger contribution to the yield than carbon monoxide or carbon dioxide which were not measured during pyrolysis experiments. The output of most compounds decreased by 500°C although water takes longer to return back to base levels. Hydrogen increases as temperatures increases towards 800°C.

Gas analysis during pyrolysis experiments was not able to measure either carbon monoxide or carbon dioxide for HDPE or LDPE as these were below detection limits but did measure a small quantity of hydrogen. The yield of these compounds is lower than values measured in biomass and this can be

observed in the lower peak size and greater noise to signal ratio in the MS measurements. At 600°C there is a slight rise in carbon monoxide which is accompanied by a minor weight loss on the DTG curve. This may be due to a char decomposition event or due to foreign matter within the recycled HDPE sample.
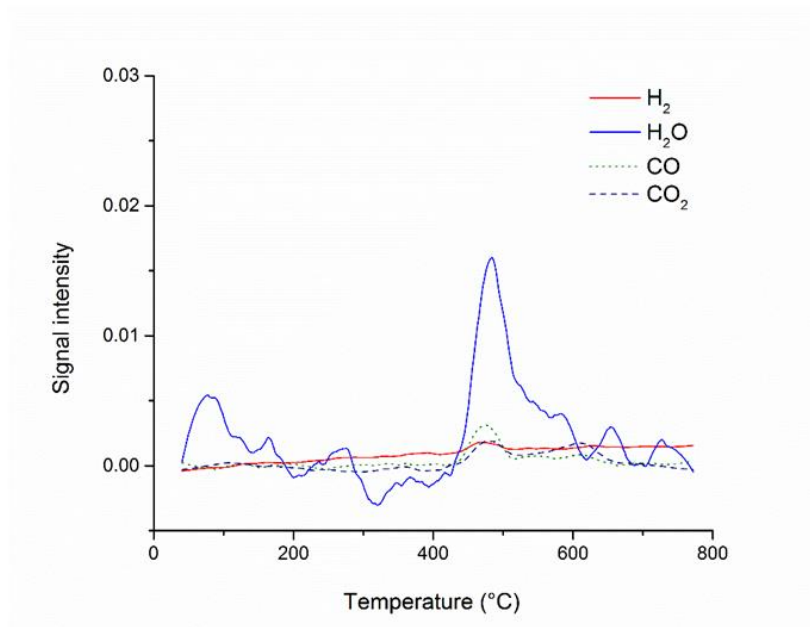
Figure 5.8: MS profile during devolatilisation of HDPE.

5.3.2.3   MS profile during devolatilisation of LDPE
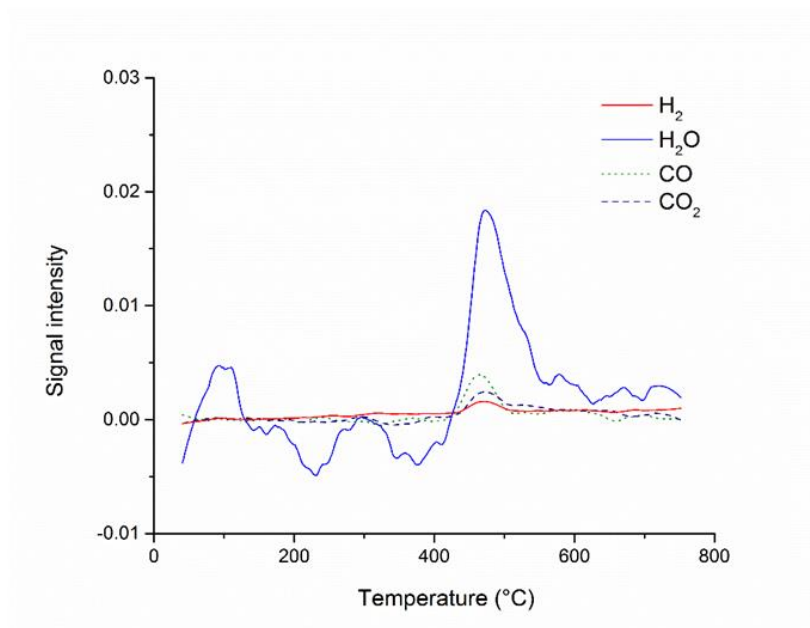
Figure 5.9: MS profile during devolatilisation of LDPE.

The LDPE MS plot is very similar to that for HDPE with the only major difference being a reduction in hydrogen gas below that of carbon dioxide where it was above in the HDPE sample. The carbon monoxide peak measured in HDPE at 600°C was not present in virgin LDPE which adds to the conclusion that it might be due to foreign material present in the HDPE rather than due to devolatilisation of the polyolefin hydrocarbons.

5.3.2.4   MS profile during devolatilisation of PP
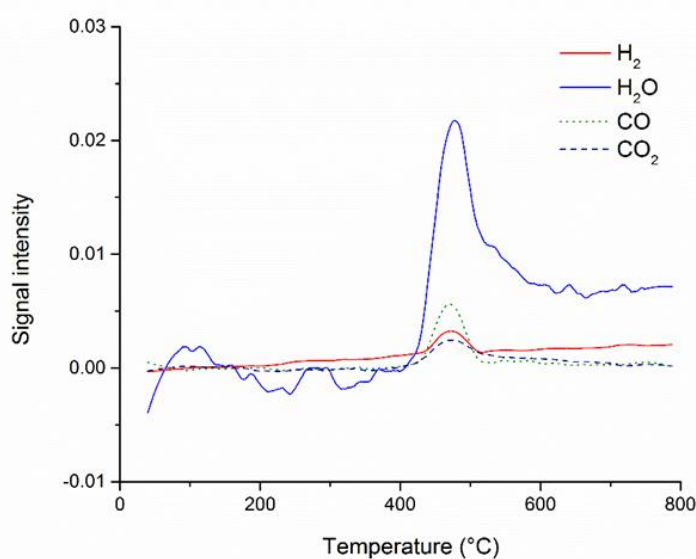
Figure 5.10: MS profile during devolatilisation of PP.

The MS profile for PP is similar to that of HDPE and LDPE although the water peak remains elevated at higher temperatures. This may be due to moisture becoming trapped in the capillary transfer line and therefore passing through to the detector over a wider temperature range. The devolatilisation of PP begins at a lower temperature than the other polyolefin samples and produced more hydrogen than carbon dioxide and more hydrogen than the HDPE and LDPE which agrees with findings from Alvarez et al. [255]. For each of the polyolefin samples the carbon monoxide yield is greater than that of carbon dioxide which is understandable in samples which have low oxygen content. As temperatures rise beyond 600°C the hydrogen yield continues to increase.

5.3.2.5   MS profile during devolatilisation of PS

The peak which is due to moisture evaporation from the sample below 100°C is absent for PS although water was produced during the devolatilisation process. The carbon monoxide peak is relatively large for PS compared to water for PS devolatilisation which may be signify that the decomposition pathway is different for PS from the polyolefin samples. Alvarez et al. [255] found that PS produced a greater proportion of hydrogen and carbon monoxide, compared to polyolefin samples, during pyrolysis at 600°C. PS does not show the same increase in hydrogen yield as temperatures are elevated beyond devolatilisation temperatures.
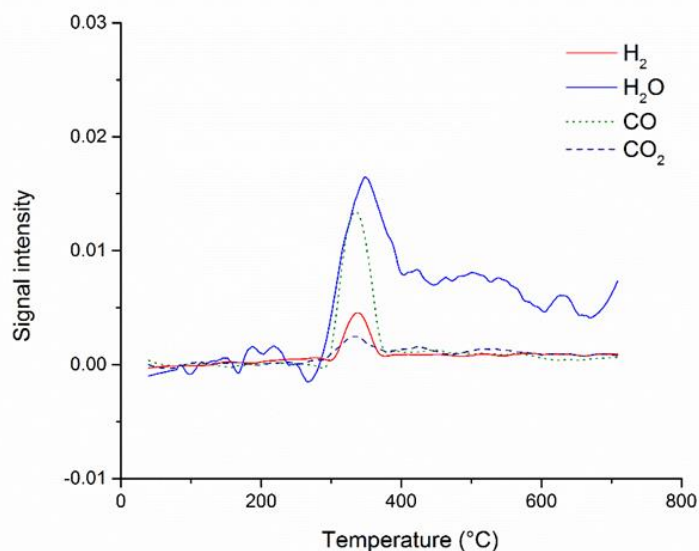
Figure 5.11: MS profile during devolatilisation of PS.

5.3.2.6   MS profile during devolatilisation of PET

The DTG data for PET showed a single devolatilisation event. The TGA-MS data include two regions of emission. The first region coincides with the temperature range of the DTG peak and the profile is similar to that of the other polymers. The main emission is water as well as carbon monoxide and carbon dioxide. There is almost no hydrogen release during this devolatilisation event. The second peak on the MS is composed of both hydrogen gas and carbon dioxide although there is little mass change on the DTG plot although a small weight loss is observed over the same temperature range. This second region

may be due to the reinforcement material within the sample as it was not observed in the other plastics.
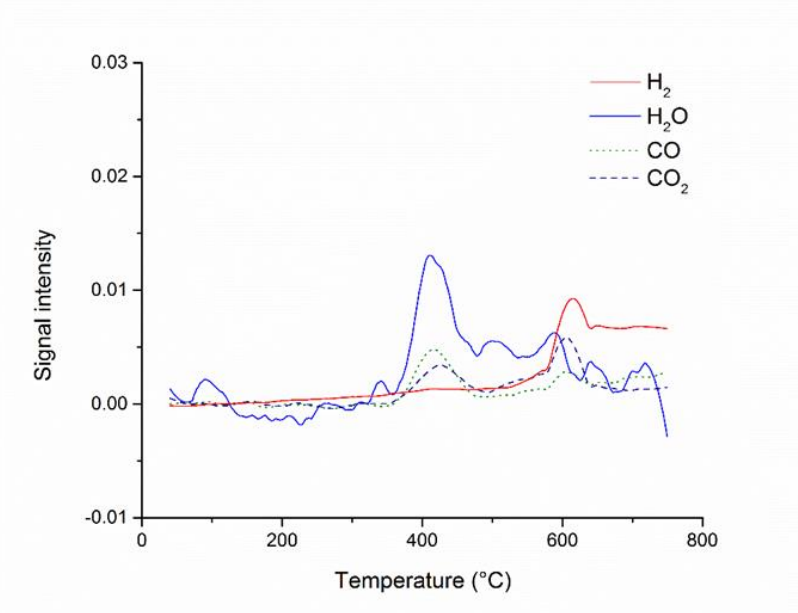
Figure 5.12: MS profile during devolatilisation of PET.

5.3.2.7 Characteristic devolatilisation temperatures for single samples

The temperature of devolatilisation can be defined using a range over which weight loss is observed however it is more useful for comparison to measure characteristic temperatures from the TG, DTG and TG-MS studies. T_{IC} is obtained from the TG plot, T_{MWL} from the DTG plot and the TG-MS may be used to determine the temperature at which peak emission of key compounds (H_2O, CO and CO_2) is observed. Table 5.3 lists the values determined for each of these characteristic temperatures for the individual biomass and plastic samples. Comparison against characteristic temperatures from co-devolatilised samples may be used to observe changes caused by devolatilisation of samples together.

Table 5.3: Characteristic temperatures (°C) during devolatilisation of single samples.

	TGA		TGA-MS		
	T_{ID}	T_{MWL}	$T_{peakH20}$	$T_{peakCO2}$	T_{peakCO}
BMS	290	360	360	360	360
HDPE	464	478	482	474	474
LDPE	454	476	476	472	468
PP	442	457	468	476	473
PS	400	416	442	424	435
PET	384	402	418	417	407

Biomass has the greatest temperature difference between the T_{ID} and T_{MWL} which highlights the broad temperature range for biomass for which hemicellulose devolatilisation starts at a lower temperature than cellulose which contributes most significantly to the peak weight loss peak. With biomass the temperature of peak emission of the key compounds is the same as that for the T_{MWL}, however, this is not the case for all the polymers where these compounds exhibit different peak temperatures. This effect is largest with PS where there is almost 20°C between the temperatures that CO_2 reaches peak emission and when H_2O reaches peak emission.

5.4 Devolatilisation of mixed samples

Devolatilisation of 1:1 mixed samples (by weight) of biomass alongside the plastics using TGA-MS was used to discover the changes to the process which are caused by mixing the samples together.

5.4.1 TG and DTG for mixed samples

The TG and DTG data for the mixed samples can give valuable information about the devolatilisation process including shifts in devolatilisation temperatures; changes in rate of devolatilisation; overlap between the samples being devolatilised; changes in the resulting proportions of char and volatiles from the process.

5.4.1.1 TGA and DTG for biomass and HDPE combined
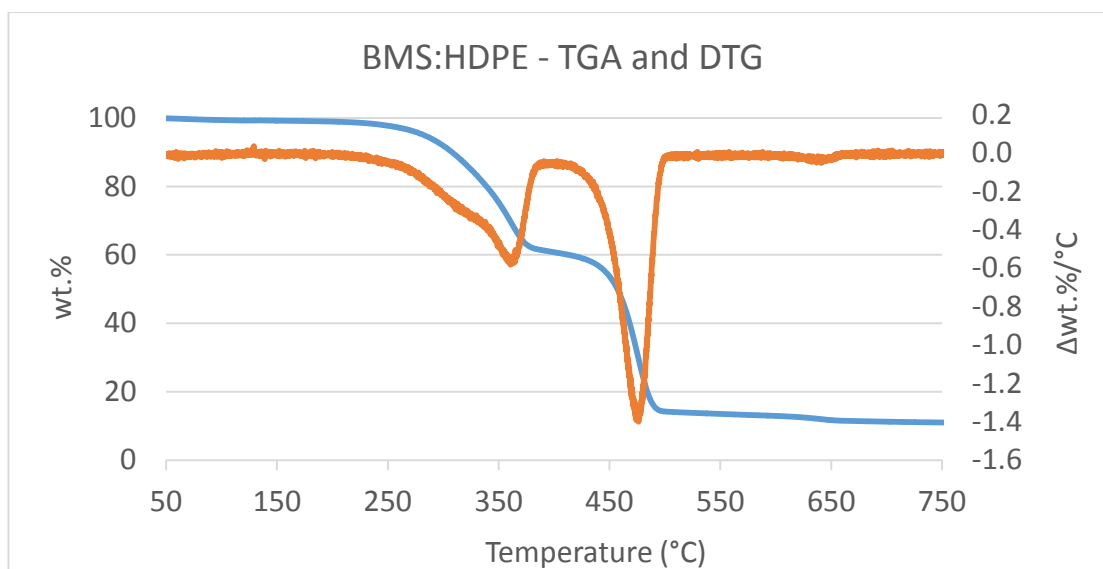
Figure 5.13: TGA and DTG during devolatilisation of biomass with HDPE.

The temperature difference between the devolatilisation of biomass and HDPE is relatively large which might lead to lower interaction between the samples during co-pyrolysis. The DTG plot (see Figure 5.13) does not appear to show a significant interaction but analysis of the temperatures, rates and yields of devolatilisation indicates that there is some interaction occurring. The onset of biomass devolatilisation as a single sample is ~200°C whereas in the sample which has been combined with HDPE the onset is delayed until ~225°C. However, there does not appear to be a significant shift to the temperature of maximum weight loss or the temperature at which devolatilisation of biomass is completed. The onset of HDPE devolatilisation appears to shift to a slightly lower temperature, however, it is challenging to estimate onset as the HDPE peak merges with the tailing end of the biomass peak. The yield of volatiles reduced for both the biomass and HDPE samples which led to a char yield of 13.9 wt.% compared to a char yield of 8.9 wt.% which was expected using calculations from single samples. This contrasts with literature where Chattopadhyay et al. [256] found synergy between biomass and HDPE led to a slight reduction in char formation. The rate of weight change at its highest point on the DTG increased slightly for the biomass sample, which may be due to several factors, with a delayed onset leading to a less broad, more rapid devolatilisation, but with a reduced volatiles yield reducing the total weigh change measured. In contrast the rate for HDPE reduced from 3.2 Δwt.%/°C to 2.8 Δwt.%/°C in the combined samples which might be due to interaction with the biomass pushing HDPE onset to a lower temperature leading to a broader HDPE peak and therefore a reduced rate at the peak temperature.

5.4.1.2   TGA and DTG for biomass and LDPE combined

The LDPE sample is very similar to the HDPE (see Figure 5.14) and the effects observed during co-devolatilisation are very similar. Addition of LDPE to the biomass causes the onset temperature of hemicellulose to increase to ~230°C where in the individual samples this was ~200°C. The effect on the peak temperature and the point at which biomass devolatilisation finishes is not alter significantly. The onset temperature for LDPE is challenging to determine as it overlaps with the biomass, but this appears to remain relatively unchanged as are the other temperatures. The volatiles released by the biomass are decreased from ~84 wt.% in the individual sample down to ~69 wt.% in the mixed sample whereas the LDPE continues to produce the same proportion of volatiles. This causes the char proportion to increase from a calculated 8.8 wt.% to 15.0 wt.% which is the same as that observed for biomass when devolatilised individually.
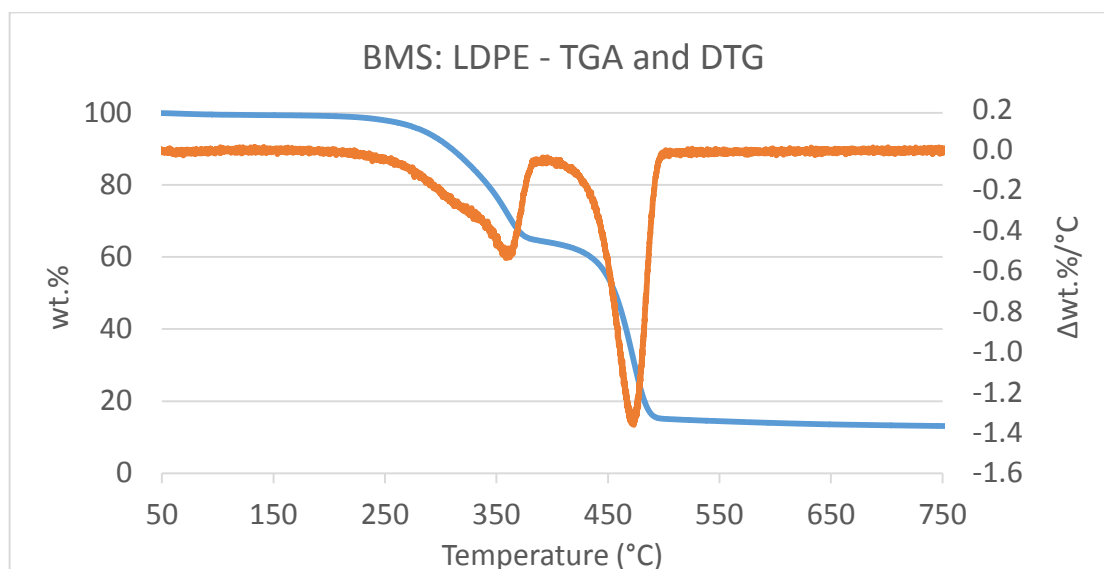
Figure 5.14: TGA and DTG during devolatilisation of biomass with LDPE.

Despite the reduced volatiles yield from biomass the rate at peak weight change does not alter significantly remaining at 1.1 Δwt.%/°C. It may be that the reduced yield is counterbalanced by the higher temperature onset of devolatilisation, such that the peak rate remains as it was. However, the LDPE reduces from 3.0 Δwt.%/°C to 2.7 Δwt.%/°C. a reduction in rate of 10% which may be caused by LDPE devolatilisation starting at a lower temperature thereby spreading the temperature range of the weight change and lowering the peak rate. Xiang et al. [191] used TGA to study the co-pyrolysis of rice straw with LLDPE and found that synergistic effects led to a lower char yield compared to

rice straw alone with the temperature at which the two samples reached peak weight loss shifting slightly to lower temperatures.

5.4.1.3   TGA and DTG for biomass and PP combined

The mixed biomass and PP sample was comparable to that of the other polyolefins except that the overlap between the two peaks was larger (see Figure 5.15). Although the onset temperature for LDPE was 10°C lower than for PP it appears that the PP has been affected by the biomass devolatilisation in a way that caused the PP to begin devolatilisation at a lower temperature. This can be observed as a 'shoulder' like feature on the DTG profile which was not present in the individual PP sample. The PP onset was at a slightly lower temperature than during than individual TGA experiment, although, the rate of devolatilisation increases faster for PP than with the other polyolefins for which a more exponential shape is observed.
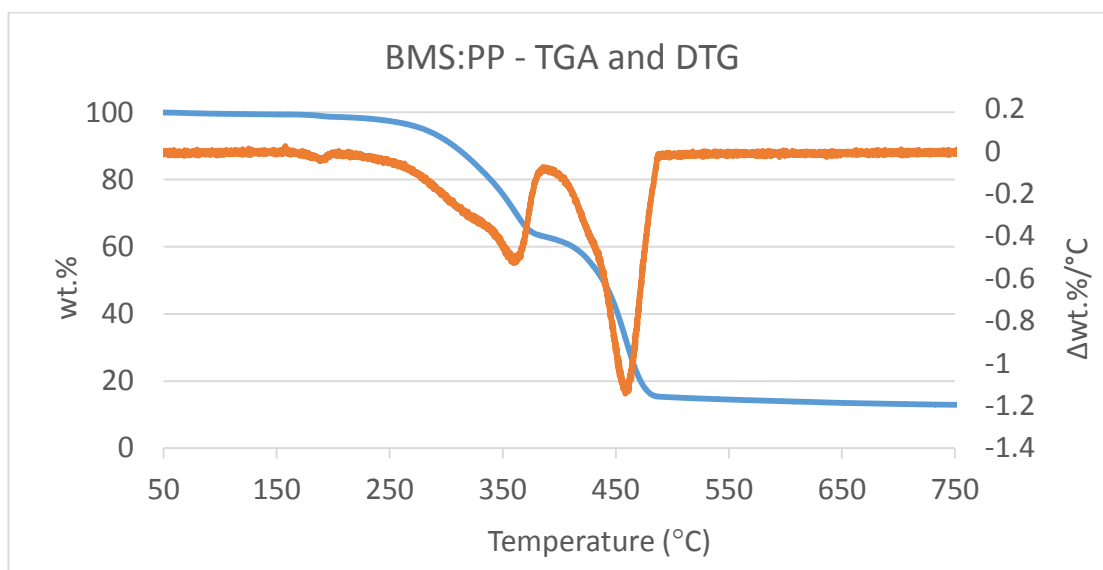
Figure 5.15: TGA and DTG during devolatilisation of biomass with PP.

The peak and final temperatures for PP remain relatively unchanged. The biomass peak onset increases in temperature to 227°C during the mixed experiments but the peak and final temperatures remain almost unchanged as with the other polyolefin samples. As with the other polyolefins combining biomass with the polymer reduces the biomass volatiles yield, in this case from 84 wt.% to 72 wt.% whilst the PP reduces only slightly. This is accompanied by an increased char yield of 15.2 wt.% greater than the calculated value of 8 wt.%. The rate at peak weight loss is slightly reduced for the biomass whilst

the PP reduced from 3.0 wt.% down to 2.6 wt.%. which is nearly a 15% reduction in rate at the point of peak weight loss. This highlights the broadening effect of mixing the biomass with the PP.

5.4.1.4 TGA and DTG for biomass and PS combined

The temperature of peak weight loss also increases slightly. As with the polyolefins, addition of the polymer led to reduced volatiles yields from the biomass sample down from 83.9 wt.% to 72.4 wt.% although the PS volatiles yield increased from 97.2 wt.% to 99.2 wt.%. Again, the char yield increased in the co-devolatilisation experiment with a yield of 13.7 wt.% compared to a value of 8.8 wt.%, calculated from the individual samples. The rate of the biomass at the point of peak weight loss reduced from 1.1 to 1.0 Δwt.%/°C with PS also decreasing slightly from 3.5 to 3.1 Δwt.%/°C.
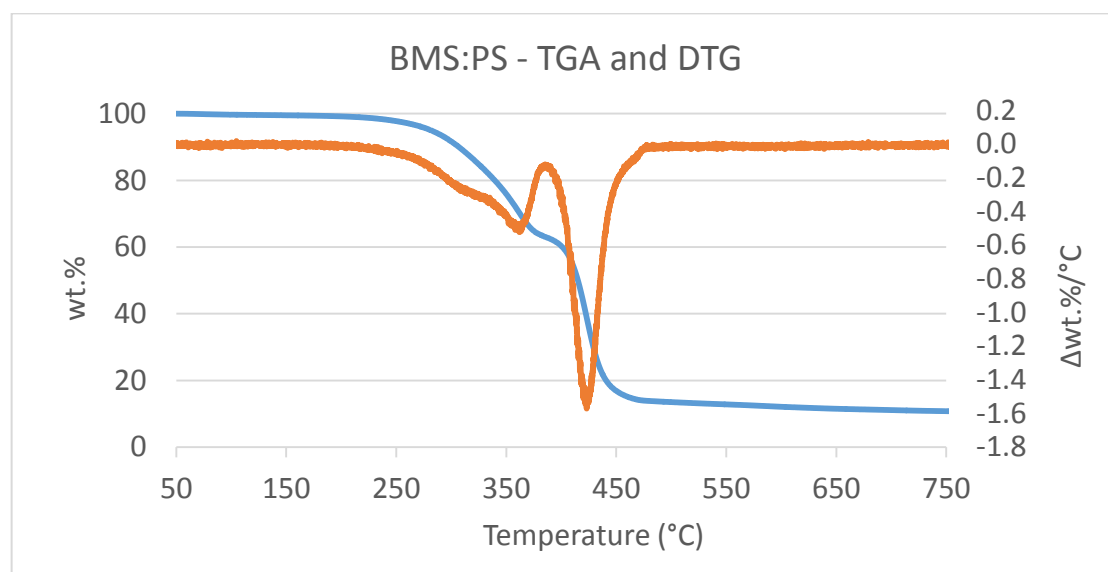
Figure 5.16: TGA and DTG during devolatilisation of biomass with PS.

Ephraim et al. [257] studied co-pyrolysis of biomass with PS and found that a limited synergy was observed, in this case leading to an increase in char yield accompanied by a decrease in oil yield. Their research suggested that secondary reactions were responsible for an increase in light hydrocarbon gases and a decrease in oil, however, these secondary reactions could not be directly observed. The synergy effects also led to an increase in hydrogen, and carbon oxides particularly in mixtures with less than 50% plastic content. As the PS content of the co-pyrolysis mixture increased carbon monoxide became

increasingly produced rather than carbon dioxide which may reflect the reduction in oxygen availability from the feedstock.

5.4.1.5 TGA and DTG for biomass and PET combined

The devolatilisation of biomass with PET was very different for the other polymers. This was mainly due to the increased overlap between the PET and the biomass devolatilisation events. This resulted in two peaks, of which the first was the most significant, containing weight loss associated with both biomass and PET. The temperature at which the secondary peak is observed indicates that this is due to PET devolatilisation alone. This is most clearly indicated by the increase of the yield from the biomass volatiles peak from 83.9 wt.% to 98.4 wt.% and a decrease in the yield from the PET peak 56.0 wt.% to 39.4 wt.%. There is only a 1% decrease in the total volatiles yield however a greater proportion of volatiles emission during the first devolatilisation peak.
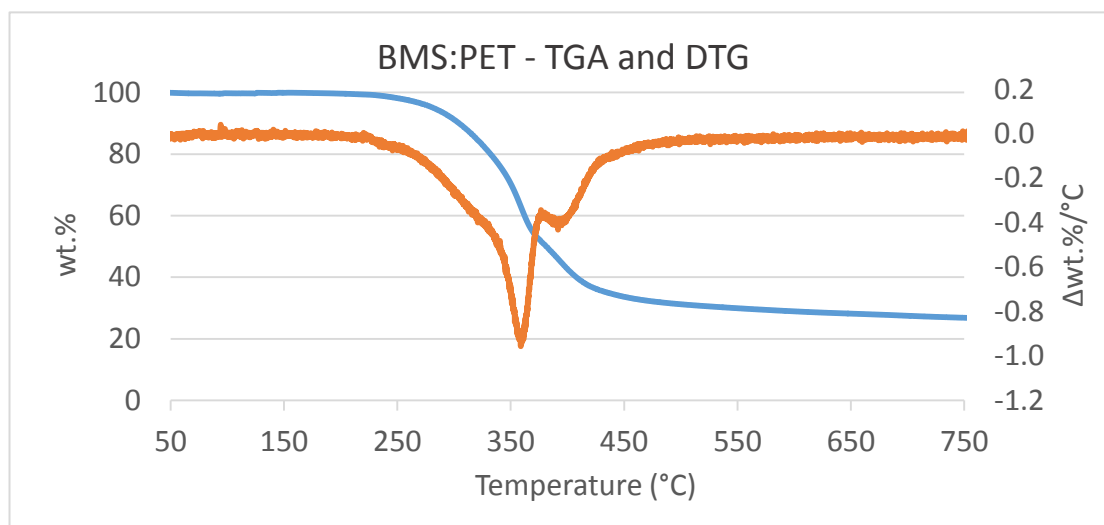
Figure 5.17: TGA and DTG during devolatilisation of biomass with PET.

This is also accompanied by an increase in the rate at peak weight loss for the first peak from 1.1 to 1.9 Δwt.%/°C and a decrease in the second peak to 0.8 from 1.1 Δwt.%/°C. Overall the rate of the two peaks is 2.7 Δwt.%/°C which is greater than the combined rate for the two individual peaks. This shows that both samples are contributing to the peak rate, thereby, causing this to increase. The char measured for the combined samples was greater than that for the individual samples increasing from 29.4 wt.% to 31.1 wt.%. As with the other polymer and biomass mixtures the onset temperature for biomass

devolatilisation increased, in this case from 201°C to 223°C although the temperature of peak weight loss for biomass did not change. The temperature at which the PET peak reached peak weight loss reduced by 10°C.

5.4.1.6   Characteristic temperatures for mixed biomass and polymer devolatilisation

Table 5.4 lists the temperatures at which devolatilisation begins, peaks and ends for each of the biomass and polymer samples during the mixed sample TGA studies. Navarro et al. [252] found that during co-devolatilisation of pine with different polymers the temperature of peak mass loss remained relatively unchanged and this was also observed in this case. Chattopadhyay et al. [256] observed a delayed onset of biomass decomposition during co-pyrolysis of plastics with biomass which was also observed during these TGA studies. They also determined that char content reduced during co-pyrolysis experiments compared to individual sample pyrolysis. However, if the low char content of the plastic samples is accounted for the char content of the combined samples is, in reality, larger than that which would be calculated from the mean value of the two samples which were combined.

Table 5.4: Temperatures (°C) at which peaks start to form, reach peak height and are finished during co-devolatilisation of mixed samples of biomass and polymers.

	Biomass peak			Polymer peak		
	T_{onset}	T_{peak}	T_{final}	T_{onset}	T_{peak}	T_{final}
BMS:HDPE	224	362	391	391	475	504
BMS:LDPE	231	362	386	386	473	502
BMS:PP	227	361	386	386	458	489
BMS:PS	224	363	384	384	423	478
BMS:PET	223	360	378	378	392	489

Table 5.5 lists the rate at the temperature of maximum weight loss as well as the char, volatiles and moisture content as determined from the TG analysis. The char yield and moisture yield are from both the biomass and the polymer sample used in each experiment and can be compared to the values determined from the individual samples. The rate at maximum weight loss and the volatiles yield are from either the biomass or the polymer where the samples devolatilise at different temperatures. If these values are compared to the

individual samples the values must be doubled to account for the 1:1 mixing ratio with each material contributing half of the original sample mass.

Table 5.5: The rate of weight loss determined for the biomass and polymer peaks and the distribution of weight loss between moisture, volatiles and char during co-devolatilisation.

	Rate at DTG$_{Max}$ 1	Rate at DTG$_{Max}$ 2	Moisture	Volatiles peak 1	Volatiles peak 2	Char
Unit	Δwt.%/°C	Δwt.%/°C	wt.%	wt.%	wt.%	wt.%
BMS:HDPE	0.57	1.40	0.8	37.6	47.7	13.9
BMS:LDPE	0.53	1.36	0.6	34.5	49.8	15.0
BMS:PP	0.52	1.31	0.6	35.9	48.2	15.2
BMS:PS	0.52	1.57	0.5	36.2	49.6	13.7
BMS:PET	0.94	0.41	0.1	49.2	19.7	31.1

As with Chattopadhyay et al. [256], Zhou et al. [177] also claimed to observe a reduction in char yield during co-pyrolysis of biomass with PP, LDPE and HDPE. However, as with Chattopadhyay this decrease is only in relation to the char from the biomass sample. Whilst in this case, combined samples of biomass and HDPE produced reduced char yield compared to the mean value from the individually pyrolysed biomass and HDPE, the char yield for biomass and PP with LDPE increased. Battacharya et al. [168] studied copyrolysis of PP and wood in an auger reactor and observed an increase in char from the mixture compared to individual samples. Sajdak and Muzyka [165] also studied the effect of co-pyrolysis of biomass and PP. In their research pine and alder wood were compared as the biomass source and in both cases an increase in char yield was observed.

5.4.2 MS profiles during devolatilisation of mixed samples

As with the individual samples the MS profile may also be used to compare the interactions between the biomass and the plastic being examined.

5.4.2.1   MS profiles during devolatilisation of Biomass with HDPE

The DTG plots show that in the case of the polyolefins and PS the weight change is greater than for the biomass samples, however, this is not reflected in the MS plot where the compounds yields are related to the amount of oxygen

content in the samples. This is much higher in the biomass sample than the polymers, with the exception of PET. The biomass related emissions are reasonably unchanged from the individual sample with a slight increase in the proportion of carbon dioxide compared to carbon monoxide. This increase is also observed with the HDPE emissions where carbon monoxide has reduced to the same level as carbon dioxide having been greater in the individual sample. The most significant change is the increase in hydrogen emissions which are greater in the mixed sample than in the individual samples particularly as higher temperatures (600-800°C) are reached.
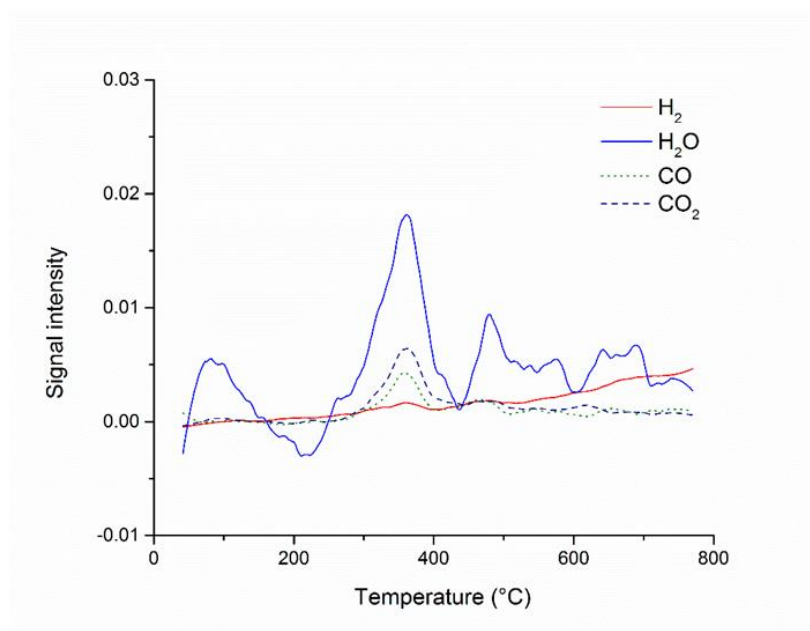
Figure 5.18: MS profile during devolatilisation of biomass with HDPE.

5.4.2.2 MS profiles during devolatilisation of Biomass with LDPE

For biomass and LDPE, the peaks are similar to those in the individual samples both in both the carbon oxides and the hydrogen yields. This may indicate that the differences observed in the mixing of biomass and HDPE could be due to impurities introduced by using a recycled material. There appears to be a greater overlap between biomass and LDPE than in the case of biomass and HDPE.
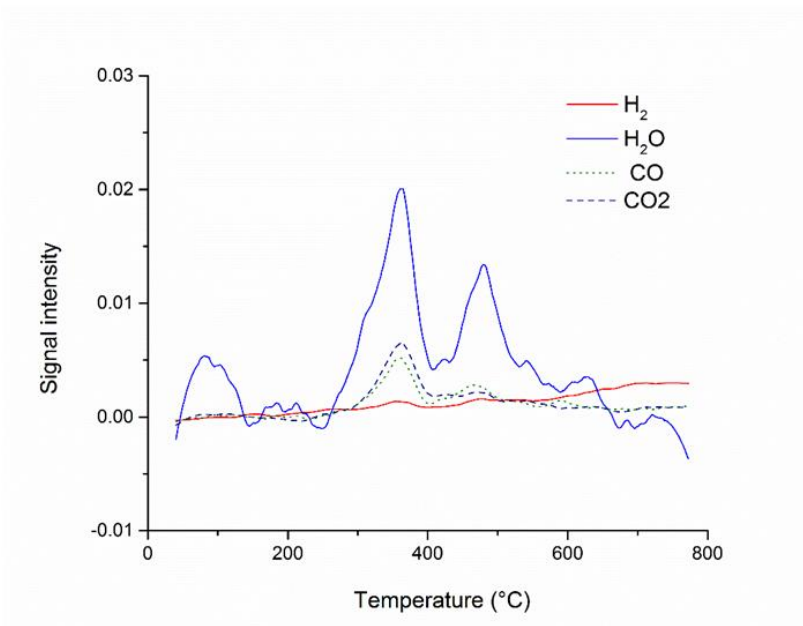
Figure 5.19: MS profile during devolatilisation of biomass with LDPE.

5.4.2.3 MS profiles during devolatilisation of Biomass with PP

With the biomass and PP mixture the biomass profile during thermal degradation is unchanged, however, in the PP emissions the yield of hydrogen has reduced with the proportion of carbon dioxide increasing to similar levels to that of the carbon monoxide where in the individual samples the carbon monoxide yield was larger. It may be that the elevated oxygen content of the biomass compared to the PP allows for more complete oxygenation of the carbon oxide which was limited in the oxygen poor PP sample. This would mean that the PP was removing oxygen from the biomass sample through interactions, as it devolatilised which would be potentially beneficial for reducing the oxygen content of bio-oils. The overlap between biomass and PP is much greater than with the other polyolefin samples. Sajdak and Muzyka [165] examined the gaseous products during co-pyrolysis of pine and PP and found that whilst H_2 remained at a similar level to the individual samples both carbon dioxide and carbon monoxide were increased in the co-pyrolysis sample.
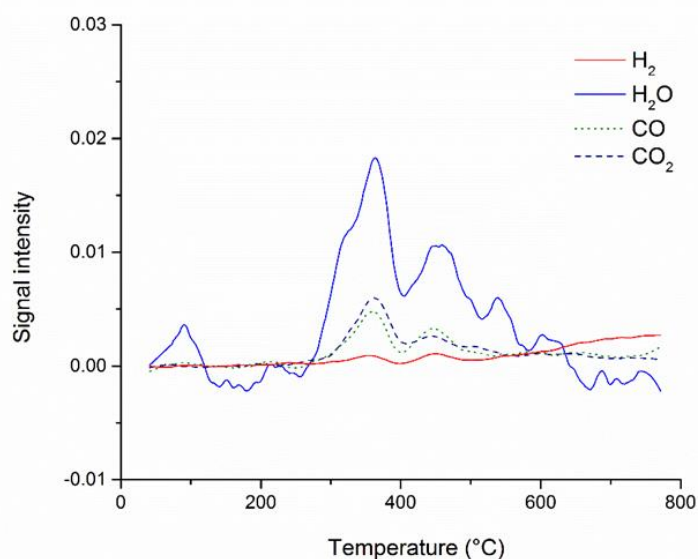
Figure 5.20: MS profile during devolatilisation of biomass with PP.

5.4.2.4 MS profiles during devolatilisation of Biomass with PS

There is a significant overlap in the emission peaks for biomass and PS and differences are observed in both the biomass and the plastic MS profiles. The most obvious change in the biomass profile is in the carbon monoxide emissions which follows a different temperature profile to the carbon dioxide. The carbon oxides previously matched closely to cellulose decomposition however in this case the carbon monoxide exhibits similarities to both the hemicellulose and cellulose decomposition with a clear 'shoulder' feature. The PS emissions are also changed from the individual sample devolatilisation with a large increase in the carbon dioxide yield. The low oxygen content of the PS may indicate that the oxygen necessary for carbon dioxide formation is from the biomass sample. Ephraim et al. [257] studied the co-pyrolysis of biomass and PS and measured the gas emissions. Their study found that the proportions of carbon dioxide was higher than carbon dioxide in the biomass sample and the inverse was true in the PS sample. The carbon oxide emissions observed by Ephraim et al. were very low compared to biomass. This contrasts to the results obtained during this study. The PS sample used by Ephraim et al. was a virgin plastic whereas the PS used in this study was a recycled material. This may account for the big difference in carbon oxides emissions with oxygen content in pure plastics at a lower level than in a sample which has been processed and may have been adulterated with oxygen containing additives. Ephraim et al. found that as the PS content increased the proportion of carbon oxides shifted towards carbon monoxide.
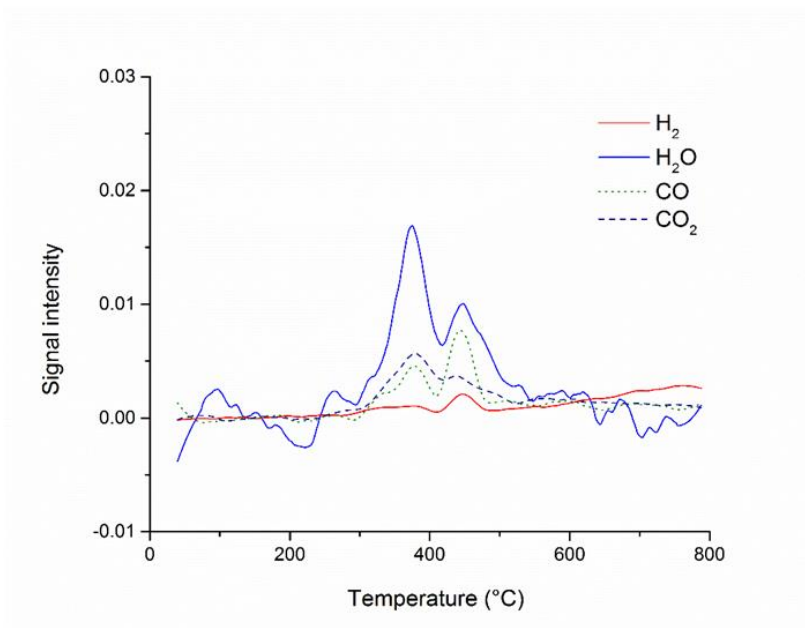
Figure 5.21: MS profile during devolatilisation of biomass with PS.

5.4.2.5 MS profiles during devolatilisation of Biomass with PET

The sample containing biomass and PET had the greatest overlap in the DTG plots and this is also observed in the MS plot. The DTG plot showed two peaks which is observed in the water emissions, however, this is not observed as a peak in the carbon oxides rather as a lengthened tail on the biomass peak. The emissions of carbon dioxide were increased in the mixed sample with the carbon monoxide remaining consistent with that expected from the individual samples.
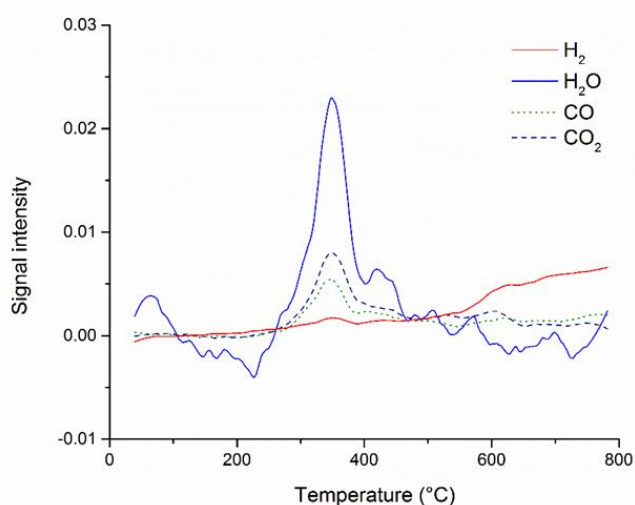
Figure 5.22: MS profile during devolatilisation of biomass with PET.

5.4.2.6 Characteristic temperatures for mixtures of biomass with plastics both from TGA/ DTG and MS data

The synergy between the biomass and the plastic samples may be observed in three ways, a change in the product yields, a change in the rates of devolatilisation and a change in the temperature at which devolatilisation occurs. Characteristic temperatures may be used to compare the temperature at which devolatilisation occurs between different samples, this allows for comparison also between individual samples and those which have been combined. Table 5.6 lists the characteristic temperatures for the peaks relating to biomass and plastic devolatilisation for the combined samples using data both from the TG/DTG and MS results.

Table 5.6: Characteristic temperatures (°C) for co-devolatilisation of biomass with plastics from both TG/DTG and MS results.

	Biomass peak					Plastic peak				
	T_{ID}	T_{MWL}	T_{H20}	T_{CO2}	T_{CO}	T_{ID}	T_{MWL}	T_{H20}	T_{CO2}	T_{CO}
BMS:HDPE	304	362	373	368	358	454	475	482	476	472
BMS:LDPE	304	362	363	366	366	449	473	479	476	465
BMS:PP	301	361	369	364	362	433	458	450	447	451
BMS:PS	300	363	388	386	380	409	423	446	438	445
BMS:PET	296	360	351	354	355	369	392	400	387	389

5.4.3 The effect of co-devolatilisation on biomass and plastic characteristic temperature.

Figure 5.23 shows the effect of combining biomass with PS on the characteristic temperature, T_{MWL}. For PS the temperature at which maximum weight loss is observed in the sample shifts to a higher temperature in the combined sample than in the individual sample. For biomass the temperature at which maximum weight loss is observed also increases in the combined sample but to a lower degree than for the PS. This indicates that when the biomass and PS are devolatilised together there are interactions between the samples which alter the devolatilisation process. It is not clear why the degradation of polystyrene is delayed by the presence of biomass. It may be that the free radical species which are important in this degradation process are being utilised in interactions with the biomass which delays degradation onset until elevated temperatures where more free radical species are generated.
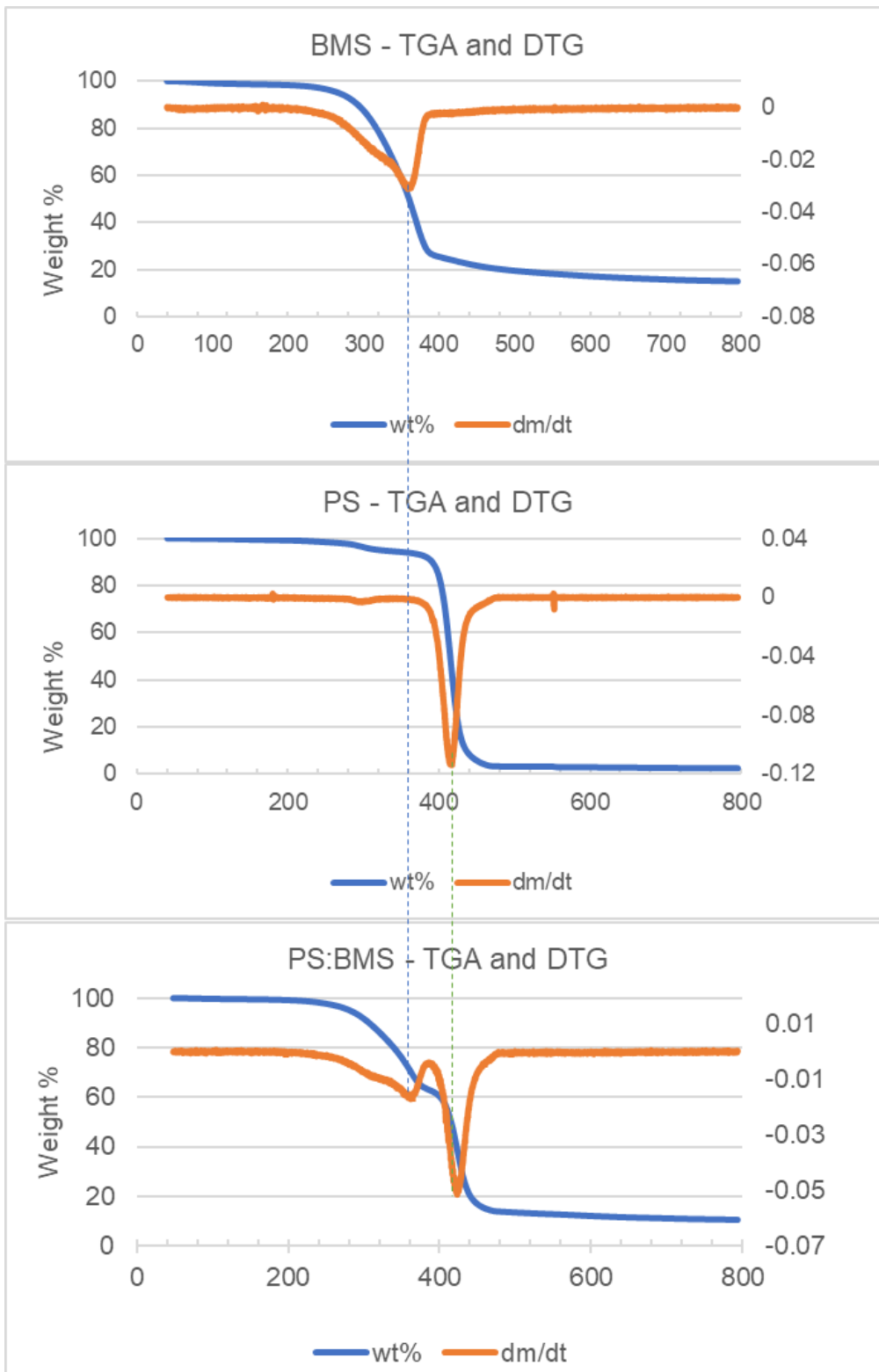
Figure 5.23: The shift observed for T_{MWL} when biomass is combined with PS.

5.4.3.1   The effect of combining biomass with HDPE on the temperature of devolatilisation

Due to limited space in the figures used for section 5.3.3 the characteristic temperatures will be labelled T1-T5 (see Table 5.7).

Table 5.7: Labels used for characteristic temperatures in section 5.3.3.

Characteristic temperature	Definition	Label
T_{ID}	Temperature of initial decomposition	T1
T_{MWL}	Temperature at maximum weight loss	T2
T_{H20}	Temperature at maximum H_2O emission	T3
T_{CO2}	Temperature at maximum CO_2 emission	T4
T_{CO}	Temperature at maximum CO emission	T5

During devolatilisation of biomass with HDPE the most significant shift is observed to the temperature of initial decomposition (T1) which denotes the onset of devolatilisation. For biomass this temperature increases whilst for the polymer it moves to a lower temperature. The other characteristic temperatures (T2-T5) relate to the point at which maximum weight loss or maximum emission of a species is observed rather than the onset. These also shift although to a lesser extent than for T1. In the individual biomass sample T2-T5 occur at the same temperature, however, in the combined sample these have diverged. This may indicate that in the individual sample all these species were produced by a single thermal decomposition mechanism or a number of mechanisms which occurred simultaneously. Whereas, in the combined sample, these mechanisms may be altered by interactions with free radical species obtained from the plastic or replaced by new mechanisms which occur through free radical based reactions.
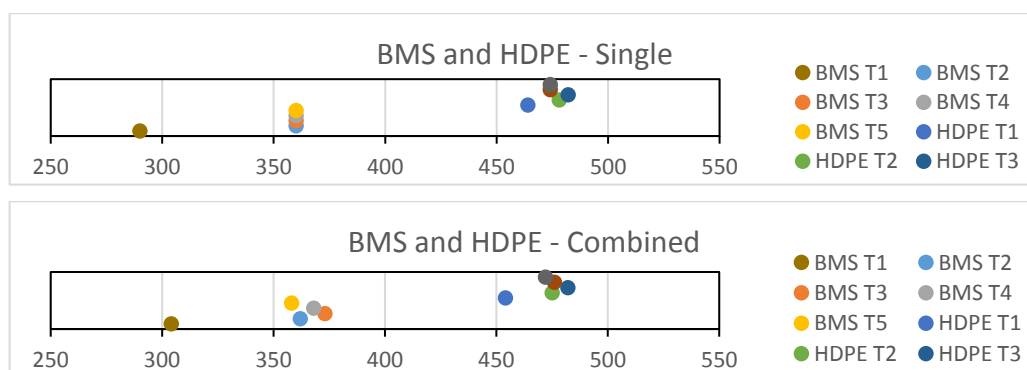
Figure 5.24: The effect of co-devolatilisation on characteristic temperatures for biomass and HDPE.

5.4.3.2   The effect of combining biomass with LDPE on the temperature of devolatilisation

As with HDPE, the LDPE sample displays a similar trend with regards to T1 (onset) and the other characteristic temperatures, T2-T5 (peak/maximum) although the change observed in the biomass sample is not as large as that for HDPE. The temperature T1 in LDPE is not altered as much as for HDPE although there is a shift in the temperature at which CO reached peak emission (T5) to a lower temperature. This was also observed in the HDPE sample but to a lesser extent.
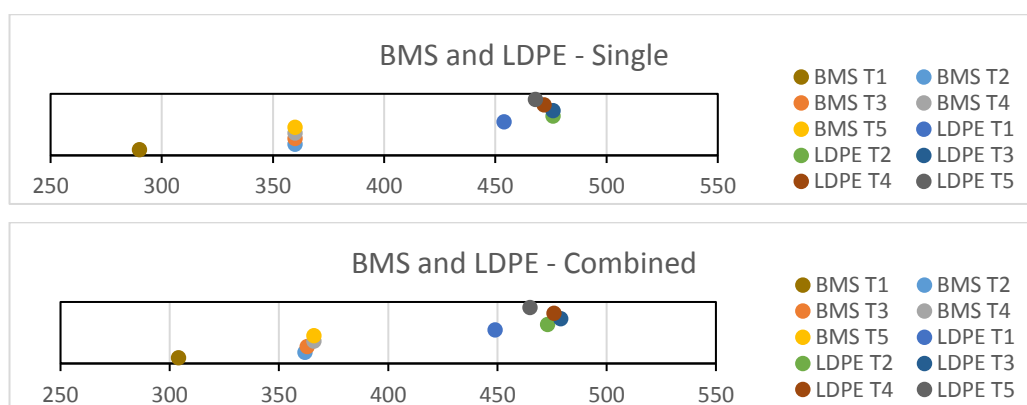
Figure 5.25: The effect of co-devolatilisation on characteristic temperatures for biomass and LDPE.

5.4.3.3   The effect of combining biomass with PP on the temperature of devolatilisation

For PP the shift which is observed for the biomass characteristic temperatures is equivalent that observed in LDPE however the change to the plastic characteristic temperatures is much larger. The PP temperature T1 moves to a lower temperature in the combined sample and the emission characteristic temperatures T3-T5 also reduce significantly indicating that the reactions which are occurring and producing these species are occurring much nearer to onset of devolatilisation than with the individual sample. This is not reflected in the value of T2 with the temperature at which weight change is at a peak is unaffected by combining the two samples during devolatilisation. This indicates that the species which are being measured (T3-T5) are not responsible for the peak weight loss or these characteristic temperatures should be the same.
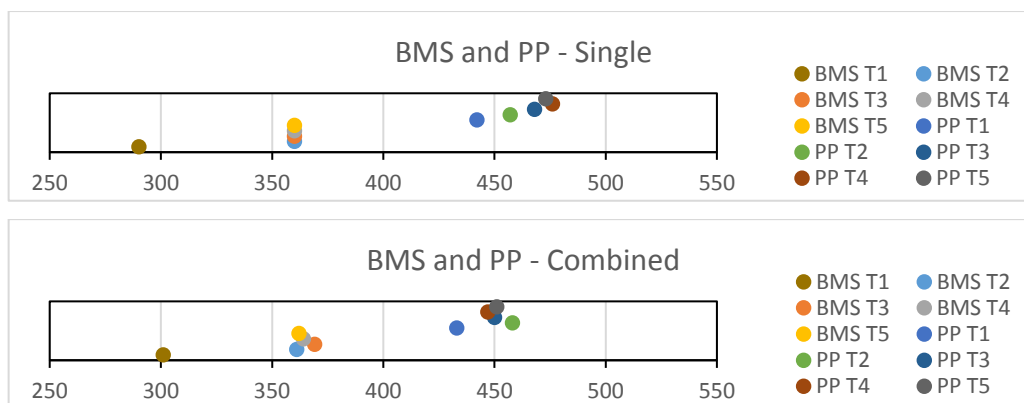
Figure 5.26: The effect of co-devolatilisation on characteristic temperatures for biomass and PP.

5.4.3.4 The effect of combining biomass with PS on the temperature of devolatilisation

In contrast to the PP sample, with PS the biomass characteristic temperatures particularly T1 and T3-T5 moved to higher temperatures by a large amount whereas the characteristic temperatures for the PS sample were relatively unaffected by combining the samples during devolatilisation. The temperatures of peak emission for PS increased marginally.
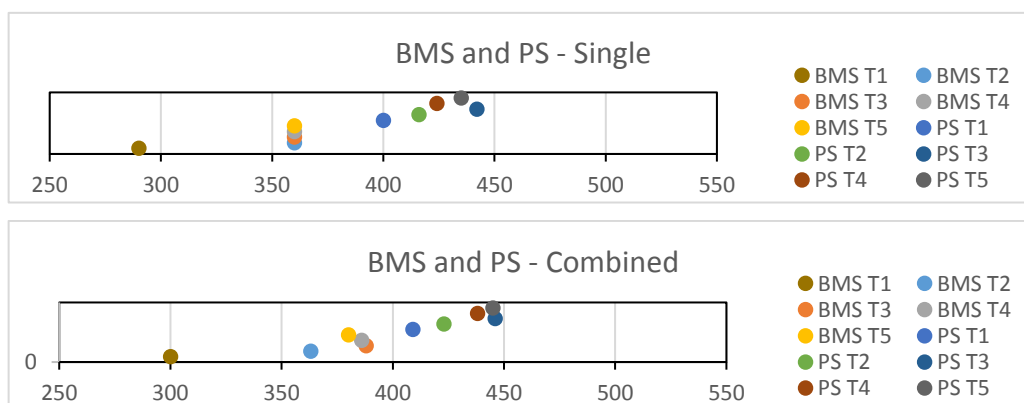
Figure 5.27: The effect of co-devolatilisation on characteristic temperatures for biomass and PS.

5.4.3.5 The effect of combining biomass with PET on the temperature of devolatilisation

In the case of biomass and PET, the onset of biomass devolatilisation was delayed to an increased temperature but the point of maximum emission of the measured species was reached at a lower temperature. This is in contrast to the other plastics. The characteristic temperatures for PET were all shifted to lower temperatures.
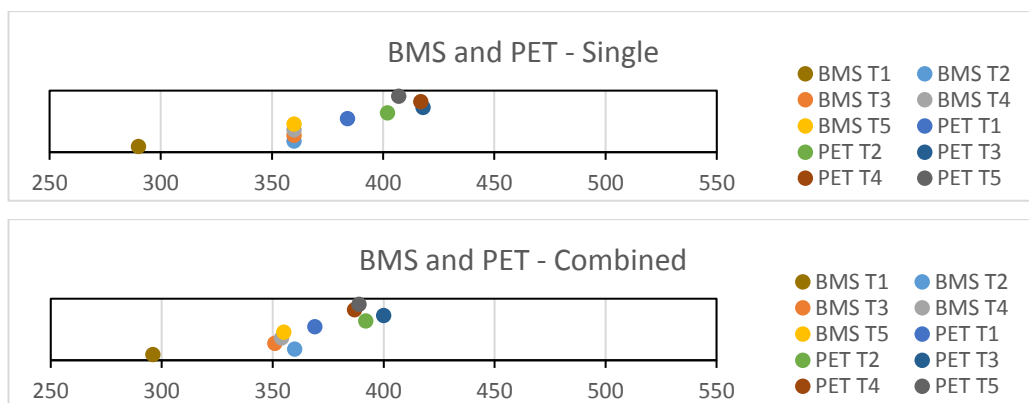
Figure 5.28: The effect of co-devolatilisation on characteristic temperatures for biomass and PET.

Table 5.8 lists the mean shift in the characteristic temperature for biomass and plastic caused by co-devolatilisation of the samples. For the polyolefin samples, the devolatilisation of biomass moved to a slightly higher temperature and the plastic to a lower temperature, this was limited for LDPE and HDPE but much larger for PP. The overall effect of both changes was that the characteristic temperatures of the two samples moved closer together in the combined sample. With PS, the characteristic temperatures of biomass moved significantly to higher temperatures whilst the plastic also moved to higher temperatures albeit by a smaller amount. The effect of this was that the character temperatures again moved closer together. In the case of PET both biomass and PET moved to lower temperatures of devolatilisation with the plastic shifting by a much larger amount than the biomass leading as with the other plastics to devolatilisation of the two samples occurring over a smaller temperature range. This indicates that there is synergy between biomass and plastics during devolatilisation although this appears to vary for each of the samples both in size of shift as well as the effect of the synergy on the temperature of devolatilisation.

Table 5.8: The mean shifts in characteristic temperatures during co-devolatilisation of biomass with polymers.

	Biomass	Polymer	Total Δ
HDPE	+7 °C	-3 °C	-10 °C
LDPE	+6 °C	-1 °C	-7 °C
PP	+5 °C	-15 °C	-21 °C
PS	+17 °C	+9 °C	-9 °C
PET	-3 °C	-18 °C	-15 °C
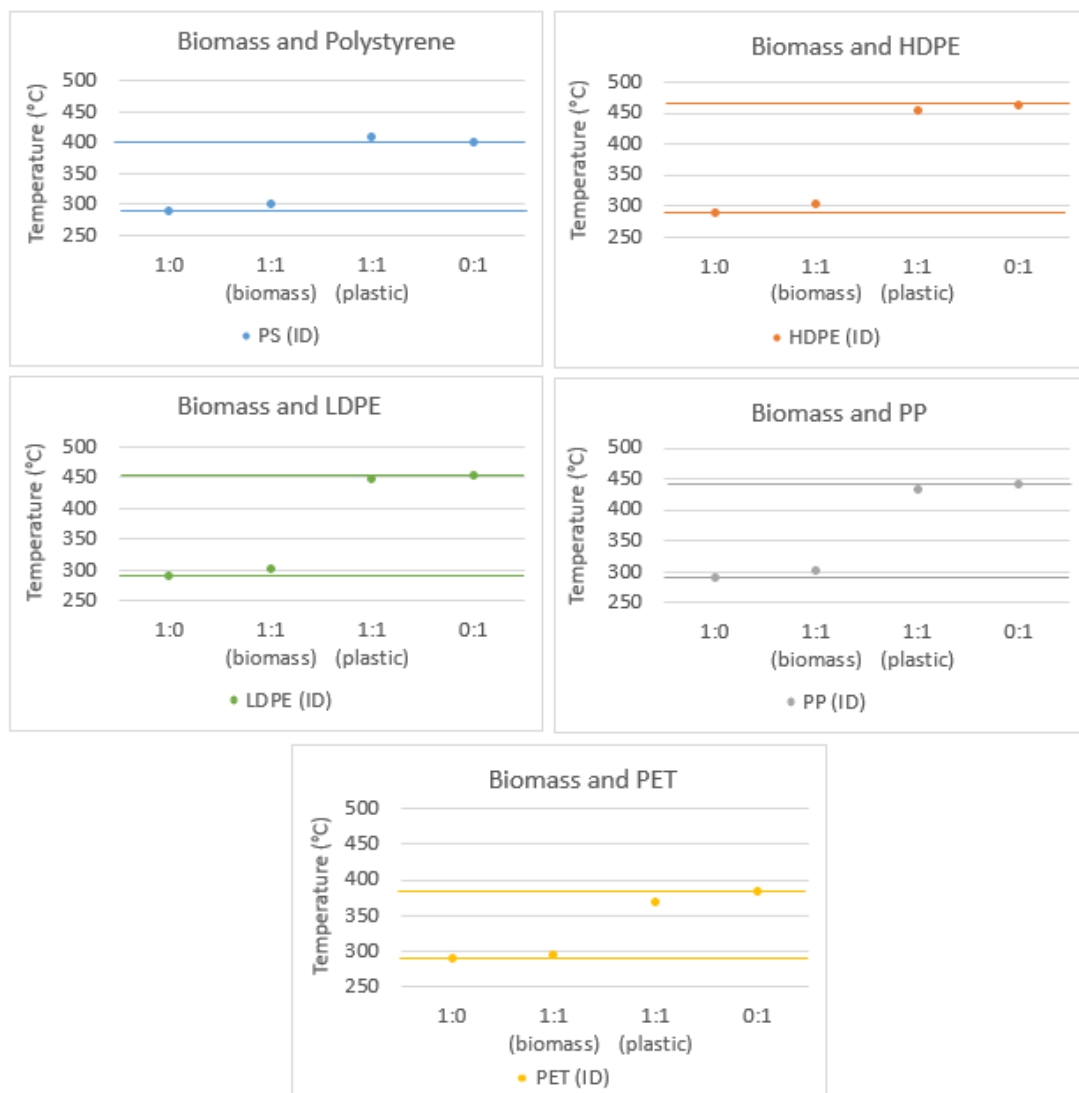
Figure 5.29: The temperature of ignition decomposition for different mixtures of biomass and plastics (1:0 – pure biomass, 0:1- pure plastic).

Figure 5.29 displays the change in temperature of initial decomposition as the mixture is changes from individual biomass (1:0) to an equal mixture (by weight) of biomass and plastic (1:1) and then as individual plastics. It can be observed that in most of the mixtures the temperatures of initial decomposition converge in the mixed samples however with polystyrene both temperatures of initial decomposition increase. This would suggest that any interactions between biomass and Polystyrene are different from those operating for the other plastics.

Jakab et al. [258] used TGA with GC/MS analysis of products to compare the devolatilisation of PP individually and in the presence of lignin, cellulose, wood and a commercial charcoal. The influence of the lignin, cellulose and wood caused the polymer to begin decomposition at a slightly lower temperature whilst the presence of the charcoal had a markedly stronger effect with the

onset temperature of decomposition for the polymer reducing substantially. Together with the analysis of the pyrolysis products, Jakab et al. concluded that charcoal formed during decomposition of biomass during co-pyrolysis is likely to act catalytically altering both the temperature and product distribution from polymer decomposition. However, the char yield from the biomass-derived samples was lower than that use in the charcoal TGA experiment and this led to a proportionately lower impact on the polymer thermal degradation. The effect of charcoal on the product distribution particularly affected the H-transfer reactions due to suggested enhancement of homolytic bond scission in the plastic. The temperature at which polystyrene decomposed in the presence of biomass increased having lowered for the other plastics. Thermal stability of plastics may be improved by intermolecular bonding which can act to shield weak points in the chemical structure [259]. It is possible that stabilising π-π stacking interactions due to electron density around aromatic rings could provide this stability increase as both biomass and polystyrene produce aromatic compounds.

Plastic melt may be the main cause for the increase in biomass decomposition onset temperature for the polyolefin and polystyrene samples with the biomass sample protected from thermal decomposition by a layer of softened plastic [260]. The divergence of the peak emission/ peak weight loss temperatures for biomass, from a single temperature in the individual sample to a range of temperatures in the combined samples, indicates that there may also be changes to the thermal decomposition mechanism during co-devolatilisation.

5.5 Conclusion

Thermal degradation begins at a lower temperature for the biomass sample examined compared to the plastic samples examined. This difference between the temperature at which biomass and the plastic degraded was higher for some of plastics than others. The difference between biomass and HDPE/LDPE was the largest observed and at a temperature increase of $10°Cmin^{-1}$ the thermal degradation of biomass was near completion prior to that of the HDPE and LDPE initiating. This means that using the same heating profile, in the two-stage fixed-bed reactor, for co-pyrolysis there is likely to be limited interactions between the vapours for the biomass and the polyolefin plastics. This might mean that for biomass and the polyolefin compounds there is limited interaction due to the vapours from the biomass passing from the reactor prior to the devolatilisation of the plastic starting. The interactions between biomass with polystyrene and biomass with PET are likely to be more

abundant due to the separation in degradation temperatures being smaller. During thermal degradation of biomass with the plastics it was possible to observe a shift in the temperature of initial decomposition and maximum weight loss compared to experiments using the individual samples. It is possible that the reduction in degradation temperature observed in the polyolefins and PET is due to the biomass char acting as an in-situ catalyst. This might have an effect on the formation of products as well as the temperatures of degradation due to possible reactions of the volatiles on the surface of the biomass char. This may be possible even though the vapours may be evolved over a different temperature range to the biomass sample. The biomass degradation in most cases began at a higher temperature during thermal degradation of biomass with the plastics. This may be due to encapsulation of the biomass particles by melted plastic. It is possible that this might increase the effect of heterogeneous reactions with the volatiles from the biomass sample potentially reacting with the surface of the plastic more readily if encapsulated. These results identify a limitation with the heating rate used during the two-stage fixed-bed reactor which is likely to be insufficient for complete mixing between the volatiles from the plastics with those form the biomass. It is likely that a higher heating rate would result in greater mixing of vapours which might therefore produce more interactions during co-pyrolysis.

Chapter 6: Co-pyrolysis of biomass with plastics

6.1 Introduction

The purpose of chapter 6 is to examine the effect of co-pyrolysis in the two-stage, fixed-bed reactor on the yield and composition of pyrolysis products. This chapter will begin by examining the pyrolysis products including the oil produced during pyrolysis of the individual plastic samples (HDPE, LDPE, PP, PET and PS) (objective 5). These results will then be used to identify whether catalytic co-pyrolysis of biomass and plastics at a 1:1 mixing ratios (by weight) may lead to variation in the pyrolysis products as compared to individually pyrolysed biomass and plastic samples (objective 6). Chapter 6 will also examine whether changes to the mixing ratio (1:1, 4:1 & 9:1) of biomass and three of the plastics (HDPE, PET and PS) may lead to variations in the pyrolysis products identified (objective 7). Temperature programmed oxidation will also be used to examine coke deposition during co-pyrolysis of biomass with the plastics to identify if certain co-pyrolysis mixtures might enhance or reduce coke formation (objective 13).

6.2 Pyrolysis of plastics

The oils produced during co-pyrolysis may exhibit improved or degraded characteristics compared to the same quantities of samples individually pyrolysed and then combined post pyrolysis. However, miscibility issues are possible when combining pyrolysis oils. Martinez et al. [166] observed that oils produced from co-pyrolysis of biomass with waste tyres and plastics can utilise radical interactions to stabilise the resulting liquid and therefore make it more suitable for use as a fuel or for mixing with current petroleum derived feedstocks. Stabilisation is also possible through the use of polar solvents such as methanol [261] however this will further increase the oxygen content of the oil and add to miscibility issues with petroleum feedstocks [27]. As well as improvements to oil stability or miscibility through interaction between the samples, it may be possible to produce an oil with lower oxygen content thereby reducing inherent miscibility challenges between bio-oil and petroleum derived oils.

6.2.1 Product yields from pyrolysis of plastics with ZSM-5

Pyrolysis of the biomass with ZSM-5 at 500°C gave a liquid yield of ~48 wt.% and an oil yield of ~14 wt.%. In contrast to this the yields from the plastics were much greater with liquid yields in the range 38 wt.% to 86 wt.% and oil yields in

the range 20 wt.% to 81 wt.% (see Table 6.1). The plastics (excluding PET) contained very little oxygen or moisture and this means that much less water is evaporated from the sample or produced during dehydrogenation reactions. This in turn meant that the liquid yield was mainly composed of compounds which may be considered oil. The plastic which produced the greatest oil yield was polystyrene (PS), followed by the polyolefins (high-density polyethylene (HDPE), low-density polyethylene (LDPE) and polypropylene (PP)) and then Polyethylene terephthalate (PET) which produced the lowest oil yield even if the reinforcement material (30 wt.%) is discounted. Reinforcement is common for PET materials which require high mechanical strength, however this presents problems with regards to recycling of PET and other glass reinforced plastics (GRP). Glass reinforced plastics are composite materials which contain glass fibres embedded within plastics to produce a material with improved properties compared to the unmodified plastic. This may alter many aspects of the material such as durability, mechanical strength, conductivity, impact resistance and weight but also provides greater challenges for recycling or disposal. One solution which has been identified as an economical and sustainable process for recycling of GRPs is pyrolysis [262-264]. This study aims to address whether glass reinforced PET may also be suitable for use during co-pyrolysis with biomass, thereby presenting a cost-effective recycling pathway with valuable by-products.

Sharuddin et al. [265] studied pyrolysis of polystyrene, polyethylene, polyethylene terephthalate and polypropylene which were also used in this research and found that of the plastic samples PS produced the highest liquid yield. This was also confirmed by Onwudili et al. [92] who found that heating of polyethylene and polystyrene individually in an autoclave for one hour led to a higher liquid yield for PS than LDPE. At 425ºC, the liquid yield of PS was 97.4 wt.% compared to 89.5 wt.% for LDPE although increasing temperature towards 425°C increased the liquid yield. Any further temperature increases above 425°C reduced the liquid yield due to a significant increase in char formation. This increase in char formation during temperature increases was due to secondary and tertiary reactions of pyrolysis vapours constrained inside the autoclave. In experimental methods which do not constrain the pyrolysis vapours, increasing temperatures and heating rates of plastic pyrolysis caused a reduction of liquid and char yield through thermal decomposition. This caused an increased gas yield equivalent to the loss in char and liquid yield [94, 265-267].

Sharuddin et al. [265] found that for LDPE the best liquid yield was recorded below 550ºC and comparison between plastics (LDPE, PET, and PP) by Fakhrhoseini et al. [266] at 500ºC determined the PP (80.65 wt.%) liquid yield to be the highest followed by LDPE (76.5 wt.%) and with PET (32.13 wt.%) much lower still. These values compare closely with those found in this research. PP had a higher liquid yield than either LDPE or HDPE, however, it was determined that the water content was also higher for PP the other polyolefins leading to an oil yield between that of LDPE and HDPE.

The char yield found by Fakhrhoseini et al. [266] for PET was at 7.6% which is relatively large considering that this was a virgin material. This may be due to formation of benzoic acid during PET thermal decomposition, a compound which can plasticise and lead to solid deposition. This is an issue as the deposits can cause clogging of equipment as well as being acidic [265, 268] . Char yields of 13.7 wt.% were determined for pyrolysis of PET at 500°C even after discounting the reinforcement material which is a much larger than with the other plastics.

Table 6.1: Yields of pyrolysis products for plastics with ZSM-5 at 500°C. The value in brackets for PET is a calculated pyrolysis yield if the reinforcement material was not present.

	Char (wt.%)	Liquid (wt.%)	Gas (wt.%)	Water (wt.%)	Oil (wt.%)	Mass balance (wt.%)
LDPE	0.0	72.5	30.9	6.1	66.4	103.7
HDPE	6.6	64.3	37.2	10.4	53.9	98.0
PP	0.5	75.1	31.6	12.5	62.6	104.6
PET	39.6	38.1	24.4	18.6	19.5	98.3
PS	1.4	86.4	8.2	6.4	88.5	97.5
Biomass	25.1	48.3	25.6	34.4	13.9	101.4

The plastics used in this experiment were pyrolysed in the presence of a catalyst, ZSM-5. Sharuddin et al. [265] observe that a solid acid catalyst such as ZSM-5 will generally increase the light hydrocarbon gas fraction (C_3-C_{11}) at the expense of the heavier hydrocarbon fraction (C_{12}-C_{20}) with the effect more pronounced as the acidity increases. This can be achieved by decreasing the Si/Al ratio in a ZSM-5 catalyst which increases the number of acid sites in the

material. This has the effect of potentially increasing the gasoline fuel range products by cracking larger hydrocarbon compounds although it will also increase the proportion of short chain hydrocarbons (C_1-C_4) which are gaseous at room temperature and pressure. The acid strength of the catalyst can be optimised to maximise the gasoline fuel range products from pyrolysis.

The char content remaining after pyrolysis of the plastic samples followed the same order as the ash content determined by proximate analysis with char and ash relatively similar in magnitude. The plastic with the lowest char yield was LDPE which allows for a larger liquid yield compared to another sample such as biomass with a much larger char yield (25.6 wt.%). At pyrolysis temperatures the char from biomass could not be entirely volatilised as would be the case in a combustion process, with an oxidising atmosphere [10, 38]. Whereas, in the case of the plastics the amount of remaining char was much lower, this compares to results obtained by Peng et al. [103]. As well as lower char content the plastics also contained less water [10, 58] which also increases the oil yield as a proportion of sample compared to biomass. Water is also formed during removal of oxygen during upgrading reactions which will be increased due to the presence of available oxygen in biomass samples compared to the polyolefins and PS. PET al.so contains much oxygen, but it is in a form which makes it more available for decarbonylation and decarboxylation rather than hydrodeoxygenation reactions. Honus et al. [269] compared the gaseous products from pyrolysis of PS, PE and PET and these plastics produced similar gas yields to one another but varied from the results for biomass [270]. Figure 6.1 shows the liquid yield for biomass and the plastics subdivided according to oil yield and water yield. It is clear that whilst the liquid yield from biomass is smaller than for the plastics, there is a large component of water in the biomass liquid yield. This means that the oil yield is considerably smaller for biomass compared to the plastics.
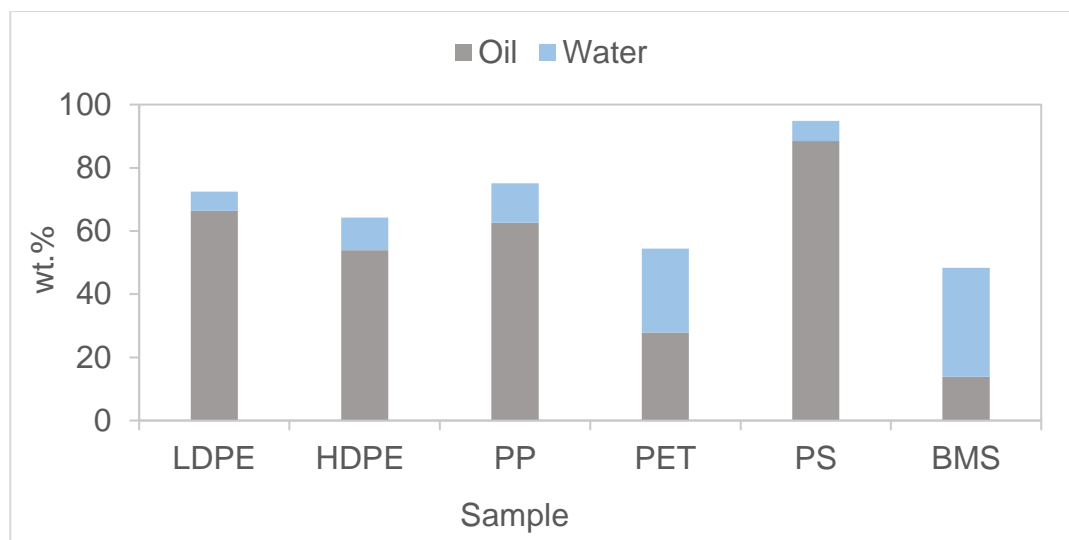
Figure 6.1: Liquid yield from catalytic pyrolysis of plastics and biomass at 500°C, with the water and oil portions of the liquid shown separately. The PET yield is corrected to discount the reinforcement material.

The gas yield for catalytic pyrolysis of each of the plastics is shown in Figure 6.2 and there are distinct differences between the polyolefin, PET and PS samples. The polyolefin sample produced the highest gas yield of which short chain hydrocarbon gases (C_2-C_4) were the major product with only a small proportion of hydrogen and methane. Pyrolysis of the biomass sample produced ~1 mmol/g hydrocarbon gases in contrast to the polyolefin samples which produced between 7-9 mmol/g, with HDPE contributing the highest value and LDPE the lowest. The oil yield shown in Figure 6.1 shows the converse effect with a range between 53 – 66 wt.%. In regard to the oil yield, LDPE produced the highest value and HDPE the lowest. HDPE as well as producing the highest hydrocarbon gases yield, also produced the highest hydrogen gas and methane yields of all the plastic samples. Non-catalytic pyrolysis of recycled HDPE and LDPE (500°C) by Sogancioglu et al. [89] produced ~88 wt.% and ~69 wt.% liquid from HDPE and LDPE respectively with ~10 wt.% and ~21 wt.% gases. This is the reverse from the results undertaken in this study although their work undertaken without a catalyst. The higher gas yield for LDPE was attributed by Sogancioglu et al., to LDPE being more readily cracked due to branching of the plastic. It is clear that the introduction of a catalyst has increased the gaseous yield with a reduction in liquid yield. This reduction in liquid yield is greater for the HDPE sample than the LDPE sample however this may be due to variations in char yield with the Sogancioglu samples producing ~5 wt.% lower char and ~9 wt.% higher char for HDPE and LDPE respectively. Whilst the results from this research and the results from

Sogancioglu for HDPE and LDPE are reversed there is a possible cause for this variation which could be due to the char. Bridgwater et al. [27] observe that with biomass the char is able to act as a catalyst leading to vapour cracking. Whilst the char present from these recycled plastics may be substantially varied from that of biomass it is evident that for both sets of results the highest gas yield/ lowest liquid yield is achieved in the sample which contains a considerably higher char yield. It may be that an active species or a number of species are enhancing the cracking of the polyolefins.
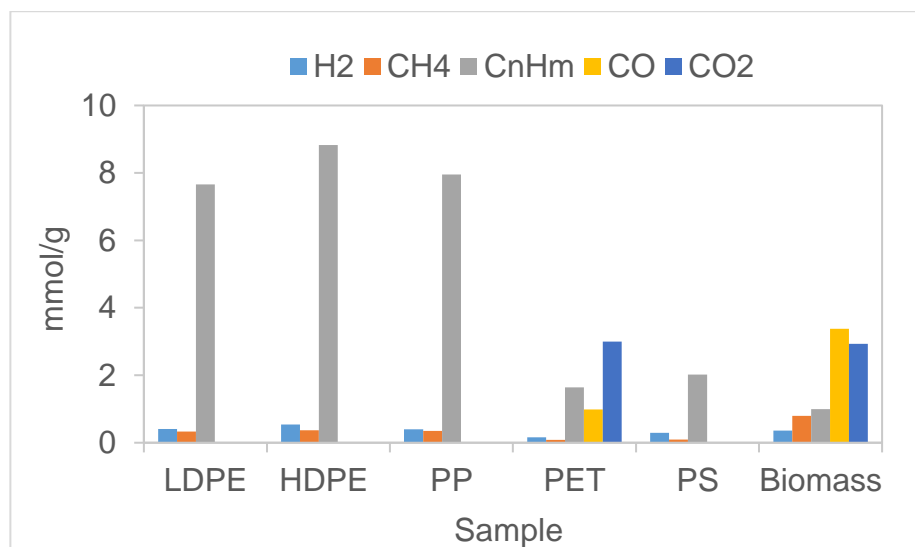
Figure 6.2: The composition of the gas collected during catalytic pyrolysis of plastics at 500°C with ZSM-5 as catalyst.

Carbon dioxide or carbon monoxide were not detected for the polyolefin samples which may indicate that they were absent or below detection limits. The absence of these gases is partially due to low oxygen content in the samples with any oxygen which was present having been retained in the oil, the char or may have become water through dehydrogenation reactions.

The PET sample produced a higher yield of hydrocarbon gases than the biomass sample and also a higher carbon dioxide content despite the sample being diluted through reinforcement. Whilst the hydrocarbon gases are lower than with the polyolefin samples the oxygenated gases are much higher and unsurprisingly carbon dioxide is the main gas product as it is already present within the PET ester functional group. Carbon dioxide and carbon monoxide have both been shown to be produced during PET decomposition [96, 99, 100].

The PS sample also produced a greater hydrocarbon gas yield than biomass although much less than the polyolefins samples. The PS sample contained very little oxygen such that it was not detected by oxygen analysis and there

was no carbon dioxide or carbon monoxide measured during analysis. This may account for the high liquid yield in PS.

The high hydrocarbon yields for the polyolefins mean that these gases might be particularly useful for combustion to provide process heat. Onwudili et al. [92] used a batch autoclave process to pyrolysis LDPE and found that the gases obtained to be between 50.8 and 52.7MJ/kg which is a little lower than that of methane gas at 55 MJ/kg [271] and comparative to natural gas 42-55 MJ/kg. However, in this research nitrogen was used as a carrier gas and continually passed through the reactor such that the collected gas would be far more dilute.
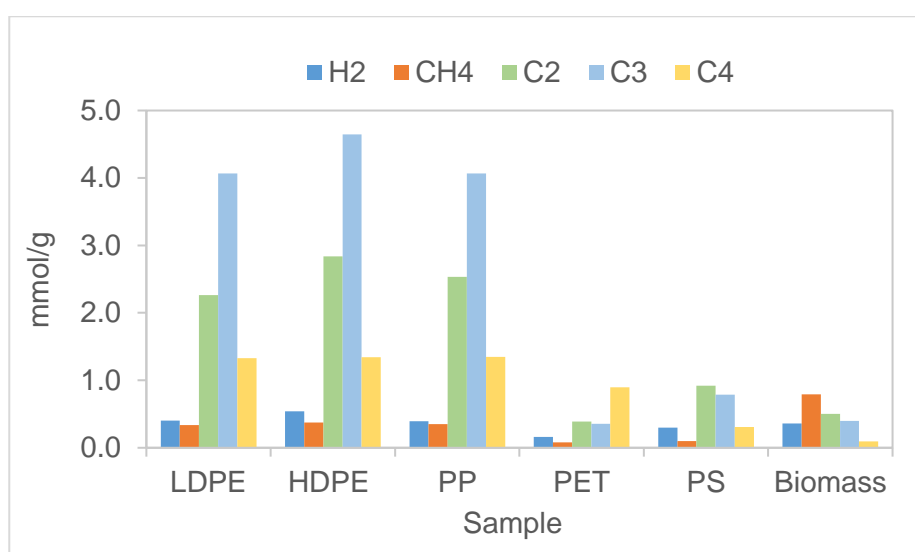
Figure 6.3: The composition of the non-oxygen containing fraction of the gases collected during pyrolysis of plastics with ZSM-5 catalyst.

Figure 6.3 details the hydrocarbon gas yields from the oil derived from the catalytic pyrolysis of the plastics in greater detail. The yield of hydrogen and methane from the polyolefins was comparable to the levels observed with biomass. The profile of light hydrocarbon gases produced during catalytic pyrolysis with ZSM-5 was distinctive for the plastic samples with C3 favoured in the polyolefins, C4 with PET and C2 with PS. This also implies that the method of product formation is different for each. This is further supported if the molar ratio of saturated/unsaturated hydrocarbon gases is considered. The polyolefin samples gave a ratio of between 4.0-4.4, PET gave 1.3 and PS gave a ratio of 12.7. This variation in values shows that a different pathway may be responsible for product formation leading to selectivity differences for saturated and unsaturated products.

The polyolefin samples are understood to break down via random chain scission leading to unsaturated hydrocarbons selectively whereas the PS is understood to undergo both random chain scission as well as end-chain scission [94]. PET decomposes via different pathways thereby not producing such high selectivity towards unsaturated products which are favoured during free radical reaction mechanisms instead producing linear alkanes and carbon oxides [96, 97, 272].

The addition of ZSM-5 catalysts to a pyrolysis reactor increases gas yields to a large degree. Rezaei et al. [123] compared the product yields for catalytic and non-catalytic pyrolysis of different biomass feedstocks. ZSM-5 increased the gas output from pyrolysis of corncob from 14 wt.% to 26 wt.%, wood waste shavings from 25 wt.% to 37 wt.% and beech wood from 18 wt.% to 26 wt.%. These increases in gas yield were accompanied by reductions in oil yield with reductions in oil yield of approximately 50% in each case.

6.2.2 Pyrolysis oil composition of plastics (ZSM-5)

As well as the yield of the products it is also important to examine the composition of the oils to discover if these are suitable for fuel use. The same properties are examined as were used for chapter 4 to allow for comparison between biomass and the plastics.

Table 6.2: Proportion of compounds in plastic derived pyrolysis oil which were aromatic, oxygenated or in the fuel range C_5-C_{12}.

	LDPE	HDPE	PP	PET	PS
Aromatic (%)	28.7	37.0	33.0	100.0	100.0
Aliphatic (%)	71.3	63.0	67.0	0.0	0.0
Oxygenated (%)	0.0	0.6	0.6	11.0	0.0
Non-oxygenated (%)	100.0	99.4	99.4	89.0	100.0
C_5-C_{12} (%)	49.1	55.4	67.2	96.5	76.3
$\geq C_{13}$ (%)	50.9	44.6	32.8	3.5	23.7
Uni-cyclic (%)	34.4	41.2	42.7	61.9	57.0
Bi-cyclic (%)	0.4	0.3	0.3	34.6	32.1
Tri-cyclic (%)	0.0	0.0	0.1	3.4	5.5
Quad-cyclic (%)	0.0	0.0	0.1	0.1	5.5
Linear (%)	65.1	58.5	56.8	0.0	0.0

6.2.2.1 Aromatic Compounds

Lopez et al. [273] examined catalytic pyrolysis of waste plastics in a semi batch process (40% PE, 35% PP, 18% PS, 4% PET and 3% PVC) with ZSM-5 catalyst and operating temperature at 500°C and determined that 98.6% of the oil compounds were aromatic even though a majority of the sample was derived from polyolefin samples. Li et al. [167] pyrolysed LDPE, PP and PS at 550°C using a pyroprobe combined with GC for quantitive analysis and ZSM-5 as the catalyst. The aromatic compounds made up 28.3 C% of the compounds produced during catalytic fast pyrolysis of LDPE, 35.4 C% for PP and 80.2 C% of the products from PS.
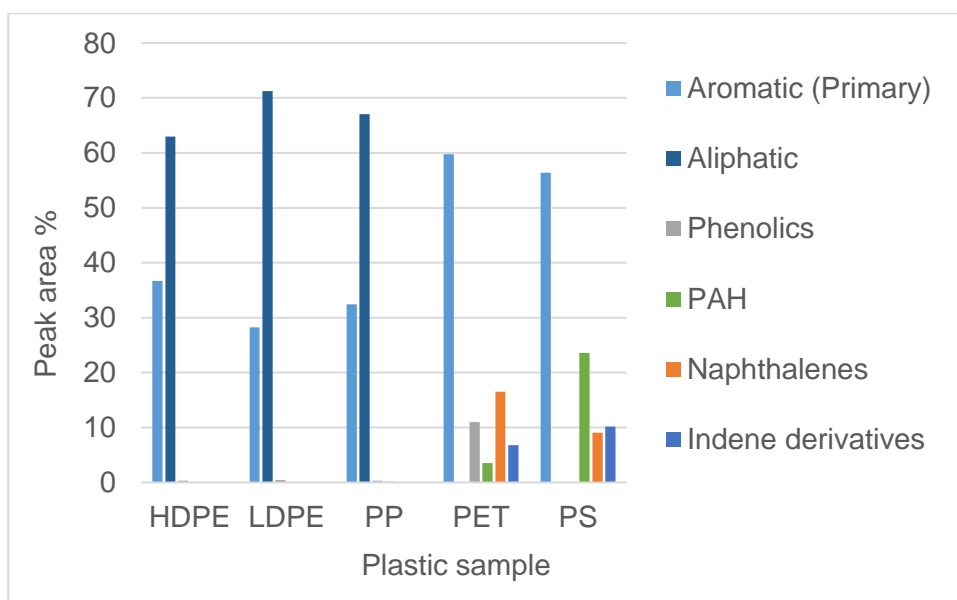
Figure 6.4: Oil composition categorised by compound type for different plastics.

Figure 6.4 shows the types of compounds identified from the pyrolysis oils. The polyolefin oils are composed of aliphatic compounds with a moderate proportion of primary aromatic compounds. In contrast the oils derived from PS and PET contain a large proportion of primary aromatics and a small proportion of other compound types such as phenolics, naphthalenes and indene derivatives and PAH compounds. This PAH group is largest for PS where is makes up ~20% of the compounds identified by GC-MS.

6.2.2.2 Compound molecular size

Table 6.2 shows the proportion of the compounds identified in the oils collected from pyrolysis of plastics at 500°C which are within the molecular size range for

gasoline (C_5-C_{12}). In the biomass sample 97.2% of the compounds were within this fuel range whereas with the plastics the best performing is PET at 96.5%. This is within the standard deviation for C_5-C_{12}, whilst the other plastics are far lower with PS at 76%, PP at 67%, HDPE at 55% and LDPE at 49%. The compounds which lie outside the fuel range may still be utilised through further cracking however this is likely to add further cost and energy input. Compounds which contain more than 12 carbon atoms and also contain aromatic rings are often polyaromatic. Polyaromatic compounds are often toxic and are precursors for tar and coke formation. In oils derived from pyrolysis of polyolefin samples which contain significant proportion of non-fuel range compounds there are no PAH compounds identified. The sample which contains the highest proportion of PAH compounds is PS.

6.2.2.3   Oxygen containing compounds

Whilst the pyrolysis oils from plastics contain much higher proportions of compounds which do not comply with the molecular fuel range for gasoline they are much more suitable for fuel use than biomass oils in terms of oxygen containing compounds. For biomass it was determined that of the compounds identified in the pyrolysis oils ~37% contained oxygen whilst in the plastic with the highest proportion of oxygenated compounds identified, PET this value is only 11% with lower values for the other plastics. The plastics with the lowest proportion of oxygenated compounds identified were PS and LDPE, for which no compounds were identified which contained oxygen. The main cause of the low oxygen values is that the samples which were plasticised contained very little oxygen which, present as impurities rather than as part of the chemical structure which for all but PET contain no oxygen. As oxygen was not introduced at any other point other than potentially as moisture there would be little source for oxygen in the oils.

The only plastic which contains higher oxygen content was PET for which 33 wt.% of the chemical structure is oxygen and further oxygen is present as glass reinforcement. However, although it contains similar levels of oxygen to biomass the proportion of oxygen containing compounds was much lower. This indicates that oxygen was being removed from the liquid fraction. Some of the oxygen was removed as carbon dioxide and some carbon monoxide as these were present in the gas phase and a large amount was removed as water as this was measured in the liquid sample however it is also likely that an amount was deposited in the solid state also as PET decomposed to form terephthalic acid and these tend to plasticise and deposit on available surfaces. It is difficult

to assess how much of this type of deposition was present although a white deposit was observed on some of the surfaces after pyrolysis.

The other plastics produced very few oxygenated compounds in the pyrolysis oils which is expected considering the low oxygen content of the samples. This low oxygen content may be useful during co-pyrolysis to produce oils which are both miscible and also have low oxygen content.

6.2.2.4 Cyclic and linear compounds

Figure 6.5 shows the cyclic and linear compounds identified in the pyrolysis oils from the plastics. As with previous criteria, the three polyolefin compounds are very similar with a mixture of unicyclic and linear compounds and are different to the PS and PET. PET contained the highest yield of primary aromatic compounds so it is not unexpected to find that it also has the highest yield of unicyclic compounds which includes both primary aromatic and phenolic compounds. PS contains both naphthalene compounds and other bi-cyclic compounds which might be considered PAH whereas PET contains a greater number of naphthalene compounds. For both PS and PET only around 60% of compounds identified belonged to the primary aromatic category with the majority of other compounds being PAH. The main type of PAH compound identified in the oils derived from PS and PET was naphthalene. The polyolefin by contrast had lower unicyclic content but the remainder was linear compounds which are not as high risk for coke and tar formation.
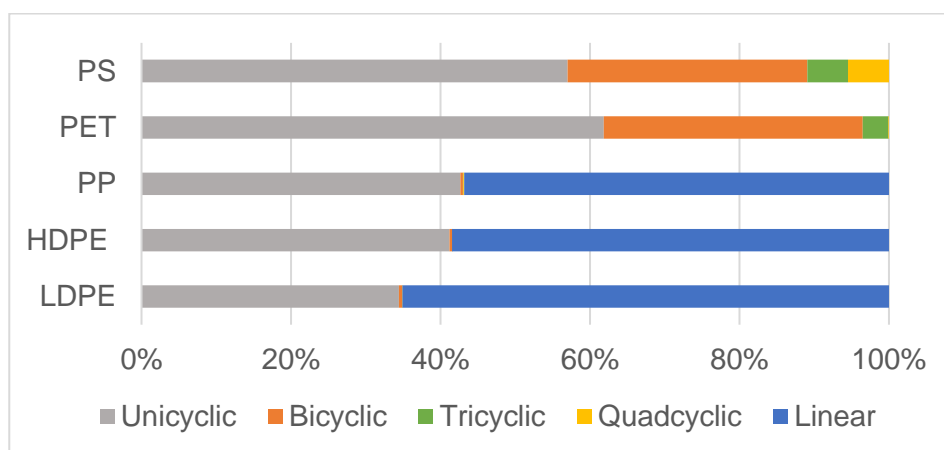
Figure 6.5: The proportion of cyclic and linear compounds found in the pyrolysis oil from plastics, with ZSM-5 catalyst.

6.2.2.5   Overview of plastics pyrolysed with ZSM-5

The results from the pyrolysis of the polyolefin plastic samples were very similar to each other, they devolatilise to produce a high yield of oil and a smaller yield of gas which is mostly hydrocarbon (C_3) with very little char material. The oil produced is a mixture of linear and unicyclic compounds with some aromatic compounds but mostly aliphatic and around half the oil yield was within the fuel range (C_5-C_{12}). The proportion of oxygenated compounds was very low.

The PET contained a large proportion of reinforcement material which reduced the oil yield from pyrolysis as a proportion of the original material, but this was still higher than for biomass if the reinforcement is accounted for. The gas yield was larger than for the other plastic samples except LDPE and the oil yield was lower than for the other plastics used (reinforcement accounted). The oil composition however was reasonable with most of the compounds in the fuel range and aromatic with lower oxygenated content than with biomass even though higher than the other plastics. The only drawback was a relatively high bicyclic yield which is not as favourable for fuel use as unicyclic and linear compounds. These bicyclic compounds are more suited to diesel fuel production or as chemical feedstocks.

The pyrolysis of PS gave the greatest oil yield with only a small percentage of gas and very little char. As well as this the oil was aromatic and had no oxygenated compounds determined from GC-MS analysis. The only downsides being the reduced fuel range proportion compared to PET, although this is offset by the increased oil yield, and the slightly higher bi-cyclic, tri-cyclic and quad-cyclic yields which are potential causes of tar and coke formation.

6.3 Co-pyrolysis of biomass and plastics (1:1 ratio)

The pyrolysis oils from biomass alone had some serious failings for potential fuel use, particularly the low oil yield and high proportion of oxygenated compounds in the oil. The use of an ex-situ ZSM-5 catalyst was able to reduce this, however, 37% of the compounds identified in the pyrolysis oil still contained oxygen. On the positive side, the molecular size of compounds was suitable for the fuel range for the biomass sample with catalytic upgrading to a high degree. In comparison the pyrolysis of plastics was able to produce a much higher oil yield with very low oxygen content, but in this case the proportion of PAH compounds was high for PET and PS and the yield of high molecular weight compounds was high for the polyolefins. Both sets of materials have significant problems were they to be used for production of fuels, however, both

sets of samples also have characteristics which make them suitable for oil use and crucially these are different for both sets. This introduces the possibility of co-pyrolysis with the aim of producing an oil for which the poor properties are minimised whilst adding stability and miscibility which are understood to improve through co-pyrolysis with certain plastics [164, 166].

There is also another advantage of co-pyrolysis, which is the introduction of hydrogen in as part of the plastic chemical structure causing an increase of the (H/C_{eff}) ratio. This allows for removal of oxygen whilst still providing enough hydrogen for viable formation of suitable pyrolysis oils. If this (H/C_{eff}) ratio is low as is the case with biomass, there is a dual effect that reduces oxygen removal in the form of water and increases the coke formation as hydrogen is unavailable for oil compound formation [159, 160]. In this was co-pyrolysis with plastics may have the potential to reduce oxygen content and coke deposition in biomass derived oils. There is also the advantage that waste plastics such as PS may be recycled and provide a high oil yield.

6.3.1 Co-pyrolysis yield of biomass and plastics (1:1) with ZSM-5

Table 6.3 shows the yields of pyrolysis products obtained from catalytic pyrolysis of biomass and plastics at a ratio of 1:1 and ZSM-5 as the catalyst. The values which would be achieved by direct mixing of pyrolysis oils from plastics and biomass pyrolysed as individual samples is was calculated from individual experiments and is shown in brackets alongside the measured value. This is a theoretical mixture assuming no reaction between the combined oils and assuming miscibility which may not be valid in a real mixing process.

Table 6.3: Yields from catalytic co-pyrolysis of plastics and biomass (1:1) with ZSM-5. Calculated values for mixtures of individual samples in brackets for comparison with measured results.

	Char (wt.%)	Liquid (wt.%)	Gas (wt.%)	Water (wt.%)	Oil (wt.%)	Mass balance (wt.%)
BMS:LDPE	12.5 (12.8)	53.5 (60.9)	35.0 (29.0)	31.5 (20.2)	22.0 (40.1)	95.4
BMS:HDPE	15.5 (16.1)	55.0 (56.8)	32.5 (32.2)	30.3 (22.4)	24.7 (33.9)	103.3
BMS:PP	14.5 (13.0)	49.5 (62.2)	34.5 (29.3)	14.1 (23.5)	35.4 (38.2)	96.0
BMS:PET	37.5 (32.6)	33.0 (43.7)	22.5 (25.7)	23.3 (26.5)	9.7 (16.7)	93.2
BMS:PS	16.0 (13.6)	65.0 (72.1)	18.5 (17.6)	17.4 (20.1)	47.6 (47.3)	98.2
BMS	25.1	48.3	25.6	34.4	13.9	101.4
LDPE	0	72.5	30.9	6.1	66.4	103.7
HPDE	6.6	64.3	37.2	10.4	53.9	98
PP	0.5	75.1	31.6	12.5	62.6	104.6
PET	39.6	38.1	24.4	18.6	19.5	98.3
PS	1.4	86.4	8.2	6.4	88.5	97.5

Co-pyrolysis on liquid yields of biomass with plastics led to a reduction in liquid yields for each of the plastics examined. The smallest reduction in liquid yield was measured for biomass with HDPE (1.8 wt.%) and PS (7.1 wt.%) with the greatest reduction for biomass and PET (10.7 wt.%) and PP (12.7 wt.%). As well as changes to liquid yields there were also reduction in oil yields from the pyrolysis of all the plastics other than PS which remained relatively unchanged. The highest reduction in pyrolysis oil yield was LDPE with a reduction of 18 wt.%. The result for PP is particularly noteworthy with liquid yield reducing by a comparatively high amount whilst oil yield only reduced marginally. If these results are correct this would suggest that the water yield for PP is significantly less than for that of the other polyolefin samples (LDPE and HDPE). One reason for this is that less oxygen has been removed from the mixed sample through hydrodeoxygenation. This may result in an increased oxygen content of the oils. In regard to char content, the polyolefin samples were relatively unchanged whereas the char produced by biomass and PS increased by 2.5 wt.% and that for biomass and PET by 5 wt.%.
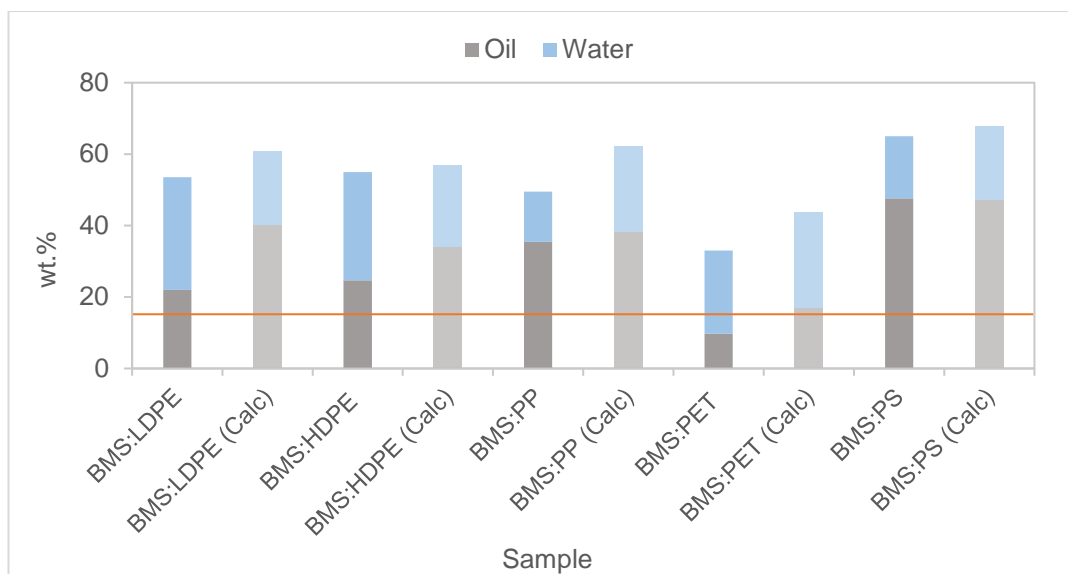
Figure 6.6: The liquid products from co-pyrolysis of plastics and biomass (1:1) with ZSM-5 catalyst alongside calculated values.

Figure 6.6 compares the calculated values to those that were measured for biomass and plastics at a 1:1 mixing ratio. The orange line has been placed on the graph to show the oil yield from biomass pyrolysis with ZSM-5. The samples which brought about the largest increase in oil yield were PP and PS. PET led to a reduced oil yield although this was without accounting for the reinforcement material which at this point is 13 wt.% of the sample. If the reinforcement is accounted for the oil yield increases to ~11 wt.% which is still lower than for that of biomass alone. It is likely that some of this reduction is due to increased char yield. The result for PS matched very closely with the calculated values whereas the other samples varied significantly.

During pyrolysis of the polyolefin samples the gas yields were higher than expected, this contrasts with yields from pyrolysis of PS where the decrease in liquid yield was counteracted by an increased char and gas yield. For pyrolysis of PET the increased char yield is balanced by a decrease in gas yield. The gas yields decreased by 4.3 wt.% for PS and 3.2 wt.% for PET respectively in the co-pyrolysis samples compared to values calculated from the individual biomass and plastic samples. The increase in gases during pyrolysis of the polyolefin samples was mostly due to an increase in the hydrocarbon gases and methane although there was a reduction in both carbon dioxide and carbon monoxide. This is likely to cause an increase in oxygenated compounds in the co-pyrolysis oils when compared to the oils from pyrolysis of individual samples. For pyrolysis of PET there was a reduction in hydrocarbon gases and a slight reduction in carbon dioxide, carbon monoxide and methane. The hydrogen gas

yield was fractionally increased. For co-pyrolysis of biomass with PS the carbon dioxide and carbon monoxide yields were approximately 8 wt.% and 10 wt.% higher than values calculated from individual pyrolysis of biomass and polystyrene. This included small increases in hydrocarbon gases, and hydrogen and a small decrease in methane formation.
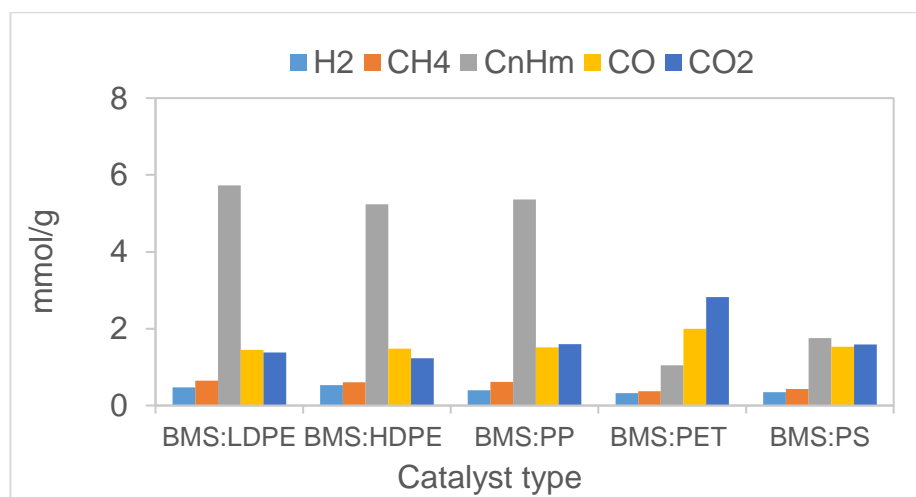
Figure 6.7: The composition of the gas collected during co-pyrolysis of biomass and plastic (1:1) (without nitrogen) with ZSM-5 catalyst.

The increase in hydrocarbon gas yield involved a relatively large increase in both C_2 and C_3 hydrocarbons. Table 6.4 gives the ratio of unsaturated to saturated hydrocarbon gases produced during individual and co-pyrolysis. There is little change in the polyolefin samples where the hydrocarbon yield is dominated by cracked products from the polyolefin rather than the biomass whereas there is a significant change in the case of PET. The low ratio for PET was particularly due to butane as a gaseous product however this is no longer present in co-pyrolysis with biomass and the resulting gases are strongly unsaturated.

Table 6.4: The ratio of unsaturated to saturated hydrocarbon gases, C_2-C_4, in the gas yield.

	LDPE	HDPE	PP	PET	PS	Biomass
Individual	4.0	4.3	4.4	1.3	12.7	7.6
Co-pyrolysis	4.2	4.1	4.5	11.7	10.4	-

6.3.2 Co-pyrolysis oil composition of biomass and plastics (1:1) with ZSM-5 catalyst

In order to assess whether co-pyrolysis is beneficial for fuel production it is necessary to consider both the pyrolysis oil yield as well as the composition of that oil. Table 6.5 shows the types of compounds which were identified during co-pyrolysis of biomass and plastics with calculate values derived from individual samples in brackets.

Table 6.5: Proportion of compounds in biomass and plastic derived co-pyrolysis oil which were aromatic, oxygenated, cyclic/linear or in the fuel range (C_5-C_{12}). Calculated values for mixtures of individual samples in brackets.

	BMS:LDPE	BMS:HDPE	BMS:PP	BMS:PET	BMS:PS
Aromatic (%)	52.5 (41.0)	42.1 (50.4)	43.1 (45.0)	100.0 (99.7)	95.6 (99.9)
Aliphatic (%)	47.5 (59.0)	57.9 (50.0)	56.9 (55.0)	0.0 (0.3)	4.4 (0.1)
Oxygenated (%)	12.3 (6.1)	11.7 (8.0)	10.2 (6.9)	19.7 (21.4)	2.1 (5.0)
Non-oxygenated (%)	87.7 (93.9)	88.3 (92.0)	89.8 (93.0)	80.3 (78.6)	97.9 (95.0)
C_5-C_{12} (%)	66.2 (57.4)	51.8 (64.4)	72.1 (72.6)	89.1 (96.8)	75.7 (79.3)
≥C_{13} (%)	33.8 (42.6)	48.2 (35.6)	27.9 (27.4)	10.8 (3.2)	24.3 (20.7)
Uni-cyclic (%)	49.4 (42.8)	40.4 (50.1)	49.3 (49.9)	65.7 (70.8)	62.2 (61.0)
Bi-cyclic (%)	3.1 (2.8)	1.7 (3.3)	0.8 (2.8)	27.1 (26.0)	24.6 (29.5)
Tri-cyclic (%)	0.0 (0.5)	0.0 (0.6)	0.0 (0.6)	7.1 (3.2)	6.1 (5.1)
Quad-cyclic (%)	0.0 (0.0)	0.0 (0.0)	0.0 (0.1)	0.1 (0.1)	2.8 (4.7)
Linear (%)	47.5 (53.8)	57.9 (46.0)	49.9 (46.6)	0.0 (0.0)	4.4 (0.0)

6.3.2.1 Aromatic compounds

The overall trend observed for the aromatic compounds in the pyrolysis oils from co-pyrolysis of polyolefins is an increase compared to the oils from individual plastics. However, if this is compared to predicted values for mixtures of biomass and polyolefins there is only an increase for LDPE when compared to calculated values. If compared to results from biomass pyrolysis there is a decrease in aromatic compounds. For PET the aromatic content remains high during co-pyrolysis which is not surprising considering that for pyrolysis of both biomass and PET high aromatic yields were produced for both. For PS the

decrease in aromatic compounds identified in the co-pyrolysis sample is only small.

When the specific types of aromatic compounds are considered there are further changes observed. In the case of the polyolefins the proportion of primary aromatic compounds identified in the co-pyrolysis oils is not changed much compared to the individual plastic samples but there is an approximately 10% reduction in the proportion of aliphatic compounds and this is counterbalanced by around 10% increase in phenolic compounds compared to values estimated for co-pyrolysis of biomass and polyolefins based on individual pyrolysis results.
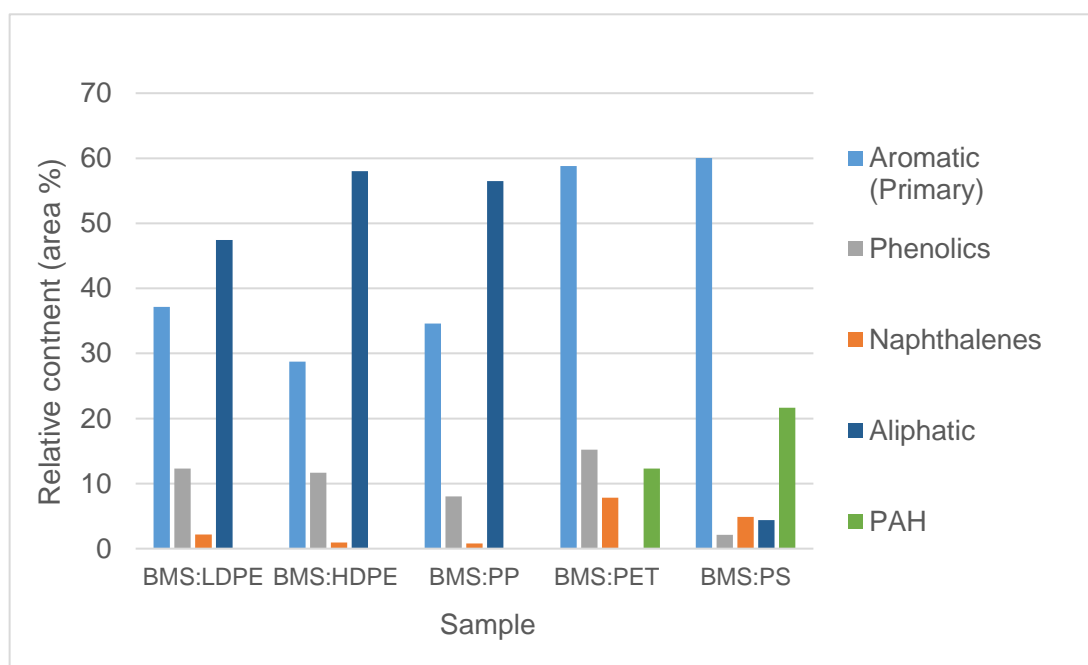
Figure 6.8: Oil composition categorised by compound type for co-pyrolysis of biomass with plastics (1:1) with ZSM-5.

For PET the primary aromatic content increases from ~50% in the biomass and ~60% in the plastic to ~60% in the mixture. This is accompanied by a reduction in phenolic compounds with ~33% in biomass and ~11% in the plastic becoming ~15% in the mixture when we would expect closer to 22%. There is also a reduction in the proportion of naphthalene compounds below that of the individual plastic or the biomass and an increase in PAH to a level greater than either sample individually.

With PS the primary aromatic compounds identified increases above the level of either individual sample with a reduction in naphthalene compounds below

the level seen for either sample. However, there is also an increase in PAH compounds with the proportion staying similar to that for PS although this contributes the dominant proportion of the oil. There is also a small proportion of linear compounds not identified in either biomass or PS.

6.3.2.2 Compound molecular size

The C_5-C_{12} proportion for biomass was much higher than for the plastics at 97.2% of all identified compounds and this higher than for the plastics, although PET was not far below (96.5%). It would therefore be expected that a mixture of the two pyrolysis oils would lead to an increase in the fuel range proportion compared to the plastics. This was the case for LDPE and PP and in the case of LDPE this increased even above the calculated value for the mixture. However, for HDPE, PET and PS there was a decrease in fuel range compounds below even that for the individual plastics. This may indicate that there are reactions occurring between the compounds produced by biomass and those from the plastics which are producing larger compounds and therefore the proportion of fuel range compounds is reduced. Alternatively, it may be that coke deposition on the catalysts is causing a reduced effectiveness of the catalyst and therefore the templating properties of the catalyst is being degraded.

6.3.2.3 Oxygen containing compounds

The proportion of oxygenated compounds is important for a number of properties of the oil including pH, stability and miscibility and it is therefore one of the most important criteria to consider. Talmadge et al. [41] suggested that a beneficial strategy might be to reduce the oxygen content of bio-oils to around 7 wt.% through hydroprocessing. This would ensure the bio-oils can be incorporated into existing petroleum upgrading infrastructure. Further reduction in oxygen content below this level would be beneficial, however it would require costly and energy intensive hydroprocessing. This research has examined deoxygenation achieved through metal-zeolitic cracking and co-pyrolysis rather than hydroprocessing but the same deoxygenation strategy would still be valid in this case. This research used semi-quantitive analysis to determine the deoxygenation capability of different catalysts and plastic co-feeds and the oxygenated compounds values could be cautiously applied to estimate oxygen content. The oxygen content of three compounds which were identified in pyrolysis oils, phenol, cresol and guaiacol contain 17 wt.%, 15 wt.% and 26 wt.% oxygen respectively. It is therefore likely that the semi-quantitive values determined for proportions of oxygenated compounds in the oil samples are larger than the elemental oxygen content (wt.%) of those oils. Therefore, an oil

which contains 7% oxygenated compounds is likely to contain less than 7 wt.% oxygen.

The oils derived from the pyrolysis of polyolefin and biomass mixtures contained a greater proportion of oxygenated compounds than the individual plastics and also higher levels than might be expected from calculations of mixed pyrolysis oils however at ~10-12% they were much lower than the 37.3% oxygenated compounds identified in the individual biomass sample.

The oxygenated content for biomass and PET derived oils was lower than that of biomass and was lower even compared to the calculated value for the mixture (predicted from pyrolysis of individual biomass and PET samples), however the measured value, 19.7% of identified compounds is above the oils derived from the other biomass and polymer mixtures. It is relatively low considering the high oxygen content in the initial samples of both biomass and PET.

The oil derived from pyrolysis of biomass and PS produced the lowest oxygenated compound proportion with 2.1% of identified compounds containing oxygen. This is below the calculated value which was 5.0% and is considerably below the 7% level proposed by Talmadge et al. [41].

6.3.2.4   Cyclic and linear compounds

The proportion of unicyclic compounds in the product oils increased for each of the plastics during co-pyrolysis compared to individual samples apart from HDPE for which a small reduction was observed caused by an increase in bi-cyclic compounds. The two samples with the greatest increase in unicyclic compounds was LDPE and PS which increased by 15% and 5% respectively and produced values higher than those calculated from the individual samples. Whilst this represents a small improvement for fuel use these cyclic compound proportions are far more similar to the oils derived from the individual plastic samples rather than the biomass samples which is unsurprising considering the greater oil yield per gram of sample for the plastics than for the biomass. This effect is particularly large in the case of PS where almost 90 wt.% of the original sample becomes oil compared to approximately 14 wt.% for the biomass.

6.3.3 Temperature programmed oxidation for analysis of coke deposition of ZSM-5 used during individual and co-pyrolysis

Table 6.6 gives the TPO results for the catalyst used during pyrolysis and co-pyrolysis of biomass and plastics. Pyrolysis of PET produced the greatest

coke deposition at 5.5 wt.% which is higher than any of the values determined during the TPO of catalysts used with biomass. The highest value obtained during metal impregnated catalysis was 4.7 wt.%, determined for 5%-Fe and 5%-Mg impregnated ZSM-5. The lowest was obtained for cobalt at 1.7 wt.% which was slightly over half that obtained for biomass with unmodified ZSM-5. In this case the PS and HDPE both produced lower coke deposition than biomass with HDPE deposition at only 1.1 wt.%. When co-pyrolysis was used the coke deposition was slightly above the mean result from the individual biomass and plastic samples for HDPE and PS. For PET which had the largest coke deposition the coke deposition was lower than the mean value of individually pyrolysed biomass and PET. The results for the catalysts used during co-pyrolysis are between 2.5 wt.% and 2.8 wt.% which is around what might be expected from the pyrolysis of individual samples.

Table 6.6: TPO results for the catalysts which were used during pyrolysis and co-pyrolysis of biomass and plastics.

Sample	Catalyst	Temp 1st Δ (°C)	1st Δ (wt.%)	Temp 2nd Δ (°C)	2nd Δ (wt.%)	Total Δ (wt.%)
BMS	Sand	-	-	-	-	-0.2
BMS	ZSM-5	20-300	0.8	400-800	2.3	3.1
PS	ZSM-5	-	-	400-800	1.9	1.9
HDPE	ZSM-5	20-300	1.0	400-800	0.2	1.1
PET	ZSM-5	20-300	2.0	400-800	3.5	5.5
BMS / PS (1:1)	ZSM-5	20-300	1.1	400-800	1.7	2.8
BMS / HDPE (1:1)	ZSM-5	20-300	1.3	400-800	1.2	2.5
BMS / PET (1:1)	ZSM-5	20-300	1.0	400-800	1.6	2.7

Biomass

x20K

PS

x20K

PET
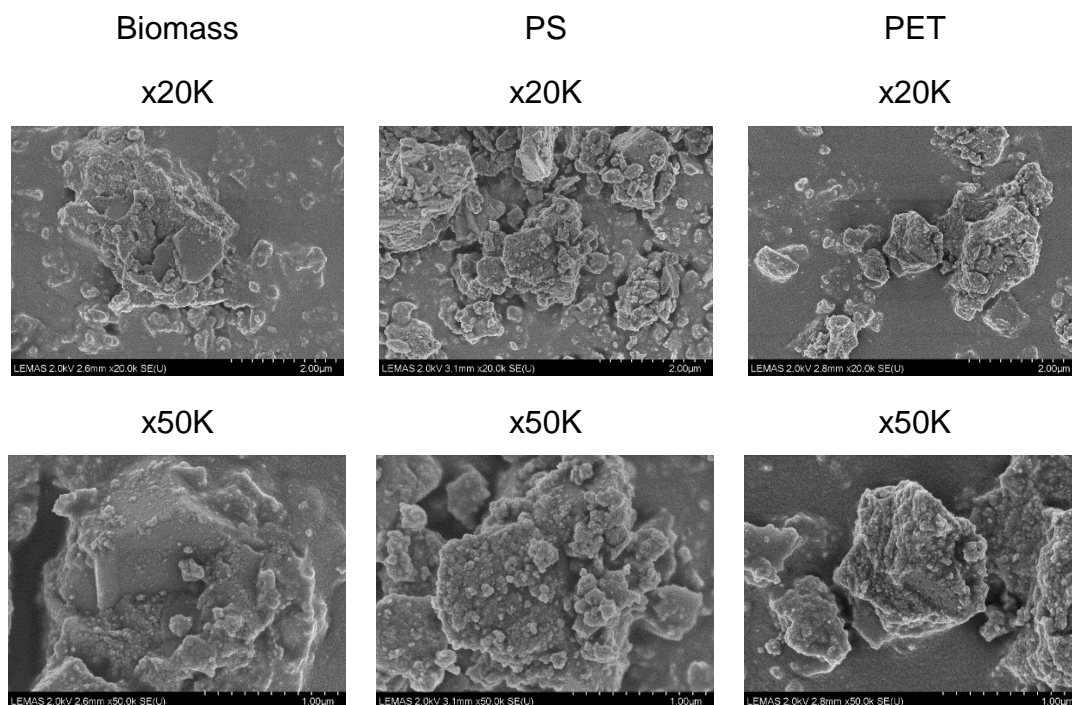
x20K

x50K

x50K

x50K

Figure 6.9: SEM imaging of char on surface of ZSM-5 after pyrolysis of individual samples at 20,000 (x20K) and 50,000 (x50K) magnification.

Biomass / PS

x20K

Biomass / PET
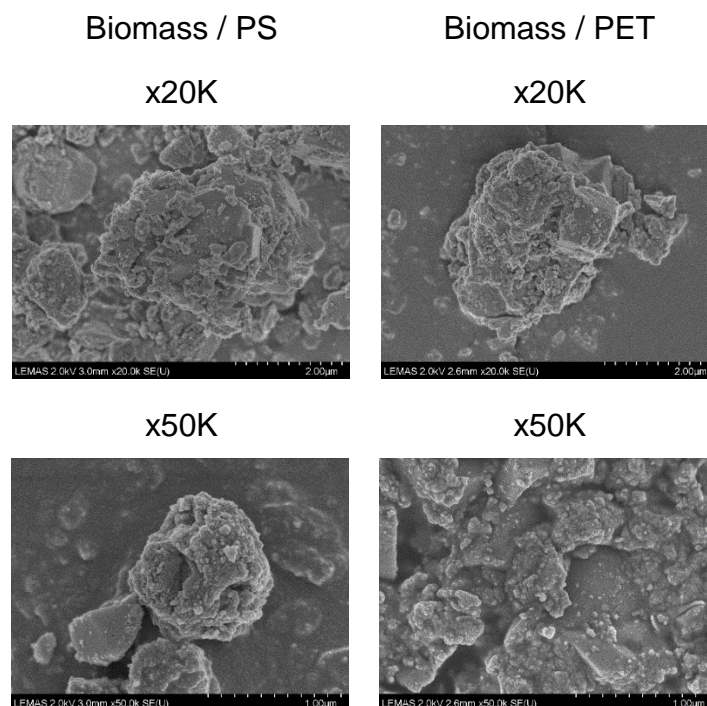
x20K

x50K

x50K

Figure 6.10: SEM imaging of char on surface of ZSM-5 after co-pyrolysis of samples at 20,000 (x20K) and 50,000 (x50K) magnification.

Figure 6.9 shows the coke deposition on the surface of ZSM-5 catalyst using SEM imaging. The hexagonal / angular material with a porous surface is the

ZSM-5 catalyst onto the surface of which is significant coke deposition. For all the samples there is inconsistent coke deposition with regions which are relatively free of coke and other regions which are heavily deposited. The SEM imaging only allows for the external coke deposition, so this technique can not give a clear understanding of internal coke deposition. The coke deposition is relatively consistent in appearance across the samples although the deposition is slightly different on the biomass sample. On the catalyst from the biomass sample the coke appears to be amorphous and composed of fine particles which have merged and clumped together into layers. Whereas, in the plastic samples the coke has formed into great numbers of small nodules. In comparison to the TPO results, there does appear to be a significant decrease in coke coverage for the co-pyrolysis catalyst in the case of PET, however this is not easily quantified using this technique. The coke deposition for co-pyrolysis of biomass and PS appears to be flakier in appearance than for the individual samples. This may be due to flattening of the nodules or just a coating of these nodules with the fine coke particles observed with the biomass sample.

6.4 Co-pyrolysis of biomass and HDPE with different mixing ratios

The mixing ratio for biomass and plastic may contribute to differences in the yields and composition of co-pyrolysis products. It is valuable to be able to understand whether effects from co-pyrolysis are due to bulk mixing of plastic pyrolysis oil with bio-oil, or whether the plastic is able to react with the bio-oils in a way that increases the yield and quality of the oil. The results may also be important for designing co-pyrolysis reactors and being able to control or optimise certain products. The polyolefin samples have given relatively consistent results so for these experiments HDPE was used to represent the polyolefin samples [91]. HDPE was chosen, rather than PP or LDPE, because it is a large constituent of municipal solid waste which is routinely collected and separated for recycling (unlike PP) [274]; and in this case is a recycled material (unlike LDPE).

6.4.1 Pyrolysis yields for Co-pyrolysis of biomass and HDPE with different mixing ratios

Table 6.7 gives the pyrolysis product yields which were determined from catalytic co-pyrolysis of biomass and HDPE at 500°C with ZSM-5 catalyst at different mixing ratios (1:1,4:1 and 9:1).

Table 6.7: Pyrolysis yields for catalytic co-pyrolysis of biomass and HDPE at different mixing ratios. Calculated mixing values in brackets.

	Char (wt.%)	Liquid (wt.%)	Gas (wt.%)	Water (wt.%)	Oil (wt.%)	Mass balance (wt.%)
BMS:HDPE (9:1)	23.0 (23.7)	51.5 (50.8)	29.0 (28.1)	31.9 (32.0)	19.6 (17.9)	100.1
BMS:HDPE (4:1)	21.1 (21.8)	48.7 (52.3)	33.7 (29.1)	25.2 (29.6)	23.6 (21.9)	99.6
BMS:HDPE (1:1)	15.5 (16.1)	55.0 (56.8)	32.5 (32.2)	30.3 (22.4)	24.7 (33.9)	103.3
BMS	25.1	48.3	25.6	34.4	13.9	101.4
HDPE	6.6	64.3	37.2	10.4	53.9	98

The predicted yields which were calculated from pyrolysis of individual samples show that the char content should decrease as the proportion of plastic increases. The results from the experiments show that this does happen with predicted results and measured results within 1 wt.% although char content was marginally lower than predicted for each result.

The gas yield was predicted to increase as the proportion of HDPE in the sample increased which is unsurprising considering the high hydrocarbon gas yield during HDPE pyrolysis. This trend is observed for the mixing ratio 9:1 and 1:1, however, the result for 4:1 is higher than predicted by ~5 wt.%.

The liquid yield is predicted to increase as the proportion of plastic in the mixture increases as with the gas yield and this is observed when changing between the mixing ratio from 9:1 to 1:1, but there is a complication in that the liquid yield reduced in the 4:1 mixing ratio. Table 6.7 shows the proportions of oil and liquid for the three mixtures and it is clear that the oil yield increases as the proportion of plastic increases yet the effect is not the same for the water yield. The water yield for the mixing ratio 4:1 is reduced compared to the other two measurements which might mean that the oil would contain a greater proportion of oxygen since less oxygen was removed through hydrodeoxygenation. However, the gas yields also need to be considered.
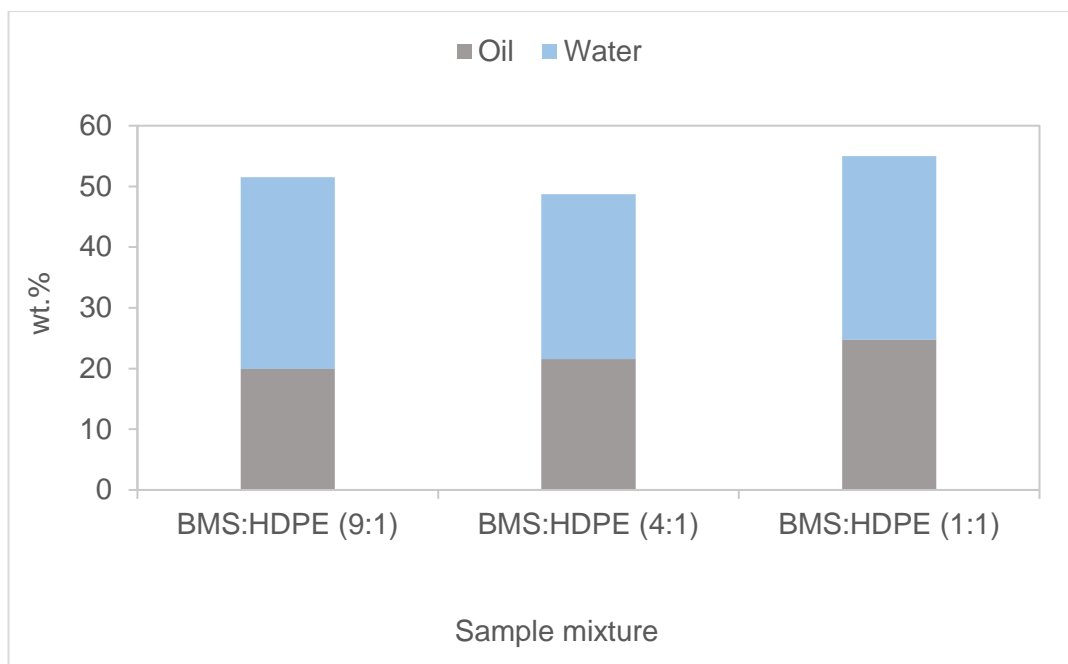
Figure 6.11: Liquid yield from catalytic co-pyrolysis of biomass with HDPE at various mixing ratios.

Figure 6.12 shows the composition of the gases which were produced during co-pyrolysis of the biomass and HDPE at different mixing ratios. As the proportion of plastic increases (from 9:1-1:1), the proportion of hydrocarbon gases increases, and the proportion of carbon oxides decreases. If the specific values of the gas composition is examined in detail a more complex picture emerges. At a mixing ratio of 1:1, the amount of hydrocarbon gases is ~6% higher than would be expected from calculations. The carbon monoxide peak is ~12% lower and carbon dioxide is ~10% lower. So, although the gas yield as a mass is as expected there has been a shift in the composition with an increase in hydrocarbon gases and a significant decrease in carbon oxides. This is likely to result in an oil which has more oxygen present than predicted from individual samples as less oxygen is removed through carbonylation or carboxylation.

At 4:1, the hydrocarbon gases are reduced ~16%, carbon monoxide reduced ~5% and carbon dioxide increased ~11%. At this mixing ratio the hydrocarbon gases have increased further, however, unlike at 1:1, the component of oxygen removing gases has increased. Although, carbon monoxide decreased, carbon dioxide increased a greater amount and removes two oxygen atoms for each removed by carbon monoxide.

At 9:1, the hydrocarbon gases increase ~16%, carbon monoxide decreased by ~7% and carbon dioxide increased by ~6%. This constitutes an increase in oxygen removing gases although not as large as for the 4:1 mixture ratio

although as was observed previously less water was produced during pyrolysis of the 4:1 mixture so the deoxygenation potential of the two mixtures, 4:1 and 9:1, are potentially similar. This indicates that the pyrolysis oil which is produced should contain more oxygen than predicted from individual samples, for the 1:1 mixture but less for both the 4:1 and 9:1 mixtures.
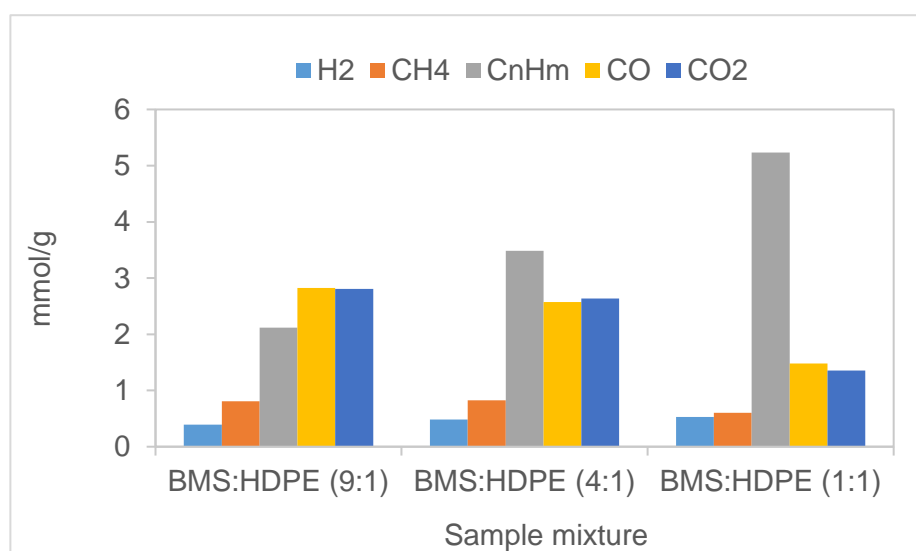
Figure 6.12: The composition of the gas collected during catalytic co-pyrolysis of biomass with HDPE at different mixing ratios.

6.4.2 Oil composition for co-pyrolysis of biomass with HDPE at various mixing ratios

Both the composition of the oils and the yield are important considerations for optimising the process towards gasoline range fuels or chemical feedstock and these two criteria are linked. Changing the composition of the oil will often results in measurable changes to the yields of pyrolysis products. Although this may not be the case where changes are confined to a particular product type, i.e. conversion of primary aromatic compounds into PAH compounds. This would leave the oil yield unaffected, but additional hydrogen gas might be detected.

Table 6.8: Proportion of compounds in catalytic (ZSM-5) co-pyrolysis oil which were aromatic, oxygenated, cyclic or in the gasoline fuel range (C_5-C_{12}), with different mixtures of biomass and HDPE. Calculated values for mixtures in brackets.

	BMS:HDPE (9:1)	BMS:HDPE (4:1)	BMS:HDPE (1:1)
Aromatic (%)	88.5 (81.4)	77.6 (69.6)	42.1 (50.4)
Aliphatic (%)	11.5 (18.6)	22.4 (30.4)	57.9 (49.6)
Oxygenated (%)	15.2 (26.7)	11.6 (19.8)	11.7 (8.5)
Non-oxygenated (%)	84.8 (73.3)	88.4 (80.2)	88.3 (91.5)
C_5-C_{12} (%)	88.7 (85.1)	85.8 (77.2)	51.8 (64.4)
≥C_{13} (%)	11.3 (14.9)	14.2 (22.8)	48.2 (35.6)
Uni-cyclic (%)	72.0 (68.4)	66.8 (62.9)	40.4 (51.1)
Bi-cyclic (%)	15.8 (9.5)	10.7 (7.6)	1.7 (3.3)
Tri-cyclic (%)	0.7 (1.8)	0.0 (1.4)	0.0 (0.6)
Quad-cyclic (%)	0.0 (0.1)	0.0 (0.1)	0.0 (0.0)
Linear (%)	11.5 (20.2)	22.4 (28.0)	57.9 (45.9)

Table 6.8 shows the proportions of compounds which were identified using GC-MS and the compound type to which these belong. The proportion of compounds, belonging to each category has been predicted, through calculations from product yield and composition of individual samples, and is included in brackets.

The proportion of aromatic compounds in the oil decreases as the proportion of HDPE increases which is understandable considering that biomass contains aromatic rings in the lignin component and HDPE contains no aromatic rings naturally. However, this reduction in aromatic rings is greater than was predicted through calculations, with more (~7%) aromatic than expected at a mixing ratio of 9:1 and less (~13%) at a mixing ratio of 1:1. If we examine the cause of this reduction by interpreting the data for molecular size in Table 6.8, we discover that the proportion of long chain hydrocarbons (≥C_{13}) has

increased and with aromatics reduced (primary aromatics ~4%, phenolics ~10%). There was an increase of hydrocarbon gases of ~12% which indicates that cracking reactions have increased, however, this cracking appears to have mainly affected the biomass sample and its aromatic compounds rather than the LDPE linear hydrocarbons where cracking has been reduced. Potentially, the radicals from the HDPE sample are assisting with the cracking of the biomass, lignin aromatics, whilst coke deposition on the catalyst is then hindering catalytic cracking of the HDPE compounds which are volatilised at a higher temperature.

This effect is not observed in the mixtures where biomass is a higher proportion of the sample. Where biomass is the dominant fraction of the sample the linear proportion is largely diminished and the unicyclic proportion is increased. There is again a more complex situation here than mere bulk mixing. The proportion of linear compounds for 9:1 and 4:1 is lower than that predicted and the unicyclic and bicyclic are larger than expected. The reduction in linear aliphatics may be attributed to an increase in thermal or catalytic cracking, producing an increase in short chain hydrocarbon gases (C_2-C_4), however, this would not account for the increase in unicyclic compounds which was also observed in the pyrolysis oils.

 The increase in unicyclic compounds is mainly observed as an increase in primary aromatic compounds which in the 9:1 and 4:1 mixtures are ~14% higher than expected. Phenolics compounds in contrast reduce by ~9% and ~5% respectively. Therefore, at these mixing ratios, where biomass is the dominant proportion of the sample, reactions are taking place which convert linear hydrocarbons into primary aromatic compounds. Linear hydrocarbons are also being increasingly removed through cracking.

There is a third effect, which is regarding to oxygenated compounds. It can be observed that phenolic compounds are lower than expected for the biomass dominant mixing ratios (9:1 and 4:1) and higher than expected for the 1:1 mixing ratio. The overall effect is that the proportion of oxygenated compounds reduces significantly in the biomass dominant mixtures which is exactly the same trend that was expected from the gas and water analysis which showed an increased oxygen removal for 9:1 and 4:1 and a reduced oxygen removal in 1:1. The overall effect of this is that whilst oxygen content reduces from 9:1 to 4:1, it remains unchanged as the mixture progresses to a 1:1 ratio. Figure 6.13 shows that over this same change in sample composition, the composition of the oils are significantly altered with a reduction in primary aromatics from 9:1 to 1:1 and the reverse effect observed in aliphatic compound yields. The fuel

range proportion is much improved for the 9:1 and 4:1 mixtures than the 1:1 mixture.
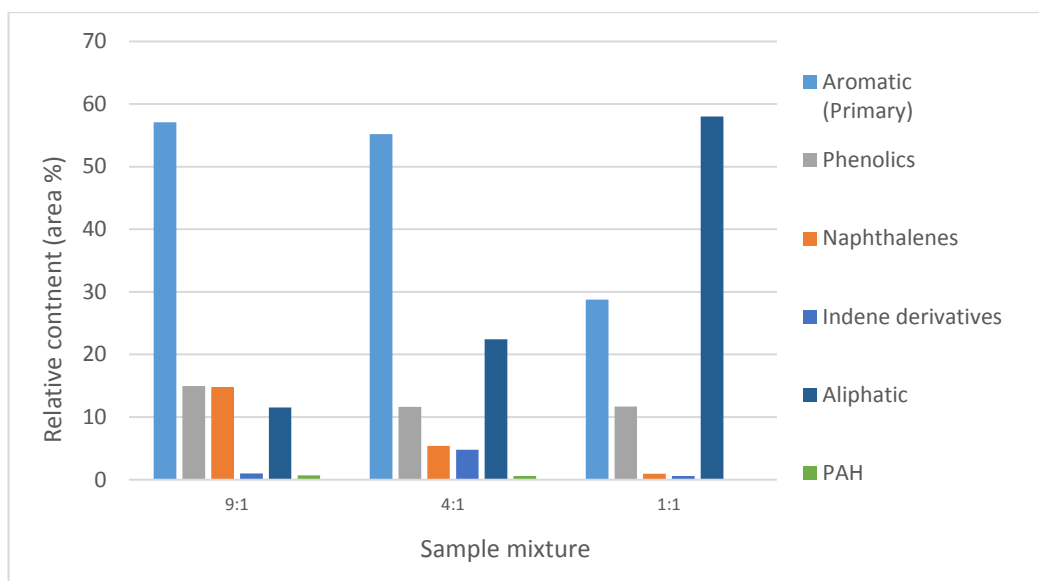
Figure 6.13: Oil composition categorised by compound type for catalytic co-pyrolysis of biomass with biomass and HDPE at different mixing ratios.

These trends taken collectively would suggest that 4:1 is the optimal mixture ratio for biomass and HDPE from the three mixtures analysed as it produces the joint lowest oxygen content whilst maintaining high primary aromatic and gasoline fuel range compounds. 4:1 was also only slightly lower than 1:1 in terms of oil yield.

6.5 Co-pyrolysis of biomass and PET with different mixing ratios

6.5.1 Pyrolysis yields for co-pyrolysis of biomass and PET with different mixing ratios

Table 6.9 gives the yields of products from catalytic co-pyrolysis of biomass and PET at 500°C with ZSM-5 catalyst. The three mixing ratios were the same used for HDPE at 9:1, 4:1 and 1:1 with biomass the larger proportion in the case of 9:1 and 4:1.

As the plastic content of the mixture increases the amount of char increased which was expected as the PET contained a reinforcement material. However, the increase is above the predicted values suggesting that the combination of the biomass and PET leads to an increased char deposition.

The gas yield decreased as the plastic increases which also follows the expected values from the individual biomass and PET samples although again at 1:1 there is a deviation from the predicted values with the gas yield below that expected.

Table 6.9: Pyrolysis yields for catalytic co-pyrolysis of biomass and PET at different mixing ratios. Calculated mixing values in brackets.

	Char (wt.%)	Liquid (wt.%)	Gas (wt.%)	Water (wt.%)	Oil (wt.%)	Mass balance (wt.%)
BMS:PET (9:1)	28.8 (27.0)	48.0 (48.1)	26.3 (26.8)	33.7 (32.8)	14.3 (14.5)	98.8
BMS:PET (4:1)	29.4 (28.4)	49.5 (47.0)	24.0 (26.5)	33.0 (31.2)	16.5 (15.0)	102.0
BMS:PET (1:1)	37.5 (32.6)	33.0 (43.7)	22.5 (25.7)	23.3 (26.5)	9.7 (16.7)	93.2
BMS	25.1	48.3	25.6	34.4	13.9	101.4
PET	39.6	38.1	24.4	18.6	19.5	98.3

The results for the liquid yield are complicated with a decrease between mixture ratios of 9:1 and 1:1 which is as predicted but the scale of the change is greater. The value for 4:1 is higher than was expected and is above even the value for 9:1. The water content decreases as the plastic proportion increases whereas the oil content is predicted to increase which explains the liquid yield variation. The liquid yield is composed of two fractions, one which increases and one which decreases as the mixture of plastic changes. The difference in scale of these changes accounts for the lack of clear trend in the liquid yield. Another remarkable result is the particularly low oil yield and mass balance for PET and BMS as 1:1 mixing ratio. This is partially due to deposition of terephthalic acid derivatives onto the top-plate of the reactor and thermocouples during the pyrolysis experiment, this presented as a white waxy deposit. In a repeated experiment using DCM as a solvent this part of the reactor was weighed pre and post pyrolysis and a larger oil yield (10.6 wt.%) and mass balance (100.3 wt.%) were determined. The increase in char yield may also be due to deposition of terephthalic acid directly onto the biomass char material and sample basket. It is clear from Figure 6.14 that there is no obvious trend across the mixtures.
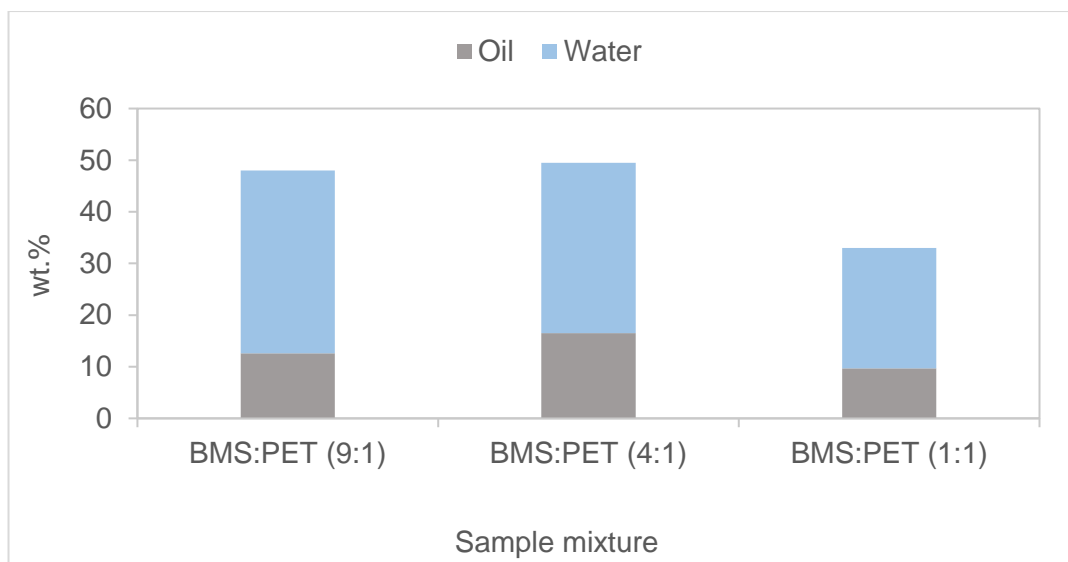
Figure 6.14: Percentage of liquid yield which is composed of water for co-pyrolysis of biomass with PET at various mixing ratios.
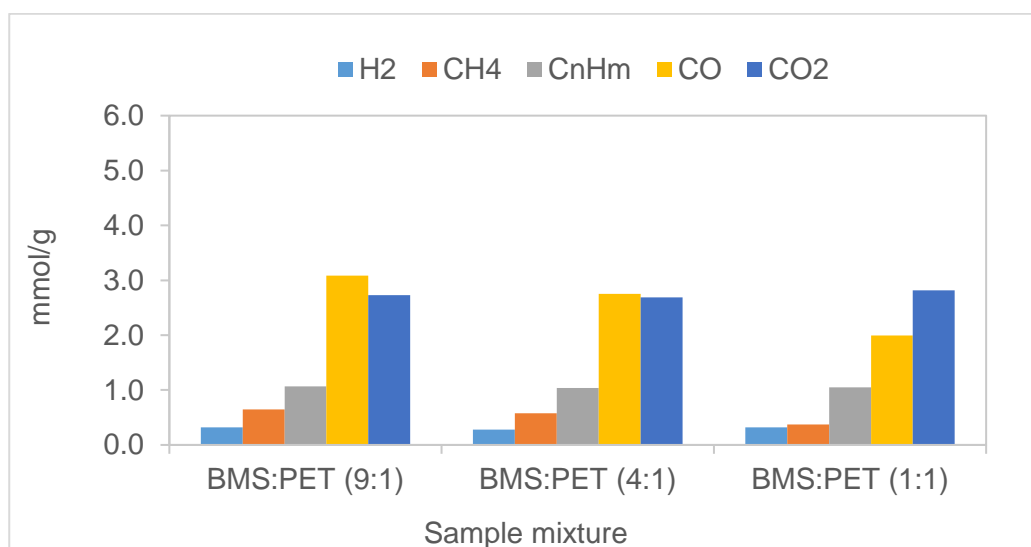
Figure 6.15: The composition of the gas collected during catalytic co-pyrolysis of biomass with PET at different mixing ratios.

Figure 6.15 gives the gas yields during pyrolysis and there is a clear shift from a gas mixture which appears similar to that for biomass towards one that is more similar to PET. The main feature of this is an increase in proportion of carbon dioxide to carbon monoxide. The hydrocarbon gases were expected to increase as the plastic fraction increased however this was not observed. The hydrocarbon gas content in the 1:1 mixture is ~20% lower than expected to be. There is no clear increase in carbon oxide gases for any of the mixtures.

6.5.2 Oil composition for co-pyrolysis of biomass with PET at various mixing ratios

Table 6.10: Proportion of compounds in catalytic (ZSM-5) co-pyrolysis oil which were aromatic, oxygenated, cyclic or in the gasoline fuel range (C_5-C_{12}), with different mixtures of biomass and PET. Calculated values for mixtures in brackets.

	BMS:PET (9:1)	BMS:PET (4:1)	BMS:PET (1:1)
Aromatic (%)	98.2 (99.5)	98.4 (99.5)	100.0 (99.7)
Aliphatic (%)	1.8 (0.5)	1.6 (0.5)	0.0 (0.3)
Oxygenated (%)	18.0 (34.0)	24.6 (30.9)	19.7 (22.5)
Non-oxygenated (%)	82.0 (66.0)	75.4 (69.1)	80.3 (77.5)
C_5-C_{12} (%)	97.5 (97.1)	95.3 (97.0)	89.2 (96.8)
$\geq C_{13}$ (%)	2.5 (2.9)	4.7 (3.0)	10.8 (3.2)
Uni-cyclic (%)	70.8 (80.1)	67.5 (77.6)	65.7 (70.8)
Bi-cyclic (%)	27.7 (16.9)	30.1 (19.4)	27.1 (25.9)
Tri-cyclic (%)	1.5 (2.8)	2.4 (2.9)	7.1 (3.1)
Quad-cyclic (%)	0.0 (0.1)	0.0 (0.1)	0.1 (0.1)
Linear (%)	0.0 (0.0)	0.0 (0.0)	0.0 (0.0)

Table 6.10 shows the types of compounds which were identified in the oils from co-pyrolysis of biomass and PET. The oil which was produced for each of the mixtures was almost entirely composed of aromatic compounds with a large proportion of the compounds belonging to the gasoline fuel range in terms of compound size. The aromatic proportion increased marginally as the proportion of PET increased and the fuel range proportion decreased a small amount although this was slightly below expectation for the 1:1 mixture where a larger than expected yield of tri-cyclic PAH compounds was produced. Figure 6.16 shows the types of aromatic compound which were found in the oil and whilst

each of the oils is relatively similar the proportion of primary aromatic compounds is largest for the 1:1 mixture. However, the oil yield was smallest for the 1:1 mixture. All three of the mixtures contain a reduced unicyclic content compared to calculations with increased bicyclic compounds, mainly naphthalenes. This effect is largest for the samples with lower PET content.
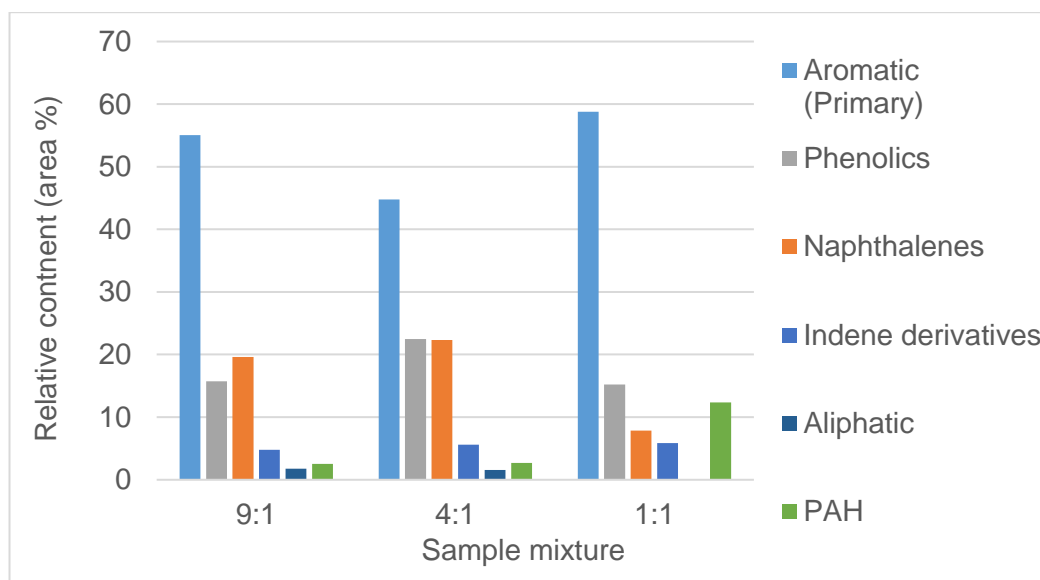
Figure 6.16: Oil composition categorised by compound type for catalytic co-pyrolysis of biomass with biomass and PET at different mixing ratios.

The proportion of oxygen containing compounds in the three oil samples whilst relatively large, appears to be far lower than the predicted values, particularly with the 4:1 and 9:1 mixing ratios. However, these values mask an important consideration. In the 1:1 mixture, 0.5% of the identified compounds was terephthalic acid; in the 4:1 mixture, 1.1% was terephthalic acid and 1.6% levoglucosan; in the 9:1 mixture 1.5% was terephthalic acid and 1.8% levoglucosan. Terephthalic acid contains atoms of oxygen for each molecule and levoglucosan contains 5 oxygen atoms for each molecule. Therefore, whilst it might appear as though the oxygen content is decreasing as the plastic content decreases, there is a large increase in two compounds which contain a very large amount of oxygen. Whereas a molecule of phenol contains 17 wt.% oxygen, a molecule of terephthalic acid and levoglucosan contain 33 wt.% and 49 wt.% oxygen respectively.

6.6 Co-pyrolysis of biomass and PS with different mixing ratios

6.6.1 Pyrolysis yields for Co-pyrolysis of biomass and PS with different mixing ratios

The yields resulting from catalytic pyrolysis of biomass and PS at 500°C is contained in Table 6.11. In contrast to PET and HDPE, there appear to be clear trends in the yields of char, liquid and gas. Figure 6.17 shows clearly that as the proportion of PS in the sample increases from 10 wt% through to 50 wt.%, the char decreases, the gas decreases and the liquid yield increases. The yield of char is greater than what was predicted in each mixture and particularly in the 1:1 mixture. The gas yield is greater than predicted for both the extreme mixtures (1:1 and 9:1) but at 4:1 is below the expected value. The converse effect is observed in the liquid yield with lower liquid yields at the extreme values and an increased liquid value at 4:1 where gas yield was reduced. This indicates that to some extent that in the 4:1 mixture, volatile compounds are being converted to molecules which are gaseous at ambient temperatures and pressures, thus resulting in a lower liquid yield.

Table 6.11: Pyrolysis yields for catalytic co-pyrolysis of biomass and PS at different mixing ratios. Calculated mixing values in brackets.

	Char (wt.%)	Liquid (wt.%)	Gas (wt.%)	Water (wt.%)	Oil (wt.%)	Mass balance (wt.%)
BMS:PS (9:1)	24.5 (23.2)	52.6 (53.8)	28.6 (25.2)	38.5 (31.6)	14.0 (21.4)	98.2
BMS:PS (4:1)	21.9 (20.8)	59.3 (58.4)	22.2 (23.3)	34.0 (28.8)	25.3 (28.8)	100.7
BMS:PS (1:1)	16.0 (13.6)	65.0 (72.1)	18.5 (17.6)	17.4 (20.1)	47.6 (47.3)	98.2
BMS	25.1	48.3	25.6	34.4	13.9	101.4
PS	1.4	86.4	8.2	6.4	88.5	97.5

Figure 6.18 shows the proportion of this liquid yield, which is composed of water and oil. As the plastic content increases there is a clear decrease water content and a clear increase in oil content. This is not unexpected as the biomass sample produced a low yield of oil and high yield of water and the PS sample had the opposite characteristics.
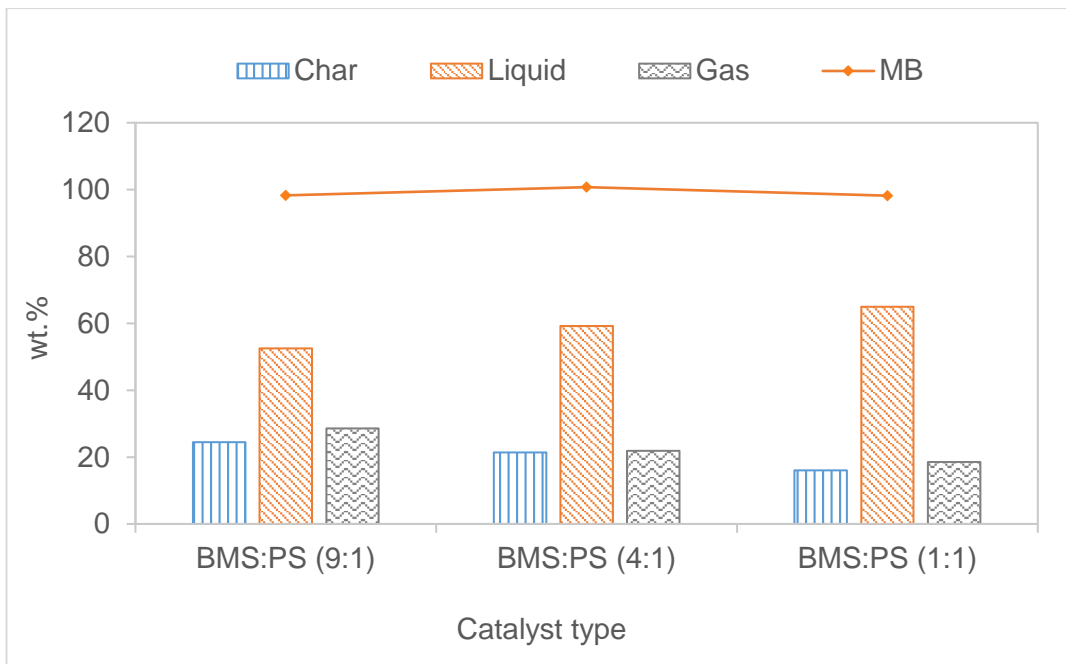
Figure 6.17: Pyrolysis yields and mass balance for biomass and PS at various mixing ratios.
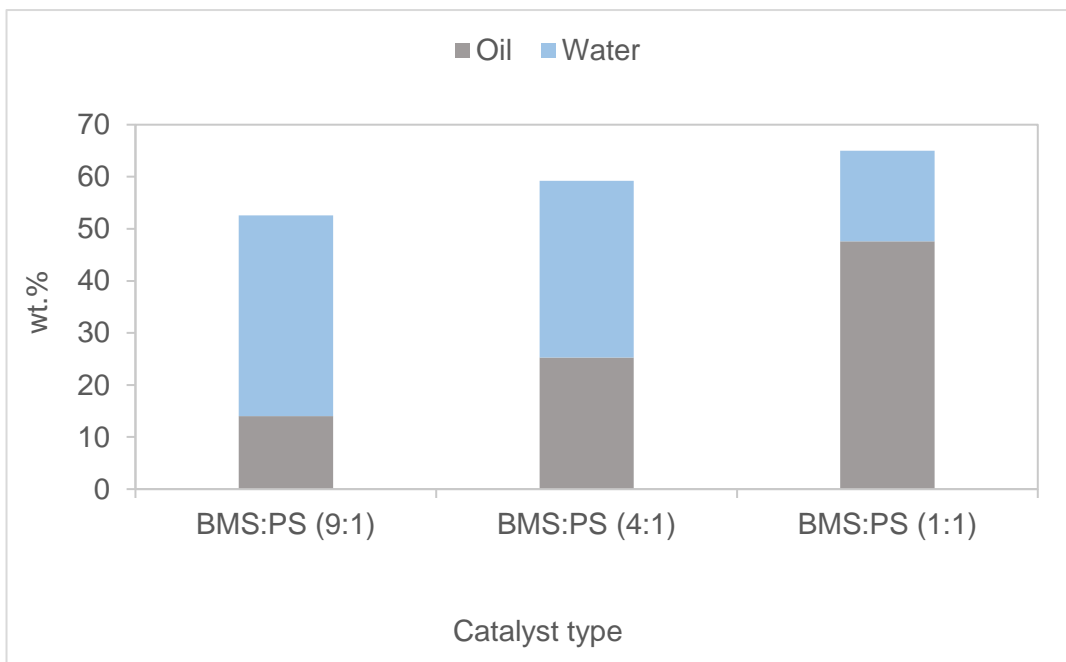
Figure 6.18: Percentage of liquid yield which is composed of water for co-pyrolysis of biomass with PS at various mixing ratios.
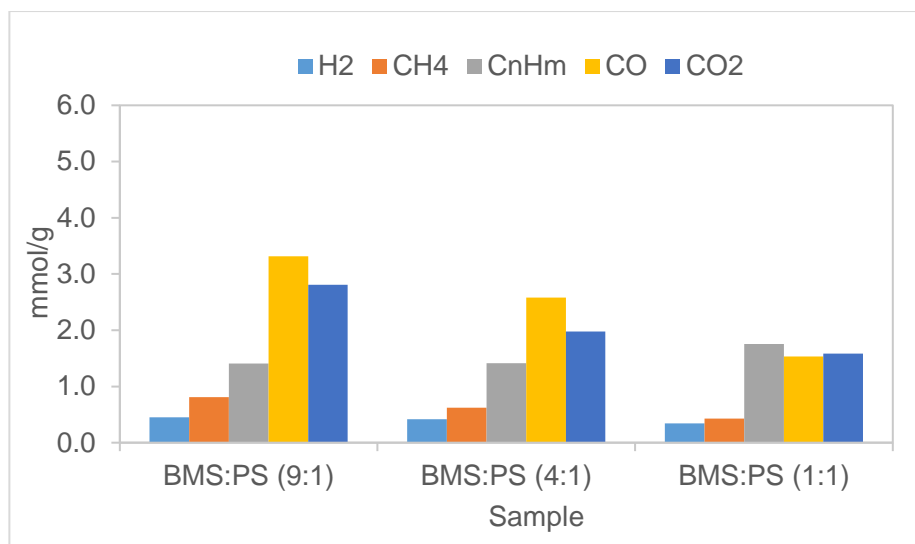
Figure 6.19: The composition of the gas collected during co-pyrolysis of biomass with PS (without nitrogen) at different mixing ratios.

The hydrogen yield increases as the proportion of biomass increases. At the 1:1 mixing ratio it is below the predicted value by ~12%, at 4:1 it is above the predicted value by ~19% and at 9:1 it is above by ~27%. This is interesting as it will be seen in the composition that the aromatic yield is expected to decrease as the biomass proportion increases, yet instead it increases. Talmadge et al. [41] explain that formation of aromatic compounds releases hydrogen and as the aromatic content increases above expectation, so the hydrogen gas content also increases above expectation. There are also significant increases in hydrocarbon gas yields (C_2-C_4) above those predicted for each of the mixtures by an increasing amount as the biomass proportion increases with increases of ~17%, ~18% and ~28% for 1:1. 4:1 and 9:1 respectively. The yield of hydrocarbon gases increases in the reverse manner with the mixture with greatest plastic content giving the highest yield. The oxygen containing gases are key to the removal of oxygen and it is observed that they increase as the biomass proportion of the mixture increases.

In the gases there is a small increase in deoxygenation for the 1:1 mixture with carbon monoxide decreasing by 9% and carbon dioxide, with twice the oxygen content, increasing by 9%. For this sample the water content decreased slightly such that deoxygenation was reduced through hydrodeoxygenation and carbonylation but increased through carboxylation.

In the 4:1 mixture there was a decrease in deoxygenation gases with carbon monoxide and carbon dioxide decreasing by 4% and 16% respectively, however in this case the water yield increased. In the 9:1 mixture both carbon

oxides increased, and water content also increased. This indicates that this sample is likely to have the largest reduction in oxygen content with hydrodeoxygenation, carbonylation and carboxylation all contributing to removal of oxygen from the oil.

6.6.2 Oil composition for co-pyrolysis of biomass with PS at various mixing ratios

The oil yield in the 1:1 mixture was equivalent to predicted values, however gas and water analysis suggests only limited deoxygenation. The oil yield at 4:1 was lower than predicted but although deoxygenation gases decreased the water yield increased by ~18% such that a small decrease or increase in deoxygenation could be possible. The oil yield at 9:1 was severely diminished from predicted values however the gas and water analysis indicate significant deoxygenation.

Table 6.12: Proportion of compounds in catalytic (ZSM-5) co-pyrolysis oil which were aromatic, oxygenated, cyclic or in the gasoline fuel range (C_5-C_{12}), with different mixtures of biomass and PS. Calculated values for mixtures in brackets.

	BMS:PS (9:1)	BMS:PS (4:1)	BMS:PS (1:1)
Aromatic (%)	100.0 (99.6)	100.0 (99.8)	95.6 (99.9)
Aliphatic (%)	0.0 (0.4)	0.0 (0.2)	4.4 (0.1)
Oxygenated (%)	16.9 (22.4)	12.6 (14.9)	2.1 (5.3)
Non-oxygenated (%)	83.1 (77.5	87.4 (85.1)	97.9 (94.7)
C_5-C_{12} (%)	91.2 (88.8)	82.9 (84.6)	75.7 (79.3)
$\geq C_{13}$ (%)	8.8 (11.2)	17.1 (15.4)	24.3 (20.7)
Uni-cyclic (%)	78.5 (72.5)	64.6 (67.3)	62.2 (60.7)
Bi-cyclic (%)	19.7 (21.4)	27.2 (25.0)	24.6 (29.5)
Tri-cyclic (%)	1.4 (3.8)	6.5 (4.4)	6.1 (5.1)
Quad-cyclic (%)	0.5 (2.2)	1.7 (3.3)	2.8 (4.7)
Linear (%)	0.0 (0.0)	0.0 (0.0)	4.4 (0.0)

The oil yield increased as the proportion of plastic in the mixture also increased and there are clear patterns which are evident in the oil composition. The aromatic ring containing compounds, oxygen containing compounds, gasoline fuel range compounds and unicyclic compounds which were identified all decreased as the plastic content increased.

In terms of the aromatic compounds there is a small reduction which was not predicted through calculations with a small quality of aliphatic compounds present in the pyrolysis oil in the 1:1 mixture. The major issue with the 1:1 mixture is the increased PAH content at almost 22% of compounds identified however, although unicyclic compounds decreased the proportion of primary aromatics remains high with very few phenolics identified. As the proportion of biomass in the mixture increases there are fewer PAH compounds but increased proportions of phenolic compounds.
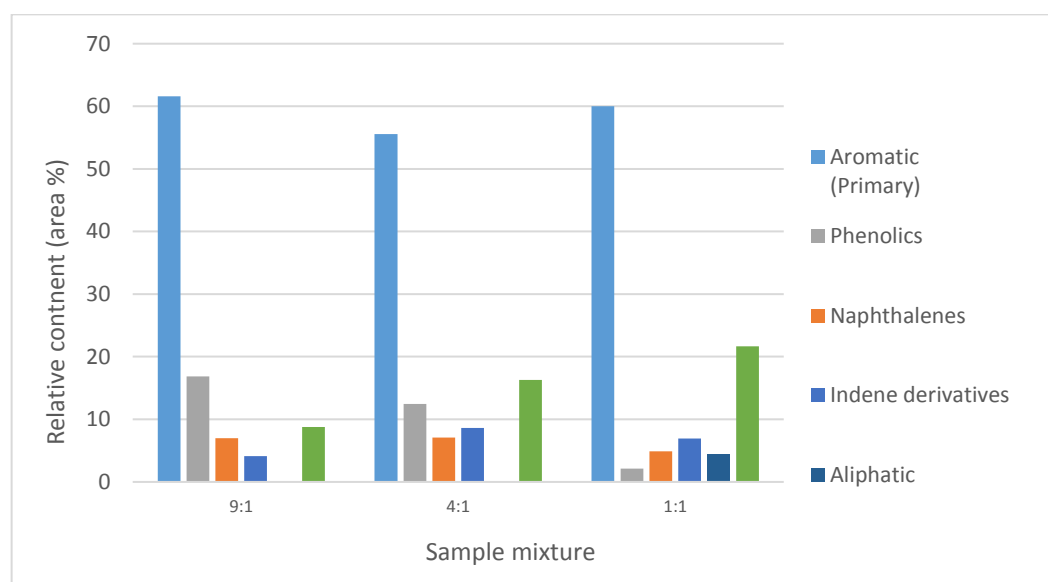
Figure 6.20: Oil composition categorised by compound type for catalytic co-pyrolysis of biomass with biomass and PS at different mixing ratios.

The oxygenated compounds in Table 6.12 show similar results to those predicted from the deoxygenation products. There is a reduction in oxygen content for all three mixtures and this is particularly high for the 9:1 mixture which had both the largest decrease in oil yield and increase in deoxygenated products. However, although there is a larger reduction compared to predicted values for the 9:1 mixture, there is still a relatively high proportion of oxygenated compounds at 16.9%. The 1:1 mixture is less effective at removing oxygen but there is also a much higher oil yield due to the increased PS content of the

blend and it might be more effective to process this oil and remove the PAH compounds if possible rather than reducing the 9:1 oil by deoxygenating and also reducing the PAH.

6.7 Chapter summary

Catalytic co-pyrolysis of biomass and plastics has been proposed as a methodology for producing upgraded pyrolysis oils [115, 161-165, 275]. The main pathways by which this upgrading is achieved is through deoxygenation and through formation of monoaromatic compounds. These products are valuable for their utilisation as a chemical feedstock with high quantities of these compounds produced and consumed each year and they are also important for the production of fuels. One of the major reaction pathways proposed for deoxygenation and aromatic formation involves reaction of furan compounds derived from cellulose with alkenes derived from plastics to produce monoaromatic compounds such as xylene with the oxygen removed as water via a Diels-Alder mechanism (see figure 2.29) [276]. Other pathways involving reactions of styrene with allene to produce indenes which can then be converted into naphthalene compounds through alkylation are possible when polystyrene is used as the co-feed plastic [115, 170].

The co-pyrolysis of biomass with the polyolefins (1:1) produced a small increase in the proportion of oxygenated compounds compared to calculations for individual biomass and plastic although this produced a reduction in the oxygen content compared to the pyrolysis oils from biomass alone. However, experiments using different mixing ratios of HDPE found that by reducing the mixing ratio of the polymer from 1:1 through to 9:1 the deoxygenation observed increased. The drawback to this approach was that the increased proportion of oxygen-rich biomass sample used increased the overall proportion of oxygen compounds slightly despite the increased oxygen removal. Using a low mixing ratio of HDPE also increased the proportion of aromatic and unicyclic compounds compared to the higher mixing ratio and optimised the oil yield as a proportion of the calculated yield. The gross oil yield was greater for the 1:1 mixing ratio though as HDPE produces more oil than the biomass per unit of mass so although the 1:1 mixture produced a lower oil yield than calculated this still resulted in a higher yield than in the low HDPE mixtures. The results at a 9:1 mixing ratio exhibit the same oil enhancement observed by Li et al. [167] with increased unicyclic aromatic formation and decreased oxygenated content.

Co-pyrolysis of biomass and PET produced poor oil yields at a 1:1 mixing ratio compared to individual pyrolysis of biomass and PET. By altering the mixing ratio to 9:1 the oil yield was improved both as a gross value and also in comparison the predicted yield. The lower mixing ratio also gave improved deoxygenation and the highest proportions of fuel range C_5-C_{12} and unicyclic compounds. The highest aromatic content was achieved in the 1:1 mixture but the reduction caused through reducing the mixing ratio was small.

Co-pyrolysis of biomass with polystyrene produce the most notable results of the plastics which were studied. The oil yield at a 1:1 mixing ratio was higher than the predicted value with the composition properties of the oils remaining largely unaltered. There was a small reduction in aromatic and fuel range compounds but there was also a reduction in the proportion of oxygenated compounds. This reduction in oxygenated compounds was relatively small at ~3% but amounted to a greater than 50% reduction in the proportion of identified oxygenated compounds. Changing the mixing ratio led to a significant reduction in oil yield as PS produces a much higher yield of oil compared to biomass for each gram of sample used but there reduction in oil yield at the 4:1 and 9:1 mixtures was greater than predicted. The proportion of oxygenated compounds increased as the proportion of polystyrene was reduced with an increase in deoxygenation. The increase in deoxygenation was not great enough, however, to remove the extra oxygen introduced by increasing the biomass in the pyrolysis sample. A benefit of reducing the proportion of polystyrene in the sample was an increase in both unicyclic and gasoline fuel range compounds although this is not large enough to compensate for the reduction in oil yield. There was also a small increase in aromatic compounds as the mixture ratio was changed from 1:1 to 9:1 and the proportion of PAH compounds was reduced in the 9:1 mixture.

6.8 Conclusion

Catalytic pyrolysis of the plastic samples (objective 5) gave very different products to those collected during pyrolysis of biomass. The liquid yields were significantly higher than those for the biomass samples and this was mainly due to the comparative low char formation during pyrolysis of the plastic samples. The liquid products from the plastics also contained a low proportion of water which is due to low moisture in the initial samples and low oxygen content in the samples allowing for limited formation of water through hydrodeoxygenation. Polystyrene gave a particularly high oil yield as a proportion of the initial sample with low char and gas yields whereas the

polyolefin samples contributed relatively high yields of gas which contained a high proportion of short chain aliphatic compounds from catalytic cracking of the longer straight chain hydrocarbons which compose the polyolefin plastics. The compounds identified in the oils from the polyolefin samples contained a high proportion of aliphatic and primary aromatic compounds which are suitable for fuel use although many of the aliphatic chain lengths are larger than the C_5-C_{12} range which is best suited for fuels. The polystyrene oils contained suitable primary aromatics as well as a high proportion of polyaromatic compounds which are unsuitable. The oil from the PET pyrolysis contained a high proportion of fuel range compounds however this was offset by a relatively low liquid/ oil yield. It is likely that deposition of terephthalic acid and benzoic acid onto the reactor contributed to this lower oil yield although formation of char and coke also appears high. Although only a limited proportion of the oxygen from the PET is apparent in the pyrolysis oils this may be partially due to the oxygen containing oil compounds derived from PET degradation being prone to polymerisation and deposition onto the reactor and catalyst. There are deoxygenation reactions occurring during catalytic pyrolysis of PET, particularly through carbon dioxide formation, however, this is not large enough to account for all of the reduction in oxygen in the oils compared to the original sample. Each of the plastics samples produces less than ideal products for oil production.

Co-pyrolysis of the biomass with the plastics has the potential to allow for reactions which might improve the characteristics of the oils from biomass whilst at the same time improving the oils from the plastic samples. Improvements to the oils were achieved merely due to mixing of the biomass and plastic oils together during co-pyrolysis. The temperature of degradation of the polyolefin samples is above that of the biomass and this is likely to explain the limited interactions observed between the two constituents during pyrolysis. This may be the reason that during co-pyrolysis of these samples there was very limited effect on the pyrolysis products which could not be explained by additive effects from mixing. This suitability of the biomass oils was improved through dilution of the oxygenated compounds using the non-oxygen containing compounds from the polyolefin samples, but this could potentially be completed through post-pyrolysis mixing as well as through co-pyrolysis. When the proportion of biomass was increased compared to that of the polyolefin a greater degree of deoxygenation was observed than calculated for additive mixing. This might indicate that interactions are taking place, potentially within the pores of the catalyst, which are not observed during bulk co-pyrolysis. In the 1:1 mixture a high proportion of the biomass volatiles are expected to have

passed through to the condensers prior to the degradation of biomass. However, during co-pyrolysis with a higher proportion of biomass than plastic, the yield of deoxygenation compounds increases as the proportion of biomass in the pyrolysis sample increased although this was not a big enough effect to counteract the increase in oxygen caused by biomass being a greater proportion of the mixture. It would be useful to examine co-pyrolysis of biomass and polyolefin samples at a higher heating rate to examine if simultaneous thermal degradation could allow for further interactions between the volatiles leading to improved deoxygenation.

Co-pyrolysis of biomass with polyethylene terephthalate gave lower oil yields than during individual pyrolysis which appears to have been caused by an increase in char and coke formation during co-pyrolysis. It is possible that the char from the biomass sample is either acting as a natural catalyst or just as an additional surface onto which the PET volatiles may become deposited. Reducing the proportion of PET to biomass gave improved oil yields and deoxygenation however any improvements were very limited and potentially just due to a lower deposition of coke onto the catalyst leading to deoxygenation reactions on the catalyst remaining more active during catalytic pyrolysis. The results for co-pyrolysis of biomass and PET do not support the suitability of producing fuel from this feedstock.

Co-pyrolysis of biomass with polystyrene gave improved deoxygenation compared to the individual samples. The high oil yield from the polystyrene compared to biomass ensured that at a 1:1 (by weight) mixing ratio the oil contained more compounds from the individually pyrolysed polystyrene than the individually pyrolysed biomass. However, there was a small increase in deoxygenation via formation of carbon oxides and a lower proportion of oxygenated compounds identified in the oil than expected in an additive mixture. As the proportion of biomass was increased this deoxygenation also increased leading to a lower content of oxygenated compounds identified compared to calculated values as the proportion of biomass in the mixture increased. Whilst the deoxygenation reactions were most effective at a higher biomass proportion this potential improvement in oil suitability is counteracted by an increased oxygen content due to a higher proportion of biomass in the sample. Therefore, the greatest improvement in oxygen content is achieved in a mixture with more biomass but the lowest proportion of oxygenated compounds identified is achieved in a mixture with more polystyrene.

These results show that by changing the mixing ratio of the co-pyrolysis feed the pyrolysis products can also be changed using additive effects with the

resulting yields reflecting the properties of the individual components of the mixture (objectives 6 & 7). However, there are also co-pyrolysis interactions (synergistic effects) which lead to deoxygenation or formation of aromatic compounds and these reactions appears to be most active at mixing ratios which contain more biomass. The resulting product yields and compositions are influenced by both factors so these need to be considered if co-pyrolysis is utilised for fuel production.

Coke deposition (objective 13) onto the ZSM-5 catalyst was particularly high in the case of PET and low for HDPE however during co-pyrolysis the coke deposition for each of the biomass and plastic mixtures appears to be approximately the same value. This coke deposition represents a slight improvement in the mixture of biomass with PET but is around midway for the mixtures of biomass with the other plastics. This indicates that co-pyrolysis of biomass with these plastics is unlikely to lead to severe enhancement or reduction of coke deposition onto the catalyst during ex-situ pyrolysis although this has not been confirmed for the metal-impregnated ZSM-5 catalysts.

Chapter 7: Catalytic co-pyrolysis of biomass and polystyrene with metal impregnated ZSM-5

7.1 Introduction

Chapter 6 examined the co-pyrolysis of biomass and PS in the two-stage, fixed-bed reactor, with the resulting oils showing potential as a pathway towards fuel production through analysis of the composition and yields of the oils. At a mixing ratio of 1:1 the major issue with the oil was a PAH content which exceeded 20% of the compounds identified in the oil. This PAH content could be reduced by using a mixture with lower plastic content, however, this resulted in a lower oil yield and increased oxygenated content. Chapter 7 examines the possibility of using metal impregnated ZSM-5 catalysts which were previously used in chapter 4 to improve the co-pyrolysis oils by reducing the content of oxygenated and PAH compounds in the oil, whilst retaining oil yields. The chapter will initially examine the effect of the metal impregnated ZSM-5 catalysts at a 1:1 mixing ratio and will compare this against the results obtained at a 4:1 mixing ratio. This is to identify which catalysts are most effective for a particular mixture with variations in the efficacy of an individual catalyst potentially identifying variations in how the catalyst function (objective 9). Further analysis was conducted using the gallium impregnated ZSM-5 catalyst to identify the effect of wider changes in mixing ratio (1:1, 4:1, 19:1, 99:1 and 1:0) and varying temperature of the catalyst bed (450°C, 500°C, 550°C, 600°C) on the products of pyrolysis. This focuses both on the types of compounds identified in the oil as well as the yields of the various pyrolysis products (objective 10). Simulated distillation was used to compare the effect of the various changes in co-pyrolysis mixing ratio and catalyst to identify the extent of upgrading of the pyrolysis oils through the various pathways. This was compared against the profile for a standard fuel (objective 13).

7.2 Catalytic co-pyrolysis at 1:1 mixing ratio

The metal-impregnated catalyst used in chapter were used as ex-situ catalysts for the upgrading of the volatiles produced during co-pyrolysis of biomass and polystyrene at a 1:1 mixing ratio (by weight). Table 7.1 gives the product yields for catalytic pyrolysis of biomass and PS with each of the metal catalysts as well as unmodified ZSM-5 and sand which represents a non-catalytic pyrolysis. Sand was used, as its elemental composition (SiO_2) is similar to zeolites whilst not catalytically active. The sand ensures that pyrolysis vapours are exposed to similar conditions in both the catalytic experiments and blank.

Table 7.1: Product yields during catalytic co-pyrolysis of biomass with PS at 500°C at a mixing ratio of 1:1, with metal impregnated catalysts.

	Char (wt.%)	Liquid (wt.%)	Gas (wt.%)	Water (wt.%)	Oil (wt.%)	Mass balance (wt.%)
ZSM-5 (Ga-5%)	14.5	67.0	14.0	16.7	50.3	100.4
ZSM-5 (Co-5%)	13.5	68.0	22.5	15.3	52.7	102.1
ZSM-5 (Cu-5%)	14.5	64.5	16.0	16.6	47.9	102.7
ZSM-5 (Fe-5%)	13.5	64.5	17.0	17.5	47.0	97.8
ZSM-5 (Ni-5%)	14.0	51.0	25.0	13.4	37.6	99.0
ZSM-5	16.0	65.0	18.5	17.4	47.6	98.2
Sand	13.0	71.5	10.0	18.6	52.9	97.5

There is little variation expected in the char yield as each sample is exposed to the same conditions of pyrolysis and the char remains separate from the catalyst throughout. The calculated char yield from the individual samples was 13.6 wt.% and most of the samples are within 1 wt% of this value.

The liquid yield is greatest for the non-catalytic experiment which is consistent with other non-catalytic experiments where liquid yields are high and gaseous yields are low as is this case here. The surprising result is the water content which is greater with sand than that for ZSM-5 where in pyrolysis of biomass as an individual sample the water content was higher in the catalytic experiment due to increased hydrodeoxygenation reactions. The oil yield with sand is also above that of the ZSM-5 catalyst.

In terms of the different catalysts the liquid yield was highest for gallium and cobalt. These were a little above the value for ZSM-5 (2-3 wt.%) which had an equivalent liquid yield to copper and iron and the lowest value was obtained for nickel which was significantly reduced (see Figure 7.1). Generally a larger liquid yield resulted in a smaller gas yield with the converse effect also observed. This gas yield was highest for nickel and lowest for gallium (excluding sand) which represented the upper and lower range of liquid yield. However, there were some results which do not fit this pattern such as cobalt which both a high liquid yield and high gas yield and copper which has a low gas yield and yet does not have a high gas yield. The high gas yield for nickel is also not large enough to account for the even larger loss in liquid yield. This is because with co-pyrolysis of biomass and PS alongside these catalysts the residue has increased higher than previously seen. Residue is measured as the change in weight of the

reactor and catalyst during pyrolysis. There are factors which reduce this weight such as drying of the reactor (1.2kg) and the catalyst (4g) during pyrolysis and factors which increase this value such as coke deposition on the reactor and catalyst. In most of the experiments this value has remained below 0.1g. From the experiments here, three of the catalysts exceeded this value with residue for gallium, copper and nickel producing residue of 5 wt.%, 7.5 wt.% and 9 wt.% respectively. This residue which is mostly due to coke deposition is the reason for the lower than suggested liquid yield for nickel and copper and the reason that cobalt produces a higher liquid yield than gallium whilst still producing a high gas yield.

The oil yield follows a similar trend to the liquid yield with cobalt and gallium providing the highest oil yield, copper, iron and unmodified ZSM-5 approximately the same and with nickel producing the lowest oil yield by a margin of 9.4 wt.% and this despite the low water yield for nickel. Cobalt produced a relatively low water yield although not as low as for nickel with ZSM-5 and iron responsible for the highest water yields.
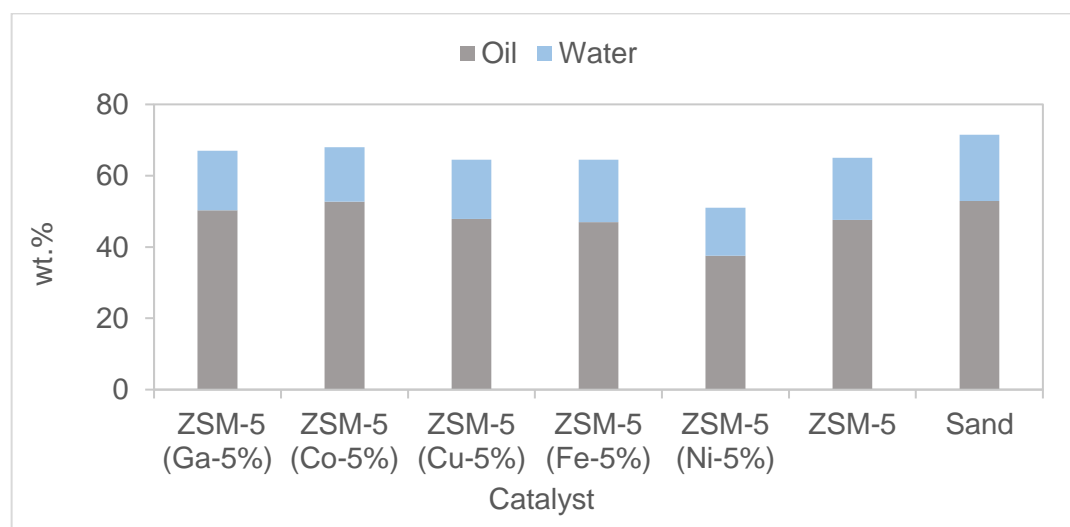
Figure 7.1: Liquid yield from catalytic co-pyrolysis of biomass with PS (1:1) with different ZSM-5 catalysts and sand.
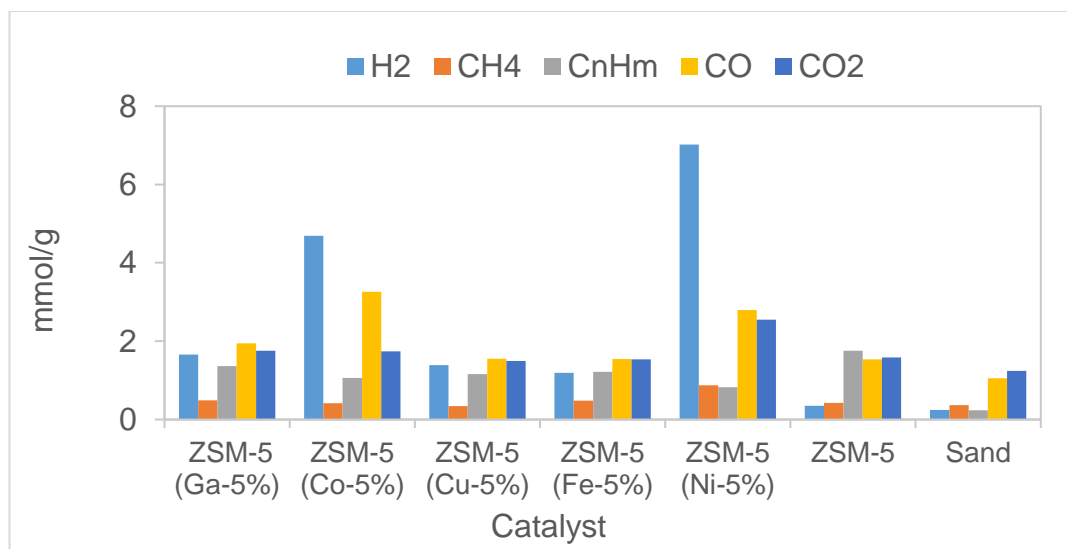
Figure 7.2: The composition of the gas collected during catalytic co-pyrolysis of biomass and PS (1:1) at 500°C with various catalysts.

From the gas analysis it is observed that the non-catalytic experiment produced the lowest gas yield (Figure 7.2) which included the lowest yield of carbon dioxide, carbon monoxide, hydrogen and hydrocarbon gases. By contrast the ZSM-5 catalyst increases the yield of each of these gases with the largest increase in the hydrocarbon gases which increased from 0.24 to 1.8 mmolg^{-1}. This follows the accepted understanding that ZSM-5 catalyst are able to promote cracking, decarbonylation, decarboxylation and dehydrogenation reactions although the elevated water yield suggests that hydrodeoxygenation is promoted in the non-catalytic result contrary to expectation [41, 105]. It may be possible that the reduction of carbon based deoxygenation reactions allows greater availability of oxygen atoms which may react with readily available hydrogen due to polystyrene cracking.

The hydrogen yield is much greater for each of the metal impregnated ZSM-5 catalysts than for the unmodified ZSM-5 with that of cobalt and nickel particularly large. Literature results such as those from Veses et al. [134] which studied offline upgraded of bio-oils collected from woody biomass pyrolysed at 450°C in an auger reactor, found that nickel impregnated catalysts produced high hydrogen gas yields. The research compared H-ZSM-5 with metal impregnated ZSM-5 (Mg, Ni, Cu, Ga and Sn) with the findings that for nickel loaded ZSM-5, 5.7% (v/v) of the gas composition was hydrogen whilst for the other metal catalysts and unmodified ZSM-5 the values ranged between 0.9% and 2.5%. Iliopoulou et al. [136] compared pyrolysis of beech wood in a three zone fixed bed tubular reactor at 500°C with upgrading achieved through nickel

and cobalt impregnated (wet impregnation) ZSM-5 catalyst. The hydrogen yield measured by online GC for the ZSM-5 (pure) catalyst was 0.04 wt.%. Loading of nickel and cobalt on the ZSM-5 increased this value to 0.25 wt.% and 0.12 wt.% respectively at 5 wt.% metal loading. This value was increased to 0.45 wt.% for nickel loaded ZSM-5 at 10 wt.% of metal but did not increase with increased cobalt loading.

This formation of hydrogen gas is potentially advantageous as it is then available for deoxygenation reactions, however, the detection of the hydrogen in the gas bag suggests much of this gas has not been utilised for deoxygenation. The low water content of nickel and cobalt also suggest that rather than promotion of deoxygenation, there might have been some removal of water to produce hydrogen gas. This loss of hydrogen also has a potential disadvantage in that it is likely to lead to a reduction in (H/C_{eff}) ratio which is associated with an increased coke formation. Kim et al. [160] explain that to produce high yields of aromatic and olefin (alkene) through pyrolysis a sample with a high (H/C_{eff}) ratio is required as these compounds require both hydrogen and carbon to be produced. Biomass is not suitable for this because the high oxygen content consumes hydrogen such that a carbon rich and hydrogen deficient material remains. This remaining material does not contain enough hydrogen to produce the types of compound desired. Co-feeding biomass with alcohols or plastics is one possible route to alleviating this hydrogen deficiency and allow for increased production of olefins and aromatics [41, 160, 277]. It is not possible to know if the high residue deposition in the case of nickel was due to a reduced (H/C_{eff}) ratio but this might be the case. If this is occurring in the case of nickel then it is unexplained why the residue weight for cobalt which also produced high hydrogen gas yield was negligible. It might be that the availability of gaseous hydrogen in the case of cobalt was being utilised for increasing the (H/C_{eff}) of the vapours whereas in nickel this was not occurring and the hydrogen gas only acted to deplete the abundance of hydrogen. Interestingly there were also increased hydrogen gas yields for the other metal impregnated catalysts although significantly lower than either cobalt or nickel. It is not possible through these results to determine whether these produced higher hydrogen yields which were then utilised for hydrodeoxygenation or whether this hydrogen gas was produced and passed unaffected from the reactor. It was observed by Yung et al. [155] that nickel oxide impregnated ZSM-5 catalysts underwent in-situ reduction during catalytic pyrolysis of biomass so it is also likely that the formation of hydrogen from these other metal impregnated catalysts might also lead to in-situ reduction.

Hydrocarbon yields were higher for the metal impregnated catalysts than for sand but were lower than those measured for the unmodified ZSM-5. This might indicate a reduction in cracking reactions in these catalysts. This may simply be due to reduction in surface area which occurred during the impregnation process although reduction in acidity could also be involved.

The deoxygenation gases carbon monoxide and carbon dioxide were highest in nickel, cobalt and gallium which were above the value for the unmodified ZSM-5 catalyst. The values for copper and iron were slightly below that of ZSM-5. The result for cobalt is notable as carbon monoxide formation as a molar yield is greater than carbon dioxide formation (see Figure 7.2). The proportion of carbon monoxide compared to carbon dioxide when using cobalt impregnated ZSM-5 (5 wt.%) is higher than that observed by Iliopoulou et al. [136] although they did measurer a lower molar proportion of carbon dioxide than carbon monoxide in the gas yield. Results by Veses et al. [134] indicating that gallium and nickel can also lead to elevated carbon monoxide yield compared to carbon dioxide which is also observed in Figure 7.2 although Veses et al. [134] did not include a cobalt impregnated ZSM-5 catalyst for comparison. These elevated carbon monoxide yields might imply that decarbonylation is promoted rather than decarboxylation however it may also indicate that there is not enough oxygen present thereby carbon monoxide is produced preferentially to carbon dioxide. Deoxygenation involves reactions with both carbon and hydrogen so it is important to consider both the removal of water as well as the removal of carbon oxides.

The oxygen content of the oils produced in this set of experiments are very low which presents issues with comparing values which are close to the standard deviation of the analysis methodology. One way to improve the confidence is to compare against a second analytical methodology. For each of the experiments the main deoxygenation products (CO, CO_2 and H_2O) have been measured and it is possible to use knowledge of the original sample to calculate the amount of oxygen which has been removed and therefore how much remains in the sample oil and char.
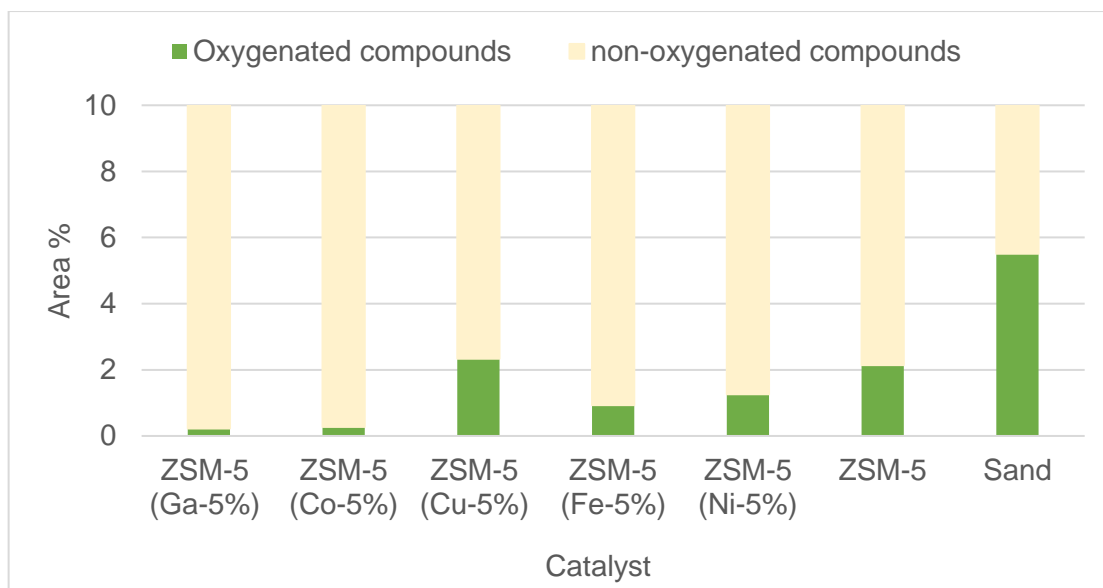
Figure 7.3: The proportion of oxygenated and non-oxygenated compounds identified in the oil from catalytic pyrolysis of biomass and PS (1:1) with various catalysts.
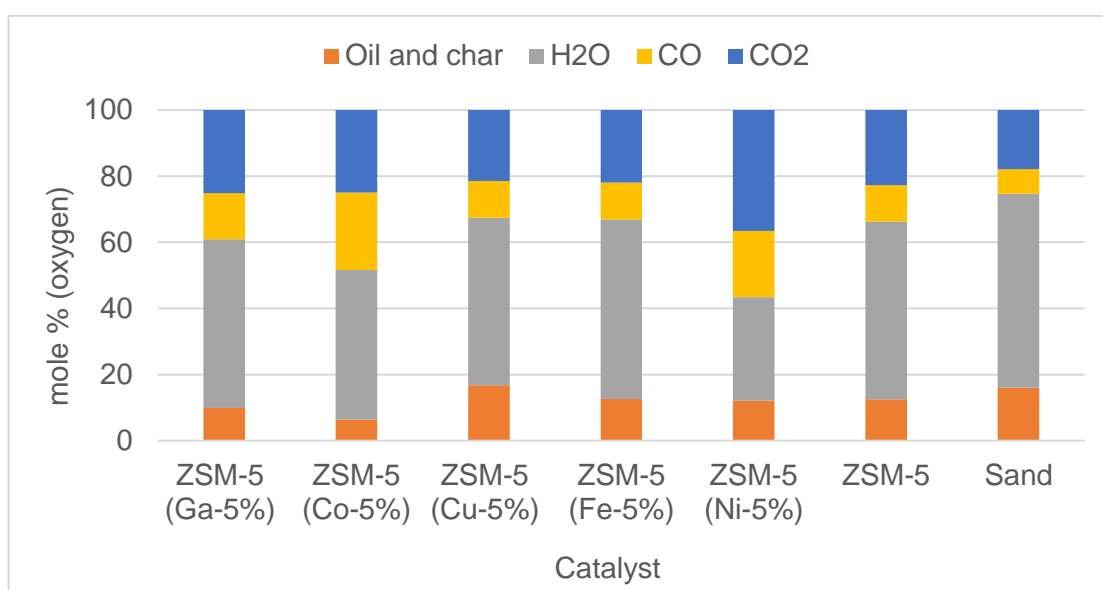
Figure 7.4: The fate of oxygen which was present in the initial sample which has been removed through deoxygenation reactions in the form of carbon monoxide, carbon dioxide and water.

Figure 7.3 plots the proportion of compounds within the oil from catalytic pyrolysis of biomass and PS at a mixing ratio of 1:1 which was identified using GC-MS as containing oxygen. This can be compared to Figure 7.4 which shows the fate of oxygen which was present in the original samples and lost to the sample in the form of carbon monoxide, carbon dioxide and water. Whilst these do not match up exactly there are several notable points which may be

compared. The two samples which had the lowest oxygenated compounds, used gallium and cobalt impregnated ZSM-5 catalyst and also had the largest proportion of deoxygenation products measured by GC and Karl-Fischer titration. The two samples which had the highest proportion of oxygenated compounds as measured by GC-MS, used sand and copper impregnated ZSM-5 as the catalyst and also had the lowest proportion of deoxygenation products. Although in this case the copper and sand were not as clearly distinguished as through the GC-MS where sand had significantly more (>3%) oxygenated compounds than the copper sample. The third point of comparison is between sand and unmodified ZSM-5 which shows the same trend in both data sets although again the distinction is not as clear with unmodified ZSM 5 producing similar deoxygenation products as iron and nickel which in the GC-MS data ranged over a 1% difference.

Table 7.2: Oil composition during catalytic co-pyrolysis of biomass with PS at a mixing ratio 1:1, with different catalysts.

	ZSM-5 (Ga-5%)	ZSM-5 (Co-5%)	ZSM-5 (Cu-5%)	ZSM-5 (Fe-5%)	ZSM-5 (Ni-5%)	ZSM-5	Sand
Aromatic (%)	100.0	100.0	100.0	100.0	100.0	95.6	97.7
Aliphatic (%)	0.0	0.0	0.0	0.0	0.0	4.4	2.3
Oxygenated (%)	0.2	0.3	2.3	0.9	1.3	2.1	5.5
Non-oxygenated (%)	99.8	99.7	97.7	99.1	98.7	97.9	94.5
C_5-C_{12} (%)	71.2	78.5	76.9	80.0	82.0	75.7	76.2
$\geq C_{13}$ (%)	28.8	21.5	23.1	20.0	18.0	24.3	23.8
Uni-cyclic (%)	57.9	69.9	69.0	75.0	74.4	62.2	76.7
Bi-cyclic (%)	27.9	20.2	22.3	15.9	18.5	24.6	18.6
Tri-cyclic (%)	10.7	6.9	7.7	7.0	4.9	6.1	2.3
Quad-cyclic (%)	3.5	3.0	1.0	2.1	2.1	2.8	0.6
Linear (%)	0.0	0.0	0.0	0.0	0.0	4.4	1.9

With these limitations in the analysis it is not possible to definitively confirm which metal impregnated catalysts are superior to each other in terms of deoxygenation but general trends can be observed. Copper appears to be the least effective as this was found in both datasets with gallium and cobalt almost certainly the most effective as this was also found in both datasets. Sand appears to be less effective at deoxygenation than the ZSM-5 based catalysts based entirely upon the big variation in the GC-MS data. ZSM-5, nickel and iron are approximately equivalent as though there are differences in the GC-MS results they are close enough together that they may not be definitively distinguished from each other.

Comparison of sand with unmodified ZSM-5 in the gas products indicated an increase in cracking reactions and this is also observed in the oil analysis. There is a reduction in unicyclic compounds as well as aromatic compounds when the catalyst was introduced and this was accompanied by an increase in the proportion of linear compounds. There was also an increase in PAH compounds with two/three/four aromatic rings which caused a slight decrease in the proportion of compounds between C_5-C_{12}.

Gallium and cobalt impregnation of ZSM-5 were both effective for reducing the oxygen content, however, varied in terms of some of the other criteria. Although every metal impregnated catalyst produced aromatic compounds, gallium produced the lowest proportion of unicyclic compounds with the main cause of this a large increase in the proportion of bi-cyclic compounds as well as an increase in larger PAHs. This gave gallium the lowest proportion of compounds in the C_5-C_{12} range. In contrast to this cobalt increased the proportion of uni-cyclic and C_5-C_{12} compounds compared to unmodified ZSM-5 mainly through a reduction in PAHs. Copper had a high oxygenated compound proportion similar to ZSM-5 and in terms of its other characteristics was somewhere between cobalt and unmodified ZSM-5. Iron and nickel had the middle range of oxygenated compounds but in terms of the other categories were the top metal impregnated catalysts. Nickel had the highest proportion of C_5-C_{12} compounds and the highest proportion of unicyclic compounds led by a reduction in PAHs compared to ZSM-5. Iron was just slightly lower in both criteria.
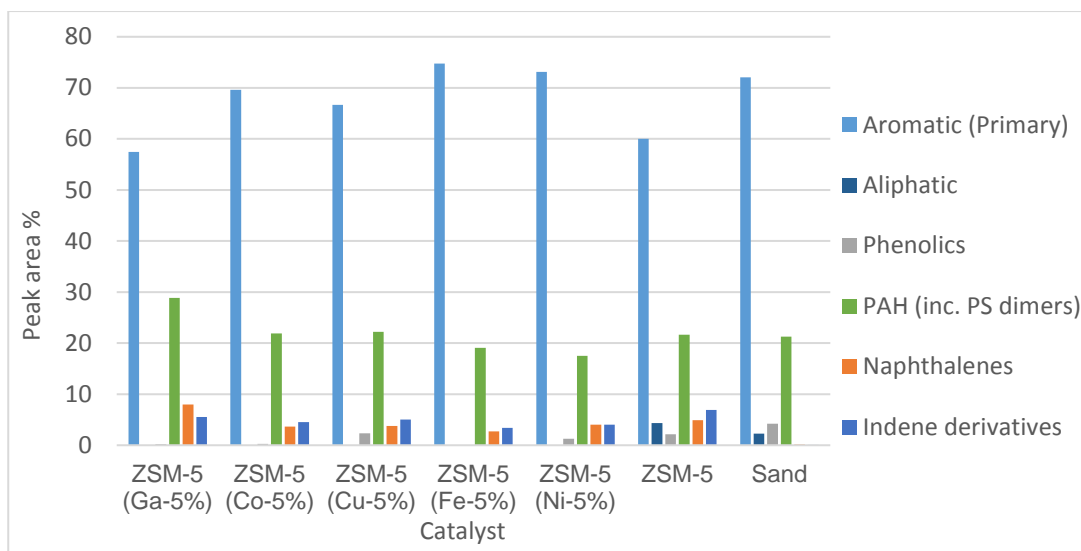
Figure 7.5: Types of compounds which comprise the aromatic component of the oil from catalytic co-pyrolysis (1:1).

Primary aromatics are those which contain a single aromatic ring and do not contain oxygen which means they are valuable for use both as fuel compounds and as chemical feedstocks. In terms of the primary aromatic yield (see Figure 7.5) iron and nickel performed the best and exceeded ZSM-5 by over 10%. Cobalt was slightly lower than iron and nickel from the aspect of primary aromatic yield however it had a lower proportion of oxygenated compounds. Gallium reduced the proportion of oxygenated compound but there was an increase in PAH compounds which significantly reduced the yield of primary aromatic compounds. In terms of oi yield, cobalt was the highest followed by gallium with nickel the lowest and iron the second lowest.
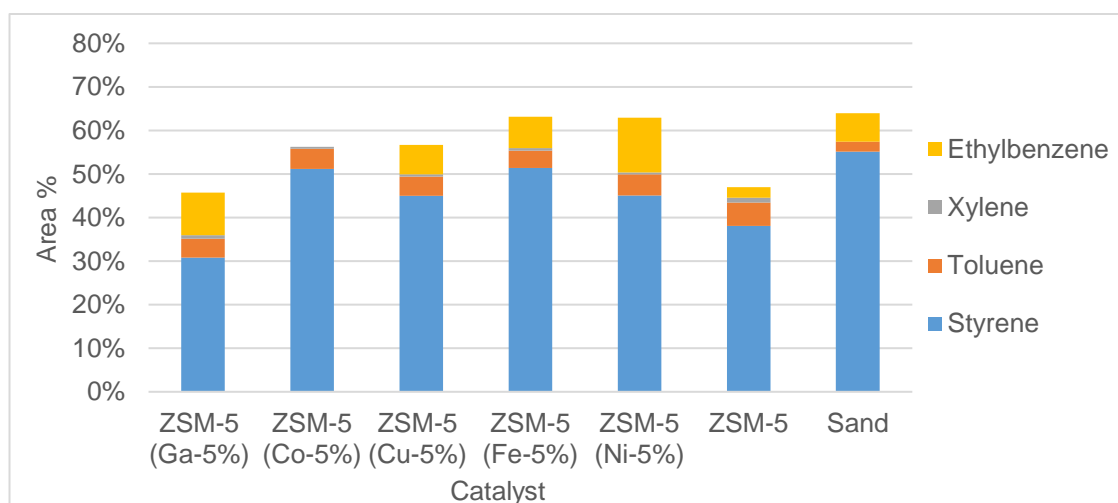
Figure 7.6: The main constituents of the primary aromatic fraction from catalytic co-pyrolysis of biomass and PS at a mixing ratio 1:1.

The primary aromatic fraction is composed of styrene to a high degree with a limited proportion of toluene, xylene and ethylbenzene. The introduction of a catalyst in each case reduced the yield of styrene with an increased toluene yield in each case. With nickel impregnated ZSM-5 resulted in the largest increase in ethylbenzene formation with gallium, the next highest. Cobalt produced little xylene or ethylbenzene.

The International Energy Agency considers ethylene, propylene, benzene toluene and xylene (BTX) to be high value chemicals and, as part of understanding the impact of chemical production on the environment, has modelled the increase in these chemicals from 2012 to 2050 using both a high-demand and low-demand scenario [196]. The 2012 figures place this production for OECD nations at ~175Mt and for non-OECD nations ~150Mt. By 2050 the demand for OECD nations is expected to increase to between ~190-210Mt and for the non-OECD to between 450-475Mt. BTEX is a significant requirement currently obtained from catalytic cracking and steam reforming of naphtha [195] Figures from the US department of energy [194] placed US production of benzene, toluene, xylene, ethylbenzene and styrene in 1998 at 6.8Mt, 3.8Mt, 4.1Mt, 6.3Mt and 5.2Mt respectively. Ethylbenzene was used to produce styrene which in turn was used to produce polystyrene. Although it is possible to recover styrene from petrochemical feedstocks and pyrolysis products. This is beneficial as styrene has a higher value as a chemical than as a motor fuel constituent [193, 278].

7.3 Catalytic co-pyrolysis at 4:1 mixing ratio

Catalytic co-pyrolysis of biomass and polystyrene a mixing ratio of 1:1, with metal impregnated catalysts has some advantageous features and some disadvantageous features. The oxygenated content of the oils has been reduced in many cases through the catalytic co-pyrolysis however it was initially relatively low. The proportion of PAH including PS dimers, however, remains relatively unchanged although this increased for gallium impregnated ZSM-5, a catalyst which produced particularly low oxygenated content. The high content of styrene may also make these oils more suited for chemical production rather than fuel production. Co-pyrolysis of biomass with PS in chapter 6 found that a higher biomass proportion produced an oil with increased oxygenated content and reduced PAH content compared to the 1:1 mixture. If the same effects observed utilising metal impregnated catalysts at a 1:1 mixture are observed in a 4:1 mixture this may be more suitable for fuel use with lower PAH content and

decreased oxygenated content although this is unlikely to reduce as much as with the 1:1 mixture.

Table 7.3: Product yields during catalytic co-pyrolysis of biomass with PS at a mixing ratio 4:1, with various metal impregnated catalysts.

	Char (wt.%)	Liquid (wt.%)	Gas (wt.%)	Water (wt.%)	Oil (wt.%)	Mass balance (wt.%)
(ZSM-Cu-5%)	22.5	48.5	27.5	27.9	20.6	102.0
(ZSM-Ga-5%)	21.5	51.0	28.5	29.7	21.3	102.7
(ZSM-Co-5%)	22.0	41.5	34.0	27.3	14.2	98.8
(ZSM-Fe-5%)	21.0	44.0	27.5	26.3	17.7	97.0
ZSM-5	22.0	59.5	22.3	34.1	25.4	100.0
Sand	21.0	65.0	13.4	24.6	40.4	98.4

Table 7.3 gives the product yields measured during catalytic co-pyrolysis of biomass and polystyrene with metal-impregnated ZSM-5 catalysts at a 4:1 mixing ratio. The gas yield is lowest for the non-catalytic pyrolysis experiment with only that of ZSM-5 increased by ~9 wt.% and those of the metal impregnated ZSM-5 catalysts increased even further. The highest gas yield was determined for cobalt and gallium with greater than twice the gas output for the non-catalytic experiment. The liquid and oil yields followed the same order with sand producing the highest liquid/oil yield followed by unmodified ZSM-5 and then the metal-based catalysts with the highest liquid and oil yield of the metal impregnated ZSM-5 for gallium and iron and the lowest for cobalt which had the highest gas yield. The unmodified ZSM-5 produced the greatest proportion of water followed by the gallium with sand producing the lowest water. Gallium produced a high gas yield and high water yield therefore it might be expected to contain a low proportion of oxygenated compounds whereas sand produced the opposite effect so it may be expected to produce a higher proportion of oxygenated compounds. In contrast to the 1:1 mixing ratio where oil yields were similar for the metal impregnated catalysts to the unmodified ZSM-5, with the 4:1 mixing ratio, the oil yield is reduced for each of the metal impregnated catalysts to some extent with iron and cobalt reduced by ~8 wt.% and ~13 wt.% respectively.

In the 1:1 mixture, the cobalt based catalyst produced high oil yield and low oxygen content whilst retaining primary aromatic compounds. In contrast, the gallium-based catalyst produced lower oil yields and whilst it produced low

oxygenated content, caused loss of primary aromatic compounds through formation of PAHs. The copper-based catalyst produced slightly lower oil yields than cobalt and retained primary aromatic content but had elevated oxygenated content compared to the cobalt catalyst. The oil yield for cobalt impregnated catalyst this 4:1 mixture for the cobalt catalyst is particularly low which is surprising considering the high oil yield during the experiments with catalytic co-pyrolysis of biomass and polystyrene at a 1:1 mixing ratio (see Figure 7.6).
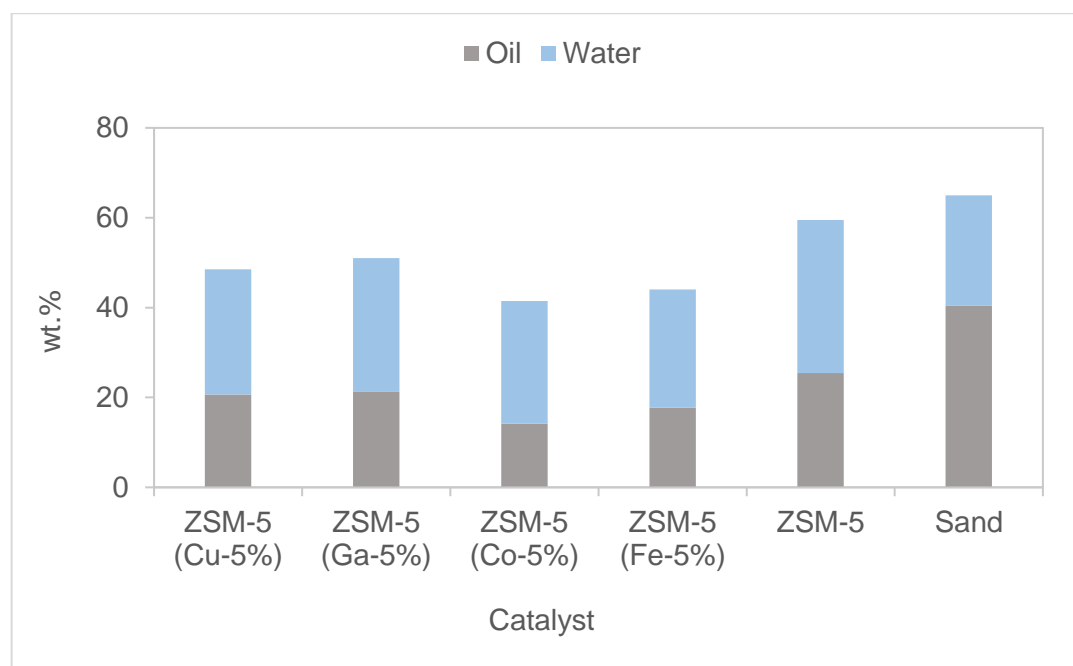
Figure 7.6: Liquid yield from catalytic co-pyrolysis of biomass with PS (4:1) with different ZSM-5 catalysts and sand.
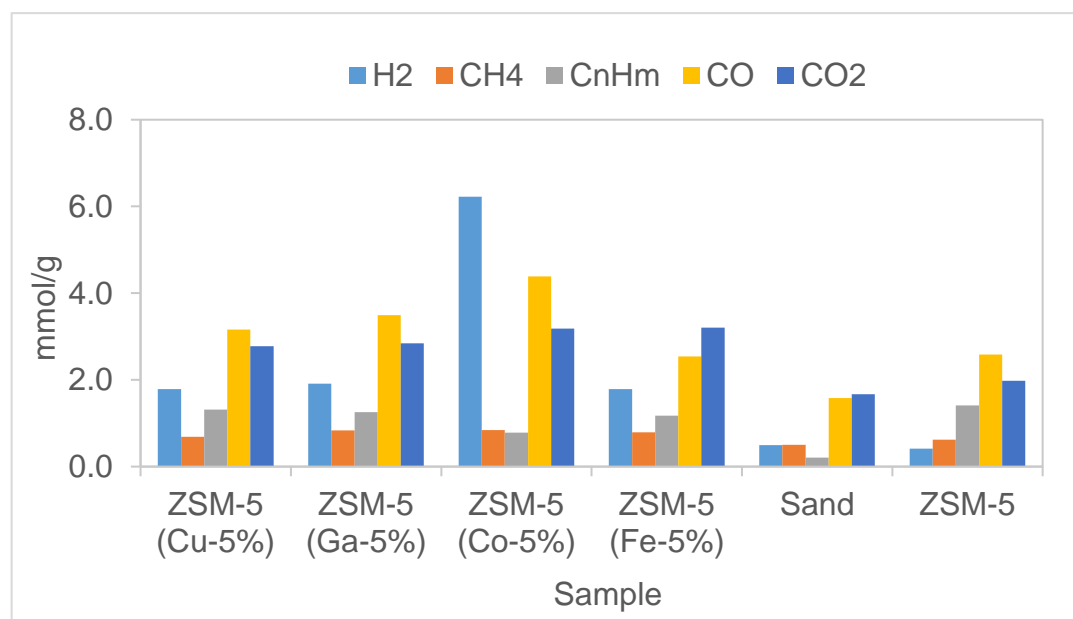
Figure 7.7: The composition of the gas collected during catalytic co-pyrolysis of biomass and PS (4:1) at 500°C with various catalysts.

There are two factors which explain this reduction in oil yield and both relate to the gas produced. Deoxygenation is able to reduce the oil yield through two main pathways. Firstly, producing water reduces the oil yield by removing oxygen and hydrogen with 89% of the compound mass due to oxygen. Secondly, production of carbon oxides also reduces the oil yield by removing carbon and oxygen with 57% of carbon monoxide mass due to oxygen and 73% of carbon dioxide due to oxygen. During deoxygenation of biomass it is important to remove oxygen through carbon dioxide to minimise mass loss and limit reductions to the (H/C_{eff}) ratio which is important for formation of oil compounds rather than coke. However, when polymers are present (H/C_{eff}) is increased significantly thereby hydrodeoxygenation is more attractive as there is hydrogen available and this reduces the mass of oil, to a smaller degree, per oxygen atom removed.

Using the gallium impregnated ZSM-5 as an example, it can be observed that with catalytic pyrolysis of biomass as an individual sample the deoxygenation to produce water and carbon oxides reduces the oil yield below that of non-catalytic pyrolysis and to similar levels to ZSM-5 despite lower coke deposition on the catalyst. This oil yield increases on addition of PS in the 4:1 mixture despite oxygenated content decreasing significantly. For the cobalt catalyst the oil yield decreased on addition of the PS at a mixing ratio of 4:1. Part of this decrease was due to greater deoxygenation compared to gallium both through increased water as well as carbon oxides production. The gallium catalyst achieved the deoxygenation through hydrodeoxygenation more than did the cobalt catalyst and cobalt also utilised greater carbonylation than did gallium, both effects would decrease the oil mass for cobalt for each oxygen atom removed than for gallium. The secondary effect is that whilst gas and water products for the gallium catalyst were mainly due to deoxygenation cobalt produced both deoxygenation products and also produced high hydrogen gas yields (see Figure 7.7) although these were less critical for mass loss due to the low molecular mass of hydrogen gas. This was also the case at a 1:1 mixing ratio but the gallium catalyst oil yield was reduced through high residue deposition (5 wt.%) most likely in the form of coke whereas cobalt did not.

The copper and iron catalysts were not as deoxygenating as the gallium and cobalt (see Figure 7.8) which was mostly through lower water yield. Copper produced slightly lower gas yield than gallium but produced 2 wt.% more residue leading to a similar oil yield whereas iron produced 3 wt.% more residue than gallium which again led to slightly lower oil yields.
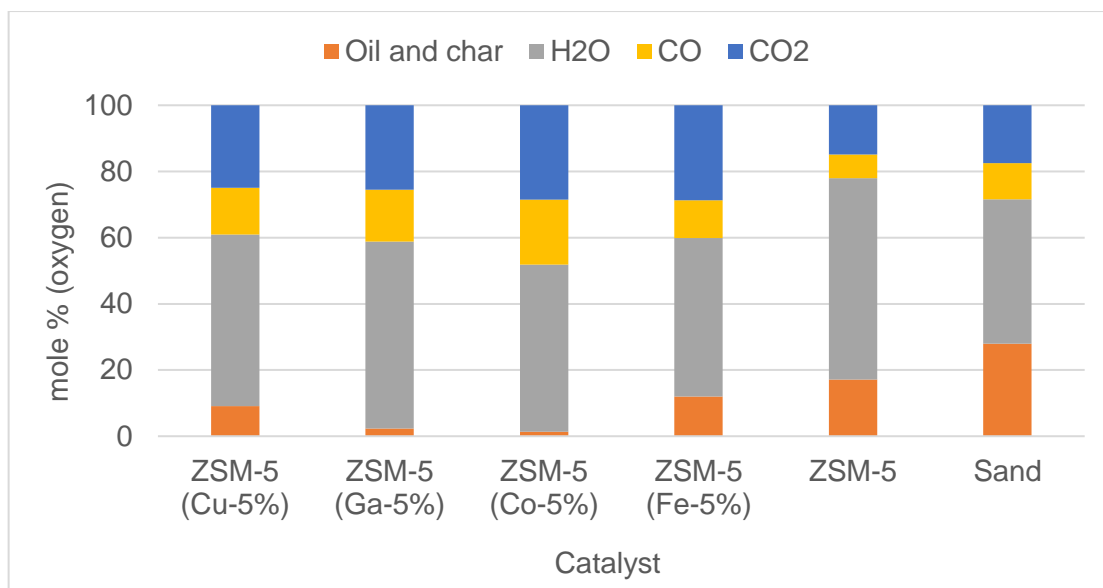
Figure 7.8: Oxygen removal during catalytic co-pyrolysis of biomass and PS at a mixing ratio of 4:1 with various catalysts.

Table 7.4: Oil composition during catalytic co-pyrolysis of biomass with PS at a mixing ratio 4:1, with different catalysts.

	ZSM-5 (Cu-5%)	ZSM-5 (Ga-5%)	ZSM-5 (Co-5%)	ZSM-5 (Fe-5%)	ZSM-5	Sand
Aromatic (%)	100.0	100.0	100.0	100.0	100	98.3
Aliphatic (%)	0.0	0.0	0.0	0.0	0	1.7
Oxygenated (%)	3.7	1.2	2.0	3.5	12.6	12.4
Non-oxygenated (%)	96.3	98.8	98.0	96.5	87.4	87.6
C_5-C_{12} (%)	77.1	84.4	70.8	82.4	82.9	71.6
$\geq C_{13}$ (%)	22.9	15.6	29.2	17.6	17.1	28.4
Uni-cyclic (%)	61.9	75.3	65.5	71.2	64.6	72.7
Bi-cyclic (%)	27.6	19.0	21.4	21.7	27.2	20.0
Tri-cyclic (%)	9.0	4.4	11.4	6.0	6.5	6.1
Quad-cyclic (%)	1.5	1.3	1.8	1.1	1.7	0.0
Linear (%)	0.0	0.0	0.0	0.0	0.0	1.2

Table 7.4 shows the types of compounds which were identified in the oils for each of the catalysts with co-pyrolysis of biomass and PS at a 4:1 mixing ratio. The oxygenated compound values compared reasonably closely to the removal of oxygen calculated through deoxygenation reactions. The gallium and cobalt catalysts were the least oxygen containing in both cases but the deoxygenation products suggest that cobalt might be slightly more deoxygenating than gallium although the variation between values is below standard deviation. Figure 7.8 places iron and copper next in order in terms of deoxygenating products and this compares to the GC-MS results in the table. Unmodified ZSM-5 produced lower deoxygenation products than the metal catalysts and sand produced few still so it would be expected that that sand would contain a greater proportion of oxygen containing compounds than ZSM-5 and this would be expected to be higher than for the metal-impregnated catalysts. Table 7.4 shows that the oil from ZSM-5 contained more oxygenated compounds than the metal catalysts however this is not increased for sand. If the oxygenated compounds are examined more closely it is found that for ZSM-5 11.2% of the compounds contained one oxygen atom and 1.4% contained two oxygen atoms, whereas in contrast, for sand only 3.0% of compounds contained one oxygen atom and 9.5% contained two or more oxygen atoms. This shows that although both samples contain a similar proportion of oxygen containing compounds, there is more oxygen contained in the oxygenated compounds when using sand instead of a ZSM-5. This then matches with the oxygen contain as predicted from the deoxygenation products.

In the 4:1 Mixture the gallium loaded catalyst produced the highest proportion of gasoline fuel sized molecules which was slightly above that of the iron loaded and unmodified ZSM-5. The lowest was for cobalt which was lower even than that of sand. This same trend was not observed in the unicyclic compounds with copper and unmodified ZSM-5 containing a particularly large proportion of bi-cyclic compounds (PS dimers) which were marginally outside the fuel range. Once again gallium had the most optimal value in regards to unicyclic compounds with 75.3% of compounds containing a single cyclic ring compared to 57.9% in the 1:1 biomass/ and polystyrene mixture with a significant reduction in bi-cyclic, tri-cyclic and quad-cyclic compounds. The lowest result for uni-cyclic compounds was for copper loaded ZSM-5 at 61.9% down from 69.0% with an increase in PAHs. Gallium loaded zeolites including wet impregnation of ZSM-5 have been examined by Li et al. [186] in literature for catalytic co-pyrolysis of biomass and LDPE using a pyroprobe microreactor. Impregnation of ZSM-5 with 5 wt.% gallium increased the yield of desirable oil compounds (monoaromatic and alkenes) from 37.6C% to 38.8C% and

monoaromatic from ~23 C% to ~27 C%. This was accompanied by a reduction in polyaromatic carbon from ~5 C% to ~3 C% and char/coke also reduced marginally. The research attributed this increase in monoaromatic compounds to a conversion of light alkanes derived from the polyolefin into monoaromatic compounds. Often the conversion of saturated alkanes to unsubstituted alkenes is the limiting step in production of aromatics from polymers, however, the gallium and Brönsted acid sites appears to catalyse dehydrogenation reactions for conversion of alkanes to alkenes [279, 280]. This subsequently allows for increased aromatic production due to aromatization of alkenes. There is very limited literature regarding co-pyrolysis yields for other metal-zeolite catalysts. Stanton et al. [135] compared pyrolysis of biomass with metal-impregnated ZSM-5 in an inert atmosphere and in the presence of hydrogen gas. The use of hydrogen led to an increased proportion of two and three ring aromatic compounds when using the metal loaded catalysts whereas hydrogen donation through the addition of PS does not appear to increase PAH compounds to any significant degree.
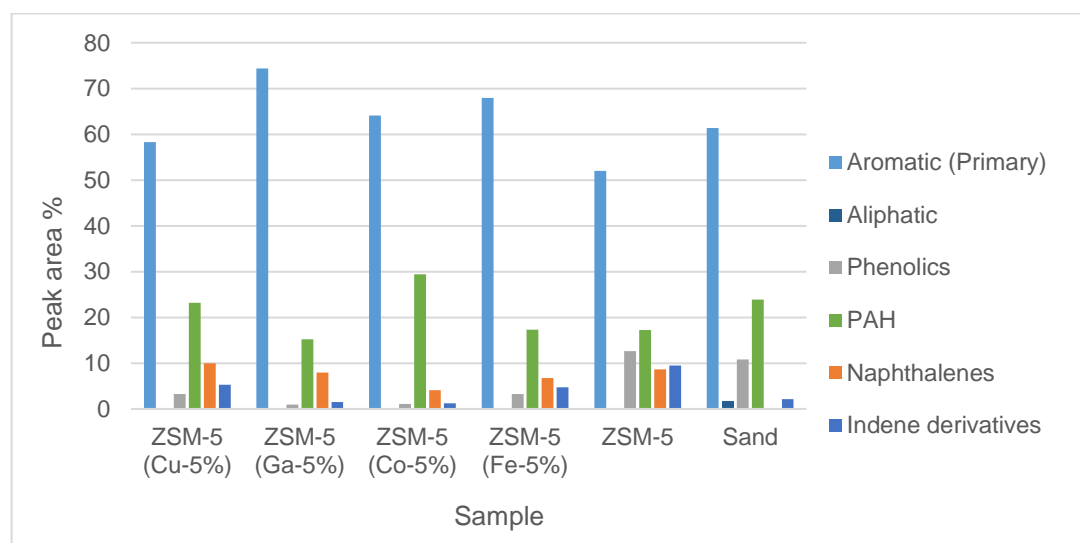
Figure 7.9: Types of compounds which comprise the aromatic component of the oil from catalytic co-pyrolysis (4:1).

Figure 7.9 shows the types of aromatic compounds which are present in the oil samples from the various catalysts. The highest proportion of primary aromatics is observed for gallium and iron although if the size of the oil yield is accounted the yield of primary aromatics is large in the non-catalytic samples. The proportion of PAH is largest for cobalt and sand although in general these values are lower than in the 1:1 mixture but then so too is the primary aromatic content.
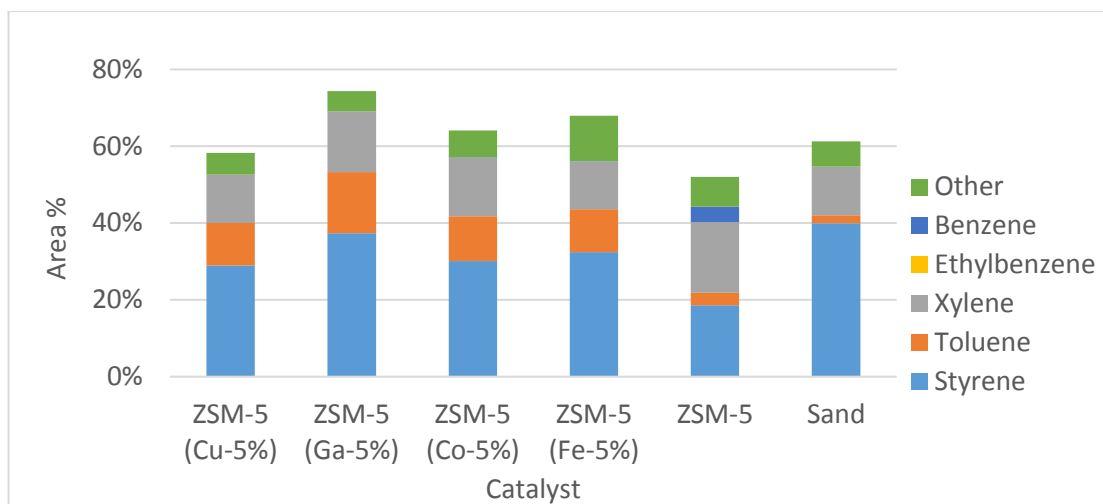
Figure 7.10: The main primary aromatic constituents of the oil from catalytic co-pyrolysis of biomass and PS at a mixing ratio 4:1 with various catalysts.

In comparison to the 1:1 mixture, in the 4:1 there is a large reduction is styrene content although it is still a major component. This is reduced to varying extents depending on the catalyst used with gallium retaining the highest styrene proportion and ZSM-5 the lowest proportion. However, the main change in composition is an increase in toluene yield when using the metal impregnated catalysts.

7.4 Effect of temperature on products from Catalytic co-pyrolysis of biomass with PS (4:1)

Co-pyrolysis and catalytic pyrolysis together have allowed for a variety of product distributions to be reached. There are other factors which may also potential to provide further variation including catalytic effects. The temperature at which the catalyst is held during pyrolysis is one such factor which can alter the effectiveness of the catalyst for various reactions. This section (section 7.4) examines the effect of varying the temperature of gallium impregnated ZSM-5 (5%) between 450°C and 600°C.

Table 7.5: Product yields during catalytic co-pyrolysis of biomass with PS at a mixing ratio 4:1, using gallium impregnated ZSM-5 (5%), at various temperatures.

	Char (wt.%)	Liquid (wt.%)	Gas (wt.%)	Water (wt.%)	Oil (wt.%)	Mass balance (wt.%)
450°C	21.5	53.5	21.0	33.6	20.9	98.4
500°C	21.5	51.0	28.5	29.7	21.3	102.7
550°C	23.5	51.5	27.0	27.7	23.8	103.0
600°C	19.0	50.0	27.0	25.6	24.4	96.4

As the catalyst temperature is increased, there was a decrease in the liquid yield. This was due to the combination of two contrasting effects. The oil yield increased as the catalyst temperature increased, however, the water yield decreased and to a higher degree than the oil yield increased. It is likely that some of this oil increase was due to a reduced loss of oil yield in the formation of water although it is also probable that the reduction in gas yield from 500°C to 600°C also allowed for a greater oil yield across this same temperature range. The gas yield increases by 7.5 wt.% from 450C to 500°C and then reduces slightly through to 550°C where it remains stable through to 600°C. This suggests that at higher temperatures there is likely to be a greater oxygen content in the oils because of reduced hydrodeoxygenation.

The gas composition gives insight into the activity of the catalyst. From 450°C to 500°C there is an increase in each of the gas products (see Figure 7.11) suggesting that the catalyst is becoming more active as temperatures increase. After 500°C the products of most products stabilise. C_2-C_4 reduces slightly from 500-600°C over which range the methane yield increases slightly and carbon oxides are at their peak at 500°C before reducing as the temperature increases further. The only gas product which continues to increase with catalyst temperature is hydrogen gas which increases as water yield is decreases. For deoxygenation through carbon oxides this is at its peak around 500°C. At lower temperatures hydrodeoxygenation is higher but carbon oxide deoxygenation lower and at temperatures above 500°C all types of deoxygenation decrease.
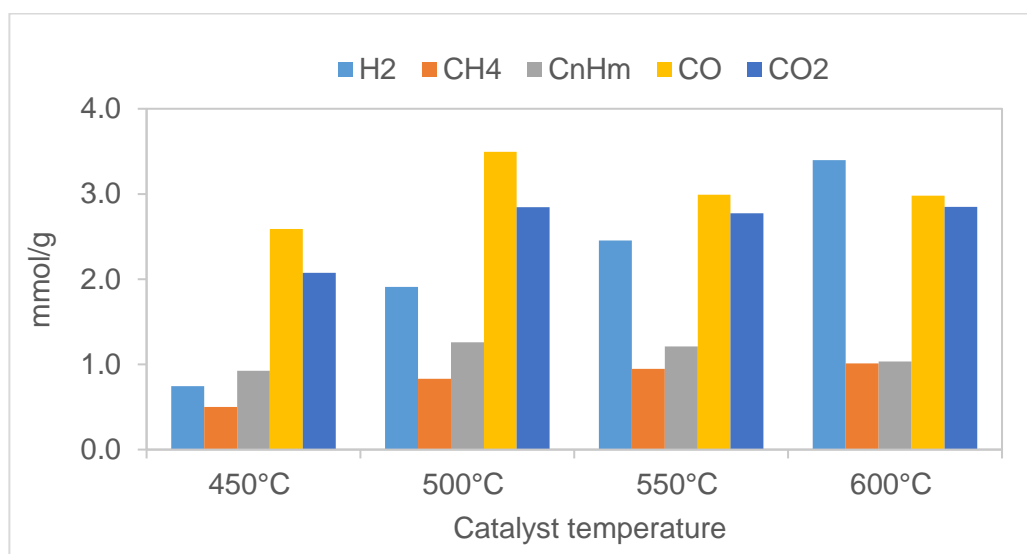
Figure 7.11: The composition of the gas collected during catalytic co-pyrolysis of biomass and PS (4:1) with Ga-ZSM-5 (5%) across a range of catalyst temperatures.

From analysis of the oil it is observed that both the oil at 450C and 500C had equivalent proportions of oxygenated compounds with an increase at 550°C and 600°C which follows the correlation from the deoxygenation products.

The oil yield was slightly higher at 500°C compared to 450°C with C_5-C_{12} proportion higher at 450°C. Whilst 500°C produced the highest proportion of deoxygenation gases, it also produced the highest proportion of PAH compounds larger than C_{13}.

Table 7.6: Oil composition during catalytic co-pyrolysis of biomass with PS at a mixing ratio 4:1, with Ga-ZSM-5 (5%) across a range of temperatures.

	450°C	500°C	550°C	600°C
Aromatic (%)	100	100	100	100
Aliphatic (%)	0	0	0	0
Oxygenated (%)	1.1	1.2	4.8	5.3
Non-oxygenated (%)	98.9	98.8	95.2	94.7
C_5-C_{12} (%)	89.1	84.4	88.6	91.1
$\geq C_{13}$ (%)	10.9	15.6	11.4	8.9
Uni-cyclic (%)	76.7	75.3	74.3	75.2
Bi-cyclic (%)	19.0	19.0	23.7	20.8
Tri-cyclic (%)	3.8	4.4	1.8	3.1
Quad-cyclic (%)	0.5	1.3	0.2	0.9
Linear (%)	0.0	0.0	0.0	0.0

Table 7.6 shows the proportions of aromatic, oxygenated, cyclic and fuel range compounds identified in the oils produced during catalytic co-pyrolysis of biomass with polystyrene at a 4:1 mixing ratio at varying temperatures. The proportion of primary aromatic compounds was largest at 450°C and this decreased by a small amount as the temperature increased to 550 and 600°C with an increase in phenolics and naphthalene compounds (see Figure 7.12). However, generally there was little variation compared to the results from different catalysts. The primary aromatics were mainly composed of styrene with toluene and xylene present in each case with a general decline in the proportion of primary aromatic compounds as temperatures were increased (see Figure 7.13).
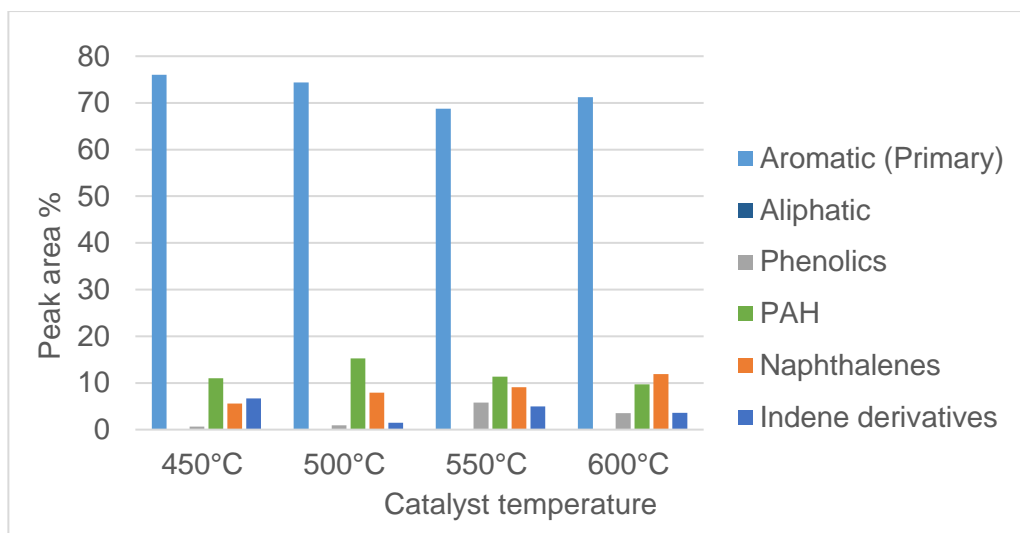
Figure 7.12: Types of compounds which comprise the aromatic component of the oil from catalytic co-pyrolysis (4:1) with Ga-ZSM-5 (5%) over a range of temperatures.
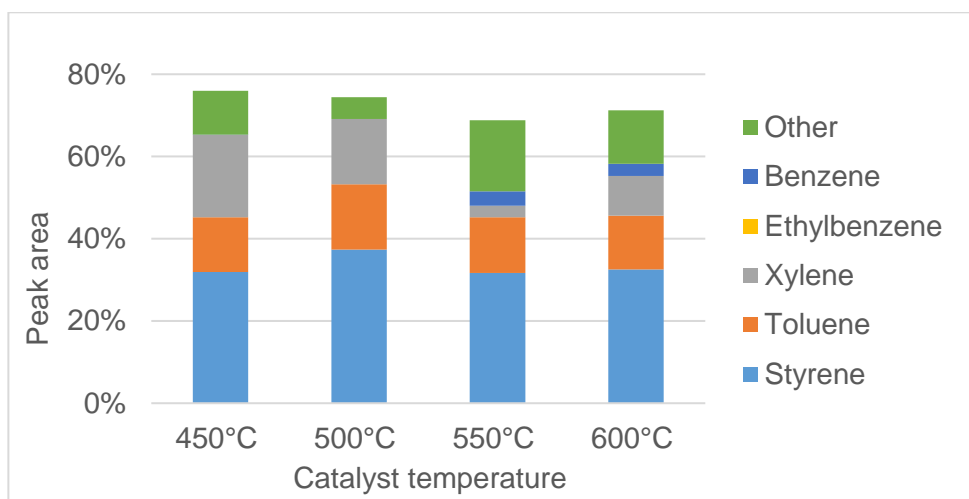
Figure 7.13: The main primary aromatic constituents of the oil from catalytic co-pyrolysis of biomass and PS at a mixing ratio 4:1 with Ga-ZSM-5 (5%) over a range of temperatures.

7.5 The effect of mixing ratio on the products of catalytic co-pyrolysis

The mixing ratio has a large impact on the types of compounds which are present in the oil from catalytic co-pyrolysis of biomass and PS. There are variations introduced simply through mixing of compounds derived from the two different samples as well as catalytic upgrading effects.

Table 7.7: Product yields during catalytic co-pyrolysis of biomass with PS using gallium impregnated ZSM-5 (5 wt.%), at various mixing ratios.

	Char (wt.%)	Liquid (wt.%)	Gas (wt.%)	Water (wt.%)	Oil (wt.%)	Mass balance (wt.%)
1:1	14.5	67.0	14.0	16.7	67.4	100.4
4:1	21.5	51.0	28.5	29.7	21.7	102.5
19:1	24.0	45.5	30.5	26.2	17.6	101.5
99:1	25.0	44.0	32.0	35.0	8.0	97.8
1:0	25.3	49.0	25.8	34.9	13.3	99.5

Biomass produced more char than PS so it is unsurprising that as the biomass content increases from 50 wt.% of the sample through to 100 wt.% of the sample that the char content also increases. There is also an increase in gas yield as the biomass content increases, however, the gas yield for 100 wt.% biomass is lower than nearly all of the co-pyrolysis mixtures. This indicates that reactions are occurring in the co-pyrolysis mixtures which are producing gas. The liquid yield decreases as the proportion of biomass increases which is as expected due to the high liquid yield of PS, however, as with the gas yield, the value for the pure biomass sample is not in keeping with this trend due to the reduced gas production. As with the liquid yield the oil yield also decreases with increased biomass with the pure biomass again producing a higher oil yield than the trend would suggest. The correlation between water yield and mixing ratio is not as clear. There is a general increase as the biomass yield increases which is expected both due to the high moisture content in the biomass sample and the high oxygen content for water production, however the values for the 4:1 and 19:1 mixtures do not hold to this pattern. It appears as though hydrodeoxygenation is reduced for this mixture although the cause of this is unclear.
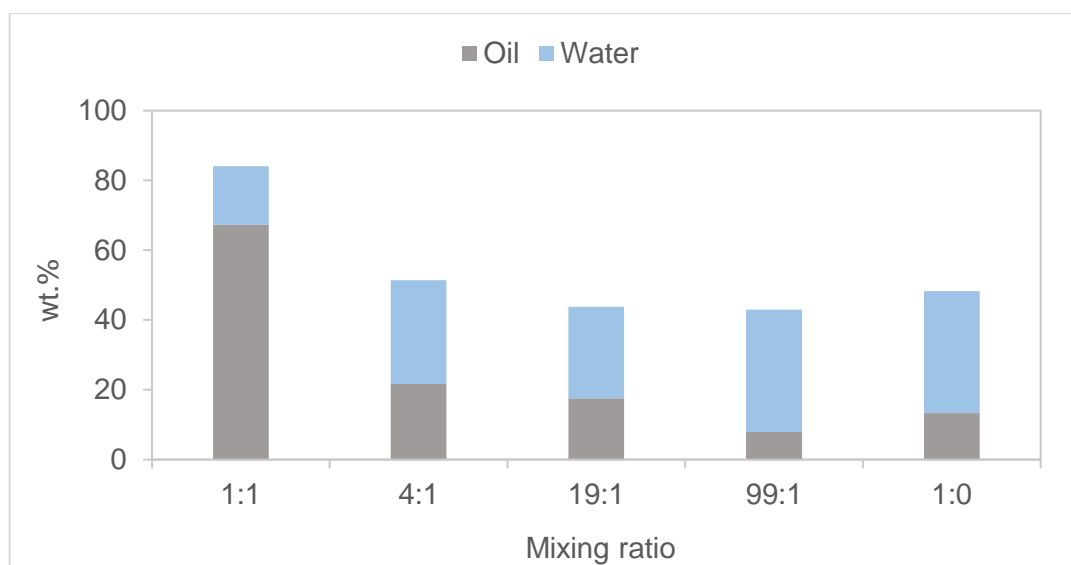
Figure 7.14: Liquid yield from catalytic co-pyrolysis of biomass with PS with different with Ga-ZSM-5 (5%) at different mixing ratios.

Figure 7.15 gives the gas composition determined for each pyrolysis experiment. The deoxygenation gases are lowest for the 1:1 mixture which contained the lowest amount of oxygen and were much larger for the other mixture ratios. The sample with the highest deoxygenation through carbon oxides was the 19:1 mixture which may explain why the deoxygenation through water was lower for this mixture. 99:1 and 1:0 contained more oxygen in the sample with carbon oxides reduced compared to 19:1 so it is probable that the oils from these experiments contain elevated proportions of oxygenated compounds compared to the 19:1 mixture. The products of cracking (C_2-C_4) are highest in the 99:1 sample which clearly breaks the correlation in this value reducing from the 1:1 mixture to the 1:0 mixture for each of the other samples and may account for the particularly low oil yield in this case.
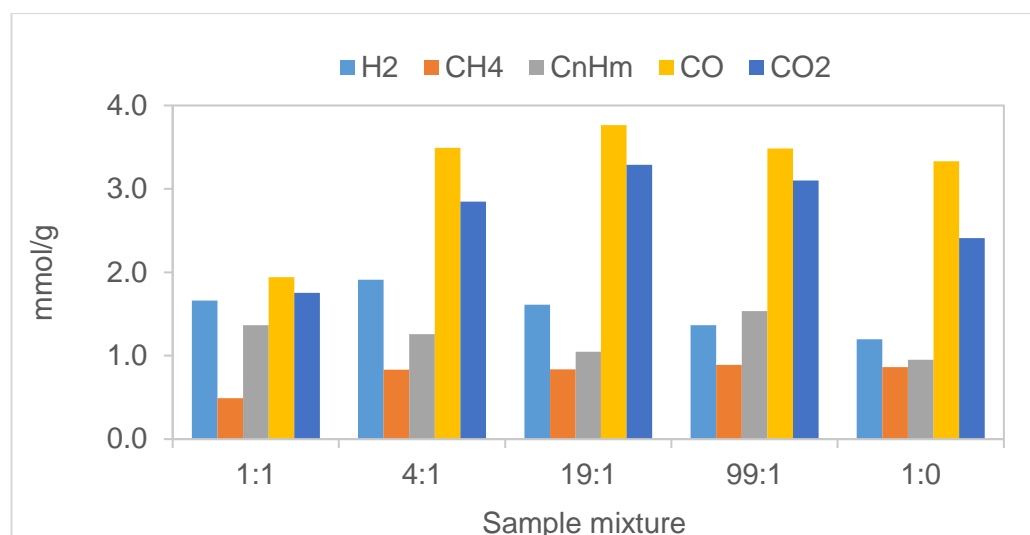
Figure 7.15: The composition of the gas collected during catalytic co-pyrolysis of biomass and PS with Ga-ZSM-5 (5 wt.%) at different mixing ratios.

Table 7.8: Oil composition during catalytic co-pyrolysis of biomass and PS with Ga-ZSM-5 (5 wt.%) at different mixing ratios.

	1:1	4:1	19:1	99:1	1:0
Aromatic (%)	100	100	100	100	100
Aliphatic (%)	0	0	0	0	0
Oxygenated (%)	0.2	1.2	9.4	12.9	25.8
Non-oxygenated (%)	99.8	98.8	90.6	87.1	74.2
C_5-C_{12} (%)	71.2	84.4	95.6	99.6	99.4
$\geq C_{13}$ (%)	28.8	15.6	4.4	0.4	0.6
Uni-cyclic (%)	57.7	75.3	82.6	84.0	79.3
Bi-cyclic (%)	27.8	19.0	16.5	15.9	20.6
Tri-cyclic (%)	11.0	4.4	0.6	0.1	0
Quad-cyclic (%)	3.5	1.3	0.3	0.0	0
Linear (%)	0.0	0.0	0.0	0.0	0

There is substantial variation in the oxygenated, cyclic and C_5-C_{12} compounds due to varying the mixture ratio of the samples. The aromatic compounds were unaffected with all identified compounds containing aromatic rings for all the mixtures. As the proportion of biomass increases in the mixture this led in each case to an increase in oxygenated compounds although there was also an

increase in the proportion of C_5-C_{12} compounds. The variation in oxygenated compounds between 99% biomass and 100% biomass was very large with the addition of 1 wt.% PS reducing the oxygenated compounds by almost 50%. In contrast the variation in C5-C12 between 99% and 100% biomass was only 0.2% which is below standard deviation and should be considered equivalent. The cyclic compounds are also affected by the mixing ratio with increasing biomass proportion increasing the unicyclic compounds and reducing the PAH proportion this is beneficial, however, in the case of 100% biomass the PAH increases with naphthalenes the main PAH product.
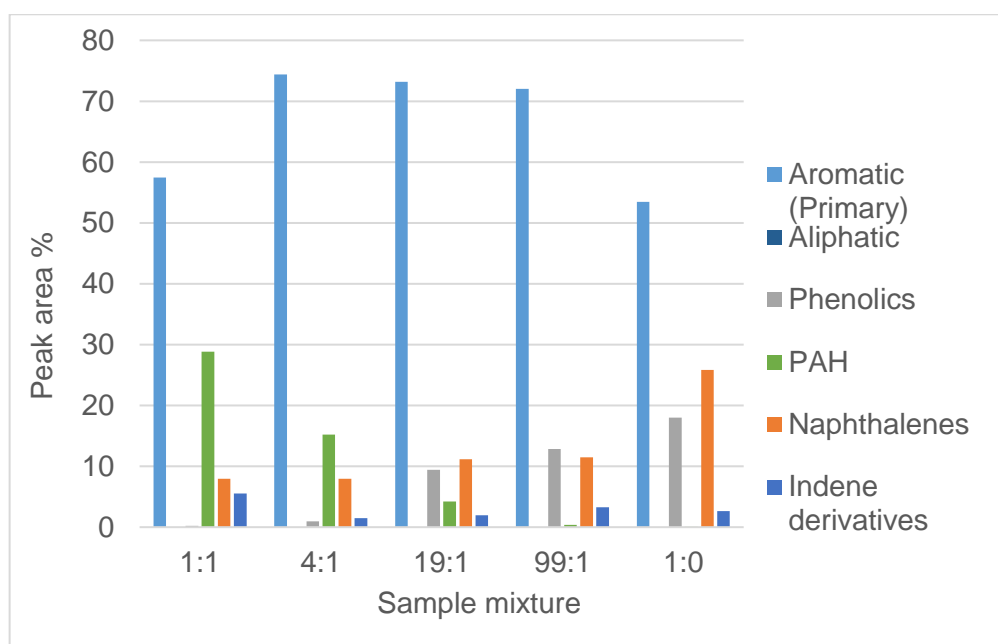
Figure 7.16: Types of compounds which comprise the aromatic component of the oil from catalytic co-pyrolysis of biomass and PS with Ga-ZSM-5 (5 wt.%) at different mixing ratios.

The proportion of primary aromatic compounds is highest for the mixtures with an increase in PAH (excluding naphthalenes) as the PS share increases and an increase in naphthalenes and phenolics as the biomass proportion increases (see Figure 7.16). As the proportion of biomass increases there is an observable increase in toluene with other primary aromatics also observed with increased PS leading to greater styrene product yield and loss of xylene in favour of ethylbenzene (see Figure 7.17).
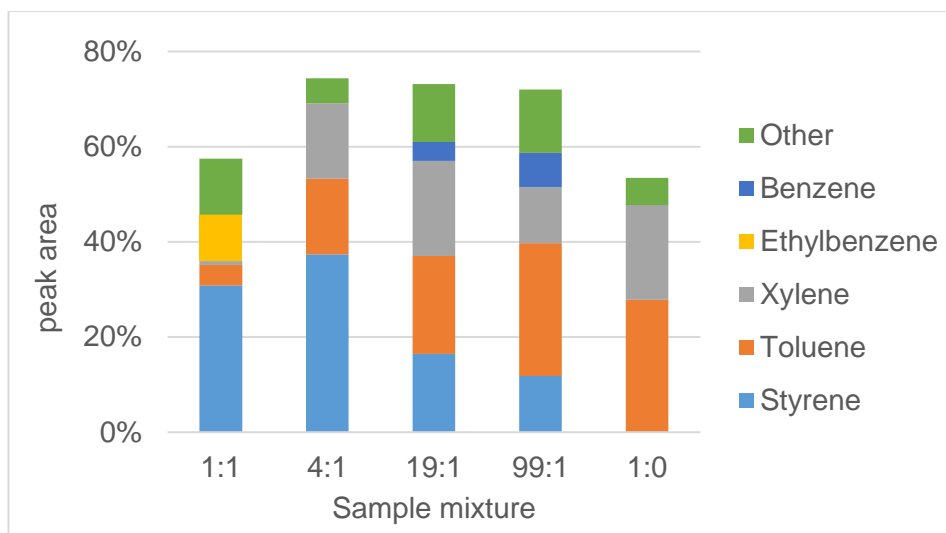
Figure 7.17: The main primary aromatic constituents of the oil from catalytic co-pyrolysis of biomass and PS 1 with Ga-ZSM-5 (5 wt.%) at different mixing ratios.

7.6 Simulated distillation of catalytic co-pyrolysis oils

Simulated distillation shows the range of temperatures over which an oil sample will distil which may then be compared against the range which would be expected for a petroleum fuel. This range which is due to different compounds in the oil becoming volatile once they reach their boiling point. A major factor effecting boiling temperature is the molecular carbon number with a greater number of carbon atoms leading to elevated boiling points. However, the presence of oxygen can substantially increase boiling points with oxygenated compounds having boiling points far in excess of those for a similar sized no-oxygenated hydrocarbon [41].

The simulated distillation results from this research are shown in Figure 7.18 and are similar to results obtained by Muhammad et al. [281] examining oils produced through catalytic and non-catalytic pyrolysis of polymers. The introduction of a catalyst improved the proportion of oil which is volatile at temperatures below 150°C to a high degree, with an increase from 0% through to between 30-70% for various combinations of catalytic co-pyrolysis. This is still lower than values expected for a gasoline [282, 283] for which greater than 80% of the sample is volatilised by this temperature. The results for biomass which was individually pyrolysed show that the addition of the unmodified ZSM-5 catalyst significantly improves the low temperature volatility considerably and this is then improved further by the use of gallium impregnated ZSM-5. The major reason for this improvement is a reduction in oxygenated compounds. The 1:1 mixture ratio had a very similar result to

gallium impregnated ZSM-5 at 150°C for both the modified and unmodified catalyst however the substantial increased PAH compounds caused lower proportions of volatilised compounds between 200°C and 500°C. The mixtures which contained greater proportions of biomass were more similar to gasoline than those with greater PS (see Figure 7.18) although all of the oils examined would need processing to produce a fuel with the same properties as those of gasoline.
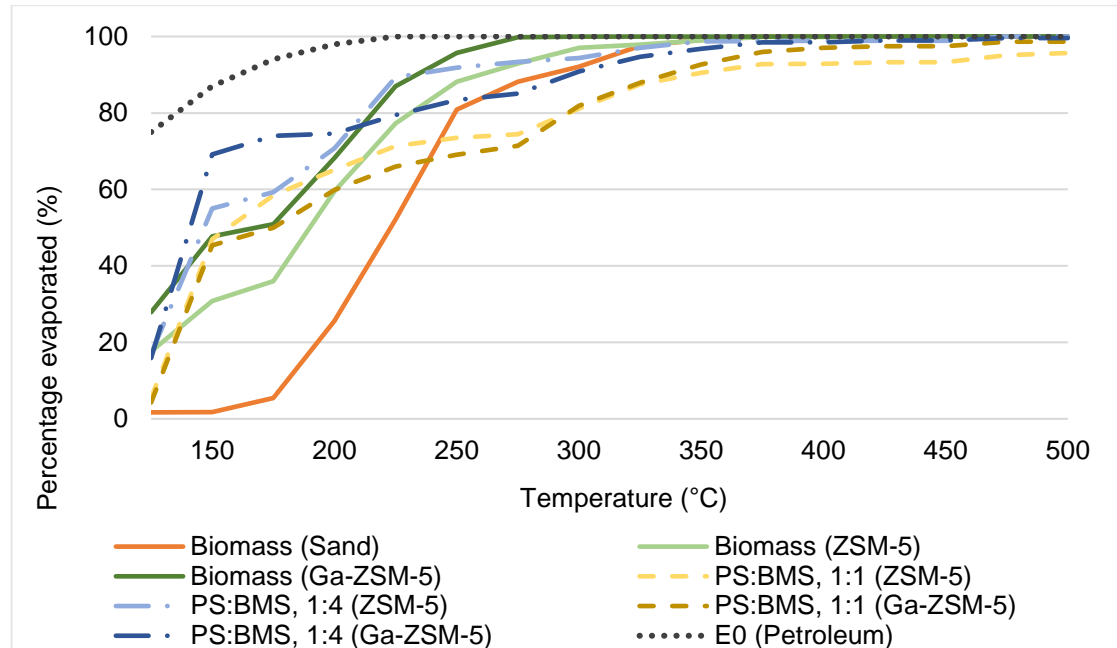
Figure 7.18: Simulated distillation profiles for various catalytic co-pyrolysis oils compared against petroleum (E0).

Whilst there is observable improvement through catalytic co-pyrolysis of biomass and PS, these oils have not been improved enough through this methodology to render them suitable for an automotive application. The low volatility of the oils would reduce the combustion rate of the fuel within the cylinder of an engine which can impact on the cycle timings of an engine with the potential to reduce the cycle efficiency and lead to incomplete combustion of the fuel. This is particularly problematic in engines with rapid cycle rates such as those used for road transportation although this is less problematic in lower rate engines such as generators or for maritime applications which run using fuel oil. However, it is important to restrict the amount of phenolics and styrene as these may contribute to failure of fuel pumps and filters if present in high concentrations. Phenolic compounds such as 4-cumyl-phenol (4-(1-methyl-1-phenylethyl)-phenol) have been linked to thickening of oils leading to damage

of equipment through increased load and seizing of mobile components with styrene linked to formation of polystyrene which has been identified in blocked fuel filters. Failure of engines, leading to loss of power is a particular danger in maritime applications [284, 285].

The co-pyrolysis with PS brings about beneficial changes in the oil produced during pyrolysis of biomass, particularly with regards to oxygen content. However, there are also drawbacks to this approach with the styrene presenting a particular possibility for valorisation but also a concern if high concentrations remain in the oil. It is clear that further offline upgrading would be required beyond that presented by online ex-situ catalysis. Hydroprocessing would be suitable for this and the improvement in oil properties, particularly the reduction in oxygen content would reduce the quantity of hydrogen needed to provide further upgrading.

7.7 Conclusion

Catalytic co-pyrolysis using metal-impregnated ZSM-5 catalysts was able to facilitate deoxygenation of the pyrolysis oils from biomass and polystyrene, particularly in the case of gallium and cobalt impregnated ZSM-5. This deoxygenation follows the three main pathways with deoxygenation through decarbonylation, decarboxylation and hydrodeoxygenation. Gallium impregnated ZSM-5 and cobalt impregnated ZSM-5 both utilise a mixture of these three reaction pathways. At a 1:1 mixing ratio of biomass and polystyrene the deoxygenation reactions for the metal-impregnated ZSM-5 catalysts were generally close in scale to those for the unmodified ZSM-5. Gallium and cobalt impregnated ZSM-5 showed greater deoxygenation than unmodified ZSM-5 from measuring deoxygenation products (Karl-Fischer titration and GC) and this was consistent with the proportions of oxygenated products identified using GC-MS. When the mixing ratio of biomass to polystyrene was 4:1 the proportion of oxygenated compounds in the oils increased for ZSM-5 (unmodified). As the oxygen content of the feedstock has increased considerably, due to the increase in proportion of biomass with a high oxygen content and the reduction in polystyrene which has a low oxygen content and produces a high oil yield, this follows expectation. However, at the 4:1 mixing ratio the deoxygenation of the metal-modified catalysts was more effective compared to the ZSM-5 (unmodified) particularly for gallium and cobalt.

The oil yield was also affected by the change in feedstock mixture ratio. It was observed that with gallium and cobalt impregnated ZSM-5 the method of deoxygenation (decarbonylation, decarboxylation or hydrodeoxygenation) was

a strong factor in determining the size of the oil yield. For a feedstock with more polystyrene (1:1 mixture), deoxygenation using gallium modified ZSM-5 which uses hydrodeoxygenation predominantly led to coke formation and therefore reduced oil yields. In a feedstock which contained a lower proportion of polystyrene (4:1) deoxygenation using cobalt modified ZSM-5 which deoxygenates predominately through carbon oxides led to an observable loss in oil yield compared to gallium though in both cases similar levels of deoxygenation were observed for the two catalysts. These findings show that although different metal-impregnated catalysts may promote deoxygenation to a similar degree a particular catalyst may be more suited to a specific feedstock. This is especially clear in the case of oil yield and this might require than feedstock processing for catalytic-pyrolysis needs to be carefully controlled in order to maximise oil yields.

The temperature of the catalyst bed in the reactor was examined using gallium impregnated ZSM-5 (objective 10). Changing the temperature of the catalyst bed from 450°C to 500°C decreased deoxygenation via water formation whilst at the same time increasing the formation of carbon oxides. This produced only a small effect on the overall deoxygenation during this temperature increase from 450-500°C, however, further temperature increases reduce the water formation further whilst leaving the carbon oxide formation relatively stable. The overall effect of this was that an increase in temperature above 500°C reduces deoxygenation reactions using the gallium modified ZSM-5 catalyst but the reduction was not considerable.

Thermal degradation of biomass and the plastic samples was practically complete by 500°C (see chapter 5) which makes this an efficient temperature for the devolatilisation region in the two-stage fixed-bed reactor. Temperatures of between 450-500°C are suitable for the catalyst bed in the two-stage reactor as this maximises oil yield whilst also maximising deoxygenation reactions which are useful for producing oils suitable for fuel use. Increasing the temperature further would reduce the energy efficiency of the reactor with little additional gain other than a slight increase in oil yield although this gain in oil yield is mainly due to an increase in oxygen content, which is undesirable.

The mixing ratio was also examined using gallium modified ZSM-5 catalyst to upgrade the volatiles from co-pyrolysis of biomass and polystyrene (objective 10). It was clear that as the biomass proportion of the mixture increased the oil yield decreased and the oxygen content of the oils increased, however, it is probable that the optimal mixture ratio for fuel use would be somewhere between a 4:1 and 19:1 mixture of biomass and polystyrene. In the 1:1 and 1:0

mixtures there is significant formation of polyaromatic hydrocarbon compounds compared to the intermediate mixtures. During individual pyrolysis of biomass, the PAHs formed were mainly naphthalene and indene compounds whereas as the polystyrene content of the mixture was increased, the polyaromatic hydrocarbons are mostly due to dimers and trimers of styrene. The 4:1 mixture ratio gives a good compromise of results with high primary aromatic yield whilst retaining high oil yields, low phenolic content and low PAH content. It is possible that a slightly different mixture could give an improved yield and composition however only a limited range of mixtures were examined. The results obtained at each mixture ratio might vary if a different catalyst was used besides gallium impregnated ZSM-5 and that might be a suitable target for further research.

Simulated distillation was used to compare the different combinations of catalysts and mixtures against a standard gasoline fuel to identify the extent of any improvement in the upgrading process (objective 13). It was clear that both co-pyrolysis using polystyrene as well as catalytic pyrolysis were able to affect the distillation profile of the pyrolysis oils produced and that this improved the profile of the oil compared to non-catalytic pyrolysis of biomass. However, the oils which were produced, whilst becoming closer in profile towards a standard petroleum fuel, were not improved enough to stand as a replacement for a petroleum fuel. Further upgrading would be required to produce fuels using these pyrolysis oils for any of the combinations of catalyst and co-pyrolysis used. It is worth noting that the improvements which have been possible through these processes might be used to upgrade pyrolysis oils to a level where they could be readily upgraded using standardised petrochemical approaches. This might even include co-processed alongside crude oils using current petroleum refining equipment and processes. However, before co-processing could be considered or undertaken, further analysis would be required to assess the suitability of the oils to ensure that this would not introduce problems to the process through issues such as miscibility problems or potential corrosion of the refinery infrastructure.

Primary aromatics including styrene, benzene, toluene, xylene and ethylbenzene were produced during catalytic pyrolysis of both polystyrene and biomass and the mixture of these products could be modified to some extent through alteration of the mixing ratio. If it is economically feasible to extract styrene from the pyrolysis oil mixtures it may be possible to utilise co-pyrolysis to upgrade the oils from biomass through deoxygenation before extracting the styrene to increase the economic return possible for the overall process.

Chapter 8: Conclusions and further work

8.1 Catalytic pyrolysis of biomass

- A biomass sample was pyrolyzed using a two-stage fixed-bed reactor with the gaseous, liquid and solid products collected, yields measured, and the composition of the solid and gaseous fractions analysed. The liquid yield was mainly composed of aromatic hydrocarbon compounds, aliphatic hydrocarbons and water. Analysis of the oil using GC-MS identified 100% of the compounds as containing oxygen. This liquid would not be suitable for use as a fuel or for fuel production due to its corrosive nature. It would also be unstable and have a low energy density due to the high oxygen content. The gaseous pyrolysis products contained carbon dioxide, carbon monoxide, methane, short-chain hydrocarbons and hydrogen.

- When ZSM-5 was used as an ex-situ catalyst for upgrading of the vapours which are produced during pyrolysis of biomass some of the products of pyrolysis were changed in composition as well as yield. The char yield was not affected by the use of an ex-situ catalyst as the sample and the catalyst were not brought into contact. The gaseous products were altered in two major ways. There was an increase in methane and short-chain hydrocarbons, particularly alkenes which are formed during zeolitic cracking of alkane compounds. There was also an increase in carbon monoxide and carbon dioxide which are produced during decarbonylation and decarboxylation of biomass respectively. The liquid yield collected from pyrolysis using ZSM-5 as an ex-situ catalyst was also substantially altered in comparison to non-catalytic pyrolysis with a large increase in water formation through hydrodeoxygenation of biomass. This removal of oxygen as water along with those deoxygenation products in the gas phase (carbon dioxide and carbon monoxide) corresponded with a large decrease in oxygenated compounds identified in the pyrolysis oils. The removal of oxygen from the compounds identified in the pyrolysis oils would produce an oil which is more suitable for fuel use than that produced without the benefit of the catalyst. The drawback of this catalytic upgrading is a reduction in the yield of oil compounds which was reduced by the removal of oxygen as well as the carbon and hydrogen atoms necessary to facilitate the oxygen removal. There was also a reduction in oil yield due to the

catalytic cracking with an equivalent increase in gaseous yield. There was also an increase in PAH compounds during pyrolysis with the ZSM-5 catalyst. The presence of these compounds in fuels should be kept to a minimum due to their role in coke formation and their toxicity and although some limited amount may be present in fuel they are preferably avoided.

- Metal impregnated (Cu, Co, Ni, Ga, Fe, Mg and Zn) ZSM-5 catalysts were produced using wet impregnation with a 5 wt.% loading of metal. These were used for ex-situ catalytic pyrolysis of the biomass sample. The metal impregnated catalysts had a limited effect on the pyrolysis products. For most of the metal modified catalysts there was little effect on the liquid yield, or a limited reduction compared to unmodified ZSM-5. However, for cobalt, copper and zinc impregnated ZSM-5 there was a small increase in oil yield with the other catalysts remaining at approximately the same oil yield as for the unmodified ZSM-5. Care must be exercised when considering the liquid yield during pyrolysis as this includes water which may be derived directly from the feedstock or may be formed during deoxygenation reactions. Both nickel and cobalt produced high yields of hydrogen gas as well as increased carbon oxide yields during catalytic pyrolysis of biomass compared to unmodified ZSM-5. This might make these catalysts more suitable for gasification processes rather than for pyrolysis. The high hydrogen yields were also accompanied by a reduction in formation of water compared to the unmodified catalyst. This meant that the liquid yields for both cobalt and nickel were lower than expected however, despite the lower liquid yield, the oil yield for both was not reduced.

- Cobalt, copper and gallium impregnated ZSM-5 produced oils in which the proportion of oxygenated compounds reduced compared to the unmodified ZSM-5 whilst nickel, magnesium and iron impregnated catalysts had increased oxygenated compounds. The reduction and increase in identified oxygenated products in the oils were consistent with the increase or decrease of deoxygenation products during pyrolysis. The improvement in the oil yields and composition, using these metal-impregnated catalysts in comparison to the unmodified ZSM-5 was relatively limited. In many of the catalysts any improvements in oxygen content of the oils was counteracted by an increase in undesirable PAH compounds. It is also possible that some of these

catalysts may be more effective with a different loading of metal on the ZSM-5. Zinc and magnesium have been examined in literature with different findings observed at different metal loadings. The ZSM-5 material appears to become susceptible to pore blockage by magnesium and zinc at higher metal loadings it is possible a 1 wt.% metal content would have been more suitable for catalytic pyrolysis using these metals [137,156, 158].

8.2 Thermal decomposition of biomass and plastics

- Thermal decomposition of the plastic (HDPE, LDPE, PP, PET, PS) and biomass samples using TGA-MS analysis was used to study the temperatures over which these materials decomposed and the temperature range over which key pyrolysis products were formed. The analysis was conducted using the same heating profile as that used during the experiments using the two-stage fixed-bed reactor. It was observed that the biomass decomposed at a lower temperature than the plastic samples.

- Thermal degradation of the polyethylene terephthalate and polystyrene samples started during the same temperature range as the degradation of the biomass sample although at a higher temperature whereas the degradation of the polyolefin plastics initiated at near to the temperature at which the biomass had completed thermal degradation. Due to this variation in degradation temperatures it is likely that the interactions between volatile species from the PS and PET samples and biomass will be considerably greater than those with the polyolefin samples. During co-pyrolysis of biomass with the polyolefin samples the volatiles from biomass are likely to have been produced and passed through the reactor prior to formation of volatiles from the polyolefin. In this case any interactions are likely to be limited to solid(liquid)-gaseous interactions between the hot plastic sample and the volatiles from the biomass sample and solid-gaseous interactions between the char from the biomass and the volatiles from the plastic. It is possible there are gaseous-gaseous interactions between biomass volatiles remaining in the porous catalyst and the volatiles from the plastic, but the scale of these interactions will be limited by the pore volume of the catalyst.

- During TGA-MS experiments using (1:1) mixtures of the biomass and plastics it was observed that in most cases the initial temperature of the biomass decomposition changed towards a higher temperature with the initial decomposition of the plastic sample shifting to a lower temperature. It is possible that the increase in onset for the biomass is due to encapsulation of the biomass sample by melting plastic material and the decrease in onset for the plastics is due to in-situ catalysis of the thermal degradation of the plastics due to the presence of catalytically active biomass char. The biggest convergence of degradation temperatures for biomass and the plastics was observed with biomass and PP with the onset of thermal degradation for the samples shifting 21°C closer together than during individual experiments. Changes detected in the devolatilisation products were limited in scope, although some changes in hydrogen production and formation of deoxygenation products was detected. The degradation of polystyrene was different to the other plastic samples with the temperature of thermal degradation moving to a higher temperature when combined with biomass. It is possible that this might be due to interactions between the PS and the biomass which lead to biomass degradation whilst reducing the availability of radical species required to initiate polystyrene decomposition. At the least it indicates that polystyrene interacts with biomass in a different manner to the other plastics examined.

8.3 Catalytic pyrolysis of plastics

- Catalytic pyrolysis of plastics (HDPE, LDPE, PP, PET and PS) in the two-stage fixed-bed reactor gave high liquid yields compared to those observed for pyrolysis of biomass which is mainly due to a low formation of char (excluding PET) during decomposition of these plastics. The liquid yields produced from the plastic samples contained a lower proportion of water compared to those collected during catalytic pyrolysis of biomass. This is due to a smaller water content of the initial feedstock and a lower formation of water through hydrodeoxygenation as the low oxygen contents of the plastics do not provide the available oxygen for hydrodeoxygenation to occur. This gives an oil yield for the plastic samples which is much larger than that for biomass.

- The compounds identified in the oils from catalytic pyrolysis of the plastics (excluding PET) contained a low proportion of oxygenated

compounds which is as would be expected considering the low oxygen content of the initial samples however there are drawbacks to direct pyrolysis of the plastics. The catalytic pyrolysis of polystyrene produced a high proportion of PAH compounds and high molecular weight aromatic compounds ($>C_{13}$) whereas the pyrolysis of the polyolefin compounds produced high proportions of high molecular weight ($>C_{13}$) aliphatic compounds. The PET produced a relatively high proportion of PAH compounds as well as a considerable yield of char most likely due to deposition of terephthalic acid and benzoic acid species. Whilst these oils do not contain the same undesirable oxygenated compounds as those present in the biomass pyrolysis oils, they would be problematic for fuel use due to their high molecular weight and PAH compounds. Further upgrading would be required before they were suitable to be used for fuels.

8.4 Catalytic co-pyrolysis of biomass and plastics

- Catalytic co-pyrolysis of biomass and plastics was undertaken using the two-stage fixed-bed reactor at different mixture ratios with the pyrolysis product yields and compositions examined to identify if it would be possible to produce oils which are more suitable for fuel use than the oils from individual pyrolysis of biomass or plastics.

- Co-pyrolysis of biomass with polyolefins at a 1:1 mixing ratio gave oils which were similar to predicted values calculated from the two individually pyrolysed samples. These oils had lower oxygenated content than the oils from biomass alone and lower proportions of high molecular weight compounds than those from the polyolefins alone. However, this variation appears to be due to additive effects rather than due to any interactions between the two constituents during pyrolysis. It is likely that the difference in temperature of thermal degradation is a major cause of this absence of interactions between the samples. This shortage of interaction could potentially be improved by increasing the heating rate such that devolatilisation of both samples occurs near to simultaneously. When a mixing ratio which contained a greater proportion of biomass was used (4:1, 9:1) the number of deoxygenation reactions appeared to increase slightly which may be an indication that the polyolefin vapours are interacting with the volatiles from biomass pyrolysis which are remaining within the pores of the catalyst. However,

the overall effect of increasing the proportion of biomass in the mixture is to produce an oil less suited to fuel use due to increased oxygen content in the oil.

- Co-pyrolysis of biomass with PET gave oils which were similar in nature to oils predicted for the mixtures of biomass and PET used with limited interactions observed. In general, the oil yields were poor during co-pyrolysis of biomass with PET due to an increase in coke formation although this could be minimised by reducing the proportion of PET in the mixture. However, this produced co-pyrolysis oils which were less poor, and these oils would still require intensive upgrading to be considered for fuel use. The co-pyrolysis did not produce oils which were more suited for fuel use than either of the oils produced during individual pyrolysis.

- Co-pyrolysis of biomass with polystyrene gave the most promising results with interactions between the biomass and polystyrene constituents producing an increase in deoxygenation products and a reduction in oxygenated compounds identified in the oils. The highest oil yields were achieved in at a 1:1 mixing ratio of biomass and polystyrene with oil yields decreasing as the ratio of biomass in the mixture was increased. This was due to two effects. The high oil yield of polystyrene compared to that of biomass meant that the oil yield decreased as the proportion of biomass increased due to additive effects. However, there was also a decrease in the yield of oil as the proportion of biomass was increased further than that predicted by calculation. This was due to an increase in water and gas formation. The increase in water and gas yield at the cost of the oil yield was due to increased formation of deoxygenation products. The increase in deoxygenation products was consistent with a reduction in oxygenated compounds identified in the oil during GC-MS analysis. These non-additive effects act counter to the additive effects such that increasing the proportion of biomass in the mixture increases the deoxygenation of the oils but results in an increase in overall oxygenated compounds due to the increased oxygen content of the sample mixture used as the feedstock for pyrolysis.

- The change in co-pyrolysis sample mixture can be used to alter the pyrolysis products. In general, the pyrolysis product yields and

compositions reflect the properties of the individual samples in the mixture. However, it can also be observed that there are co-pyrolysis interactions which change the pyrolysis products. This has been most clearly seen through deoxygenation reactions or formation of aromatic compounds. Consideration needs to be given to both effects. These non-additive effects were most clearly observed during co-pyrolysis of biomass with polystyrene.

- Catalytic co-pyrolysis of biomass and the plastics did not produce a large enhancement or reduction in coke deposition on the catalysts with values approximately midway between those for individual biomass and individual plastics.

8.5 Co-pyrolysis of biomass and PS with metal impregnated ZSM-5 catalysts

- Co-pyrolysis of biomass and polystyrene with ex-situ metal impregnated ZSM-5 catalysts was examined at different mixing ratios to identify the effect this might produce on the yield and composition of pyrolysis products. By comparing the metal-impregnated catalysts against the unmodified ZSM-5 catalyst at different mixing ratios of biomass and polystyrene it was possible to identify differences in the function of the catalysts which could produce improved pyrolysis oils.

- Catalytic co-pyrolysis of biomass and polystyrene at a mixing ratio of 1:1 gave small improvements in oil yield compared to the unmodified ZSM-5 in most cases. The metal impregnated catalysts also appeared to improve the deoxygenation of the pyrolysis oils to a small extent. The catalysts which produced the greatest deoxygenation / lowest oxygenated compounds identified in the oil were cobalt and gallium impregnated ZSM-5 whilst several of the other catalysts gave apparent improvement compared to the unmodified ZSM-5 albeit within the range of standard deviation. Several of the catalysts (Ga, Ni, Cu) produced high coke deposition at a 1:1 mixture ratio which reduced the oil yield with the effect most severe on the nickel catalyst which produced both high residue formation and high hydrogen gas formation.

- At a 4:1 mixing ratio of biomass to polystyrene the proportion of oxygenated compounds in the oils from un-modified ZSM-5 catalysis and non-catalytic pyrolysis increased significantly compared to the 1:1 mixture. However, the values for the metal-impregnated catalysts remained lower than expected. As with the 1:1 mixing ratio, gallium and cobalt produced the greatest deoxygenation effect and the lowest proportion of oxygenated compounds was identified in the oils produced using these catalysts. In this case however, the oil yield for cobalt was severely diminished both compared to the other metal-impregnated catalysts and compared to the unmodified ZSM-5. The unmodified ZSM-5 produced a higher oil yield compared to the metal impregnated catalysts in the 4:1 mixture however this is due to much lower deoxygenation occurring for the unmodified ZSM-5 catalyst compared to the metal-impregnated catalysts. The large reduction in oil yield for cobalt appears to be due to deoxygenation reactions producing high yields of carbon monoxide and thereby removing oxygen at the cost of carbon atoms required for a high oil yield. In contrast, gallium impregnated ZSM-5 removes a greater proportion of oxygen via hydrodeoxygenation thereby limiting the loss to the oil yield. The formation of residue/ coke is much reduced in the 4:1 mixture such that the oil yield for gallium is not reduced by coke formation as it was in the 1:1 mixture.

- The results for gallium and cobalt impregnated ZSM-5 would indicate that in the 1:1 mixture where polystyrene makes up a high proportion of the sample, deoxygenation with gallium impregnated ZSM-5 predominately using hydrodeoxygenation led to formation of coke and loss in oil yield. In contrast deoxygenation using cobalt impregnated ZSM-5 which utilised predominately decarbonylation did not lead to coke formation, thereby, retaining higher oil yields. In the 4:1 mixture there was more oxygen to be removed than the 1:1 mixture. By using carbon to remove this oxygen mainly through decarbonylation as with cobalt impregnated ZSM-5 has a much more significant effect on the oil yield than in the 1:1 mixture. Both gallium and cobalt impregnated ZSM-5 were effective at deoxygenation but each was suited to one particular feedstock more than another, particularly with regards to oil yield retention. If metal-impregnated ZSM-5 catalysts are utilised for co-pyrolysis it would be important to control the feedstock composition

to ensure that the oil yields were maximised as the effectiveness of the catalyst appears to be reliant on the composition of the feedstock.

8.6 Temperature of co-pyrolysis

- Changing the temperature of the catalyst bed used for pyrolysis of biomass and polystyrene with the gallium-impregnated ZSM-5 catalyst altered the reactions which were acting to remove oxygen from the oils. As the temperature increases from 450°C deoxygenation via hydrodeoxygenation reduces and deoxygenation via decarbonylation and decarboxylation. Above 500°C deoxygenation through carbon oxides does not increase significantly. The overall effect is that deoxygenation is highest between 450°C and 500°C and above this temperature it becomes reduces to a limited degree. The oil yield increases slightly above 500°C but as this is due to a small increase in oxygen content it is not an advantageous increase in oil yield for fuel production. These temperature effects were only measured using the gallium-impregnated ZSM-5 so it is possible that a different range of temperatures might be more suitable were a different metal-impregnated catalyst investigated. Changing the temperature of the catalyst had an effect on the production of hydrogen which increased as the temperature was increased, and this was accompanied by a small reduction in primary aromatic compounds. It is possible that the formation of hydrogen is therefore related to the reduction in primary aromatic compounds. The change in temperature had a limited effect on the proportion of PAH compounds identified however it did change the type of PAH compounds formed with naphthalene compounds more prevalent at higher temperatures.

8.7 The effect of mixing ratio on co-pyrolysis

- Changing the mixing ratio has a large impact on the oil yield and composition during catalytic co-pyrolysis. At a 1:1 mixture ratio of biomass and polystyrene with gallium impregnated ZSM-5 the oil yield was the highest of the mixtures considered. As the proportion of biomass was increased the oil yield decreased and the proportion of compounds identified which were phenolic or oxygenated increased. In order to maximise the oil yield and the proportion of oil compounds which do not contain oxygen a high polystyrene proportion should be used in the sample mixture. However, in the 1:1 mixture the proportion of PAH

compounds is at its highest and this decreases as the mixture tends towards pure biomass at which point it increases again. The mixtures which exhibits the highest deoxygenation and highest primary aromatic content is the 4:1 mixture which is possibly the optimal mixture for fuel production as it retains relatively high oil yields and low oxygenated content whilst also containing a lower PAH content than the 1:1 mixture.

- Primary aromatic compounds such as styrene have a higher value as a chemical than they would receive as part of a fuel, however, it is potentially challenging to remove these compounds from a complex oil such as those pyrolysis oils produced in this research. If styrene is able to be extracted at a reasonable cost, there would be the potential to use co-pyrolysis of biomass and polystyrene to upgrade the biomass compounds through deoxygenation before extracting the styrene to add value to the process. This proposal would depend on the feasibility of extracting the styrene, however if this was achieved then the 4:1 mixture might be the most suitable as it optimises the deoxygenation of the biomass oils and it is the oil mixture which contains the highest proportion of styrene.

- If fuel is being produced without removal of styrene this mixture might be problematic due to the high proportion of styrene as a proportion of the oil. It is possible that this could introduce handling or processing issues if conditions were present which caused polymerisation to occur. In this case a mixture with lower polystyrene content might be favourable as a change in mixture from 4:1 through to a 99:1 has a minimal effect on the types of compounds in the oil (lower PAH but higher oxygenated compounds) but reduces the proportion of styrene significantly. Although the drawback to this is that oil yields decrease as the proportion of polystyrene in the feedstock are reduced.

8.8 Simulated distillation and overview

- Simulated distillation of catalytic co-pyrolysis oils was used to provide a comparison against a standard motor gasoline (E0). The non-catalytic pyrolysis of biomass provided a poor match to gasoline and this is improved through use of ZSM-5 and further improved by the gallium-impregnated ZSM-5. However, these pyrolysis oils are still unsuitable for

fuel use when compared to the standard gasoline. Alteration of the mixing ratio was able to improve the distillation profile at lower temperature however, this reduced the fitting at higher temperatures particularly through the formation of PAH compounds. All of the oils produced through combinations of metal-impregnated catalysts and co-pyrolysis used in this research would need to be upgraded considerably before utilisation as a fuel was possible. The changes which have been achieved through catalytic co-pyrolysis has improved these oils to a degree where less forceful conditions would be needed to upgrade these oils further which would be economically and energetically beneficial. It may even be possible to upgrade some of the catalytic co-pyrolysis oils in this research through co-processing alongside crude oil. However, further research would be necessary to confirm if this could be achieved without damaging or degrading the refining process and equipment. It would also need to be established if this could be achieved at an economically feasible cost.

- The results from this research indicate that there is a potential pathway for production of both chemical feedstock compounds and fuels through catalytic co-pyrolysis. For both applications there are still major limitations to the utilisation of this technology. For production of fuels it is clear that control of the products is of paramount importance particularly to be able to control size of compounds such that they are appropriate to use in fuels, the remove the oxygen which is present in the initial feedstock and for inhibition of PAH compounds.

- Changing of the mixing ratio between biomass and plastic in the feedstock was able to provide some control of molecular size but this was mainly through additive effects rather than reactions between the constituent components. Use of different catalysts also provided some control over molecular size however this had the drawback of producing increased coke deposition or increased PAH formation at times.

- Deoxygenation was clearly observed during catalytic pyrolysis and this was enhanced during pyrolysis of biomass with polystyrene which reduced oxygen content both through deoxygenation and through additive effects which effectively dilute the oxygen content in the feedstock. This was also advantageous due to the high efficiency of oil

formation through polystyrene pyrolysis for which PAH formation was reduced through interactions with the biomass. The metal impregnated ZSM-5 catalysts also contributed to deoxygenation reactions particularly where biomass was present as a higher proportion of the feedstock although these deoxygenation reactions were most effective in the feedstock mixtures which contained more oxygen initially and therefore any improvement gained through oxygen removal was countered by an increase in total oxygen in the feedstock which passed into the oils.

- The catalysts which were utilised during this research were basic in design and utilisation and it may be possible that more sophisticated catalysts are able to improve the deoxygenation and size templating of the oil compounds. Whilst improvements were observed through catalytic co-pyrolysis the oils which were produced remained unsuitable for fuel use and further upgrading would be required before they might be utilised to produce fuels.

- It must also be considered that the feedstocks which were examined though this research were chosen to be representative of 'real-world' samples however they had to be homogenous and high quality to ensure that feedstock variation did not contribute excessively to variation observed in the results. If catalytic co-pyrolysis of biomass and plastics was commercialised the biomass and plastics would most likely be using feedstocks which are of a lower quality. This would to impact the results of pyrolysis in several ways including increased moisture content of oils, poisoning of catalyst, natural in-situ catalysis caused by metals present in the biomass and plastic feedstocks as well as potential emission of heavy metals in the gaseous products or concentration of heavy metals within the oils themselves. Further work would be needed to ensure that these effects could be avoided or minimised. These lower-quality feedstocks would also affect the composition and yield of oils produced.

8.9 Further work

- This research used a two-stage fixed-bed reactor to run the catalytic pyrolysis experiments in a manner which allows for detailed analysis of the products of pyrolysis both in terms of yield and composition and this is assisted by the equipment which allows for separation of the various pyrolysis products as well as control over the conditions the feedstock is

exposed to. However, the equipment which would be utilised during a commercial operation would have different design requirements which may have a major impact on the pyrolysis products. A commercial operation would be expected to use a continuous feed process with high heating rates and in-situ catalysis. It would be valuable to examine how these feedstocks and catalysts might be affected by using a reactor such as a fluidised bed reactor in order to observe the effect this produces on the yield and the composition of the pyrolysis products as well as the effectiveness of the catalysts. It would be expected that in this type of reactor the particle sizes of the catalyst and feedstock would be a much more important factor in determining the pyrolysis products. The increased heating rate would have an impact as would the vapour residence time within the reactor. There would potentially be higher catalyst degradation due to contact between the char from the feedstock with the catalyst particles. The major advantage of this methodology would be an increase in interactions between the volatiles produced by biomass and the plastic feedstock due to rapid heating of the samples such that near simultaneous thermal degradation of the feedstock might produce an increase in non-additive interactions which could be valuable for further upgrading of the pyrolysis vapours. This would be particularly important for the polyolefin plastics where the temperature of thermal degradation is outside the range of thermal degradation of the biomass.

- The research undertaken here has focused on relatively high-quality feedstocks however if this process is to be commercialised it is probable that a wider variety of feedstocks would be used. It would be expected that these would include lower-grade materials due to the high availability and lower cost of these materials compared to virgin and highly processed recycled material which have value for other purposes. This would introduce further issues into the pyrolysis process which would need to be understood and minimised for the process to be viable. The key contaminants are likely to include metal elements such as alkali and alkaline earth metals as well as heavy metals such as cadmium and mercury. Further research would be needed to identify and understand the fate of elements such as these during catalytic co-pyrolysis. It is important to understand if these elements might contaminate the oils or pass into the gas phase and become airborne pollutants which would require pollution mitigation. These elements might also act as catalysts and change the yield and composition of pyrolysis products or might

affect the economics of the process by causing detriment to equipment or deactivation of the catalysts.

- Recycled or waste plastics used in a large-scale process might not be as thoroughly separated as those used during this research which has utilised high-grade recycled plastic sources. Mixtures which include multiple different plastic types may interact with each other during co-pyrolysis in a manner which might be advantageous for fuel production or might introduce further issues. The presence of halogenated plastics such as Polyvinylchloride (PVC) could also have a damaging effect on the process and equipment as well as producing pollution. It would be valuable to identify how the presence of mixtures such as those including PVC affect the pyrolysis process however great care would be needed if studying this to ensure any halogenated by-products are appropriately handled. This might pose a risk to the operator of the equipment and may be detrimental to pyrolysis and analytical equipment so appropriate risk assessment must be undertaken.

- Elemental analysis would be useful to give further insight into the quantities of oxygen which partitions into the oils during pyrolysis. This was not examined during this research due to the uncertainty introduced to the elemental analysis when testing volatile oils. It would be extremely valuable to develop and validate a procedure to ensure that the values obtained using the methodology were representative for the samples examined. This would be an excellent tool which would add greater understanding and confidence to the results obtained during this research which have been limited though use of semi-quantitive methodologies. It might also be useful to develop HPLC, GC-FID or NMR methodologies to be utilised alongside GC-MS to give further understanding of the whole oil sample where GC-MS is limited to providing data on the compounds in the oil which lie between a range of molecular sizes.

- It would also be useful to examine the effect of metal loading percentage on the effectiveness of the metal-impregnated ZSM-5 catalyst as results during this research and literature have indicated that magnesium and zinc impregnated ZSM-5 may be less effective at higher metal loadings due to blockage of pores in the catalyst.

References

1. IEA. *Key world energy statistics 2019*. [Online]. 2019. [Accessed 17 October 2019]. Available from: https://webstore.iea.org/key-world-energy-statistics-2019.

2. UNFCCC. *KP Introduction – Kyoto Protocol*. [Online]. 2018. [Accessed 29 August 2018]. Available from: https://unfccc.int/process/the-kyoto-protocol

3. IPCC. *Climate Change 2013: The Physical Science Basis*. [Online]. 2018. [Accessed 29 August 2018]. Available from: http://www.ipcc.ch/report/ar5/wg1/

4. EC. *Environment – Waste*. [Online]. 2018. [Accessed 29 August 2018]. Available from: http://ec.europa.eu/environment/waste/index.htm

5. BEIS. *Energy Consumption in the UK (ECUK) 2018*. [Online]. 2018. Available from: https://www.gov.uk/government/statistics/energy-consumption-in-the-uk

6. DFT. *Vehicle licensing statistics: Quarter 3 (Jul-Sept) 2017*. [Online]. 2017. [Accessed 26 June 2018]. Available from: https://assets.publishing.service. gov.uk/government/uploads/system/uploads/attachment_data/file/666905/ Vehicle-Stats-Release-2017-Q3.pdf

7. BP. *BP Statistical review of world energy - June 2018*. [Online]. 2018. [Accessed 26 July 2018]. Available from: https://www.bp.com/ content/dam/bp/en/corporate/pdf/energy-economics/statistical-review/bp-stats-review-2018-oil.pdf

8. Vaclav, S. *Energy and civilisation: A history. Cambridge:* MIT Press. 2017

9. Klass, D. *Biomass for renewable energy, fuels, and chemical*. San Diego: Academic Press. 1998.

10. Van Loo, S. and Koppejan., J., *The handbook of biomass combustion and co-firing.* London: Earthscan, 2008.

11. Speight, J.G. *Handbook of petroleum product analysis*. Hoboken: John Wiley and sons, Inc., 2002.

12. EC*. Biofuels – Land use change*. [Online]. 2018. [Accessed 28 August 2018]. Available from: https://ec.europa.eu/energy/en/topics/renewable-energy/ biofuels/land-use-change

13. Edinburgh University. *Energy from waste and wood*. [online]. 2007. [Accessed 18 July 2016]. Available from: http://energyfromwasteandwood.weebly.com/ generations-of-biofuels.html.

14. ETIP Bioenergy. *Advanced biofuels in Europe*. [online]. 2018. [Accessed 18 July 2018]. Available from: http://www.etipbioenergy.eu/?option=com_content &view=article&id=287#generations

15. Geyer, R., Jambeck, J.R. and Law, K.L. Production, use, and fate of all plastics ever made. *Science Advances*, 2017, **3**(7), DOI:10.1126/sciadv.1700782. [Accessed 26 July 2018]. Available from: http://advances.sciencemag.org/content/3/7/e1700782.full

16. Melero, J.A., Iglesias, J. and Garcia, A. Biomass as renewable feedstock in standard refinery units. Feasibility, opportunities and challenges. *Energy and Environmental Science.* [Online]. 2012, **5**(6), pp. 7393-7420. [Accessed 27 August 2018]. Available from: http://dx.doi.org/10.1039/C2EE21231E

17. Carpenter, D., Westover, T.L., Czernik, S. and Jablonski W. Biomass feedstocks for renewable fuel production: a review of the impacts of feedstock and pretreatment on the yield and production distribution of fast-pyrolysis oils and vapours. *Green Chemistry.* [Online]. 2014, **16**(2), pp. 384-406. [Accessed 27 August 2018]. Available from: http://dx.doi.org/10.1039/C3GC41631C

18. Welfle, A., Gilbert P. and Thornley P. Securing a bioenergy future without imports. *Energy Policy.* [Online]. 2014, **68**, pp.1-14. [Accessed 26 July 2018]. Available from: https://www.sciencedirect.com/science/article/pii/S03014215513012093

19. RECOUP. *UK Household Plastics collection survey 2017*. [Online]. 2017. [Accessed 26 July 2018]. Available from: http://www.recoup.org/p/275/publications

20. DEFRA. *UK Statistics on waste - Feb 2018.* [online]. 2018. [Accessed 26 July 2018]. Available from: https://assets.publishing.service.gov.uk/government/uploads/system/uploads/attachment_data/file/683051/UK_Statisticson_Waste_statistical_notice_Feb_2018_FINAL.pdf.

21. Forest Research. *Tools and resources – Fuels* [online]. 2018 [Accessed 28 August 2018]. Available from: https://www.forestresearch.gov.uk/tools-and-resources/biomass-energy-resources/fuel/

22. DRAX. *Sustainability - responsible sourcing.* [Online]. 2018. [Accessed 28 August 2018]. Available from: https://www.drax.com/sustainability/sourcing/

23. DECC. *UK Bioenergy Strategy.* [Online]. 2012. [Accessed 15/06/2018]. Available from: https://www.gov.uk/government/publications/uk-bioenergy-strategy

24. Chatham House. *Woody biomass for power and heat: impacts on the global climate.* [Online]. 2017. [Acessed 25/07/2018]. Available from: https://www.chathamhouse.org/publication/woody-biomass-power-and-heat-impacts-global-climate

25.   IEA Bioenergy. *Response to Chatham House report "Woody Biomass for Power and Heat: Impacts on the Global Climate"* [Online]. 2017. [Accessed 25/07/2018]. Available from: https://www.chathamhouse.org/sites/default/files/publications/2017-04-05-IEABioenergy.pdf

26.   Lee, S. Chapter 15: Thermochemical conversion of biomass In: Lee, S., Speight, J. and Loyalka, S. eds. *Handbook of alternative fuel technologies*. Boca Raton: CRC Press, 2015, pp. 471-522.

27.   Bridgewater, A.V. Review of fast pyrolysis of biomass and product upgrading. *Biomass and Bioenergy.* 2012, **38**, pp.68-94.

28.   Dahlquist E. Simulations of combustion and emissions characteristics of biomass-derived fuels. In: Dahlquist, E. ed. *Technologies for converting biomass to useful energy: combustion, gasification, pyrolysis, torrefaction and fermentation.* [Online]. Boca Raton: CRC Press, 2013, pp. 1-5. [Accessed 7 November 2017]. Available from: https://www.taylorfrancis.com/books/e/9780429217135.

29.   Poritosh, R. and Gorrety, D. Prospects for pyrolysis technologies in the bioenergy sector: A review. *Renewable and Sustainable Energy Reviews.* [Online]. 2017, **77**, pp. 59-69. [Accessed 29 August 2018]. Available from: http://www.sciencedirect.com/science/article/pii/S1364032117304719

30.   Liu, C., Wang, H., Karim, A.M., Sun, J. and Wang, Y. Catalytic fast pyrolysis of lignocellulosic biomass. *Chemistry Society Reviews.* [Online]**.** 2014, **43**(22), pp.7594-7623. [Accessed 12 February 2016]. Available from: https://www.sciencedirect.com/science/article/pii/S001623611400287

31.   Boslaugh, S.E. Encyclopaedia Britannica – Pyrolysis [Online]. 2019. [Accessed 16 January 2019]. Available from: https://www.britannica.com/science/pyrolysis.

32.   Staš, M., Kubička, D., Chuboba, J. and Pospíšil, M. Overview of analytical methods used for chemical characterization of pyrolysis bio-oil. *Energy & Fuels.* [Online]. 2014. **28**(1), pp.385-402. [Accessed 16 January 2014]. Available from: https://doi.org/10.1021/ef402047y.

33.   Wang, S., Dai, G., Yang, H. and Lu, Z. Lignocellulosic biomass pyrolysis mechanism: A state-of-the-art review. *Progress in Energy and Combustion Science.* [Online]. 2017. **62**, pp.33-86. [Accessed 7 January 2019]. Available from: http://www.sciencedirect.com/science/article/pii/S0360128517300266.

34.   Di Blasi, C. Modeling chemical and physical processes of wood and biomass pyrolysis. *Progress in Energy and Combustion Science.* [Online]. 2008. **34**(1), pp.47-90. [Accessed 8 November 2018]. Available from: http://www.sciencedirect.com/science/article/pii/S0360128507000214.

35. Asadieraghi M., Wan Daud, W.M.A. and Abbas, H.F. Model compound approach to design process and select catalysts for in-situ bio-oil upgrading. *Renewable and Sustainable Energy Reviews*. [Online]. 2014. **36**, pp.286-303. [Accessed 8 November 2018]. Available from: http://www.sciencedirect.com/science/article/pii/S1364032114002883.

36. Aggarwal, S.K. Simulations of combustion and emissions characteristics of biomass-derived fuels. In: Dahlquist, E. ed. *Technologies for converting biomass to useful energy: combustion, gasification, pyrolysis, torrefaction and fermentation*. [Online]. Boca Raton: CRC Press, 2013, pp. 5-34. [Accessed 16 January 2018]. Available from: https://www.taylorfrancis.com/books/e/9780429217135.

37. Papari, S. and Hawboldt, K. A review on condensing system for biomass pyrolysis process. *Fuel Processing Technology*. [Online]. 2018. **180**, pp.1-13. [Accessed 17 January 2019]. Available from: http://www.sciencedirect.com/science/article/pii/S0378382018310142.

38. Pattiya, A. Fast pyrolysis. In: Rosendahl, L. ed. *Direct thermochemical liquefaction for energy applications.* [Online]. Duxford: Woodhead publishing, 2018, pp.3-23.

39. Huber, G.W. and Corma, A. Synergies between Bio- and oil refineries for the production of fuels from biomass. *Angewandte Chemie International Edition.* [Online]. 2007. **46**(38), pp.7184-7201. [Accessed 19 November 2018]. Available from: https://onlinelibrary.wiley.com/doi/abs/10.1002/anie.200604504.

40. Guedes, R.E, Luna, A.S. and Torres, A.R. Operating parameters for bio-oil production in biomass pyrolysis: A review. *Journal of Analytical and Applied Pyrolysis.* [Online]. 2018. **129**, pp.134-149. [Accessed 8 January 2018]. Available from: https://www.sciencedirect.com/science/article/pii/S0165237017305697.

41. Talmadge, M.S., Baldwin, R.M., Biddy, M.J., Mccormick, R.L., Beckham, G.T., Ferguson, G.A., Czernik, S., Magrini-Bair, T.D, Foust, T.D., Metelski, P.D., Hetrick, M.R. and Nimlos, M.R. A perspective on oxygenated species in the refinery integration of pyrolysis oil. *Green Chemistry*. [Online]. 2014. **16**(2), pp.407-453. [Accessed 15 November 2018]. Available from: https://pubs.rsc.org/en/content/articlelanding/2014/gc/c3gc41951g#!divAbstract.

42. Morali, U. and Şensöz, S. Pyrolysis of hornbeam shell (Carpinus Betulus L.) in a fixed bed reactor: characterisation of bio-oil and bio-char. *Fuel.* [Online]. 2015. **150**, pp.672-678. [Accessed 21 January 2019]. Available from: https://www.sciencedirect.com/science/article/pii/S0016236115002574.

43. Şensöz, S., Demiral, I. and Ferdi, G.H. Olive bagasse (Olea Europea L.) pyrolysis. *Bioresource Technology,* [Online]. 2006. **97**(3), pp.429-436. [Accessed 21 January 2019]. Available from: https://www.sciencedirect.com/science/article/pii/S0960852405001653.

44. Bridgwater, A.V. and Peacocke, G.V.C. Fast pyrolysis processes for biomass. *Renewable and Sustainable Energy Reviews.* [Online]. 2000. **4**(1), pp.1-73. [Accessed 21 January 2019]. Available from: https://www.sciencedirect.com/science/article/pii/S1364032199000076.

45. Akhtar, J. and Saidina, A.N. A review on operating parameters for optimum liquid oil yield in biomass pyrolysis. *Renewable and Sustainable Energy Reviews.* [Online]. 2012. **16**(7), pp.5101-5109. [Accessed 21 January 2019]. Available from: https://www.sciencedirect.com/science/article/pii/S136403211200367X.

46. Biradar, C.H., Subramanian, K.A. and Dastidar, M.G. Production and fuel quality upradation of pyrolytic bio-oil from Jatropha Curcas de-oiled seed cake. *Fuel.* [Online]. 2014. **119**, pp.81-89. [Accessed 22 January 2019]. Available from: https://www.sciencedirect.com/science/article/pii/S001623611301106X.

47. Sulaiman, F. and Abdullah, N. Optimum conditions for maximising pyrolysis liquids of oil palm empty fruit bunches. *Energy.* [Online]. 2011. **36**(5), pp.2352-2359. [Accessed 22 January 2019]. Available from: https://www.sciencedirect.com/science/article/abs/pii/S0360544210007735.

48. Alvarez, J., Lopez, G., Amutio, M., Bilbao, J. and Olazar, M. Bio-oil production from rice husk fast pyrolysis in a conical spouted bed reactor. *Fuel.* [Online]. 2014. **128**, pp.162-169. [Accessed 23 January 2019]. Available from: https://www.sciencedirect.com/science/article/pii/S0016236114002221.

49. Abdullah, N. and Gerhauser, H. Bio-oil derived from empty fruit bunches. *Fuel.* [Online]. 2008. **87**(12), pp.2606-2613. [Accessed 23 January 2019]. Available from: https://www.sciencedirect.com/science/article/pii/S0016236108000720.

50. Volli, V. and Singh, R.K. Production of bio-oil from de-oiled cakes by thermal pyrolysis. *Fuel.* [Online]. 2012. **96**, pp.579-585. [Accessed 23 January 2019]. Available from: https://www.sciencedirect.com/science/article/pii/S0016236112000282.

51. Encinar, J.M, Beltrán, F.J., Ramiro, A. and González, J.F. Pyrolysis/gasification of agricultural residue by carbon dioxide in the presence of different additives: influence of variables. *Fuel Processing Technology.* [Online]. 1998. **55**(3), pp.219-233. [Accessed 23 January 2019]. Available from: https://www.sciencedirect.com/science/article/pii/S0378382098000526.

52. Islam, M.R., Parveen, M. and Haniu, H. Properties of sugarcane waste-derived bio-oils obtained by fixed-bed fire-tube heating pyrolysis. *Bioresource Technology*. [Online]. 2010. **101**(11), pp.4162-4168. [Accessed 23 January 2019]. Available from: https://www.ncbi.nlm.nih.gov/pubmed/20133132.

53. Pattiya, A. and Suttibak, S. Production of bio-oil via fast pyrolysis of agricultural residues from cassava plantations in a fluidised-bed reactor with a hot vapour filtration unit. *Journal of Analytical and Applied Pyrolysis.* [Online]. 2012. **95**, pp.227-235. [Accessed 23 January 2019]. Available from: https://www.sciencedirect.com/science/article/pii/S0165237012000319.

54. Kim, S.W., Koo, B.S., Ryu, J.W., Lee, J.S., Kim, C.J., Lee, D.H., Kim, G.R. and Choi, S. Bio-oil from the pyrolysis of palm and Jatropha wastes in a fluidized bed. *Fuel Processing Technology*. [Online]. 2013. **108**. Pp.118-124. [Accessed 23 January 2019]. Available from: https://www.sciencedirect.com/science/article/pii/S0378382012001713.

55. Apaydin-Varol, E., Pütün, E.E. and Pütün, A.E. Slow pyrolysis of pistachio shell. *Fuel.* [Online]. 2007. **86**(12), pp.1892-1899. [Accessed 23 January 2019]. Available from: https://www.sciencedirect.com/science/article/pii/S0016236106004893.

56. Makibar, J., Fernandez-Akarregi, A.R., Amutio, M., Lopez, G. and Olazar, M. Performance of a conical spouted bed pilot plant for bio-oil production by poplar flash pyrolysis. *Fuel Processing Technology.* [Online]. 2015. **137**, pp.283-289. [Accessed 23 January 2019]. Available from: https://www.sciencedirect.com/science/article/pii/S0378382015001216.

57. Agblevor, F.A. and Besler, S. Inorganic compounds in biomass feedstocks. 1. Effect on the quality of fast pyrolysis oils. *Energy & Fuels.* [Online]. 1996. **10**(2), pp.293-298. [Accessed 22 January 2019]. Available from: https://pubs.acs.org/doi/10.1021/ef950202u.

58. Liu, W.J., Li, W.W., Jiang, H. and Yu H.Q. Fates of chemical elements in biomass during its pyrolysis. *Chemical Reviews.* [Online]. 2017. **117**(9), pp.6367-6398. [Accessed 8 November 2018]. Available from: https://pubs.acs.org/doi/abs/10.1021/acs.chemrev.6b00647.

59. Pattiya, A. Catalytic pyrolysis. In: Rosendahl, L. ed. *Direct thermochemical liquefaction for energy applications.* [Online]. Duxford: Woodhead publishing, 2018, pp.29-64.

60. Zakzeski, J., Bruijnincx, P.C.A, Jongerius, A.L. and Weckhuysen, B.M. The catalytic valorization of lignin for the production of renewable chemicals.

Chemical Reviews. [Online]. 2010. **110**(6), pp.3552-3599. [Accessed 24 January 2019]. Available from: https://pubs.acs.org/doi/abs/10.1021/cr900354u.

61. Demirbaş, A. Calculation of higher heating values of biomass fuels. *Fuel.* [Online]. 1997. **76**(5), pp.431-434. [Accessed 28 January 2019]. Available from: https://www.sciencedirect.com/science/article/pii/S0016236197855202.

62. Wang, H., Male, J. and Wang, Y. Recent advances in hydrotreating of pyrolysis bio-oil and its oxygen-containing model compounds. *ACS Catalysis.* [Online]. 2013. **3**(5), pp.1047-1070. [Accessed 28 January 2019]. Available from: https://pubs.acs.org/doi/abs/10.1021/cs400069z.

63. Shafizadeh, F. Introduction to pyrolysis of biomass. *Journal of Analytical and Applied Pyrolysis.* [Online]. 1982. **3**(4), pp.283-305. [Accessed 28 January 2019]. Available from: https://www.sciencedirect.com/science/article/pii/016523708280017X.

64. Kilzer, F.J and Broido, A. Speculations on the nature of cellulose pyrolysis. *Pyrodynamics.* [Online]. 1965. **2**, pp.151-163. [Accessed 28 January 2019]. Available from: https://www.fs.fed.us/psw/publications/broido/psw_1965_broido001_kilzer.pdf.

65. Piskorz, J. Radlein, D.S.A.G., Scott, D.S. and Czernik, S. Pretreatment of wood and cellulose for production of sugars by fast pyrolysis. *Journal of Analytical and Applied Pyrolysis.* [Online]. 1989. **16**(2), pp.127-142. [Accessed 28 January 2019]. Available from: https://www.sciencedirect.com/science/article/pii/0165237089850120.

66. Banyasz, J.L., Li, S., Lyons-Hart, J. and Shafer, K.H. Gas evolution and the mechanism of cellulose pyrolysis. *Fuel.* [Online]. 2001. **80**(12), pp.1757-1763. [Accessed 28 January 2019]. Available from: https://www.sciencedirect.com/science/article/pii/S0016236101000606.

67. Anca-Couce, A. Reaction mechanisms and multi-scale modelling of lignocellulosic biomass pyrolysis. *Progress in Energy and Combustion Science.* [Online]. 2016. **53**, pp.41-79. [Accessed 7 January 2019]. Available from: https://www.sciencedirect.com/science/article/pii/S0360128515300150.

68. Banyasz, J.L., Li, S., Lyons-Hart, J. and Shafer, K.H. Cellulose pyrolysis: the kinetics of hydroxyacetaldehyde evolution. *Journal of Analytical and Applied Pyrolysis.* [Online]. 2001. **57**(2), pp.223-248. [Accessed 28 January 2019]. Available from: https://www.sciencedirect.com/science/article/pii/S0165237000001352.

69. Burhenne, L., Messemer, J., Aicher, T. and Laborie M.P. The effect of the biomass components lignin, cellulose and hemicellulose on TGA and fixed bed

pyrolysis. *Journal of Analytical and Applied Pyrolysis.* [Online]. 2013. **101**, pp.177-184. [Accessed 8 November 2018]. Available from: https://www.sciencedirect.com/science/article/pii/S0165237013000168.

70. Wang, S., Ru, B., Lin, H. and Luo Z. Degradation mechanism of monosaccharides and xylan under pyrolytic conditions with theoretical modelling on the energy profiles. *Bioresource Technology.* [Online]. 2013. **143**, pp.378-383. [Accessed 29 January 2019]. Available from: https://www.sciencedirect.com/science/article/pii/S0960852413009450.

71. Shafizadeh, F., Mcginnis, G.D. and Philpot C.W. Thermal degradation of xylan and related model compounds. *Carbohydrate Research.* [Online]. 1972. **25**(1), pp. 23-33. [Accessed 29 January 2019]. Available from: https://www.sciencedirect.com/science/article/abs/pii/S0008621500827421.

72. Patwardhan, P.R., Brown, R.C. and Shanks, B.H. Products distribution from the fast pyrolysis of hemicellulose. *ChemSusChem.* [Online]. 2011. **4**(5), pp.636-643. [Accessed 29 January 2019]. Available from: https://onlinelibrary.wiley.com/doi/abs/10.1002/cssc.201000425.

73. Cho, J., Chu, S., Dauenhauer, P.J. and Huber, G.W. Kinetics and reaction chemistry for slow pyrolysis of enzymatic hydrolysis lignin and organosolv extracted lignin derived from maplewood. *Green Chemistry,* [Online]. 2012. **14**(2), pp.428-439. [Accessed 30 January 2019]. Available from: https://pubs.rsc.org/en/content/articlelanding/2012/gc/c1gc16222e#!divAbstract.

74. Zhou, S., Pecha, B., Van Kuppevelt, M., Mcdonald, A.G. and Garcia-Perez, M. Slow and fast pyrolysis of Douglas-fir lignin: importance of liquid-intermediate formation on the distribution of products. *Biomass and Bioenergy.* [Online]. 2014. **66**, pp.368-409. [Accessed 30 January 2019]. Available from: https://www.sciencedirect.com/science/article/pii/S0961953414001937.

75. Kim, Y.M., Jae, J., Myung, S., Sung, B.H., Dong, J.I. and Park, Y.K. Investigation into the lignin decomposition mechanism by analysis of the pyrolysis product of Pinus radiata. *Bioresource Technology.* [Online]. 2016. **219**, pp.371-377. [Accessed 30 January 2019]. Available from: https://www.sciencedirect.com/science/article/pii/S0960852416311221.

76. Kosa, M. Ben, H., Theliander and Ragauskas A.J. Pyrolysis oils from CO_2 precipitated Kraft lignin. *Green Chemistry.* [Online]. 2011. **13**(11), pp.3196-3202. [Accessed 30 January 2019]. Available from: https://pubs.rsc.org/en/content/articlelanding/2011/gc/c1gc15818j#!divAbstract.

77. Wang, S., Guo, X., Wang, K. and Luo, Z. Influence of the interaction of components on the pyrolysis behaviour of biomass. *Journal of Analytical and*

Applied Pyrolysis. [Online]. 2011. **91**(1), pp.183-189. [Accessed 30 January 2019]. Available from: https://www.sciencedirect.com/science/article/pii/ S0165237011000350.

78. Collard, F.X. and Blin, J. A review on pyrolysis of biomass constituents: mechanisms and composition of the products obtained for the conversion of cellulose, hemicelluloses and lignin. *Renewable and Sustainable Energy Reviews.* [Online]. 2014. **38**, pp.594-608. [Accessed 30 January 2019]. Available from: https://www.sciencedirect.com/science/article/pii/ S136403211400450X.

79. Hosoya, T., Kawamoto, H. and Saka, S. Cellulose-hemicellulose and cellulose-lignin interactions in wood pyrolysis at gasification temperature. *Journal of Analytical and Applied Pyrolysis.* [Online]. 2007. **80**(1), pp.118-125. [Accessed 30 January 2019]. Available from: https://www.sciencedirect.com/ science/article/pii/S0165237007000125.

80. Hosoya, T., Kawamoto, H. and Saka, S. Solid/liquid- and vapor- phase interactions between cellulose- and lignin-derived pyrolysis products. *Journal of Analytical and Applied Pyrolysis.* [Online]. 2009. **85**(1), pp.237-246. [Accessed 30 January 2019]. Available from: https://www.sciencedirect.com/ science/article/pii/S016523700800199X.

81. Sipilä, K., Kuoppala, E., Fagernäs, L. and Oasmaa, A. Characterization of biomass-based flash pyrolysis oils. *Biomass and Bioenergy.* [Online]. 1998. **14**(2), pp.103-113. [Accessed 4 February 2019]. Available from: https://www.sciencedirect.com/science/article/pii/S0961953497100241.

82. Branca, C., Giudicianni, P. and Di Blasi, C. GC/MS characterisation of liquids generated from low-temperature pyrolysis of wood. *Industrial & Engineering Chemistry Research.* [Online]. 2003. **24**(14), pp.3190-3202. [Accessed 4 February 2019]. Available from: https://pubs.acs.org/doi/abs/10.1021/ ie030066d.

83. Oasmaa, A., Elliott, D.C. and Korhonen, J. Acidity of biomass fast pyrolysis bio-oils. *Energy & Fuels.* [Online]. 2010. **24**(12), pp.6548-6554. [Accessed 4 February 2019]. Available from: https://pubs.acs.org/doi/10.1021/ef100935r.

84. Thangalazhy-Gopakumar, S., Adhikari, S., Ravindran, H., Gupta, R.B., Fasina, O., Tu, M. and Fernando, S.D. Physiochemical properties of bio-oil produced at various temperatures from pine wood using an auger reactor. *Bioresource Technology.* [Online]. 2010. **101**(21), pp.8389-8395. [Accessed 4 February 2019]. Available from: https://www.sciencedirect.com/science/ article/pii/S0960852410008965?via%3Dihub.

85.   Encinar, J.M. and Gonzalez, J.F. Pyrolysis of synthetic polymers and plastic wastes kinetic study. *Fuel Processing Technology.* [Online]. 2008. **89**(7), pp.678-686. [Accessed 4 February 2019]. Available from: https://www.sciencedirect.com/science/article/pii/S0378382007002809.

86.   Kiran, N., Ekinci, E. and Snape, C.E. Recycling of plastic wastes via pyrolysis. *Resources, Conservation and Recycling.* [Online]. 2000. **29**(4), pp.273-283. [Accessed 4 February 2019]. Available from: https://www.sciencedirect.com/science/article/pii/S0921344900000525.

87.   B.P. Federation. Plastics recycling. [Online]. 2019. [Accessed 4 February 2019]. Available from: http://www.bpf.co.uk/sustainability/plastics_recycling.aspx.

88.   Williams, P.T. and Williams, E.A. Fluidised bed pyrolysis of low density polyethylene to produce petrochemical feedstock. *Journal of Analytical and Applied Pyrolysis.* [Online]. 1999. **51**(1), pp.107-126. [Accessed 5 February 2019]. Available from: https://www.sciencedirect.com/science/article/pii/S016523709900011X.

89.   Sogancioglu, M., Yel, E. and Ahmetli, G. Pyrolysis of waste high density polyethylene (HDPE) and low density polyethylene (LDPE) plastics and production of epoxy composites with their pyrolysis chars. *Journal of Cleaner Production.* [Online]. 2017. **165**, pp.369-381. [Accessed 13 December 2018]. Available from: https://www.sciencedirect.com/science/article/pii/S0959652617316037.

90.   Williams, E.A., and Williams, P.T. The pyrolysis of individual plastics and a plastic mixture in a fixed bed reactor. *Journal of Chemical Technology & Biotechnology.* [Online]. 1997. **70**(1), pp.9-20. [Accessed 5 February 2019]. Available from: https://onlinelibrary.wiley.com/doi/abs/10.1002/%28SICI%291097-4660%28199709%2970%3A1%3C9%3A%3AAID-JCTB700%3E3.0.CO%3B2-E.

91.   Aguado, R., Elordi, G., Arrizabalaga, A., Artetxe, M., Bilbao, J. and Olazar, M. Principal component analysis for kinetic scheme proposal in the thermal pyrolysis of waste HDPE plastics. *Chemical Engineering Journal.* [Online]. 2014. **254**, pp.357-364. [Accessed 9 November 2018]. Available from: https://www.sciencedirect.com/science/article/pii/S1385894714007177.

92.   Onwudili, J.A., Insura, N. and Williams, P.T. Composition of products from the pyrolysis of polyethylene and polystyrene in a closed batch reactor: Effects of temperature and residence time. *Journal of Analytical and Applied Pyrolysis.* [Online]. 2009. **86**(2), pp.293-303. [Accessed 30 November 2018]. Available from: https://www.sciencedirect.com/science/article/pii/S0165237009001119.

93.   Westerhout, R.W.J., Waanders, J., Kuipers, J.A.M and Van Swaaij, W.P.M. Recycling of polyethene and polypropylenein a novel bench-scale rotating cone reactor by high-temperature pyrolysis. *Industrial & Engineering Chemistry Research.* [Online]. 1998. **37**(6), pp.2293-2300. [Accessed 5 February 2019]. Available from: https://pubs.acs.org/doi/abs/10.1021/ie970704q.

94.   Demirbas, A. Pyrolysis of municipal solid wastes for recovery of gasoline-range hydrocarbons. *Journal of Analytical and Applied Pyrolysis.* [Online]. 2004. **72**(1), pp.97-102. [Accessed 30 November 2018]. Available from: https://www.tandfonline.com/doi/abs/10.1080/10916466.2015.1110594.

95.   Scott, D.S., Czernik, S.R., Piskorz, J. and Radlein, D.S.A.G. Fast pyrolysis of plastic wastes. *Energy & Fuels.* [Online]. 1990. **4**(4), pp.407-411. [Accessed 5 February 2019]. Available from: https://pubs.acs.org/doi/abs/10.1021/ef00022a013.

96.   Grause, G., Handa, T., Kameda, T., Mizoguchi, T. and Yoshioka, T. Effect of temperature management on the hydrolytic degradation of PET in a calcium oxide filled tube reactor. *Chemical Engineering Journal.* [Online]. 2011. **166**(2), pp. 523-528. [Accessed 6 February 2019]. Available from: https://www.sciencedirect.com/science/article/pii/S1385894710010946.

97.   Grause, G., Kaminsky, W. and Fahrbach, G. Hydrolysis of poly(ethylene terephthalate) in a fluidised bed reactor. *Polymer Degradation and Stability.* [Online]. 2004. **85**(1), pp.571-575. [Accessed 6 February 2019]. Available from: https://www.sciencedirect.com/science/article/pii/S0141391003003963.

98.   Artetxe, M., Lopez, G., Amutio, M., Elordi, G., Olazar, M. and Bilbao, J. Operating conditions for the pyrolysis of poly-(ethylene terephthalate) in a conical spouted-bed reactor. *Industrial & Engineering Chemistry Research.* [Online]. 2010. **49**(5), pp.2064-2069. [Accessed 6 February 2019]. Available from: https://pubs.acs.org/doi/abs/10.1021/ie900557c.

99.   Brems, A., Baeyens, J., Vandecasteele, C. and Dewil, R. Polymeric cracking of waste polyethylene terephthalate to chemicals and energy. *Journal of the Air & Waste Management Association.* [Online]. 2011. **61**(7), pp.721-731. [Accessed 6 February 2019]. Available from: https://www.tandfonline.com/doi/full/10.3155/1047-3289.61.7.721.

100.   Du, S., Valla, J.A., Parnas, R.S. and Bollas, G.M. Conversion of polyethylene terephthalate based waste carpet to benzene-rich oils through thermal, catalytic and catalytic steam pyrolysis. *ACS Sustainable Chemistry & Engineering.* [Online]. 2016. **4**(5), pp.2852-2860. [Accessed 6 February 2019]. Available from: https://pubs.acs.org/doi/abs/10.1021/acssuschemeng.6b00450.

101.   Mu, W. Lignin pyrolysis components and upgrading – Technology review. *BioEnergy Research.* [Online]. 2013. **6**(4), pp.1183-1204. [Accessed 30 January 2019]. Available from: https://link.springer.com/article/10.1007/s12155-013-9314-7.

102.   Cheng, Y.T. Jae, J., Shi, J., Fan, W. and Huber, G.W. Production of renewable aromatic compounds by catalytic fast pyrolysis of lignocellulosic biomass with bifunctional Ga/ZSM-5 catalysts. *Angewandte Chemie.* [Online]. 2012. **124**(6), pp.1416-1419. [Accessed 9 January 2019]. Available from: https://onlinelibrary.wiley.com/doi/full/10.1002/ange.201107390.

103.   Lu, P., Huang, Q., Bourtsalas, A.C, Chi, Y. and Yan, J. Synergistic effects on char and oil production by the co-pyrolysis of pine wood, polyethylene and polyvinyl chloride. *Fuel.* [Online]. 2018. **230**, pp.359-367. [Accessed 3 December 2018]. Available from: https://www.sciencedirect.com/science/article/pii/S0016236118308950?via%3Dihub.

104.   Li, X., Zhang, H., Li, J., Su, L., Zuo, J., Komarneni, S. and Wang, Y. Improving the aromatic production in catalytic fast pyrolysis of cellulose by co-feeding low-density polyethylene. *Applied Catalysis A: General.* [Online]. 2013. **455**, pp.114-121. [Accessed 13 November 2018]. Available from: https://www.sciencedirect.com/science/article/pii/S0926860X13000756.

105.   Mortensen, P.M, Grunwaldt, J.D., Jensen, P.A., Knudsen, K.G. and Jensen, A.D. A review of catalytic upgrading of bio-oil to engine fuels. *Applied Catalysis A: General.* [Online]. 2011. **407**(1), pp.1-19. [Accessed 6 February 2019]. Available from: https://www.sciencedirect.com/science/article/pii/S0926860X11005138.

106.   French, R. and Czernik, S. Catalytic pyrolysis of biomass for biofuels production. *Fuel Processing Technology.* [Online]. 2010. **91**(1), pp.25-32. [Accessed 13 November 2018]. Available from: https://www.sciencedirect.com/science/article/pii/S0378382009002392.

107.   Transport Policy.net. *EU: Fuels: Diesel and gasoline.* [Online]. 2018. [Accessed 19 November 2018]. Available from: https://www.transportpolicy.net/standard/eu-fuels-diesel-and-gasoline/.

108.   Keller, T.C., Rodrigues, E.G. and Pérez-Ramirez, J. Generation of basic centers in high-silica zeolites and their application in gas-phase upgrading of bio-oil. [Online]. 2014. **7**(6), pp.1729-1738. [Accessed 5 June 2019]. Available from: https://onlinelibrary.wiley.com/doi/abs/10.1002/cssc.201301382.

287

109. Fernando, S.D. and Gunawardena, D.A. Methods and applications of deoxygenation for the conversion of biomass to petroleum products. In: Matovic, M.D. ed. *Biomass Now – Cultivation and Utilization.* [Online]. London: IntechOpen, 2013, pp.273-298. [Accessed 5 June 2019]. Available from: https://www.intechopen.com/books/biomass-now-cultivation-and-utilization/methods-and-applications-of-deoxygenation-for-the-conversion-of-biomass-to-petrochemical-products.

110. Elliott, D.C. Historical developments in hydroprocessing bio-oils. *Energy & Fuels.* [Online]. 2007. **21**(3), pp.1792-1815. [Accessed 8 February 2019]. Available from: https://pubs.acs.org/doi/10.1021/ef070044u.

111. Al-Sabawi, M. and Chen J. Hydroprocessing of biomass-derived oils and their blends with petroleum feedstocks: A review. *Energy & Fuels.* [Online]. 2012. **26**(9), pp.5373-5399. [Accessed 8 February 2019]. Available from: https://pubs.acs.org/doi/abs/10.1021/ef3006405.

112. Furimsky, E. Hydroprocessing challenges in biofuels production. *Catalysis Today.* [Online]. 2013. **217**, pp.13-56. [Accessed 8 February 2019]. Available from: https://www.sciencedirect.com/science/article/pii/S0920586112008176.

113. Sadeghbeigi, R. Chapter 4 – FCC catalysts. In: Sadeghbeigi, R. ed. *Fluidic catalytic cracking handbook.* [Online]. Oxford: Butterworth Heinemann, 2012, pp.87-115. [Accessed 5 June 2017]. Available from: https://www.sciencedirect.com/book/9780123869654/fluid-catalytic-cracking-handbook.

114. Weitkamp, J. Zeolites and catalysis. *Solid State Ionics.* [Online]. 2000. **131**(1-2), pp.175-188. [Accessed 11 February 2019]. Available from: https://www.sciencedirect.com/science/article/pii/S0167273800006329.

115. Zhang, X., Lei, H., Chen, S. and Wu, J. Catalytic co-pyrolysis of lignocellulosic biomass with polymers: a critical review. *Green Chemistry.* [Online]. 2016. **18**(15), pp.4145-4169. [Accessed 30 November 2018]. Available from: https://pubs.rsc.org/en/content/articlelanding/2016/gc/c6gc00911e#!divAbstract.

116. Primo, A. and Garcia, H. Zeolites as catalysts in oil refining. *Chemical Society Reviews.* [Online]. 2014. **43**(22), pp.7548-7561. [Accessed 11 February 2019]. Available from: https://pubs.rsc.org/en/content/articlelanding/2014/CS/C3CS60394F#!divAbstract.

117. Hunger, M. Catalytically active sites: generation and characterization. In: Cejka, J., Corma, A. and Zones, S. eds. *Zeolites and catalysis: synthesis, reactions and applications.* Weinheim: Wiley-VCH, 2010, pp.493-546.

118.   Shigeishi, R.A., Chiche, B.H. and Fajula, F. CO adsorption on superacid sites on dealuminated mazzite. *Microporous and Mesoporous Materials.* [Online]. 2001. **43**(2), pp.211-226. [Accessed 11 February 2019]. Available from: https://www.sciencedirect.com/science/article/pii/S1387181100003656.

119.   Jae, J., Tompsett, G.A, Foster, A.J, Hammond, K.D., Auerbach, S.M., Lobo, R.F. and Huber, G.W. Investigation into the shape selectivity of zeolite catalysts for biomass conversion. *Journal of Catalysts.* [Online]. 2011. **279**(2), pp.257-268. [Accessed 11 February 2019]. Available from: https://www.sciencedirect.com/science/article/pii/S0021951711000315.

120.   Bhatia, S. *Zeolite Catalysts: Principles and applications.* Boca Raton: CRC Press, 1989.

121.   Sadeghbeigi, R. Chapter 6 – Chemistry of FCC reactions. In: Sadeghbeigi, R. ed. *Fluidic catalytic cracking handbook.* [Online]. Oxford: Butterworth Heinemann, 2012, pp.125-135. [Accessed 5 June 2017]. Available from: https://www.sciencedirect.com/book/9780123869654/fluid-catalytic-cracking-handbook.

122.   Pham, T.N., Sooknoi, T., Crossley, S.P. and Resasco, D.E. Ketonization of carboxylic acids: Mechanisms, catalysts, and implications for biomass conversion. *ACS Catalysis.* [Online]. 2013. **3**(11), pp.2456-2473. [Accessed 1 April 2019]. Available from: https://pubs.acs.org/doi/abs/10.1021/cs400501h.

123.   Rezaei, P.S. Shafaghat, H. and Daud, W.M.A.W. Production of green aromatics and olefins by catalytic cracking of oxygenate compounds derived from biomass pyrolysis: A review. *Applied Catalysis A: General.* [Online]. 2014. **469**, pp.490-511. [Accessed 15 November 2018]. Available from: https://www.sciencedirect.com/science/article/pii/S0926860X13005784.

124.   Adjaye, J.D. and Bakhshi, N.N. Catalytic conversion of a biomass-derived oil to fuels and chemicals I: Model compound studies and reaction pathways. *Biomass and Bioenergy.* [Online]. 1995. **8**(3), pp.131-149. [Accessed 14 February 2019]. Available from: https://www.sciencedirect.com/science/article/pii/0961953495000183.

125.   Adjaye, J.D. and Bakhshi, N.N. Production of hydrocarbons by catalytic upgrading of a fast pyrolysis bio-oil Part II: Comparative catalyst performance and reaction pathways. *Fuel Processing Technology.* [Online]. 1995. **45**(3), pp.185-202. [Accessed 9 January 2019]. Available from: https://www.sciencedirect.com/science/article/pii/037838209500040E.

126.   Miskolczi, N. Juzsakova, T. and Sója, J. Preparation and application of metal loaded ZSM-5 and y-zeolite catalysts for thermos-catalytic pyrolysis of real end

of life vehicle plastics waste. *Journal of the Energy Institute.* [Online]. 2017. **92**(1), pp.118-127. [Accessed 12 November 2018]. Available from: https://www.sciencedirect.com/science/article/pii/S1743967117305585.

127. Jackson, M.A., Compton, D.L. and Boateng, A.A. Screening heterogeneous catalysts for the pyrolysis of lignin. *Journal of Analytical and Applied Pyrolysis.* [Online]. 2009. **85**(1), pp.226-230. [Accessed 14 February 2019]. Available from: https://www.sciencedirect.com/science/article/pii/S016523700800137X.

128. Williams, P.T. and Horne, P.A. The influence of catalyst type on the composition of upgraded biomass pyrolysis oils. *Journal of Analytical and Applied Pyrolysis.* [Online]. 1995. **31**, pp.39-61. [Accessed 13 February 2019]. Available from: https://www.sciencedirect.com/science/article/pii/016523709400847T.

129. Zhao, Y., Deng, L., Liao, B., Fu, Y. and Guo, Q.X. Aromatics production via catalytic pyrolysis of pyrolytic lignins from bio-oil. *Energy & Fuels.* [Online]. 2010. **24**(10), pp.5735-5740. [Accessed 14 February 2019]. Available from: https://pubs.acs.org/doi/pdf/10.1021/ef100896q.

130. Taarning, E., Osmundsen, C.M., Yang, X., Voss, B., Andersen, S.I. and Christensen, C.H. Zeolite-catalyzed biomass conversion to fuels and chemicals. *Energy & Environmental Science.* [Online]. 2011. **4**(3), pp.793-804. [Accessed 14 February 2019]. Available from: https://pubs.rsc.org/en/content/articlelanding/2011/ee/c004518g#!divAbstract.

131. Diebold, J. and Scahill, J. Biomass to gasoline In: Soltes, J. and Milne, T. eds. *Pyrolysis oils from biomass – Producing, analyzing and upgrading.* [Online.] Washington: American Chemical Society, 1988, *pp.264-276.* [Accessed 14 February 2019]. Available from: https://pubs.acs.org/isbn/9780841215368.

132. Twaiq, F.A, Zabidi, N.A.M and Bhatia, S. Catalytic conversion of palm oil to hydrocarbons: performance of various zeolite catalysts. *Industrial & Engineering Chemistry Research.* [Online]. 1999. **38**(9), pp.3230-3237. [Accessed 14 February 2019]. Available from: https://pubs.acs.org/doi/abs/10.1021/ie980758f.

133. Mullen, C.A., Tarves, P.C., Raymundi, L.M., Schultz, E.L, Boateng, A.A. and Trierweiler, J.O. Fluidized bed catalytic pyrolysis of eucalyptus over HZSM-5: Effect of acid density and gallium modification on catalyst deactivation. *Energy & Fuels.* [Online]. 2018. **32**(2), pp.1771-1778. [Accessed 19 November 2018]. Available from: https://pubs.acs.org/doi/abs/10.1021/acs.energyfuels.7b02786.

134. Veses, A., Puértolas, B., Callén, M.S. and García, T. Catalytic upgrading of biomass derived pyrolysis vapors over metal-loaded ZSM-5 zeolites: Effect of

different metal cations on the bio-oil final properties. *Microporous and Mesoporous Materials.* [Online]. 2015. **209**, pp.189-196. [Accessed 8 November 2018]. Available from: https://www.sciencedirect.com/science/article/pii/S1387181115000244.

135.   Stanton, A.R., Iisa, K., Yung, M.M. and Magrini, K.A. Catalytic fast pyrolysis with metal-modified ZSM-5 catalysts in inert and hydrogen atmospheres. *Journal of Analytical and Applied Pyrolysis.* [Online]. 2018. **135**, pp.199-208. [Accessed 19 November 2018]. Available from: https://www.sciencedirect.com/science/article/pii/S0165237018302584.

136.   Iliopoulou, E.F., Stefanidis, S.D., Kalogiannis, K.G., Delimitis, A. Lappas, A.A. and Triantafyllidis, K.S. Catalytic upgrading of biomass pyrolysis vapors using transition metal-modified ZSM-5 zeolite. *Applied Catalysis B: Environmental.* [Online]. 2012. **127**, pp.281-290. [Accessed 13 November 2018]. Available from: https://www.sciencedirect.com/science/article/pii/S0926337312003888.

137.   Zheng, Y., Wang, F., Yang, X., Huang, Y., Liu, C., Zheng, Z. and Gu, J. Study on aromatic production via the catalytic pyrolysis vapor upgrading of biomass using metal-loaded modified H-ZSM-5. *Journal of Analytical and Applied Pyrolysis.* [Online]. 2017. **126**, pp.169-179. [Accessed 19 November 2018]. Available from: https://www.sciencedirect.com/science/article/pii/S0165237017300839.

138.   Li, P., Chen, X., Wang, X., Shao, J., Lin, G., Yang, H., Yang, Q. and Chen, H. Catalytic upgrading of fast pyrolysis products with Fe-, Zr-, and Co-modified zeolites based on pyrolyzer-GC/MS analysis. *Energy & Fuels.* [Online]. 2017. **31**(4), pp.3979-3986. [Accessed 15 February 2019]. Available from: https://pubs.acs.org/doi/abs/10.1021/acs.energyfuels.6b03105.

139.   Vichaphund, S., Aht-Ong, D., Sricharoenchaikul, V. and Atong, D. Production of aromatic compounds from catalytic fast pyrolysis of Jatropha residues using metal/HZSM-5 prepared by ion-exchange and impregnation methods. *Renewable Energy.* [Online]. 20156. **79**, pp.28-37. [Accessed 15 February 2019]. Available from: https://www.sciencedirect.com/science/article/pii/S0960148114006405.

140.   Thangalazhy-Gopakumar, S., Adhikari, S. and Gupta, R.B. Catalytic pyrolysis of biomass over H+ZSM-5 under hydrogen pressure. *Energy & Fuels.* [Online]. 2012. **26**(8), pp.5300-5306. [Accessed 15 February 2019]. Available from: https://pubs.acs.org/doi/abs/10.1021/ef3008213.

141.   Iliopoulou, E.F., Stefanidis, S., Kaligiannis, K., Psarras, A.C., Delimitis, A., Triantafyllidis, K.S. and Lappas, A.A. Pilot-scale validation of Co-ZSM-5 catalyst

performance in the catalytic upgrading of biomass pyrolysis vapours. *Green Chemistry.* [Online]. 2014. **16**(2), pp.662-674. [Accessed 18 February 2019]. Available from: https://pubs.rsc.org/en/content/articlelanding/2014/GC/C3GC41575A#!divAbstract.

142. Campanella, A. and Harold, M.P. Fast pyrolysis of microalgae in a falling solids reactor: Effects of process variables and zeolite catalysts. *Biomass and Bioenergy.* [Online]. 2012. **46**, pp.218-232. [Accessed 15 February 2019]. Available from: https://www.sciencedirect.com/science/article/pii/S0961953412003376.

143. Veses, A., Puértolas, B., López, J.M., Callén, M.S., Solosona, B. and García, T. Promoting deoxygenation of bio-oil by metal-loaded hieracrchical ZSM-5 zeolites. *ACS Sustainable Chemistry & Engineering.* [Online]. 2016. **4**(3), pp.1653-1660. [Accessed 20 November 2018]. Available from: https://pubs.acs.org/doi/abs/10.1021/acssuschemeng.5b01606.

144. Xu, C., Jiang, B., Liao, Z., Wang, J., Huang, Z. and Yang, Y. Effect of metal on the methanol to aromatics conversion over modified ZSM-5 in the presence of carbon dioxide. *RSC Advances.* [Online]. 2017. **7**(18), pp.10729-10736. [Accessed 9 January 2019]. Available from: https://pubs.rsc.org/en/content/articlelanding/2017/ra/c6ra27104a#!divAbstract.

145. Zhang, S., Yang, M., Shao, J., Yang, H., Zeng, K., Chen, Y., Luo, J., Agblevor, F.A. and Chen, H. The conversion of biomass to light olefins on Fe-modified ZSM-5 catalyst: Effect of pyrolysis parameters. *Science of the Total Environment.* [Online]. 2018. **628-629,** pp.350-357. [Accessed 15 February 2019]. Available from: https://www.sciencedirect.com/science/article/pii/S0048969718303589.

146. Zhang, S., Zhang, H., Liu, X., Zhu, S., Hu, L. and Zhang Q. Upgrading of bio-oil from catalytic pyrolysis of pretreated rice husk over Fe-modified ZSM-5 zeolite catalyst. *Fuel Processing Technology.* [Online]. 2018. **175**, pp.17-25. [Accessed 22 November 2018]. Available from: https://www.sciencedirect.com/science/article/pii/S0378382018300675.

147. Zhang, H., Zheng, J. and Xiao, R. Catalytic pyrolysis of willow wood with Me/ZSM-5 (Me = Mg, K, Fe, Ga, Ni) to produce aromatics and olefins. *BioResources.* [Online]. 2013. **8**(4), pp. 5612-5621. [Accessed 15 February 2019]. Available from: https://ojs.cnr.ncsu.edu/index.php/BioRes/article/view/BioRes_08_4_5612_Zhang_Catalytic_Pyrolysis_Willow_Wood.

148. Serrano, D.P., Aguado, J. and Escola, J.M. Developing advanced catalysts for the conversion of polyolefinic waste plastics into fuels and chemicals. *ACS*

Catalysis. [Online]. 2012. **2**(9), pp.1924-1941. [Accessed 30 November 2018]. Available from: https://pubs.acs.org/doi/abs/10.1021/cs3003403.

149. Li, Q., Zhang, F., Jarvis, J., He, P., Yung, M.M., Wang, A., Zhao, K. and Song, H. Investigation on the light alkane aromatization over Zn and Ga modified HZSM-5 catalysts in the presence of methane. *Fuel.* [Online]. 2018. **219**, pp.331-339. [Accessed 19 November 2018]. Available from: https://www.sciencedirect.com/science/article/pii/S0016236118301133.

150. Park, H.J., Heo, H.S., Jeon, J.K., Kim, J., Ryoo, R., Jeong, K.E. and Park, Y.K. Highly valuable chemicals production from catalytic upgrading of radiata pine sawdust-derived pyrolytic vapors over mesoporous MFI zeolites. *Applied Catalysis B: Environmental.* [Online]. 2010. **95**(3), pp.365-373. [Accessed 26 November 2018]. Available from: https://www.sciencedirect.com/science/article/pii/S0926337310000299.

151. Cheng, Y.T. Wang, Z., Gilbert, C.J. Fan, W. and Huber, G.W. Production of p-xylene from biomass by catalytic fast pyrolysis using ZSM-5 catalysts with reduced pore openings. *Angewandte Chemie International Edition.* [Online]. 2012. **51**(44), pp.11097-11100. [Accessed 15 February 2019]. Available from: https://onlinelibrary.wiley.com/doi/full/10.1002/anie.201205230.

152. Choi, S.J., Park, S.H., Jeon, J.K., Lee, I.G., Ryu, C., Suh, D.J. and Park, Y.K. Catalytic conversion of particle board over microporous catalysts. *Renewable Energy.* [Online]. 2013. **54**, pp.105-110. [Accessed 15 February 2019]. Available from: https://www.sciencedirect.com/science/article/pii/S0960148112005204.

153. Hyun, J.P., Park, Y.K., Kim, J.S., Jeon, J.K., Yoo, K.S., Yim, J.H., Jung, J. and Jung, M.S. Bio-oil upgrading over Ga modified zeolites in a bubbling fluidised bed reactor. *Studies in Surface Science and Catalysis.* [Online]. 2006. **159**, pp.553-556. [Accessed 26 November 2019]. Available from: https://www.sciencedirect.com/science/article/abs/pii/S0167299106816563.

154. Melligan, F., Hayes, M.H.B., Kwapinski, W. and Leahy, J.J. Hydro-pyrolysis of biomass and online catalytic vapor upgrading with Ni-ZSM-5 and Ni-MCM-41. *Energy & Fuels.* 2012. [Online]. **26**(10), pp.6080-6090. [Accessed 15 February 2019]. Available from: https://pubs.acs.org/doi/abs/10.1021/ef301244h.

155. Yung, M.M, Starace, A.K., Mukarakate, C., Crow, A.M., Leshnov, M.A. and Magrini, K.A. Biomass catalytic pyrolysis on Ni/ZSM-5: Effect of nickel pretreatment and loading. *Energy & Fuels.* [Online]. 2016. **30**(7), pp.5259-5268. [Accessed 22 November 2018]. Available from: https://pubs.acs.org/doi/abs/10.1021/acs.energyfuels.6b00239.

156.   Fanchiang, W.L. and Lin, Y.C. Catalytic fast pyrolysis of furfural over H-ZSM-5 and Zn/H-ZSM-5 catalysts. *Applied Catalysis A: General.* [Online]. 2012. **419-420**, pp.102-110. [Accessed 15 February 2019]. Available from: https://www.sciencedirect.com/science/article/pii/S0926860X12000324.

157.   Niu, X., Gao, J., Wang, K., Miao, Q., Dong, M., Wang, G., Fan, W., Qin, Z. and Wang, J. Influence of crystal size on the catalytic performance of H-ZSM-5 and Zn/H-ZSM-5 in the conversion of methanol to aromatics. *Fuel Processing Technology.* [Online]. 2017. **157**, pp.99-107. [Accessed 15 November 2018]. Available from: https://www.sciencedirect.com/science/article/pii/ S0378382016311754.

158.   Fermoso, J. Hernando, H., Jana, P., Moreno, I., Přech, J., Ochoa-Hernández, C., Pizarro, P., Coronado, J.M., Čejka, J. and Serrano, D.P. Lamellar and pillared ZSM-5 zeolites modified with MgO and ZnO for catalytic fast-pyrolysis of eucalyptus woodchips. *Catalysis Today.* [Online]. 2016. **277**, pp.171-181. [Accessed 12 November 2018]. Available from: https://www.sciencedirect.com/ science/article/pii/S0920586115007671.

159.   Fan, L., Zhang, Y., Liu, S., Zhou, N., Chen, P., Cheng, Y., Addy, M., Lu, Q., Omar, M.M., Liu, Y., Wang, Y., Dai, L. Anderson, E., Peng, P., Lei, H. and Ruan, R. Bio-oil from fast pyrolysis of lignin: Effects of process and upgrading parameters. *Bioresource Technology.* [Online]. 2017. **241**, pp.1118-1126. [Accessed 21 February 2019]. Available from: https://www.sciencedirect.com/ science/article/pii/S0960852417307976.

160.   Kim, B.S, Kim, Y.S., Lee, H.W., Jae, J., Kim, D.H., Jung, S.C., Watanabe, C. and Park, Y.K. Catalytic copyrolysis of cellulose and thermoplastics over HZSM-5 and HY. *ACS Sustainable Chemistry & Engineering.* [Online]. 2016. **4**(3), pp.1354-1363. [Accessed 21 February 2019]. Available from: https://pubs.acs.org/doi/abs/10.1021/acssuschemeng.5b01381.

161.   Zhang, H., Xiao, R., Nie, J., Jin, B., Shao, S. and Xiao, G. Catalytic pyrolysis of black-liquor lignin by co-feeding with different plastics in a fluidized bed reactor. *Bioresource Technology.* [Online]. 2015. **192**, pp.68-74. [Accessed 21 February 2019]. Available from: https://www.sciencedirect.com/science/article/pii/ S096085241500704X.

162.   Hassan, H., Lim, J.K. and Hameed B.H. Recent progress on biomass co-pyrolysis conversion into high-quality bio-oil. *Bioresource Technology.* [Online]. 2016. **221**, pp.645-655. [Accessed 8 January 2019]. Available from: https://www.sciencedirect.com/science/article/pii/S0960852416312810.

163.   Uzoejinwa, B.B, He, X., Wang, S. El-Fatah Abomohra, A., Hu, Y. and Wang, Q. Co-pyrolysis of biomass and waste plastics as a thermochemical conversion technology for high-grade biofuel production: Recent progress and future directions elsewhere worldwide. *Energy Conversion and Management.* [Online]. 2018. **163**, pp.468-492. [Accessed 21 February 2019]. Available from: https://www.sciencedirect.com/science/article/pii/S0196890418301006.

164.   Abnisa, F. and Wan Daud, W.M.A. A review on co-pyrolysis of biomass: An optional technique to obtain a high-grade pyrolysis oil. *Energy Conversion and Management.* [Online]. 2014. **87**, pp.71-85. [Accessed 21 February 2019]. Available from: https://www.sciencedirect.com/science/article/pii/S019689041400630X.

165.   Sajdak, M and Muzyka, R. Use of plastic waste as a fuel in the co-pyrolysis of biomass. Part I: The effect of the addition of plastic waste on the process and products. *Journal of Analytical and Applied Pyrolysis.* [Online]. 2014. **107**, pp.267-275. [Accessed 21 February 2019]. Available from: https://www.sciencedirect.com/science/article/pii/S0165237014000709.

166.   Martínez, J.D., Veses, A., Mastral, A.M., Murillo, R., Navarro, M.V., Puy, N., Artigues, A., Bartrolí, J. and García, T. Co-pyrolysis of biomass with waste tyres: Upgrading of liquid bio-fuel. *Fuel Processing Technology.* [Online]. 2014. **119**, pp.263-271. [Accessed 25 February 2019]. Available from: https://www.sciencedirect.com/science/article/pii/S0378382013003676.

167.   Li, X., Li, J., Zhou, G., Feng, Y., Wang, Y., Yu, G., Deng, S., Huang, J. and Wang, B. Enhancing the production of renewable petrochemicals by co-feeding of biomass with plastics in catalytic fast pyrolysis with ZSM-5 zeolites. *Applied Catalysis A: General.* [Online]. 2014. **481**, pp.173-182. [Accessed 21 February 2019]. Available from: https://www.sciencedirect.com/science/article/pii/S0926860X14003391.

168.   Bhattacharya, P., Steele, P.H., Hassan, E.B.M., Mitchell, B., Ingram, L. and Pittman, C.U. Wood/plastic copyrolysis in an auger reactor: Chemical and physical analysis of the products. *Fuel.* [Online]. 2009. **88**(7), pp.1251-1260. [Accessed 25 February 2019]. Available from: https://www.sciencedirect.com/science/article/pii/S001623610900012X.

169.   Xue, Y., Kelkar, A. and Bai, X. Catalytic co-pyrolysis of biomass and polyethylene in a tandem micropyrolyzer. *Fuel.* [Online]. 2016. **166**, pp.227-236. [Accessed 25 February 2019]. Available from: https://www.sciencedirect.com/science/article/pii/S0016236115011394.

170. Cheng, Y.T. and Huber, G.W. Production of targeted aromatics by using Diels-Alder classes of reactions with furan and olefins over ZSM-5. *Green Chemistry*. [Online]. 2012. **14**(11), pp.3114-3125. [Accessed 22 February 2019]. Available from: https://pubs.rsc.org/en/content/articlelanding/2012/gc/c2gc35767d#!divAbstract.

171. Dorado, C., Mullen, C.A. and Boateng, A.A. Origin of carbon in aromatic and olefin products derived from HZSM-5 catalysed co-pyrolysis of cellulose and plastics via isotopic labelling. *Applied Catalysis B: Environmental.* [Online]. 2015. **162**, pp.338-345. [Accessed 21 February 2019]. Available from: https://www.sciencedirect.com/science/article/pii/S0926337314004044.

172. Ojha, D.K. and Vinu, R. Fast co-pyrolysis of cellulose and polypropylene using Py-GC/MS and Py-FT-IR. *RSC Advances.* [Online]. 2015. **5**(82), pp.66861-66870. [Accessed 26 February 2019]. Available from: https://pubs.rsc.org/en/content/articlelanding/2015/ra/c5ra10820a#!divAbstract.

173. Abnisa, F., Wan Daud, W.M.A., Ramalingam, S., Azemi, M.N.B.M and Sahu, J.N. Co-pyrolysis of palm shell and polystyrene waste mixtures to synthesis liquid fuel. *Fuel.* [Online]. 2013. **108**, pp.311-318. [Accessed 27 February 2019]. Available from: https://www.sciencedirect.com/science/article/pii/S0016236113001014.

174. Rutkowsji, P. and Kubacki, A. Influence of polystyrene addition to cellulose on chemical structure and properties of bio-oil obtained during pyrolysis. *Energy Conversion and Management.* [Online]. 2006. **47**(6), pp.716-731. [Accessed 28 February 2019]. Available from: https://www.sciencedirect.com/science/article/pii/S019689040500138X.

175. Dorado, C., Mullen, C.A. and Boateng, A.A. H-ZSM-5 catalysed co-pyrolysis of biomass and plastics. *ACS Sustainable Chemistry & Engineering.* [Online]. **2**(2), pp.301-311. [Accessed 21 February 2019], Available from: https://pubs.acs.org/doi/abs/10.1021/sc400354g

176. Chen, L., Wang, S., Meng, H., Wu, Z. and Zhao, J. Synergistic effect on thermal behaviour and char morphology analysis during co-pyrolysis pf paulownia wood blended with different plastic waste. *Applied Thermal Engineering.* [Online]. 2017. **111**, pp.834-846. [Accessed 21 February 2019]. Available from: https://www.sciencedirect.com/science/article/pii/S1359431116319767.

177. Zhou, L., Wang, Y., Huang, Q. and Cai, J. Thermogravimetric characteristics and kinetic of plastic and biomass blends co-pyrolysis. *Fuel Processing Technology.* [Online]. 2006. **87**(11), pp.963-969. [Accessed 1 March 2019].

Available from: https://www.sciencedirect.com/science/article/pii/
S0378382006000907.

178.   Johannes, I., Tiikma, L. and Luik, H. Synergy in co-pyrolysis of oil shale and
        pine sawdust in autoclaves. *Journal of Analytical and Applied Pyrolysis.*
        [Online]. 2013. **104**, pp.341-352. [Accessed 1 March 2019]. Available from:
        https://www.sciencedirect.com/science/article/pii/S0165237013001459.

179.   Önal, E., Uzun, B.B. and Pütün, A.E. Bio-oil production via co-pyrolysis of
        almond shell as biomass and high density polyethylene. *Energy Conversion
        and Management.* [Online]. 2014. **78**, pp.704-710. [Accessed 21 February
        2019]. Available from: https://www.sciencedirect.com/science/article/pii/
        S0196890413007437.

180.   Zhou, G., Li, J., Yu, Y., Li, X., Wang, Y., Wang, W. and Komarneni. Optimizing
        the distribution of aromatic products from catalytic fast pyrolysis of cellulose by
        ZSM-5 modification with boron and co-feeding of low-density polyethylene.
        Applied Catalysis A: General. [Online]. 2014. **487**, pp.45-53. [Accessed 21
        February 2019]. Available from: https://www.sciencedirect.com/science/article/
        pii/S0926860X14005596.

181.   Breen, J.P., Burch, R., Kulkarni, M., Mclaughlin, D., Collier, P.J. and Golunski,
        S.E. Improved selectivity in the toluene alkylation reaction through
        understanding and optimising the process variables. *Applied Catalysis A:
        General.* [Online]. 2007. **316**(1), pp.53-60. [Accessed 13 June 2019]. Available
        from: https://www.sciencedirect.com/science/article/abs/pii/
        S0926860X06006764.

182.   Kaeding, W.W. Chu, C., Young, L.B. and Butter, S.A. Shape selective reactions
        with zeolite catalysts: II. Selective disproportionation of toluene to produce
        benzene and p-xylene. *Journal of catalysis.* [Online]. 1981. **69**(2), pp.392-398.
        [Accessed 13 June 2019]. Available from: https://www.sciencedirect.com/
        science/article/pii/0021951781901743.

183.   Lin, X., Zhang, Z., Sun, J., Guo, W. and Wang Q. Effects of phosphorus-
        modified HZSM-5 on distribution of hydrocarbon compounds from wood-plastic
        composite pyrolysis using Py-GC/MS. *Journal of Analytical and Applied
        Pyrolysis.* [Online]. 2015. **116**, pp.223-230. [Accessed 25 April 2019]. Available
        from: https://www.sciencedirect.com/science/article/pii/S0165237015301935.

184.   Yao, W., Li, J., Feng, Y., Wang, W., Zhang, X., Chen, Q., Komarneni, S. and
        Wang, Y. Thermally stable phosphorus and nickel modified ZSM-5 zeolites for
        catalytic co-pyrolysis of biomass and plastics. *RSC Advances.* [Online]. 2015.

5(39), pp.30485-30494. [Accessed 24 April 2019]. Available from: https://pubs.rsc.org/en/content/articlelanding/2015/ra/c5ra02947c#!divAbstract.

185.   Zhang, H., Cheng, Y.T., Vispute, T.P., Xiao, R. and Huber, G.W. Catalytic conversion of biomass-derived feedstocks into olefin and aromatics with ZSM-5: the hydrogen to carbon effective ratio. *Energy & Environmental Science*. [Online]. 2011. **4**(6), pp.2297-2307. [Accessed 13 June 2019]. Available from: https://pubs.rsc.org/en/content/articlelanding/2011/ee/c1ee01230d/ unauth#!divAbstract.

186.   Li, J., Yu, Y., Li, X., Wang, W., Yu, G., Deng, S., Huang, J., Wang, B. and Wang, Y. Maximizing carbon efficiency of petrochemical production from catalytic co-pyrolysis of biomass and plastics using gallium-containing MFI zeolites. *Applied Catalysis B: Environmental*. [Online]. 2015. **172-173**, pp.154-164. [Accessed 21 February 2019]. Available from: https://www.sciencedirect.com/science/article/pii/S0926337315000661.

187.   Al-Yassir, N., Akhtar, M.N., and Al-Khattaf, S. Physicochemical properties and catalytic performance of galloaluminosilicate in aromatization of lower alkanes: a comparative study with Ga/HZSM-5. *Journal of Porous Materials.* [Online]. 2012. **19**(6), pp.943-960. [Accessed 14 June 2019]. Available from: https://link.springer.com/article/10.1007/s10934-011-9552-z.

188.   Fricke, R., Kosslick, H., Lischke, G. and Richter, M. Incorporation of gallium into zeolites: syntheses, properties and catalytic application. *Chemical Reviews.* [Online]. 2000. **100**(6), pp.2303-2405. [Accessed 14 June 2019]. Available from: https://www.ncbi.nlm.nih.gov/pubmed/11749288.

189.   Nowak, I., Quartararo, J., Derouane, E.G. and Vedrine, J.C. Effect of H2-O2 pre-treatments on the state of gallium in Ga/H-ZSM-5 propane aromatisation catalysts. *Applied Catalysis A: General.* [Online]. 2003. **251**(1), pp.107-120. [Accessed 14 June 2019]. Available from: https://www.sciencedirect.com/ science/article/abs/pii/S0926860X03002990.

190.   Ausavasukhi, A., Huang, Y., To, A.T., Sooknoi, T. and Resasco, D.E. Hydrodeoxygenation of m-cresol over gallium-modified beta zeolite catalysts. *Journal of Catalysis*. [Online]. 2012. **290**, pp.90-100. [Accessed 14 June 2019]. Available from: https://www.sciencedirect.com/science/article/pii/ S0021951712000759.

191.   Xiang, Z., Liang, J., Morgan, H.M., Liu, Y., Mao, H. and Bu, Q. Thermal behavior and kinetic study for co-pyrolysis of lignocellulosic biomass with polyethylene over Cobalt modified ZSM-5 catalyst by thermogravimetric analysis. *Bioresource Technology.* [Online]. 2018. **247**, pp.804-811. [Accessed

1 April 2019]. Available from: https://www.sciencedirect.com/science/article/pii/
S0960852417317431.

192. Zhang, X., Lei, H., Zhu, L., Zhu, X., Qian, M., Yadavalli, G., Wu, J. and Chen, S. Thermal behaviour and kinetic study for catalytic co-pyrolysis of biomass with plastics. *Bioresource technology.* 2016. **220**, pp233-238. [Accessed 14 June 2019]. Available from: https://www.sciencedirect.com/science/article/pii/ S0960852416311968.

193. Park, J.J., Park, K., Kim, J.S., Maken, S., Song, H., Shin, H., Park, J.W. and Choi, M.J. Characterization of styrene recovery from the pyrolysis of waste expandable polystyrene. *Energy & Fuels.* [Online]. 2003. **17**(6), pp.1576-1582. [Accessed 1 May 2019]. Available from: https://pubs.acs.org/doi/abs/10.1021/ ef030102l.

194. Department of Energy (EERE). *Energy and environmental profile of the U.S. chemical industry: chapter 4 The BTX chain: Benzene, toluene, xylene.* [Online]. 2000. [Accessed 1 May 2019]. Available from: https://www1.eere.energy.gov/manufacturing/resources/chemicals/pdfs/ profile_chap4.pdf.

195. Xiang, Y., Wang, H.m Cheng, J. and Matsubu, J. Progress and prospects in the catalytic ethane aromatization. *Catalysis Science & Technology.* [Online]. 2018. **8**(6), pp.1500-1516. [Accessed 1 May 2019]. Available from: https://pubs.rsc.org/en/content/articlelanding/2018/cy/c7cy01878a#!divAbstract.

196. International Energy Agency. *Energy technology perspectives 2015.* [Online]. 2015. [Accessed 1 May 2019]. Available from: https://www.oecd-ilibrary.org/ content/publication/energy_tech-2015-en.

197. Liverpool wood pellets. *Liverpool wood pellets.* [Online]. 2019. [Accessed 14 January 2019]. Available from: http://www.liverpoolwoodpellets.co.uk/.

198. Sigma Aldrich. *Poly(ethylene terephthalate).* [Online]. 2019. [Accessed 14 January 2019]. Available from: https://www.sigmaaldrich.com/catalog/product/ aldrich/429252?lang=en&region=GB.

199. Sigma Aldrich. *Polyethylene, low density.* [Online]. 2019. [Accessed 14 January 2019]. Available from: https://www.sigmaaldrich.com/catalog/product/aldrich/ 428043?lang=en&region=GB.

200. Imerys Performance Additives. *Recycled plastics.* [Online]. 2019. [Accessed 14 January 2019]. Available from: https://www.imerys-performance-additives.com/ your-market/recycled-plastics.

201. British Standards Institution. BS EN 14774-3:2009. Solid biofuels - *Determination of moisture content – Oven dry method.* London: BSI, 2010.

202. British Standards Institution. BS EN 15148:2009. Solid biofuels - *Determination of the content of volatile matter.* London: BSI, 2010.

203. British Standards Institution. BS EN 14775:2009. Solid biofuels - *Determination of ash content – Oven dry method.* London: BSI, 2010.

204. British Standards Institution. BS EN 15104:2011. Solid biofuels - *Determination of total content of carbon, hydrogen and nitrogen – Instrumental methods.* London: BSI, 2011.

205. Van Slycken, S., Witters, n., Meiresonne, L., Meers, E., Ruttens, A., Van Peterghem, P., Weyens, N., Tack, F.M.G. and Vangronsveld, J. Field evaluation of willow under short rotation coppice for phytomanagement of metal-polluted agricultural soils. *International Journal of Phytoremediation.* [Online]. 2013. **15**(7), pp.677-689. [Accessed 8 November 2018]. Available from: https://www.ncbi.nlm.nih.gov/pubmed/23819267.

206. Friedl, A., Padouvas, E., Rotter, H. and Varmuza, K. Prediction of heating values of biomass fuel from elemental composition. *Analytica Chimica Acta.* [Online]. 2005. **544**(1-2), pp.191-198. [Accessed 21 May 2016], Available from: https://www.sciencedirect.com/science/article/pii/S0003267005000735.

207. ECN (TNO). *Phyllis 2 Databse for biomass and waste*. [Online]. 2019. [Accessed 10 June 2019]. Available from: https://phyllis.nl/.

208. ECN (TNO). *Phyllis 2 – Untreated wood, wood, pine.* [Online]. 2019. [Accessed 8 November 2018]. Available from: https://phyllis.nl/Browse/Standard/ECN-Phyllis#pine.

209. Venderbosch, R. and Prins, W. Fast pyrolysis technology development. *Biofuels, Bioproducts and Biorefining,* [Online]. 2010. **4**(2), pp.178-208. [Accessed 8 November 2018]. Available from: https://onlinelibrary.wiley.com/doi/abs/10.1002/bbb.205.

210. Oasmaa, A. and Peacocke, C. *Properties and fuel use of biomass – derived fast pyrolysis liquids – A guide.* [Online]. Vuorimiehentie, Finland: VTT, 2010. [Accessed 17 January 2019]. Available from: https://www.vtt.fi/Documents/P731.pdf.

211. Martins Mayer, F., Teixeira, C.M., Andrade Pacheco, J.G., Telles de Souza, C., De Vila Bauer, D., Bastos Caramão, E., Da Silveira Espíndola, J., Trierweiler, J.O., Perez Lopez, O.W. and Alcaraz Zini, C. Characterization of analytical fast pyrolysis vapors of medium-density fibreboard (mdf) using metal-modified HZSM-5. *Journal of Analytical and Applied Pyrolysis.* [Online]. 2018. **136**, pp.87-95. [Accessed 19 November 2018]. Available from: https://www.sciencedirect.com/science/article/pii/S0165237018307290.

212. Yuvaraj, S., Fan-Yuan, L., Tsong-Huei, C. and Chuin-Tih, Y. Thermal decomposition of metal nitrates in air and hydrogen environments. *The Journal of Physical Chemistry B.* [Online]. 2003. **107**(4), pp.1044-1047. [Accessed 29 May 2019]. Available from: https://pubs.acs.org/doi/10.1021/jp026961c.

213. International Zeolite Association. *Database of zeolite structures – Measured powder pattern for template-free ZSM-5 (MFI).* [Online]. 2018. [Accessed 8 November 2018]. Available from: http://europe.iza-structure.org/IZA-SC/ pow_plot_VerifSyn.php?STC=MFI&patternFN=SDA-free_ZSM-5.dat.

214. Liu, R.L., Zhu, H.Q., Wu, Z.W., Qin, Z.F., Fan, W.B. and Wang, J.G. Aromatization of propane over Ga-modified ZSM-5 catalysts. *Journal of Fuel Chemistry and Technology.* [Online]. 2015. **43**(8), pp.961-969. [Accessed 12 November 2018]. Available from: https://www.sciencedirect.com/science/article/ pii/S187258131530027X.

215. Liu, N., Yuan, X., Chen, B., Li, Y. and Zhang, R. Selective catalytic combustion of hydrogen cyanide over metal-modified zeolite catalysts: From experiment to theory. *Catalysis Today.* [Online]. 2017. **297**, pp. 201-210. [Accessed 12 November 2018]. Available from: https://www.sciencedirect.com/science/article/ pii/S0920586117301888.

216. Zhang, R., Zhang, B., Shi, Z., Liu, N. and Chen, B. Catalytic behaviors of chloromethane combustion over the metal-modified ZSM-5 zeolites with diverse SiO2/Al2O3 ratios. *Journal of Molecular Catalysis A: Chemical.* [Online]. 2015. **398**, pp.223-230. [Accessed 12 November 2018]. Available from: https://www.sciencedirect.com/science/article/pii/S1381116914005299.

217. Raffi, M., Mehrwan, S., Mahmood Bhatti, T., Akhter, J.I., Hameed, A., Yawar, W. and Masood ul Hasan, M. Investigations into the antibacterial behaviour of copper nanoparticles against Escherichia coli. *Annals of Microbiology.* [Online]. 2010. **60**(1), pp.75-80. [Accessed 18 February 2019]. Available from: https://link.springer.com/article/10.1007/s13213-010-0015-6.

218. Al-Khuttaf, S., Ali, M.A. and Cejka, J. Recent developments in transformations of aromatic hydrocarbons over zeolites. In: Czeka, J., Corma, A. and Zones, S. eds. *Zeolites and catalysis – synthesis, reactions and applications.* Weinheim: Wiley VCH, 2010, pp.623-648.

219. MicrotoNano. *Targeted material selection for coating SEM samples using an SEM sputter coater.* [Online]. 2019. [Accessed 15 May 2019]. Available from: https://www.microtonano.com/TIN-Target-material-selection-for-coating-SEM-samples-using-an-SEM-sputter-coater.php.

220. University of Leeds. *Leeds electron microscopy and spectroscopy centre.* 2019. [Online]. [Accessed 10 December 2018]. Available from: https://engineering.leeds.ac.uk/info/201503/research_facilities/ 73/leeds_electron_microscopy_and_spectroscopy_centre/2.

221. Olazar, M., Aguado, R., Bilbao, J. and Barona, A. Pyrolysis of sawdust in a conical spouted-bed reactor with a HZSM-5 catalyst. *AIChE Jourrnal.* [Online]. 2000. **46**(5), pp.1025-1033. [Accessed 8 November 2018]. Available from: https://aiche.onlinelibrary.wiley.com/doi/abs/10.1002/aic.690460514.

222. Wang, B., Gao, B. and Fang, J. Recent advances in engineered biochar productions and applications. *Critical Reviews in Engineering Science and Technology.* [Online]. 2017. **47**(22), pp.2158-2207. [Accessed 9 November 2018]. Available from: https://www.tandfonline.com/doi/full/10.1080/ 10643389.2017.1418580.

223. Yildiz, G., Lathouwers, T., Toraman, H.E., Van Geem, K.M., Marin, G.B., Ronsse, F., Van Duren, R., Kersten, S.R.A and Prins, W. Catalytic fast pyrolysis pf pine wood: Effect of successive catalyst regeneration. *Energy & Fuels.*[Online]. 2014. **28**(7), pp.4560-4572. [Accessed 9 November 2018]. Available from: https://pubs.acs.org/doi/abs/10.1021/ef500636c.

224. Forest Research. *Drying biomass.* [Online]. 2019. [Accessed 7 January 2019]. Available from: https://www.forestresearch.gov.uk/tools-and-resources/ biomass-energy-resources/fuel/woodfuel-production-and-supply/woodfuel- processing/drying-biomass/.

225. Li, H., Chen, Q., Zhang, X., Finney, K.N., Shafiri, V.N. and Swithenbank, J. Evaluation of a biomass drying process using waste heat from process industries: A case study. *Applied Thermal Engineering.* [Online]. 2012. **35**, pp.71-80. [Accessed 7 January 2019]. Available from: https://www.sciencedirect.com/science/article/pii/S1359431111005473.

226. Carlson, T.R., Tompsett, G.A, Conner, W.C. and Huber, G.W. Aromatic production from catalytic fast pyrolysis of biomass-derived feedstocks. *Topics in Catalysis.* [Online]. 2009. **52**, pp.241-252. [Accessed 13 November 2018]. Available from: https://link.springer.com/article/10.1007/s11244-008-9160-6.

227. Carlson, T.R., Cheng, Y.T., Jae, J. and Huber, G.W. Production of green aromatics and olefins by catalytic fast pyrolysis of wood sawdust. *Energy & Environmental Science.* [Online]. 2011. **4**(1), pp.145-161. [Accessed 13 November 2018]. Available from: https://pubs.rsc.org/en/content/articlelanding/ 2011/ee/c0ee00341g#!divAbstract.

228. Valle, B., Gayubo, A.G., Aguayo, A.T., Olazar, M. and Bilbao, J. Seletive production of aromatics by crude bio-oil valorization with a nickel-modified HZSM-5 Zeolite catalyst. *Energy & Fuels.* [Online]. 2010. **24**(3), pp.2060-2070. [Accessed 9 November 2018]. Available from: https://pubs.acs.org/doi/abs/10.1021/ef901231j.

229. Hassan, E.B., Elsayed, I. and Eseyin, A. Production high yields of aromatic hydrocarbons through catalytic fast pyrolysis of torrefied wood and polystyrene. *Fuel.* [Online]. 2016. **174**, pp.317-324. [Accessed 13 November 2018]. Available from: https://www.sciencedirect.com/science/article/pii/S0016236116001526.

230. Shao, C., Wang, H., Atef, N., Wang, Z., Chen, B., Almalki, M., Zhang, Y., Cao, C., Yang, J. and Sarathy, S.M. Polycyclic aromatic hydrocarbons in pyrolysis of gasoline surrogates (n-heptane/iso-octane/toluene). *Proceedings of the Combustion Institute.* [Online]. 2018. **37**(1), pp.993-1001. [Accessed 15 November 2018]. Available from: https://www.sciencedirect.com/science/article/pii/S1540748918302700.

231. Kukkadapu, G., Kang, D., Wagnon, S.W., Zhang, K., Mehl, M., Monge-Palacios, M., Wang, H., Goldsborough, S.S., Westbrook, C.K. and Pitz, W.J. Kinetic modelling study of surrogate components for gasoline, jet and diesel fuels: C7-C11 methylated aromatics. *Proceedings of the Combustion Institute.* [Online]. 2018. [Accessed 15 November 2018]. Available from: https://www.sciencedirect.com/science/article/pii/S1540748918305583.

232. Javed, T., Lee, C., Alabbad, M., Djebbi, K., Beshir, M., Badra, J., Curran, H. and Farooq, A. Ignition studies of n-heptane/iso-octane/toluene blends. *Combustion and Flame.* [Online]. 2016. **171**, pp.223-233. [Accessed 15 November 2018]. Available from: https://www.sciencedirect.com/science/article/pii/S0010218016301365.

233. Zhen, X., Wang, Y. and Liu D. An overview of the chemical reaction mechanisms for gasoline surrogate fuels. *Applied Thermal Engineering.* [Online]. 2017. **124**, pp.1257-1268. [Accessed 15 November 2018]. Available: https://www.sciencedirect.com/science/article/pii/S1359431116333270.

234. Shukla, B. and Koshi, M. A novel route for PAH growth in HACA based mechanisms. *Combustion and Flame.* [Online]. 2012. **159**(12), pp.3589-3596. [Accessed 8 January 2019]. Available from: https://www.sciencedirect.com/science/article/pii/S0010218012002465.

235. Paysepar, H., Rao, K.T.V., Yuan, Z., Shui, H. and Xu, C. Improving activity of ZSM-5 zeolite catalyst for the production of monomeric aromatics/phenolics

from hydrolysis lignin via catalytic fast pyrolysis. *Applied Catalysis A: General.* [Online]. 2018. **563**, pp.154-162. [Accessed 15 November 2018]. Available from: https://www.sciencedirect.com/science/article/pii/S0926860X18303260.

236.   Chiaramonti, D., Prussi, M., Buffi, M. and Tacconi, D. Sustainable bio kerosene: Process routes and industrial demonstration activities in aviation biofuels. *Applied Energy*. [Online]. **136**, pp.767-774. [Accessed 15 November 2018]. Available from: https://www.sciencedirect.com/science/article/pii/S0306261914008769.

237.   Zhu, C. and Bollas, G.M. Gasoline selective Fischer-Tropsch synthesis in structured bifunctional catalysts. *Applied Catalysis B: Environmental*. [Online]. 2018. **235**, pp.92-102. [Accessed 15 November 2018]. Available from: https://www.sciencedirect.com/science/article/pii/S0926337318303928.

238.   Ratnasari, D.K., Nahil, M.A. and Williams, P.T. Catalytic pyrolysis of waste plastics using staged catalysis for production of gasoline range hydrocarbon oils. *Journal of Analytical and Applied Pyrolysis*. [Online]. 2017. **124**, pp.631-637. [Accessed 19 November 2018]. Available from: https://www.sciencedirect.com/science/article/pii/S0165237016306015.

239.   Marker, T.L., Felix, L.G., Linck, M.B. and Roberts, M.J. Integrated hydropyrolysis and hydroconversion (IH2) for the direct production of gasoline and diesel fuels or blending components from biomass, part 1: Proof of principle testing. *Environmental Progress & Sustainable Energy.* [Online]. 2012. **31**(2), pp.191-199. [Accessed 8 January 2019]. Available from: https://aiche.onlinelibrary.wiley.com/doi/full/10.1002/ep.10629.

240.   Li, Z., Liu, G., Cui, X., Sun, X., Li, S., Qian, Y., Jiang, C. and Lu, X. Effects of the variation in diesel fuel components on the particulate matter and unregulated gaseous emissions from a common rail diesel engine. *Fuel*. [Online]. 2018. **232**, pp.279-289. [Accessed 15 November 2018]. Available from: https://www.sciencedirect.com/science/article/pii/S0016236118310159.

241.   Borrull, F. and Marcé, R.M. Polycyclic aromatic hydrocarbons, Solid phase extraction. In: Wilson, I.D. ed. *Encyclopedia of separation science.* Oxford: Academic Press, 2000, pp.3867-3877.

242.   Lin, Y.C. and Huber, G.W. The critical role of heterogeneous catalysis in lignocellulosic biomass conversion. *Energy & Environmental Science.* [Online]. 2009. **2**(1), pp.68-80. [Accessed 19 November 2018]. Available from: https://pubs.rsc.org/en/content/articlelanding/2009/ee/b814955k#!divAbstract.

243.   Thompson, B., Machas, M. and Nielsen, D.R. Creating pathways towards aromatic building blocks and fine chemicals. *Current Opinion in Biotechnology.*

[Online]. 2015. **36**, pp.1-7. [Accessed 20 November 2018]. Available from: https://www.ncbi.nlm.nih.gov/pubmed/26264997.

244.   Liang, J., Morgan, H.M., Liu, Y., Shi, A., Lei, H., Mao, H. and Bu, Q. Enhancement of bio-oil yield and selectivity and kinetic study of catalytic pyrolysis of rice straw over transition metal modified ZSM-5 catalyst. *Journal of Analytical and Applied Pyrolysis.* [Online]. 2017. **128**, pp.324-334. [Accessed 22 November 2018]. Available from: https://www.sciencedirect.com/science/article/pii/S0165237017302358.

245.   Bayraktar, O. and Kugler, E.L. Characterization of coke on equilibrium fluid catalytic cracking cataluysts by temperature-programmed oxidation. *Applied Catalysis A: General.* [Online]. 2002. **233**(1), pp.197-213. [Accessed 2 April 2019]. Available from: https://www.sciencedirect.com/science/article/pii/S0926860X02001424.

246.   Habib, E.T., Owen, H., Snyder, P.W., Streed, C.W. and Venuto, P.B. Artificially metals-poisoned fluid catalysts: Performance in pilot plant cracking of hydrotreated resid. *Product R&D.* [Online]. 1977. **16**(4), pp.291-296. [Accessed 2 April 2019]. Available from: https://pubs.acs.org/doi/abs/10.1021/i360064a006.

247.   Gayubo, A.G., Aguayo, A.T., Atutxa, A., Valle, B. and Bilbao, J. Undesired components in the transformation of biomass pyrolysis oil into hydrocarbons on an HZSM-5 zeolite catalyst. *Journal of Chemical Technology & Biotechnology.* [Online]. 2005. **80**(11), pp.1244-1251. [Accessed 26 November 2018]. Available from: https://onlinelibrary.wiley.com/doi/full/10.1002/jctb.1316.

248.   Saldarriaga, J.F., Aguado, R., Pablos, A., Amutio, M., Olazar, M. and Bilbao, J. Fast characterization of biomass fuels by thermogravimetric analysis (TGA). *Fuel.* [Online]. 2015. **140**, pp.744-751. [Accessed 9 November 2018]. Available from: https://www.sciencedirect.com/science/article/pii/S0016236114010199.

249.   Oyedun, A.O., Tee, C.Z., Hanson, S. and Hui, C.W. Thermogravimetric analysis of the pyrolysis characteristics and kinetics of plastics and biomass blends. *Fuel Processing Technology.* [Online]. 2014. **128**, pp. 471-481. [Accessed 21 February 2019]. Available from: https://www.sciencedirect.com/science/article/pii/S0378382014003464.

250.   Al-Salem, S.M. and Lettieri, P. Kinetics of polyethylene terephthalate (PET) and polystyrene (PS) dynamic pyrolysis. *World Academy of Science, Engineering and Technology International Journal of Chemical and Molecular Engineering.* [Online]. 2010. **4**(6), pp. 402-410. [Accessed 5 March 2019]. Available from: https://www.semanticscholar.org/paper/Kinetics-of-Polyethylene-Terephthalate-

(-PET-)-and-Al-salem-Lettieri/e15608fe7a5882a6c9848d755558ed308d cbc441? navId=paper-header.

251.   Pereira, A.P.D.S, Silva, M.H.P.D., Lima Junior, E.P., Paula, A.D.S. and Tommasini, F.J. Processing and characterization of PET composites reinforced with geopolymer concrete waste. *Materials Research.* [Online]. 2017. **20**, pp.411-420. [Accessed 12 March 2019]. Available from: http://www.scielo.br/ scielo.php?script=sci_arttext&pid=S1516-14392017000800411.

252.   Navarro. M.V., Lopez, J.M., Veses, A., Callen, M.S. and Garcia, T. Kinetic study for the co-pyrolysis of lignocellulosic biomass and plastics using the distributed activation energy model. *Energy.* [Online]. 2018. **165**, pp.731-742. [Accessed 1 April 2019]. Available from: https://www.sciencedirect.com/science/article/pii/ S0360544218319030.

253.   Özsin, G. and Pütün, A.E. Insights into pyrolysis and co-pyrolysis of biomass and polystyrene: Thermochemical behaviors, kinetics and evolved gas analysis. *Energy Conservation and Management.* [Online]. 2017. **149**, pp.675-685. [Accessed 27 February 2019]. Available from: https://www.sciencedirect.com/ science/article/pii/S0196890417306945.

254.   Brems, A., Baeyens, J., Vandecasteele, C. and Dewil, R. Polymeric cracking of waste polyethylene terephthalate to chemicals and energy. *Journal of the Air & Waste Management Association.* [Online]. 2011. **61**(7), pp.721-731. [Accessed 5 March 2019]. Available from: https://www.tandfonline.com/doi/full/10.3155/ 1047-3289.61.7.721.

255.   Alvarez, J., Kumagai, S., Wu, C., Yoshioka, T., Bilbao, J., Olazar, M. and Williams, P.T. Hydrogen production from biomass and plastic mixtures by pyrolysis-gasification. *International Journal of Hydrogen Energy.* [Online]. 2014. **39**(21), pp.10883-10891. [Accessed 21 February 2019]. Available from: https://www.sciencedirect.com/science/article/pii/S0360319914012798

256.   Chattopadhay, J., Kim, C., Kim, R. and Pak, D. Thermogravimetric characteristics and kinetic study of biomass co-pyrolysis with plastics. *Korean Journal of Chemical Engineering.* [Online]. 2008. **25**(5), pp.1047-1053. [Accessed 1 April 2019]. Available from: https://link.springer.com/article/ 10.1007/s11814-008-0171-6.

257.   Ephraim, A., Pham Minh, D., Lebonnois, D., Peregrina, C., Sharrock, P. and Nzihou, A. Co-pyrolysis of wood and plastics: Influence of plastic type and content on product yield, gas composition and quality. *Fuel.* [Online]. 2018. **231**, pp.110-117. [Accessed 1 April 2019]. Available from: https://www.sciencedirect.com/science/article/pii/S001623611830783X.

258.   Jakab, E., Várhegyi, G. and Faix, O. Thermal decomposition of polypropylene in the presence of wood-derived materials. *Journal of Analytical and Applied Pyrolysis.* [Online]. 2000. **56**(2), pp.273-285. [Accessed 8 June 2019]. Available from: https://www.sciencedirect.com/science/article/pii/S0165237000001017.

259.   Ray, S. and Cooney, R.P. Chapter 7: Thermal degradation of polymer composites. In: Kutz, M. ed. *Handbook of environmental degradation of materials (second edition).* [Online]. Oxford: William Andrew Publishing, 2012, pp.213-242. [Accessed 8 June 2019]. Available from: https://www.sciencedirect.com/science/article/pii/B9780323524728000095.

260.   Burra, K.G. and Gupta, A.K. Kinetics of synergistic effects in co-pyrolysis of biomass with plastic wastes. *Applied Energy.* [Online]. 2018. **220**, pp.408-418. [Accessed 9 June 2019]. Available from: https://www.sciencedirect.com/science/article/pii/S0306261918304550.

261.   Diebold, J.P. and Czernik, S. Additives to lower and stabilize the viscosity of pyrolysis oils during storage. *Energy & Fuels.* [Online]. 1997. **11**(5), pp. 1081-1091. [Accessed 3 March 2019]. Available from: https://pubs.acs.org/doi/abs/10.1021/ef9700339.

262.   Cunliffe, A.M., Jones, N. and Williams, P.T. Pyrolysis of composite plastic waste*. Environmental Technology.* [Online]. 2003. **24**(5), pp.653-663. [Accessed 5 June 2019]. Available from: https://www.ncbi.nlm.nih.gov/pubmed/12803257.

263.   Materials today: Reinforced plastics. *Recycling glass fibre reinforced composites – history and progress (Part 1).* 2013. [Accessed 22 March 2018]. Available from: https://www.materialstoday.com/carbon-fiber/features/recycling-glass-fibre-reinforced-composites/.

264.   Cornier-Rios, H., Sundaram, P.A., and Celorie, J.T. Effect of recycling on material properties of glass-filled polyethylene terephthalate. *Journal of Polymers and the Environment.* [Online]. 2007. **15**(1), pp.51-56. [Accessed 6 June 2019]. Available from: https://link.springer.com/article/10.1007/s10924-006-0045-0.

265.   Sharuddin, A., Dayana, S., Abnisa, F., Wan Daud, W.M.A. and Aroua, M.K. A review on pyrolysis of plastic wastes. *Energy conversion and Management.* [Online]. 2016. **115**, pp.308-326. [Accessed 4 March 2019]. Available from: https://www.sciencedirect.com/science/article/pii/S0196890416300619.

266.   Fakhrhoseini, S.M. and Dastanian, M. Predicting pyrolysis products of PE, PP and PET using NRTL activity coefficient model. *Hindawi Journal of chemistry*.

[Online]. 2013. **2013**. No pagination. [Accessed 4 March 2019]. Available from: https://www.hindawi.com/journals/jchem/2013/487676/.

267.　Kumar, S. and Singh, R.K. Recovery of hydrocarbon liquid from waste high density polyethylene by thermal pyrolysis. *Brazilian Journal Chemical Engineering.* [Online]. **28**(4), pp.659-667. [Accessed 4 March 2019]. Available from: http://www.scielo.br/scielo.php?script=sci_arttext&pid=S0104-66322011000400011.

268.　Sharuddin, A., Dayana, S., Abnisa, F., Wan Daud, W.M.A. and Aroua, M.K. Energy recovery from pyrolysis of plastic waste: study on non-recycled plastics (NRP) data as the real measure of plastic waste. *Energy Conversion and Management.* [Online]. 2017. **148**, pp. 925-934. [Accessed 4 March 2019]. Available from: https://www.sciencedirect.com/science/article/pii/S0196890417305915.

269.　Honus, S., Kumagai, S., Molnar, V., Fedorko, G. and Yoshioka, T. Pyrolysis gases produced from individual and mixed PE, PP, PS, PVC and PET – part II: Fuel characteristics. *Fuel.* [Online]. 2018. **221**, pp. 361-373. [Accessed 5 March 2019]. Available from: https://www.sciencedirect.com/science/article/pii/S001623611830228X.

270.　Graca, I, Lopes, J.M., Cerqueira, H.S. and Ribeiro, M.F. Bio-oils upgrading for second generation biofuels. *Industrial & Engineering Chemistry Research.* [Online]. 2013. **52**(1), pp.275-287. [Accessed 6 March 2019]. Available from: https://pubs.acs.org/doi/10.1021/ie301714x.

271.　CRC. *Handbook of chemistry and physics 99ᵗʰ edition: Interactive table: Energy produced and carbon released from fuels – methane.* [Online]. 2018. [Accessed 4 December 2018]. Available from: http://hbcponline.com/faces/contents/InteractiveTable.xhtml?search=true&tableId=36.

272.　Al-Asadi, M. and Miskolczi, N. Pyrolysis of polyethylene terephthalate containing real waste plastics using Ni loaded zeolite catalysts. *IOP Conference Series: Earth and Environmental Science.* [Online]. 2018. **154**, no pagination. [Accessed 5 December 2018]. Available from: https://iopscience.iop.org/article/10.1088/1755-1315/154/1/012021.

273.　Lopez, A., De Marco, I., Caballero, B.M., Laresgoiti, M.F., Adrados, A. and Aranzabal, A. Catalytic pyrolysis of plastic wastes with two different types of catalysts: ZSM-5 zeolite and Red Mud. *Applied Catalysis B: Environmental.* [Online]. **104**(3), pp.211-219. [Accessed]. Available from: https://www.sciencedirect.com/science/article/pii/S0926337311001433.

274.   RECOUP. *UK Household Plastics collection survey 2017*. [Online]. 2017. [Accessed 26 July 2018]. Available from: http://www.recoup.org/p/324/uk-household-plastics-collection-survey-2018.

275.   Zhang, H., Nie, J., Xiao, R., Jin, B., Dong, C. and Xiao, G. Catalytic co-pyrolysis of biomass and different plastics (polyethylene, polypropylene, and polystyrene) to improve hydrocarbon yield in a fluidized-bed reactor. *Energy & Fuels.* [Online]. 2014. **28**(3), pp.1940-1947. [Accessed 27 February 2019]. Available from: https://pubs.acs.org/doi/10.1021/ef4019299.

276.   Williams, C.L., Chang, C.C., Do, P., Nikbin, N., Caratzoulos, D.G., Vlachos, D.G., Lobo, R.F., Fan, W. and Dauenhauer, P.J. Cycloaddition of biomass-derived furans for catalytic production of renewable p-xylene. *ACS Catalysis.* [Online]. 2012. **2**(6), pp.935-939. [Accessed 20 June 2019]. Available from: https://pubs.acs.org/doi/10.1021/cs300011a.

277.   Chantal, P., Kaliaguine, S., Grandmaison, J.L. and Mahay, A. Production of hydrocarbons from aspen poplar pyrolytic oils over H-ZSM-5. *Applied Catalysis.* [Online]. 1984. **10**(3), pp.317-332. [Accessed 17 June 2019]. Available from: https://www.sciencedirect.com/science/article/pii/016698348480127X.

278.   GTC Technology. *GT Styrene.* [Online]. 2014. [Accessed 1 May 2019]. Available from: http://www.gtctech.com/wp-content/uploads/GT-Styrene1.pdf.

279.   Lukyanov, D.B. and Vazhnova. Aromatization activity of gallium containing MFI and TON zeolite catalysts in n-butane conversion: Effects of gallium and reaction conditions. *Applied Catalysis A: General.* [Online]. 2007. **316**(1), pp.61-67. [Accessed 18 June 2019]. Available from: https://www.sciencedirect.com/science/article/abs/pii/S0926860X0600679X.

280.   Guisnet, M and Gnep, N.S. Mechanism of short-chain alkane transformation over protonic zeolites. Alkylation, disproportionation and aromatization. *Applied Catalysis A: General.* [Online]. 1996. **146**(1), pp.33-64. [Accessed 18 June 2019]. Available from: https://www.sciencedirect.com/science/article/abs/pii/0926860X96002827.

281.   Muhammad, C., Onwudili, J.A. and Williams P.T. Thermal degradation of real-world waste plastics and simulated mixed plastics in a two-stage pyrolysis-catalysis reactor for fuel production. *Energy & Fuels.* [Online]. 2015. **29**(4), pp.2683-2691. [Accessed 12 December 2018]. Available from: https://pubs.acs.org/doi/abs/10.1021/ef502749h.

282.   Andersen, V.F., Anderson, J.E., Wallington, T.J., Mueller, S.A. and Nielsen, O.J. Distillation curves for alcohol-gasoline blends. *Energy & Fuels.* [Online]. 2010.

24(4), pp.2683-2691. [Accessed 9 May 2019]. Available from: https://pubs.acs.org/doi/10.1021/ef9014795.

283. Smith, B.L. and Bruno, T.J. Improvements int the measurement of distillation curves. 3. Application to gasoline and gasoline + methanol mixtures. *Industrial & Engineering Chemistry Research.* [Online]. 2007. **46**(1), pp.297-309. [Accessed 9 May 2019]. Available from: https://pubs.acs.org/doi/10.1021/ie060937u.

284. C.E. Delft. *Blending and Bunkering – admixture of hazardous materials to bunker fuels for maritime shipping – risks and strategies.* [Online]. 2011. [Accessed 15 May 2019]. Available from: https://www.cedelft.eu/publicatie/ blending_and_bunkering%3Cbr%3Ean_analysis_of_the_bunker_fuel_supply_c hain/1193.

285. Intertanko. *Contaminated bunkers damage hundreds of ships.* [Online]. 2018. [Accessed 12 June 2019]. Available from: http://www.gard.no/Content/ 26096787/Intertanko%20paper.pdf.